

**REPORT NO.
UCD/CGM-10/02**

CENTER FOR GEOTECHNICAL MODELING

SPT-BASED LIQUEFACTION TRIGGERING PROCEDURES

BY

I. M. IDRIS

R. W. BOULANGER



**DEPARTMENT OF CIVIL & ENVIRONMENTAL ENGINEERING
COLLEGE OF ENGINEERING
UNIVERSITY OF CALIFORNIA AT DAVIS**

December 2010

SPT-BASED LIQUEFACTION TRIGGERING PROCEDURES

by

I. M. Idriss

Ross W. Boulanger

Report No. UCD/CGM-10-02

Center for Geotechnical Modeling
Department of Civil and Environmental Engineering
University of California
Davis, California

December 2010

TABLE OF CONTENTS

1. INTRODUCTION
 - 1.1. Purpose
 - 1.2. Organization of report
2. ANALYSIS FRAMEWORK
 - 2.1. Components of the stress-based framework
 - 2.2. Summary of the Idriss-Boulanger procedure
3. CASE HISTORY DATABASE
 - 3.1. Sources of data
 - 3.2. Earthquake magnitudes and peak accelerations
 - 3.3. Selection and computation of $(N_1)_{60cs}$ values
 - 3.4. Classification of site performance
 - 3.5. Distribution of data
4. EXAMINATION OF THE LIQUEFACTION TRIGGERING CORRELATION
 - 4.1. Case history data
 - 4.1.1. Variation with fines content
 - 4.1.2. Variation with effective overburden stress
 - 4.1.3. Variation with earthquake magnitude
 - 4.1.4. Variation with SPT procedures
 - 4.1.5. Case histories at strong ground motion recording stations
 - 4.1.6. Data from the 1995 Kobe earthquake
 - 4.2. Sensitivity of case history data points to components of the analysis framework
 - 4.2.1. Overburden correction factor for penetration resistance, C_N
 - 4.2.2. Overburden correction factor for cyclic strength, K_σ

- 4.2.3. Short rod correction factor, C_R
- 4.2.4. Shear stress reduction factor, r_d
- 4.2.5. Equivalent clean sand adjustment, $\Delta(N_1)_{60}$
- 4.3. Summary of re-examination of case history database
- 5. COMPARISON WITH RESULTS OF TESTS ON FROZEN SAND SAMPLES
 - 5.1. Examination of data from tests on frozen sand samples
 - 5.1.1. Test data and published correlations
 - 5.1.2. Comparison to the Idriss-Boulanger liquefaction triggering correlation
 - 5.1.3. Summary of comparisons
 - 5.2. Duncan Dam – prediction of CRR at large overburden stresses
 - 5.2.1. Background
 - 5.2.2. Laboratory test data
 - 5.2.3. Predicting the variation of CRR with depth based on SPT-based correlations
 - 5.2.4. Values of CRR and $(N_1)_{60cs}$ for Duncan Dam
 - 5.2.5. Summary of comparisons
- 6. PROBABILISTIC RELATIONSHIP FOR LIQUEFACTION TRIGGERING
 - 6.1. Probabilistic relationships for liquefaction triggering
 - 6.2. Methodology
 - 6.2.1. Limit state function
 - 6.2.1. Likelihood function
 - 6.3. Results of parameter estimation
 - 6.3.1. Results and sensitivity to assumed parameter estimation errors
 - 6.3.2. Additional sensitivity studies
 - 6.3.3. Recommended relationships
 - 6.4. Summary

7. COMPARISON TO OTHER LIQUEFACTION TRIGGERING CORRELATIONS
 - 7.1. Comparison of CRR values obtained using different triggering correlations
 - 7.2. Reasons for the differences in the triggering correlations
 - 7.3. Components affecting extrapolation outside the range of the case history data
 - 7.3.1. Role of C_N relationship
 - 7.3.2. Role of K_σ relationship
 - 7.3.3. Role of r_d relationship
 - 7.3.4. Role of MSF relationship

8. SUMMARY AND CONCLUSIONS

ACKNOWLEDGMENTS

REFERENCES

APPENDIX A: EXAMINATION OF THE CETIN ET AL. (2004) LIQUEFACTION TRIGGERING CORRELATION

APPENDIX B: SHEAR STRESS REDUCTION COEFFICIENT

APPENDIX C: COMPUTATIONS OF REPRESENTATIVE $(N_1)_{60CS}$ VALUES

SPT-based Liquefaction Triggering Procedures

1. INTRODUCTION

1.1. Purpose

This report presents an updated examination of SPT-based liquefaction triggering procedures for cohesionless soils, with the specific purpose of:

- updating and documenting the case history database,
- providing more detailed illustrations of the database distributions relative to the liquefaction triggering correlation by Idriss and Boulanger (2004, 2008),
- re-examining the database of cyclic test results for frozen sand samples,
- presenting a probabilistic version of the Idriss-Boulanger (2004, 2008) liquefaction triggering correlation using the updated case history database,
- presenting a number of new findings regarding components of the liquefaction analysis framework used to interpret and extend the case history experiences, and
- presenting an examination of the reasons for the differences between some current liquefaction triggering correlations.

The last task addresses an issue of current importance to the profession, which specifically pertains to determining the source of the differences between the liquefaction triggering correlations published by the late Professor H. Bolton Seed and colleagues (Seed et al. 1984, 1985), which were adopted with slight modifications in the NCEER/NSF workshops (Youd et al. 2001), and those published more recently by Cetin et al. (2004) and those published by Idriss and Boulanger (2004, 2008). These liquefaction triggering correlations are compared in Figure 1.1 in terms of the cyclic resistance ratio (CRR) adjusted for $M = 7.5$ and $\sigma'_v = 1$ atm versus $(N_1)_{60cs}$. The question of concern is why the correlation of $CRR_{M=7.5, \sigma'_v=1}$ versus $(N_1)_{60cs}$ proposed by Cetin et al. (2004) is significantly lower than those by Seed et al. (1984) and those by Idriss and Boulanger (2004, 2008) although they are based on largely the same case histories. Do these differences represent scientific (epistemic) uncertainty, or are they due to errors or biases in the analysis frameworks or case history interpretations that can be resolved?

This issue became important to the profession in 2010 when Professor Raymond B. Seed stated that the use of the Idriss-Boulanger correlations, and presumably the similar Seed et al. (1984) correlation, was "dangerously unconservative." He repeated such statements in a series of visits to major consulting firms and regulatory agencies, a series of e-mail messages to the EERI Board of Directors with copies to over 100 prominent individuals in the USA and abroad, and a University of California at Berkeley Geotechnical Report titled, "Technical Review and Comments: 2008 EERI Monograph (by I.M. Idriss and R.W. Boulanger)". These statements took us by surprise, caused some degree of concern within the profession, and left many people asking: "Why the controversy" and "Why in this way?" We cannot answer these questions, but we can take this opportunity to openly and carefully re-examine the key technical issues affecting liquefaction triggering correlations and to investigate the reasons for the differences among the three correlations shown in Figure 1.1.

The body of this report presents the results of this updated re-examination of SPT-based liquefaction triggering procedures. This re-examination included updating the case history database, re-examining how the case history data compare to the database of cyclic test results for frozen sand samples, re-examining the case history data in a probabilistic framework, and examining new findings regarding

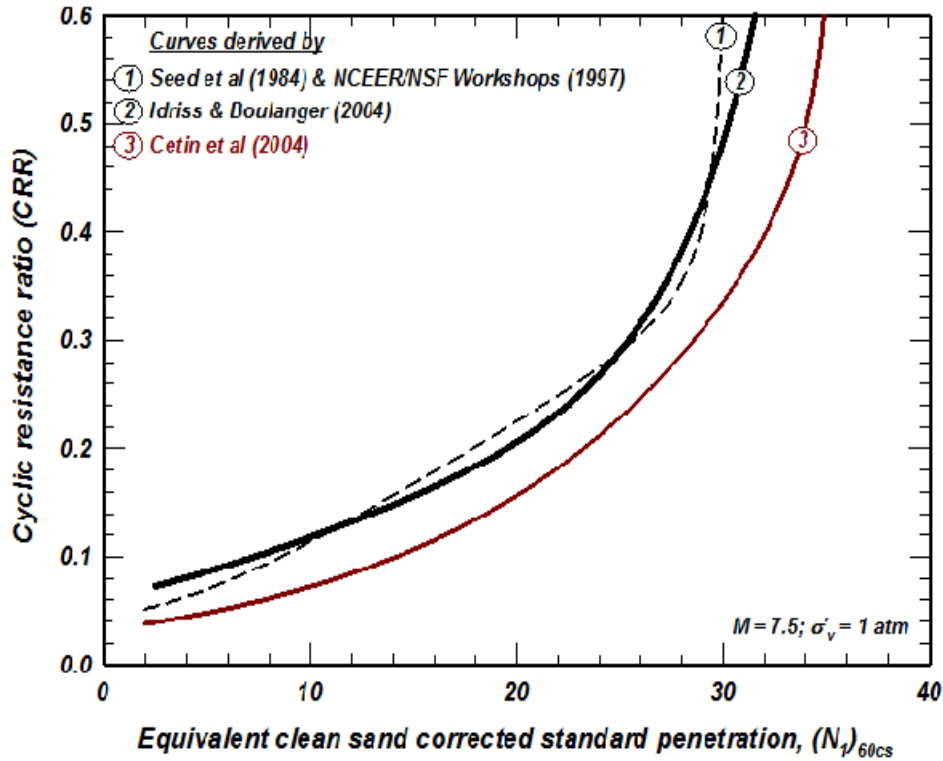


Figure 1.1. Three SPT-based liquefaction triggering curves

components of the liquefaction analysis framework. The key to this re-examination and to the development of liquefaction triggering correlations for practice, is that these various sources of information must be synthesized together, rather than viewed as separate parts. It is the synthesis of theoretical, experimental, and case history data that is particularly valuable for arriving at reasonable relationships that are consistent with the cumulative available information while overcoming the unavoidable limitations in each individual source of information.

Appendix A of this report presents the results of our examination of the reasons for the differences between the three liquefaction triggering correlations shown in Figure 1.1. This effort included examining the case history databases and analysis frameworks used by Seed et al. (1984), Youd et al. (2001), and Cetin et al. (2000, 2004) to identify the primary causes of the differences in the liquefaction triggering correlations. It had been suspected that the differences in the r_d , K_σ , and C_N relationships may have played a significant role, but it was found that they had a relatively minor effect on the resulting liquefaction triggering correlations. Instead, the differences in the liquefaction triggering correlations were found to be primarily caused by the interpretations and treatment of 8 key case histories in the Cetin et al. (2000, 2004) database. These findings were communicated to Professor Onder Cetin in the summer of 2010, but there has been no indication from him or his coauthors that these issues will be addressed. Our examination of the Cetin et al. (2000, 2004) case history database and their interpretations of these 8 key cases are presented in detail in Appendix A for the purpose of facilitating discussions and independent examinations by the profession.

It is hoped that this report will serve as a useful resource for practicing engineers and researchers working in the field of soil liquefaction. It is also hoped that this report will be a useful technical supplement to the 2008 EERI Monograph on *Soil Liquefaction During Earthquakes* by Idriss and Boulanger (2008).

1.2. Organization of report

Section 2 of this report contains an overview of the SPT-based liquefaction analysis framework for cohesionless soils, followed by a summary of the specific relationships used or derived by Idriss and Boulanger (2004, 2008).

Section 3 describes the updated database of SPT-based liquefaction/no liquefaction case histories. The selection of earthquake magnitudes, peak accelerations, and representative $(N_1)_{60cs}$ values are described, and the classification of site performance discussed.

Section 4 provides an evaluation of the SPT-based liquefaction triggering database relative to the liquefaction triggering correlation by Idriss and Boulanger (2004, 2008). The distributions of the data are examined with respect to various parameters (e.g., fines content, overburden stress, earthquake magnitude) and data sources (e.g., data from the U.S., Japan, pre- and post-1985 studies, and sites with strong ground motion recordings). In addition, the sensitivity of the database's interpretation to a number of aspects and components of the analysis framework is examined.

Section 5 contains an examination of liquefaction triggering correlations developed using the results of cyclic laboratory tests on specimens obtained using frozen sampling techniques (e.g., Yoshimi et al. 1989, 1994) and their comparison to those derived from the field case histories. This section also contains a detailed examination of the unique set of field and laboratory testing data at large overburden stresses at Duncan Dam (e.g., Pillai and Byrne 1994).

Section 6 describes the development of a probabilistic version of the Idriss and Boulanger (2004, 2008) liquefaction triggering correlation using the updated case history database and a maximum likelihood method. Sensitivity of the derived probabilistic relationship to the key assumptions is examined, and issues affecting the application of probabilistic liquefaction triggering models in practice are discussed.

Section 7 contains a comparison of CRR values computed using some of the current liquefaction triggering correlations, followed by (1) a summary of the reasons for the differences in the derived triggering correlations, and (2) an examination of new findings regarding analysis components that affect how these triggering correlations are extrapolated outside the range of the case history data.

Appendix A presents an examination of the Cetin et al. (2004) liquefaction triggering database and our findings regarding the primary reasons for the differences between the three liquefaction triggering correlations shown in Figure 1.1.

Appendix B presents background information on the development of the Idriss (1999) relationship for the shear stress reduction coefficient, r_d .

Appendix C presents the computations for the $(N_1)_{60cs}$ values in the liquefaction triggering database presented in this report.

2. ANALYSIS FRAMEWORK

2.1. Components of the stress-based framework

The stress-based approach for evaluating the potential for liquefaction triggering, initiated by Seed and Idriss (1967), has been used widely for the last 45 years (e.g., Seed and Idriss 1971, Shibata 1981, Tokimatsu and Yoshimi 1983, NRC 1985, Seed et al. 1985, Youd et al. 2001, Cetin et al. 2004, Idriss and Boulanger 2004). The basic framework, as adopted by numerous researchers, compares the earthquake-induced cyclic stress ratios (CSR) with the cyclic resistance ratios (CRR) of the soil. The components of this framework, as briefly summarized below, were developed to provide a rational treatment of the various factors that affect penetration resistance and cyclic resistance.

Earthquake-induced cyclic stress ratio (CSR)

The earthquake-induced CSR, at a given depth, z , within the soil profile, is usually expressed as a representative value (or equivalent uniform value) equal to 65% of the maximum cyclic shear stress ratio, i.e.:

$$CSR_{M,\sigma'_v} = 0.65 \frac{\tau_{\max}}{\sigma'_v} \quad (2.1)$$

where τ_{\max} = maximum earthquake induced shear stress, σ'_v = vertical effective stress, and the subscripts on the CSR indicate that it is computed for a specific earthquake magnitude (moment magnitude, M) and in-situ σ'_v . The choice of the reference stress level (i.e., the factor 0.65) was selected by Seed and Idriss (1967) and has been in use since. Selecting a different reference stress level would alter the values of certain parameters and relationships but would have no net effect on the final outcome of the derived liquefaction evaluation procedure, as long as this same reference stress level is used throughout, including forward calculations. The value of τ_{\max} can be estimated from dynamic response analyses, but such analyses must include a sufficient number of input acceleration time series and adequate site characterization details to be reasonably robust. Alternatively, the maximum shear stress can be estimated using the equation, developed as part of the Seed-Idriss Simplified Liquefaction Procedure, which is expressed as,

$$CSR_{M,\sigma'_v} = 0.65 \frac{\sigma_v}{\sigma'_v} \frac{a_{\max}}{g} r_d \quad (2.2)$$

where σ_v = vertical total stress at depth z , a_{\max}/g = maximum horizontal acceleration (as a fraction of gravity) at the ground surface, and r_d = shear stress reduction factor that accounts for the dynamic response of the soil profile.

Cyclic resistance ratio (CRR)

The soil's CRR is usually correlated to an in-situ parameter such as SPT blow count (number of blows per foot), CPT penetration resistance or shear wave velocity, V_s . SPT blow counts are affected by a number of procedural details (rod lengths, hammer energy, sampler details, borehole size) and by effective overburden stress. Thus, the correlation to CRR is based on corrected penetration resistance,

$$(N_1)_{60} = C_N C_E C_R C_B C_S N_m \quad (2.3)$$

where C_N is an overburden correction factor, $C_E = ER_m/60\%$, ER_m is the measured value of the delivered energy as a percentage of the theoretical free-fall hammer energy, C_R is a rod correction factor to account for energy ratios being smaller with shorter rod lengths, C_B is a correction factor for nonstandard borehole diameters, C_S is a correction factor for using split spoons with room for liners but with the liners absent, and N_m is the measured SPT blow count. The factors C_B and C_S are set equal to unity if standard procedures are followed.

The soil's CRR is also affected by the duration of shaking (which is correlated to the earthquake magnitude scaling factor, MSF) and effective overburden stress (which is expressed through a K_σ factor). The correlation for CRR is therefore developed for a reference $M = 7.5$ and $\sigma'_v = 1$ atm, and then adjusted to other values of M and σ'_v using the following expression:

$$CRR_{M,\sigma'_v} = CRR_{M=7.5,\sigma'_v=1} \cdot MSF \cdot K_\sigma \quad (2.4)$$

The soil's CRR is further affected by the presence of sustained static shear stresses, such as may exist beneath foundations or within slopes. This effect, which is expressed through a K_α factor, is generally small for nearly level ground conditions. It is not included herein because the case history database is dominated by level or nearly level ground conditions.

The correlation of CRR to $(N_1)_{60}$ is affected by the soil's fines content (FC) and is expressed as,

$$CRR_{M=7.5,\sigma'_v=1} = f\left[(N_1)_{60}, FC\right] \quad (2.5)$$

For mathematical convenience, this correlation can also be expressed in terms of an equivalent clean-sand $(N_1)_{60cs}$, which is obtained using the following expression:

$$(N_1)_{60cs} = (N_1)_{60} + \Delta(N_1)_{60} \quad (2.6)$$

CRR can then be expressed in terms of $(N_1)_{60cs}$, i.e.:

$$CRR_{M=7.5,\sigma'_v=1} = f\left[(N_1)_{60cs}\right] \quad (2.7)$$

where the adjustment $\Delta(N_1)_{60}$ is a function of FC.

The above framework has been used for a number of SPT-based liquefaction correlations, although the notation may be slightly different in some cases.

Important attributes of a liquefaction analysis procedure

A liquefaction analysis procedure within the above stress-based framework requires the following two attributes:

- The liquefaction analysis procedure is applicable to the full range of conditions important to practice; e.g., from shallow lateral spreads to large earth dams. Practice often results in the need to extrapolate outside the range of the case history experiences, requiring the framework to be supported by sound experimental and theoretical bases for guiding such extrapolations.
- The mechanics are consistent with those used in developing companion correlations to other in-situ parameters; e.g., SPT blow count, CPT penetration resistance, and shear wave velocity, V_s . Consistency in the mechanics facilitates the logical integration of information from multiple sources and provides a rational basis for the calibration of constitutive models for use in nonlinear dynamic analyses.

The components of the stress-based analysis framework include five functions, or relationships, that describe fundamental aspects of dynamic site response, penetration resistance, and soil characteristics and behavior. These five functions, along with the major factors affecting each, are:

- $r_d = f(\text{depth; earthquake and ground motion characteristics; dynamic soil properties})$
- $C_N = f(\sigma'_v; D_R; FC)$
- $C_R = f(\text{depth; rod stick-up length})$
- $K_\sigma = f(\sigma'_v; D_R; FC)$
- $MSF = f(\text{earthquake and ground motion characteristics; soil characteristics})$

These functions are best developed using a synthesis of empirical, experimental and theoretical methods, as ultimately the robustness of these functions is important for guiding the application of the resulting correlations to conditions that are not well-represented in the case history database.

Statistical analyses and regression methods are valuable tools for examining liquefaction analysis methods and testing different hypotheses, but the functional relationships in the statistical models must be constrained and guided by available experimental data and theoretical considerations. In the case of liquefaction triggering correlations, the use of regression models alone to derive physical relationships is not considered adequate because: (1) the case history data are generally not sufficient to constrain the development of such relationships, as illustrated later in this report; (2) any such relationship will be dependent on the assumed forms for the other functions, particularly given that four of the above five functions are strongly dependent on depth; and (3) the use of regression to define functions describing fundamental behaviors does not necessarily produce a function that can be reliably used in extrapolating the resulting correlation to conditions not well represented in the database, such as large depths. These considerations are important to the examination of the reasons for differences among some current liquefaction analysis procedures, as discussed in Section 7 of this report.

2.2. Summary of the Idriss-Boulanger procedure

The components of the analysis procedure used or derived by Idriss and Boulanger (2004, 2006, 2008) as part of their liquefaction triggering correlation are briefly summarized in this subsection.

Shear stress reduction parameter, r_d

Idriss (1999), in extending the work of Golesorkhi (1989), performed several hundred parametric site response analyses and concluded that, for the purpose of developing liquefaction evaluation procedures, the parameter r_d could be expressed as,

$$r_d = \exp[\alpha(z) + \beta(z) \cdot M]$$

$$\alpha(z) = -1.012 - 1.126 \sin\left(\frac{z}{11.73} + 5.133\right)$$

$$\beta(z) = 0.106 + 0.118 \sin\left(\frac{z}{11.28} + 5.142\right)$$
(2.8)

where z = depth below the ground surface in meters. The resulting relationship is plotted in Figure 2.1. Additional information on the development of this relationship is provided in Appendix C.

Other r_d relationships have been proposed, including the probabilistic relationships by Cetin et al. (2004) and Kishida et al. (2009b). The latter two relationships were based on large numbers of site response analyses for different site conditions and ground motions, and include the effects of a site's average shear wave velocity and the level of shaking. These alternative r_d relationships and their effects on the interpretation of the liquefaction case histories are examined in Sections 4 and 6 of this report.

Overburden correction factor, C_N

The C_N relationship used was initially developed by Boulanger (2003) based on: (1) a re-examination of published SPT calibration chamber test data covering σ'_v of 0.7 to 5.4 atm (Marcuson and Bieganousky 1977a, 1977b); and (2) results of analyses for σ'_v of 0.2 to 20 atm using the cone penetration theory of Salgado et al. (1997a, 1997b) which was shown to produce good agreement with a database of over 400

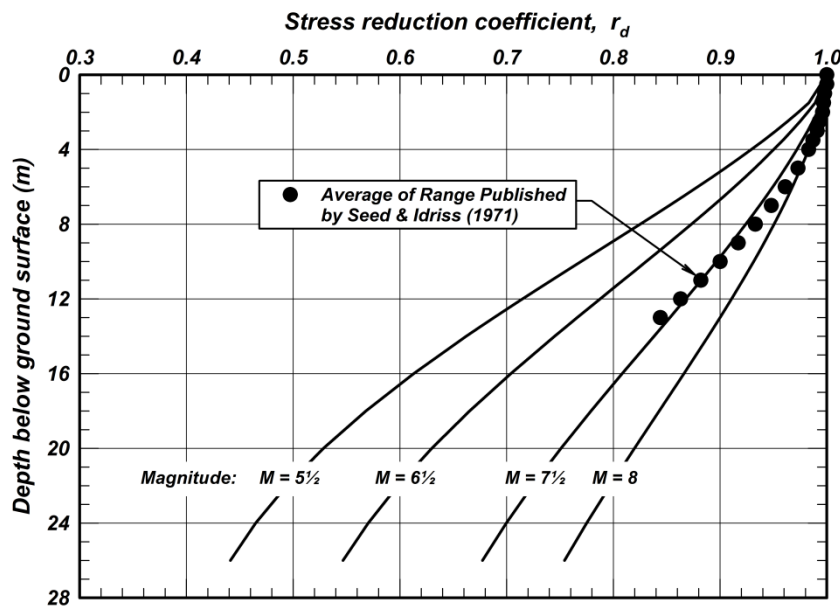


Figure 2.1. Shear stress reduction factor, r_d , relationship

CPT calibration chamber tests with σ'_v up to 7 atm. Idriss and Boulanger (2003, 2008) subsequently recommended that the D_R -dependence of the C_N relationship could be expressed in terms of $(N_1)_{60cs}$ as follows:

$$C_N = \left(\frac{P_a}{\sigma'_v} \right)^m \leq 1.7$$

$$m = 0.784 - 0.0768 \sqrt{(N_1)_{60cs}} \quad (2.9)$$

This expression requires iteration which is easily accomplished using the automatic iteration option in an Excel spreadsheet. This relationship is plotted in Figure 2.2a for a range of $(N_1)_{60cs}$ values and for effective overburden stresses up to 10 atm, and compared to the Liao and Whitman (1986) relationship in Figure 2.2b for effective overburden stresses up to 2 atm.

The limit of 1.7 on the maximum value of C_N is reached at vertical effective stresses less than about 35 kPa, which corresponds to depths less than about 2 m. This limit is imposed because these expressions were not derived or validated for very low effective stresses, and the assumed functional form will otherwise produce unrealistically large C_N values as the vertical effective stress approaches zero. Limits of 1.6 to 2.0 have been recommended by various researchers.

The recent field studies at Perris Dam by the California Department of Water Resources enabled the field-based derivation of a site-specific C_N relationship for an alluvial layer of silty and clayey sand (FC = 30-45%) that was under σ'_v ranging from 0.2 to 8.5 atm across the dam section (Wehling and Rennie 2008). These field data are evaluated relative to the above C_N relationship in Section 7; the results lend support for the dependence of C_N on $(N_1)_{60cs}$ and the use of the above expression at large depths.

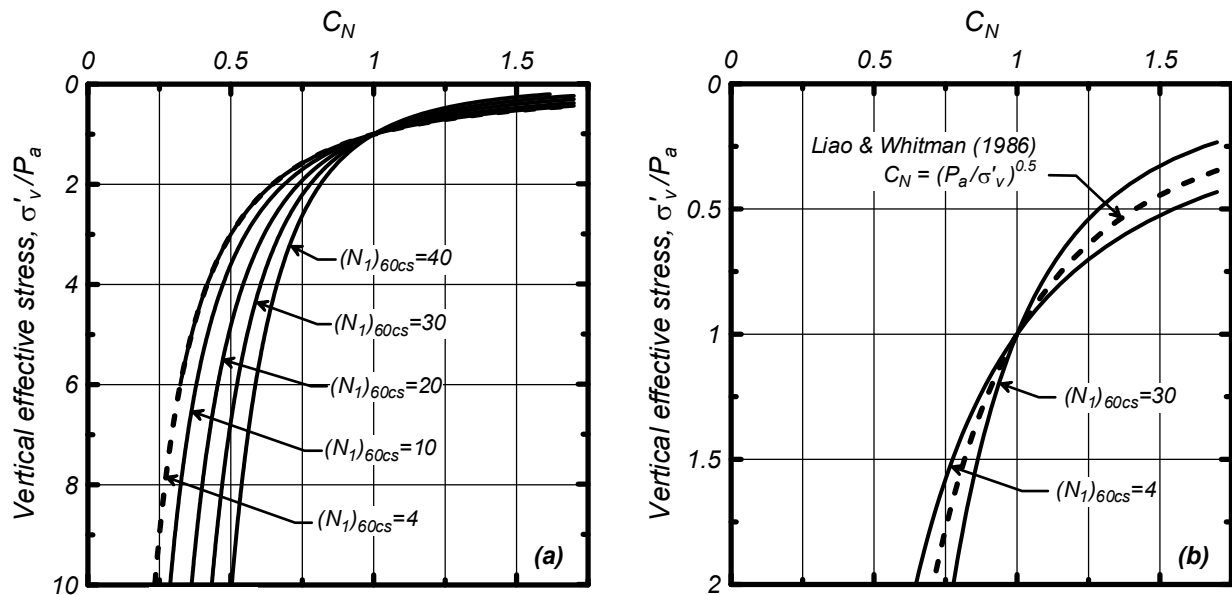


Figure 2.2. Overburden correction factor (C_N) relationship for SPT penetration resistance

Short rod correction factor, C_R

The short rod correction factor accounts for the effect of rod length on the energy transferred to the sampling rods during the primary hammer impact (e.g., Schmertmann and Palacios 1979). If the ER_m for an SPT system is measured for rod lengths greater than about 10 m, then the ER delivered with shorter rod lengths would be smaller, resulting in values of the short rod correction factor, C_R , less than unity for rod length less than 10 m. The values of C_R recommended in Youd et al. (2001) are adopted in this report and are listed below for various rod lengths:

Rod length < 3 m	$C_R = 0.75$
Rod length 3-4 m	$C_R = 0.80$
Rod length 4-6 m	$C_R = 0.85$
Rod length 6-10 m	$C_R = 0.95$
Rod length 10-30 m	$C_R = 1.00$

The rod length is the sum of the rod stick-up length (length above the ground surface) and the sampling depth. Rod stick-up lengths are often not reported or known for liquefaction case histories, so they must be estimated based on common practices and typical equipment configurations. For example, Cetin et al. (2004) used 1.2 m for donut hammers and for USGS safety hammers, and 2.1 m for all other safety hammers for cases of unreported rod stick-up length. Idriss and Boulanger (2004) accepted the values used by Seed et al. (1984) and the values by Cetin et al. (2000) for those cases not included in Seed et al. (1984). In the present re-examination, the default rod stick-up length was taken as 2.0 m for all cases from Japan and 1.5 m for all other cases. The effect of varying the assumed rod stick-up length on the interpretation of the liquefaction case histories is later shown to be unimportant.

The basis for short rod correction factors have been questioned in some recent studies. For example, Daniel et al. (2005) suggested that the energy transfer in secondary impacts may, in fact, contribute to sampler advancement. Additional studies on the combined roles of the short rod correction factor and overburden correction factor at shallow depths would be helpful.

Overburden correction factor, K_σ

The K_σ relationship used was developed by Boulanger (2003) based on: (1) showing that the CRR for a clean reconstituted sand in the laboratory could be related to the sand's relative state parameter index, ξ_R ; (2) showing that the K_σ relationship for such clean sands could be directly derived from the CRR- ξ_R relationship; and (3) deriving a K_σ relationship that was consistent with the field-based CRR- $(N_1)_{60cs}$ correlations from the corresponding field-based CRR- ξ_R relationships. Idriss and Boulanger (2008) recommended that the resulting K_σ relationship be expressed in terms of the $(N_1)_{60cs}$ values as follows:

$$K_\sigma = 1 - C_\sigma \ln \left(\frac{\sigma'_v}{P_a} \right) \leq 1.1$$
$$C_\sigma = \frac{1}{18.9 - 2.55\sqrt{(N_1)_{60cs}}} \leq 0.3 \quad (2.10)$$

The resulting relationship is plotted in Figure 2.3 for a range of $(N_1)_{60cs}$. The limit of 1.1 on the maximum value of K_σ is reached at vertical effective stresses less than about 40 kPa. This limit was imposed

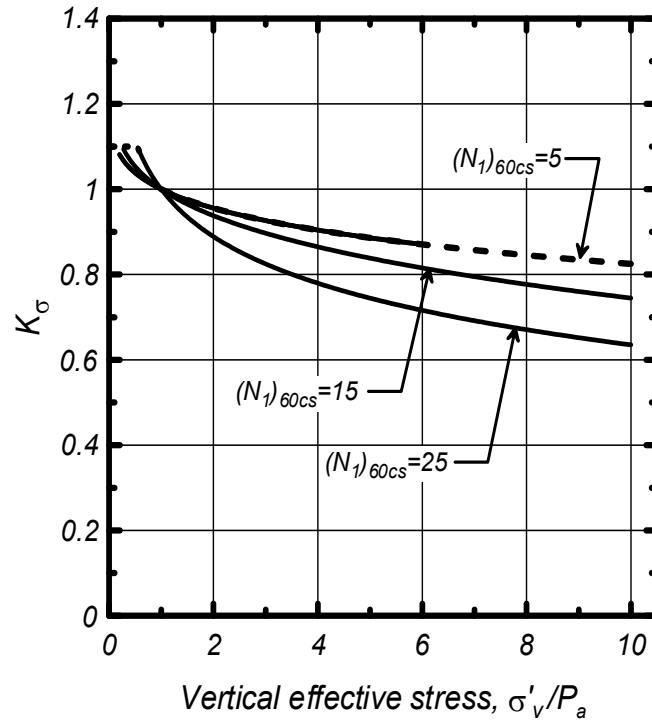


Figure 2.3. Overburden correction factor (K_σ) relationship

because these expressions were not derived or validated for very low effective stresses, and the assumed functional form is otherwise unbounded as the vertical effective stress approaches zero. The effect of omitting the limit of 1.1 for the maximum value of K_σ on the interpretation of the liquefaction case histories is later shown to be essentially unimportant.

The K_σ and C_N relationships are particularly important in applications that require extrapolation for depths greater than those covered by the case history database. Different combinations of these two relationships are evaluated using the in-situ test and frozen sand sampling data from Duncan Dam in Section 5.3.

Magnitude scaling factor, MSF

The magnitude scaling factor (MSF) is used to account for duration effects (i.e., number of loading cycles) on the triggering of liquefaction. The MSF relationship was derived by combining (1) laboratory-based relationships between the CRR and the number of equivalent uniform loading cycles, and (2) correlations of the number of equivalent uniform loading cycles with earthquake magnitude. The MSF factor is applied to the calculated value of CSR for each case history to convert to a common value of M (conventionally taken as $M = 7.5$). The MSF for sands was reevaluated by Idriss (1999), who recommended the following relationship:

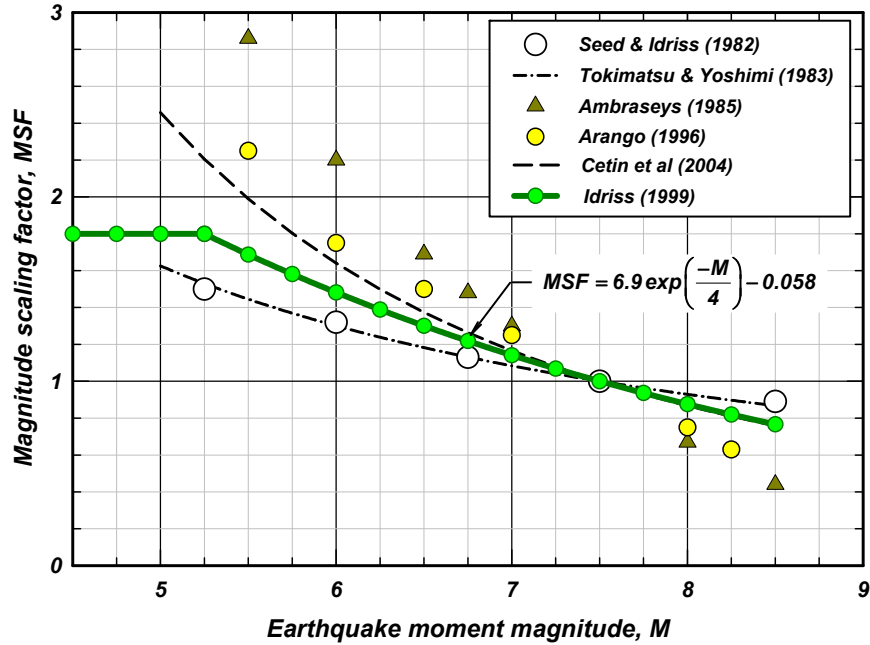


Figure 2.4. Magnitude scaling factor (MSF) relationship

$$MSF = 6.9 \cdot \exp\left(\frac{-M}{4}\right) - 0.058 \leq 1.8 \quad (2.11)$$

An upper limit for the MSF is assigned to very-small-magnitude earthquakes for which a single peak stress can dominate the entire time series. The value of 1.8 is obtained by considering the time series of stress induced by a small magnitude earthquake to be dominated by single pulse of stress (i.e., $\frac{1}{2}$ to 1 full cycle, depending on its symmetry), with all other stress cycles being sufficiently small to neglect. The resulting relationship is plotted in Figure 2.4.

Equivalent clean sand adjustment, $\Delta(N_1)_{60}$

The equivalent clean sand adjustment, $\Delta(N_1)_{60}$, is empirically derived from the liquefaction case history data, and accounts for the effects that fines content has on both the CRR and the SPT blow count. The liquefaction case histories suggest that the liquefaction triggering correlation shifts to the left as the fines content (FC) increases. This effect is conveniently represented by adjusting the SPT $(N_1)_{60}$ values to equivalent clean sand $(N_1)_{60cs}$ values (equation 2.6), and then expressing CRR as a function of $(N_1)_{60cs}$. The equivalent clean sand adjustment developed by Idriss and Boulanger (2004, 2008) is expressed as,

$$\Delta(N_1)_{60} = \exp\left(1.63 + \frac{9.7}{FC + 0.01} - \left(\frac{15.7}{FC + 0.01}\right)^2\right) \quad (2.12)$$

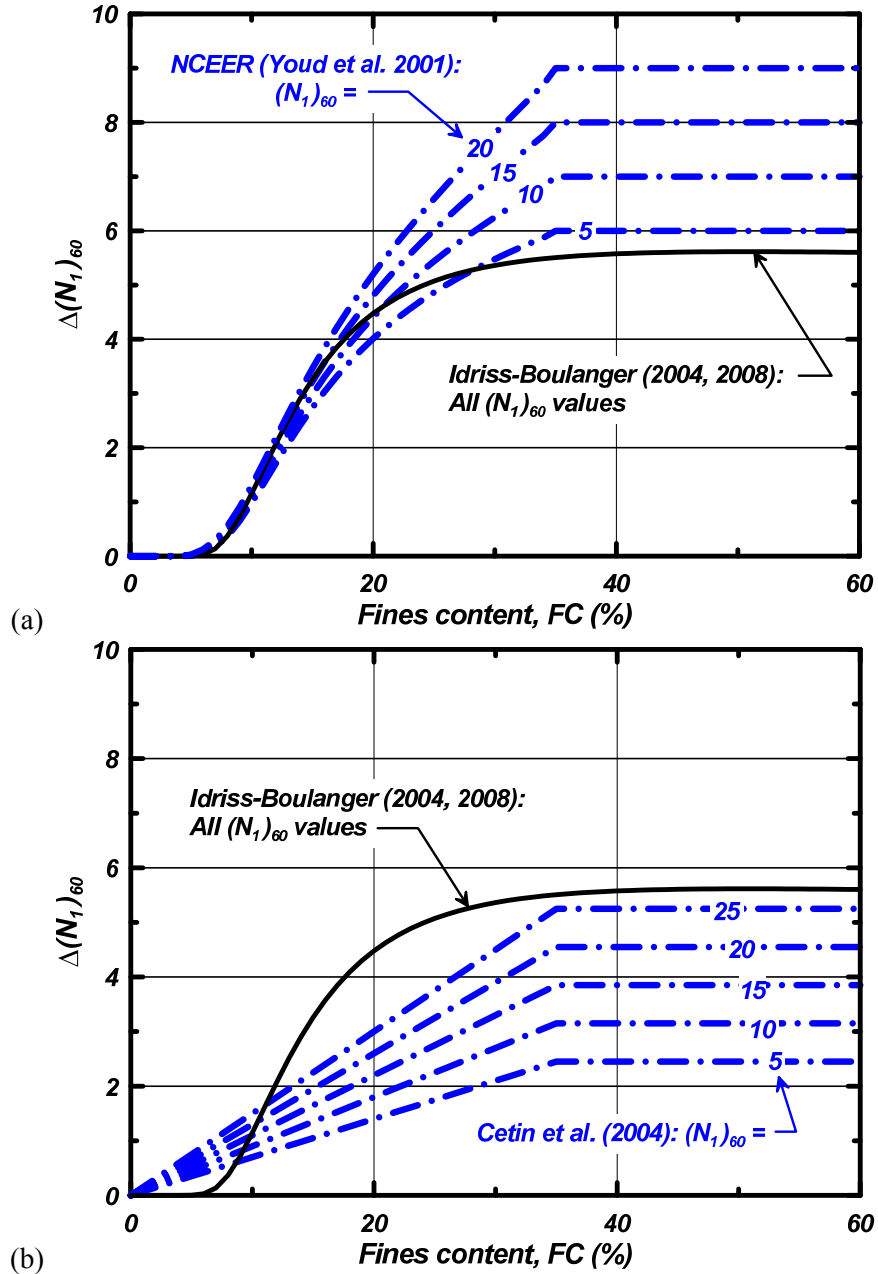


Figure 2.5. Variation of $\Delta(N_1)_{60}$ with fines content

where FC is in percent. The resulting relationships is plotted in Figure 2.5 along with: (a) the equivalent clean sand adjustments recommended in Youd et al. (2001) based on the curves originally published by Seed et al. (1984), and (b) the equivalent clean sand adjustments recommended in Cetin et al. (2004).

The equivalent clean sand adjustment is reexamined in Section 4 using the updated database.

Liquefaction triggering correlation

The correlation between the cyclic resistance ratio (CRR) adjusted to $M = 7.5$ and $\sigma'_v = 1$ atm and the equivalent clean sand $(N_1)_{60cs}$ value for cohesionless soils, as developed by Idriss and Boulanger (2004, 2008), is expressed as,

$$CRR_{M=7.5, \sigma'_v=1atm} = \exp \left(\frac{(N_1)_{60cs}}{14.1} + \left(\frac{(N_1)_{60cs}}{126} \right)^2 - \left(\frac{(N_1)_{60cs}}{23.6} \right)^3 + \left(\frac{(N_1)_{60cs}}{25.4} \right)^4 - 2.8 \right) \quad (2.13)$$

This relationship between $CRR_{M=7.5, \sigma'_v=1}$ and $(N_1)_{60cs}$ was plotted previously in Figure 1.1.

3. CASE HISTORY DATABASE

3.1. Sources of data

The SPT-based case history database used to develop the Idriss and Boulanger (2004, 2008) liquefaction correlation for cohesionless soils is updated in this report, with the following specific goals: (1) incorporating additional data from Japan; (2) incorporating updated estimates of earthquake magnitudes, peak ground accelerations, and other details where improved estimates are available; (3) illustrating details of the selection and computation of SPT $(N_1)_{60cs}$ for a number of representative case histories; and (4) presenting the distributions of the database relative to the various major parameters used in the liquefaction triggering correlation.

Idriss and Boulanger (2004) primarily used cases summarized in the databases compiled by Seed et al. (1984) and Cetin et al. (2000, 2004), except that they excluded the Kobe proprietary cases that were listed in Cetin et al. (2004). Idriss and Boulanger (2004) excluded these proprietary cases because the listing of these case histories in the Cetin et al. (2004) data report contained 21 apparently inconsistent classifications (liquefied/nonliquefied) between the top and bottom of the respective summary pages (see Appendix A for additional discussion). Idriss and Boulanger considered both sets of classifications in their 2004 work, but ultimately omitted the data from their final plots due to concerns over the inconsistency in these Cetin et al. listings and the inability to review the specific details at that time.

Idriss and Boulanger (2004, 2008) also primarily retained the values of critical depth, N_m , σ_v , σ'_v , and the product of the correction factors C_E , C_R , C_B and C_S listed by Seed et al. for the 1984 cases and by Cetin et al. for the 2000 cases. The values for the critical depth, N_m , σ_v , and σ'_v were reevaluated in the current study. The product of the correction factors C_E , C_R , C_B and C_S listed by Seed et al. for the 1984 cases and by Cetin et al. for the 2000 cases were retained in the current study, except as noted otherwise.

The Fear and McRoberts (1995) database was also a helpful reference for many of the case histories.

The updated database described in this report incorporates the 44 Kobe proprietary cases which were provided by Professor Kohji Tokimatsu (2010, personal communication), an additional 26 case histories summarized in Iai et al. (1989), and a small number of other additions. Data from the 1999 Kocaeli and Chi-Chi earthquakes have not yet been incorporated. The total number of case histories in the updated database is 230, of which 115 cases had surface evidence of liquefaction, 112 cases had no surface evidence of liquefaction, and 3 cases were at the margin between liquefaction and no liquefaction.

The individual case histories, processed using the relationships summarized in Section 2, and the key references are summarized in Table 3.1. The following sections describe the selection of earthquake magnitudes, peak accelerations, and representative $(N_1)_{60cs}$ values, discuss the classifications of site performance, and examine the distributions of the case history data.

Table 3.1. Summary of SPT-based liquefaction case history data

Earthquake & site	M	a _{max} (g)	Liq ?	Avg depth (m)	Depth GWT (m)	σ _v (kPa)	σ' _v (kPa)	Avg N _m	(N ₁) ₆₀	C _B	C _E	C _N	C _R	C _S	FC (%)	(N ₁) _{60cs}	r _d	K _σ	MSF	CSR	CSR for M=7.5, σ' _v =1	Primary source of data
<i>1944 M=8.1 Tohankai earthquake - Dec 7</i>																						
Komei	8.1	0.20	Yes	5.2	2.1	98	68	5.9	8.2	1	1.17	1.25	0.95	1	10	9.3	0.98	1.04	0.85	0.182	0.207	Kishida (1969), Seed et al (1984), Cetin et al (2000)
Ienaga	8.1	0.20	Yes	4.3	2.4	80	61	2.3	3.4	1	1.17	1.32	0.95	1	30	8.7	0.99	1.07	0.85	0.144	0.159	Kishida (1969), Seed et al (1984), Cetin et al (2000)
Meiko	8.1	0.20	Yes	3.7	2.1	69	39	1.0	1.7	1	1.17	1.70	0.85	1	27	6.9	0.99	1.08	0.85	0.225	0.245	Kishida (1969), Seed et al (1984), Cetin et al (2000)
<i>1948 M=7.3 Fukui earthquake - June 28</i>																						
Shonenji Temple	7.0	0.40	Yes	4.0	1.2	75	48	8.0	11.8	1	1.17	1.48	0.85	1	0	11.8	0.96	1.07	1.14	0.390	0.318	Kishida (1969), Seed et al (1984), Cetin et al (2000)
Takaya 45	7.0	0.35	Yes	7.5	3.7	141	104	17.3	21.1	1	1.30	0.99	0.95	1	4	21.1	0.90	0.99	1.14	0.283	0.251	Kishida (1969), Seed et al (1984), Cetin et al (2000)
<i>1964 M=7.6 Niigata earthquake - June 16</i>																						
Arayamotomachi	7.6	0.09	Yes	3.3	1.0	63	41	2.6	4.7	1	1.22	1.70	0.85	1	5	4.7	0.98	1.07	0.97	0.089	0.086	Yasuda & Tohno (1988), Cetin et al. (2000)
Cc17-1	7.6	0.16	Yes	7.0	0.9	132	72	8.0	9.9	1	1.09	1.20	0.95	1	2	9.9	0.94	1.03	0.97	0.179	0.178	Kishida (1966), Seed et al (1984), Cetin et al (2000)
Cc17-2	7.6	0.16	Yes	5.3	0.9	85	43	7.9	12.7	1	1.09	1.55	0.95	1	8	13.0	0.96	1.09	0.97	0.199	0.188	Kishida (1966), Seed et al (1984), Cetin et al (2000)
Kawagishi-cho	7.6	0.162	Yes	3.8	2.0	71	53	4.5	6.8	1	1.22	1.45	0.85	1	5	6.8	0.98	1.05	0.97	0.136	0.133	Ishihara & Koga (1981)
Old Town -1	7.6	0.18	No	7.0	1.8	132	81	18.0	22.7	1	1.21	1.10	0.95	1	2	22.7	0.94	1.03	0.97	0.179	0.178	Koizumi (1966), Seed et al (1984), Cetin et al (2000)
Old Town -2	7.6	0.18	No	10.1	1.8	190	109	20.0	23.5	1	1.21	0.97	1.00	1	2	23.5	0.90	0.99	0.97	0.184	0.191	Koizumi (1966), Seed et al (1984), Cetin et al (2000)
Rail Road-1	7.6	0.16	Yes	10.1	0.9	190	100	10.0	11.0	1	1.09	1.01	1.00	1	2	11.0	0.90	1.00	0.97	0.178	0.182	Koizumi (1966), Seed et al (1984), Cetin et al (2000)
Rail Road-2	7.6	0.16	Marginal	10.1	0.9	190	100	16.0	17.5	1	1.09	1.01	1.00	1	2	17.5	0.90	1.00	0.97	0.178	0.182	Koizumi (1966), Seed et al (1984), Cetin et al (2000)
River Site	7.6	0.16	Yes	4.6	0.6	86	47	6.0	9.4	1	1.09	1.52	0.95	1	0	9.4	0.97	1.07	0.97	0.183	0.176	Ishihara (1979), Seed et al (1984), Cetin et al (2000)
Road Site	7.6	0.18	No	6.1	2.4	115	79	12.0	14.1	1	1.09	1.13	0.95	1	0	14.1	0.95	1.03	0.97	0.162	0.162	Ishihara (1979), Seed et al (1984), Cetin et al (2000)
Showa Br 2	7.6	0.16	Yes	4.3	0.0	80	39	4.0	7.0	1	1.09	1.70	0.95	1	10	8.2	0.97	1.08	0.97	0.210	0.199	Takada et al (1965), Seed et al (1984), Cetin et al (2000)
Showa Br 4	7.6	0.18	No	6.1	1.2	115	67	27.0	35.5	1	1.21	1.14	0.95	1	0	35.5	0.95	1.10	0.97	0.191	0.178	Takada et al (1965), Seed et al (1984), Cetin et al (2000)
<i>1968 M=7.5 earthquake - April 1</i>																						
Hososhima	7.5	0.242	No	2.895	2	53	45	8.0	12.1	1	1.22	1.46	0.85	1	36	17.6	0.98	1.10	1.00	0.185	0.168	Iai et al (1989)

Earthquake & site	M	a _{max} (g)	Liq ?	Avg depth (m)	Depth GWT (m)	σ _v (kPa)	σ' _v (kPa)	Avg N _m	(N ₁) ₆₀	C _B	C _E	C _N	C _R	C _S	FC (%)	(N ₁) _{60cs}	r _d	K _σ	MSF	CSR	CSR for M=7.5, σ' _v =1	Primary source of data
<i>1968 M=8.3 Tokachi-Oki earthquake - May 16</i>																						
Aomori Station	8.3	0.213	Yes	5.7	0.0	95	38	9.0	16.5	1	1.22	1.58	0.95	1	3	16.5	0.98	1.10	0.81	0.335	0.376	Yasuda & Tohno (1988), Cetin et al (2000)
Hachinohe -2	8.3	0.23	No	6.1	2.1	115	76	28.0	35.3	1	1.21	1.10	0.95	1	5	35.3	0.98	1.08	0.81	0.221	0.254	Ohsaki (1970), Seed et al. (1984), Cetin et al (2004)
Hachinohe -4	8.3	0.23	No	4.0	0.9	75	45	16.0	23.0	1	1.21	1.40	0.85	1	5	23.0	0.99	1.10	0.81	0.246	0.276	Ohsaki (1970), Seed et al. (1984), Cetin et al (2004)
Hachinohe-6	8.3	0.23	Yes	4.0	0.6	75	42	6.0	9.1	1	1.09	1.63	0.85	1	5	9.1	0.99	1.08	0.81	0.265	0.304	Ohsaki (1970), Seed et al. (1984), Cetin et al (2004)
Nanaehama1-2-3	8.3	0.20	Yes	4.0	0.9	75	45	5.0	7.6	1	1.17	1.52	0.85	1	20	12.0	0.99	1.08	0.81	0.213	0.244	Kishida (1970), Seed et al. (1984), Cetin et al (2004)
<i>1971 M=6.6 San Fernando earthquake - Feb 9</i>																						
Juvenile Hall	6.61	0.45	Yes	6.1	4.6	112	96	3.5	3.9	1	1.13	1.03	0.95	1	55	9.5	0.92	1.01	1.26	0.312	0.246	Bennett (1989), Seed et al (1984), Cetin et al (2000)
Van Norman	6.61	0.45	Yes	6.1	4.6	112	96	7.3	8.1	1	1.13	1.03	0.95	1	50	13.7	0.92	1.01	1.26	0.312	0.245	Bennett (1989), Seed et al (1984), Cetin et al (2000)
<i>1975 M=7.0 Haicheng earthquake - Feb 4</i>																						
Panjin Chemical Fertilizer Plant	7.0	0.20	Yes	8.2	1.5	155	89	9.1	7.6	1	0.83	1.07	0.95	1	67	13.2	0.89	1.01	1.14	0.203	0.175	Shengcong & Tatsuoka (1984), Seed et al (1984), Cetin et al (2000)
Shuang Tai Zi River Sluice Gate	7.0	0.20	No	8.2	1.5	158	92	9.0	8.9	1	1.00	1.05	0.95	1	50	14.6	0.89	1.01	1.14	0.199	0.172	Shengcong & Tatsuoka (1984), Seed et al (1984), Cetin et al (2000)
Ying Kou Glass Fibre Plant	7.0	0.30	Yes	7.8	1.5	147	85	13.0	13.3	1	1.00	1.08	0.95	1	48	19.0	0.90	1.02	1.14	0.304	0.260	Shengcong & Tatsuoka (1984), Seed et al (1984), Cetin et al (2000)
Ying Kou Paper Plant	7.0	0.30	Yes	8.2	1.5	158	92	11.0	11.0	1	1.00	1.05	0.95	1	5	11.0	0.89	1.01	1.14	0.298	0.259	Shengcong & Tatsuoka (1984), Seed et al (1984), Cetin et al (2000)
<i>1976 M=7.5 Guatemala earthquake - Feb 4</i>																						
Amatitlan B-1	7.5	0.135	Yes	10.4	1.5	139	86	6.0	5.0	1	0.75	1.10	1.00	1	3	5.0	0.89	1.01	1.00	0.126	0.125	Seed et al (1979, 1984), Cetin et al (2000)
Amatitlan B-2	7.5	0.135	Marginal	4.6	2.4	55	34	8.0	9.7	1	0.75	1.70	0.95	1	3	9.7	0.97	1.10	1.00	0.138	0.126	Seed et al (1979, 1984), Cetin et al (2000)
Amatitlan B-3&4	7.5	0.135	No	10.7	3.4	137	71	16.0	14.3	1	0.75	1.19	1.00	1	3	14.3	0.89	1.04	1.00	0.149	0.144	Seed et al (1979, 1984), Cetin et al (2000)
<i>1976 M=7.6 Tangshan earthquake - July 27</i>																						
Coastal Region	7.6	0.13	Yes	4.5	1.1	87	54	9.0	11.7	1	1.00	1.37	0.95	1	12	13.8	0.97	1.06	0.97	0.130	0.125	Shengcong & Tatsuoka (1984), Seed et al (1984), Cetin et al (2000)
Le Ting L8-14	7.6	0.20	Yes	4.4	1.5	81	53	9.7	11.5	1	1.00	1.39	0.85	1	12	13.5	0.97	1.07	0.97	0.194	0.186	Shengcong & Tatsuoka (1984), Seed et al (1984), Cetin et al (2000)
Luan Nan-L1	7.6	0.22	No	3.5	1.1	62	38	19.3	24.4	1	1.00	1.49	0.85	1	5	24.4	0.98	1.10	0.97	0.226	0.211	Shengcong & Tatsuoka (1984), Seed et al (1984), Cetin et al (2000)
Luan Nan-L2	7.6	0.22	Yes	3.5	1.1	56	32	5.9	8.5	1	1.00	1.70	0.85	1	3	8.5	0.98	1.10	0.97	0.241	0.225	Shengcong & Tatsuoka (1984), Seed et al (1984), Cetin et al (2000)
Qing Jia Ying	7.6	0.35	Yes	5.3	0.9	102	59	17.0	20.1	1	1.00	1.24	0.95	1	20	24.6	0.96	1.09	0.97	0.378	0.357	Shengcong & Tatsuoka (1984), Seed et al (1984), Cetin et al (2000)
Tangshan City	7.6	0.50	No	5.3	3.1	98	75	30.0	31.6	1	1.00	1.11	0.95	1	10	32.7	0.96	1.07	0.97	0.405	0.389	Shengcong & Tatsuoka (1984), Seed et al (1984), Cetin et al (2000)

Earthquake & site	M	a _{max} (g)	Liq ?	Avg depth (m)	Depth GWT (m)	σ_v (kPa)	σ'_v (kPa)	Avg N _m	(N ₁) ₆₀	C _B	C _E	C _N	C _R	C _S	FC (%)	(N ₁) _{60cs}	r _d	K _{σ}	MSF	CSR	CSR for M=7.5, $\sigma'_v=1$	Primary source of data
Yao Yuan Village	7.6	0.20	Yes	6.1	0.9	118	67	9.0	10.5	1	1.00	1.22	0.95	1	20	15.0	0.95	1.05	0.97	0.218	0.214	Shengcong & Tatsuoka (1984), Seed et al (1984), Cetin et al (2000)
<i>1977 M=7.4 Argentina earthquake - Nov 23</i>																						
San Juan B-1	7.5	0.20	Yes	8.2	4.6	142	106	9.0	6.3	1	0.75	0.97	0.95	1	20	10.7	0.92	1.00	1.00	0.160	0.161	Idriss et al (1979), Seed et al (1984), Cetin et al (2000)
San Juan B-3	7.5	0.20	Yes	11.1	6.7	199	156	13.0	7.6	1	0.75	0.78	1.00	1	5	7.6	0.87	1.00	1.00	0.169	0.169	Idriss et al (1979), Seed et al (1984), Cetin et al (2000)
San Juan B-4	7.5	0.20	No	3.7	1.2	63	39	14.0	14.3	1	0.75	1.60	0.85	1	4	14.3	0.98	1.10	1.00	0.204	0.186	Idriss et al (1979), Seed et al (1984), Cetin et al (2000)
San Juan B-5	7.5	0.20	No	3.1	2.1	53	44	14.0	13.6	1	0.75	1.53	0.85	1	3	13.6	0.98	1.09	1.00	0.154	0.142	Idriss et al (1979), Seed et al (1984), Cetin et al (2000)
San Juan B-6	7.5	0.20	Yes	5.2	1.8	90	56	6.0	5.8	1	0.75	1.36	0.95	1	50	11.4	0.96	1.06	1.00	0.198	0.187	Idriss et al (1979), Seed et al (1984), Cetin et al (2000)
<i>1978 M=6.5 Miyagiken-Oki earthquake - Feb 20</i>																						
Arahama (A-9)	6.5	0.10	No	6.4	0.9	121	67	10.0	12.8	1	1.09	1.23	0.95	1	0	12.8	0.90	1.04	1.34	0.105	0.076	Tohno & Yasuda (1981), Seed et al (1984), Cetin et al (2000)
Hiyori-18 (site C)	6.5	0.14	No	5.2	2.4	98	71	9.0	11.1	1	1.09	1.19	0.95	1	20	15.5	0.93	1.04	1.34	0.116	0.084	Tsuchida et al (1980), Seed et al (1984), Cetin et al (2000)
Ishinomaki-2	6.5	0.12	No	3.5	1.4	66	45	3.7	5.5	1	1.09	1.61	0.85	1	10	6.7	0.96	1.07	1.34	0.109	0.076	Ishihara et al (1980), Seed et al (1984), Cetin et al (2000)
Kitawabuchi-2	6.5	0.14	No	3.4	3.1	62	59	11.0	12.3	1	1.00	1.32	0.85	1	5	12.3	0.96	1.05	1.34	0.092	0.065	Iwasaki et al (1981), Seed et al (1984), Cetin et al (2000)
Nakajima-18 (Site A)	6.5	0.14	No	6.1	2.4	115	79	12.0	14.1	1	1.09	1.13	0.95	1	3	14.1	0.91	1.03	1.34	0.120	0.088	Tsuchida et al (1979, 1980), Tohno & Yasuda (1981), Seed et al (1984), Cetin et al (2000)
Nakamura Dyke N-4	6.5	0.12	Yes	2.8	0.5	53	30	4.7	6.9	1	1.00	1.70	0.85	1	5	6.9	0.97	1.10	1.34	0.128	0.087	Iwasaki & Tokida (1980), Tohno & Yasuda (1981), Seed et al (1984), Cetin et al (2000)
Nakamura Dyke N-5	6.5	0.12	No	3.4	1.3	63	42	7.0	9.6	1	1.00	1.61	0.85	1	4	9.6	0.96	1.08	1.34	0.112	0.078	Iwasaki & Tokida (1980), Tohno & Yasuda (1981), Seed et al (1984), Cetin et al (2000)
Oiiri-1	6.5	0.14	No	6.4	4.3	106	85	9.0	9.4	1	1.00	1.10	0.95	1	5	9.4	0.90	1.02	1.34	0.102	0.075	Iwasaki et al (1978), Tohno & Yasuda (1981), Seed et al (1984), Cetin et al (2000)
Shiomi-6 (Site D)	6.5	0.14	No	4.0	2.4	75	60	6.0	7.5	1	1.09	1.34	0.85	1	10	8.6	0.95	1.05	1.34	0.108	0.077	Tsuchida et al (1979, 1980), Tohno & Yasuda (1981), Tokimatsu (1983), Seed et al (1984), Cetin et al (2000)
Yuriage Br-1	6.5	0.12	No	4.3	1.8	80	56	4.0	5.4	1	1.00	1.41	0.95	1	10	6.5	0.94	1.05	1.34	0.105	0.075	Iwasaki et al (1978), Tohno & Yasuda (1981), Seed et al (1984), Cetin et al (2000)
Yuriage Br-2	6.5	0.12	No	2.5	1.2	46	34	10.1	16.2	1	1.12	1.68	0.85	1	7	16.3	0.96	1.10	1.34	0.112	0.076	Iwasaki et al (1978), Tohno & Yasuda (1981), Seed et al (1984), Cetin et al (2000)
Yuriage Br-3	6.5	0.12	No	4.3	0.3	80	42	8.0	11.8	1	1.00	1.56	0.95	1	12	13.9	0.94	1.09	1.34	0.142	0.097	Iwasaki et al (1986), Tohno & Yasuda (1981), Seed et al (1984), Cetin et al (2000)

Earthquake & site	M	a _{max} (g)	Liq ?	Avg depth (m)	Depth GWT (m)	σ_v (kPa)	σ'_v (kPa)	Avg N _m	(N ₁) ₆₀	C _B	C _E	C _N	C _R	C _S	FC (%)	(N ₁) _{60cs}	r _d	K _{σ}	MSF	CSR	CSR for M=7.5, $\sigma'_v=1$	Primary source of data
Yuriagekami-1	6.5	0.12	No	5.5	1.8	99	63	2.0	2.5	1	1.00	1.31	0.95	1	60	8.1	0.92	1.04	1.34	0.113	0.081	Iwasaki et al (1984), Tohno & Yasuda (1981), Seed et al (1984), Cetin et al (2000)
Yuriagekami-2	6.5	0.12	No	4.3	0.9	80	47	11.0	15.1	1	1.00	1.45	0.95	1	0	15.1	0.94	1.08	1.34	0.125	0.086	Iwasaki et al (1984), Tohno & Yasuda (1981), Seed et al (1984), Cetin et al (2000)
<i>1978 M=7.7 Miyagiken-Oki earthquake - June 12</i>																						
Arahama (A-9)	7.7	0.20	Yes	6.4	0.9	121	67	10.0	12.8	1	1.09	1.23	0.95	1	0	12.8	0.95	1.04	0.95	0.223	0.225	Tohno & Yasuda (1981), Seed et al (1984), Cetin et al (2000)
Hiyori-18 (site C)	7.7	0.24	Yes	5.2	2.4	98	71	9.0	11.1	1	1.09	1.19	0.95	1	20	15.5	0.96	1.04	0.95	0.207	0.210	Tsuchida et al (1979, 1980), Seed et al (1984), Cetin et al (2000)
Ishinomaki-2	7.7	0.20	Yes	3.5	1.4	66	45	3.7	5.5	1	1.09	1.61	0.85	1	10	6.7	0.98	1.07	0.95	0.186	0.184	Ishihara et al (1980), Seed et al (1984), Cetin et al (2000)
Ishinomaki-4	7.7	0.20	No	4.5	1.4	87	57	14.2	20.9	1	1.21	1.28	0.95	1	10	22.0	0.97	1.08	0.95	0.188	0.183	Ishihara et al (1980), Seed et al (1984), Cetin et al (2000)
Kitawabuchi-2	7.7	0.28	Yes	3.4	3.1	62	59	11.0	12.3	1	1.00	1.32	0.85	1	5	12.3	0.98	1.05	0.95	0.187	0.187	Iwasaki et al (1981), Tohno & Yasuda (1981), Seed et al (1984), Cetin et al (2000)
Kitawabuchi-3	7.7	0.28	No	4.8	3.1	90	73	13.2	17.6	1	1.21	1.16	0.95	1	0	17.6	0.97	1.04	0.95	0.216	0.220	Iwasaki et al (1981), Tohno & Yasuda (1981), Seed et al (1984), Cetin et al (2000)
Nakajima 2	7.7	0.24	No	4.6	2.4	86	65	10.0	12.7	1	1.09	1.23	0.95	1	26	17.8	0.97	1.05	0.95	0.200	0.200	Tsuchida et al (1979, 1980), Tohno & Yasuda (1981), Seed et al (1984), Cetin et al (2000)
Nakajima-18 (Site A)	7.7	0.24	Yes	6.1	2.4	115	79	12.0	14.1	1	1.09	1.13	0.95	1	3	14.1	0.96	1.03	0.95	0.217	0.223	Tsuchida et al (1979, 1980), Seed et al (1984), Cetin et al (2000)
Nakamura Dyke N-1	7.7	0.32	No	3.4	0.9	63	39	19.0	26.2	1	1.12	1.45	0.85	1	4	26.2	0.98	1.10	0.95	0.329	0.315	Iwasaki & Tokida (1980), Tohno & Yasuda (1981), Seed et al (1984), Cetin et al (2000)
Nakamura Dyke N-4	7.7	0.32	Yes	2.8	0.5	53	30	4.7	6.9	1	1.00	1.70	0.85	1	5	6.9	0.99	1.10	0.95	0.346	0.332	Iwasaki (1986), Tohno & Yasuda (1981), Seed et al (1984), Cetin et al (2000)
Nakamura Dyke N-5	7.7	0.32	Yes	3.4	1.3	63	42	7.0	9.6	1	1.00	1.61	0.85	1	4	9.6	0.98	1.08	0.95	0.306	0.299	Iwasaki (1986), Tohno & Yasuda (1981), Seed et al (1984), Cetin et al (2000)
Oiiri-1	7.7	0.24	Yes	6.4	4.3	106	85	9.0	9.4	1	1.00	1.10	0.95	1	5	9.4	0.95	1.02	0.95	0.185	0.192	Iwasaki et al (1978), Tohno & Yasuda (1981), Seed et al (1984), Cetin et al (2000)
Shiomi-6 (Site D)	7.7	0.24	Yes	4.0	2.4	75	60	6.0	7.5	1	1.09	1.34	0.85	1	10	8.6	0.98	1.05	0.95	0.190	0.192	Tsuchida et al (1979, 1980), Tohno & Yasuda (1981), Tokimatsu (1983), Seed et al (1984), Cetin et al (2000)
Yuriage Br-1	7.7	0.24	Yes	4.3	1.8	80	56	4.0	5.4	1	1.00	1.41	0.95	1	10	6.5	0.97	1.05	0.95	0.216	0.218	Iwasaki et al (1978), Tohno & Yasuda (1981), Seed et al (1984), Cetin et al (2000)
Yuriage Br-2	7.7	0.24	Yes	2.5	1.2	46	34	10.1	16.2	1	1.12	1.68	0.85	1	7	16.3	0.99	1.10	0.95	0.212	0.203	Iwasaki et al (1978), Tohno & Yasuda (1981), Seed et al (1984), Cetin et al (2000)

Earthquake & site	M	a _{max} (g)	Liq ?	Avg depth (m)	Depth GWT (m)	σ_v (kPa)	σ'_v (kPa)	Avg N _m	(N ₁) ₆₀	C _B	C _E	C _N	C _R	C _S	FC (%)	(N ₁) _{60cs}	r _d	K _{σ}	MSF	CSR	CSR for M=7.5, $\sigma'_v=1$	Primary source of data
Yuriage Br-3	7.7	0.24	Yes	4.3	0.3	80	42	8.0	11.8	1	1.00	1.56	0.95	1	12	13.9	0.97	1.09	0.95	0.293	0.282	Iwasaki et al (1986), Tohno & Yasuda (1981), Seed et al (1984), Cetin et al (2000)
Yuriage Br-5	7.7	0.24	No	7.3	1.2	138	78	17.0	20.1	1	1.12	1.11	0.95	1	17	24.0	0.94	1.04	0.95	0.260	0.263	Iwasaki et al (1986), Tohno & Yasuda (1981), Seed et al (1984), Cetin et al (2000)
Yuriagekami-1	7.7	0.24	Yes	5.5	1.8	99	63	2.0	2.5	1	1.00	1.31	0.95	1	60	8.1	0.96	1.04	0.95	0.236	0.239	Iwasaki & Tokida (1980), Iwasaki et al (1984), Tohno & Yasuda (1981), Seed et al (1984), Cetin et al (2000)
Yuriagekami-2	7.7	0.24	Yes	4.3	0.9	80	47	11.0	15.1	1	1.00	1.45	0.95	1	0	15.1	0.97	1.08	0.95	0.258	0.251	Iwasaki & Tokida (1980), Iwasaki et al (1984), Tohno & Yasuda (1981), Seed et al (1984), Cetin et al (2000)
Yuriagekami-3	7.7	0.24	No	5.5	2.1	103	70	20.0	24.6	1	1.12	1.16	0.95	1	0	24.6	0.96	1.06	0.95	0.220	0.220	Iwasaki & Tokida (1980), Iwasaki et al (1984), Tohno & Yasuda (1981), Seed et al (1984), Cetin et al (2000)
<i>1979 ML=6.5 Imperial Valley earthquake - Oct 15</i>																						
Heber Road A1	6.53	0.78	No	2.9	1.8	53	42	30.4	37.8	1	1.13	1.30	0.85	1	12	40.0	0.97	1.10	1.29	0.620	0.437	Bennett et al (1981), Youd & Bennett (1983), Seed et al (1984), Cetin et al (2000)
Heber Road A2	6.53	0.78	Yes	3.7	1.8	68	50	2.0	2.9	1	1.13	1.51	0.85	1	18	7.0	0.96	1.06	1.29	0.661	0.484	Bennett et al (1981), Youd & Bennett (1983), Seed et al (1984), Cetin et al (2000)
Heber Road A3	6.53	0.78	No	4.0	1.8	79	56	13.0	16.2	1	1.13	1.29	0.85	1	25	21.2	0.95	1.08	1.29	0.690	0.493	Bennett et al (1981), Youd & Bennett (1983), Seed et al (1984), Cetin et al (2000)
Kornbloom B	6.53	0.13	No	4.3	2.7	77	62	5.0	6.2	1	1.13	1.29	0.85	1	92	11.7	0.95	1.05	1.29	0.099	0.073	Bennett et al (1984), Seed et al (1984), Cetin et al (2000)
McKim Ranch A	6.53	0.51	Yes	2.1	1.5	38	32	3.0	4.6	1	1.13	1.70	0.80	1	31	10.0	0.98	1.10	1.29	0.385	0.271	Bennett et al (1984), Seed et al (1984), Cetin et al (2000)
Radio Tower B1	6.53	0.20	Yes	3.4	2.1	62	50	2.0	2.9	1	1.13	1.49	0.85	1	64	8.5	0.96	1.06	1.29	0.154	0.112	Bennett et al (1984), Seed et al (1984), Cetin et al (2000)
Radio Tower B2	6.53	0.20	No	2.3	2.1	40	38	11.0	15.2	1	1.13	1.53	0.80	1	30	20.6	0.98	1.10	1.29	0.132	0.093	Bennett et al (1984), Seed et al (1984), Cetin et al (2000)
River Park A	6.53	0.24	Yes	1.8	0.3	35	20	3.0	4.6	1	1.13	1.70	0.80	1	80	10.2	0.98	1.10	1.29	0.266	0.187	Bennett et al (1981), Youd & Bennett (1983), Seed et al (1984), Cetin et al (2000)
Wildlife B	6.53	0.17	No	4.6	1.2	87	54	7.1	10.3	1	1.13	1.36	0.95	1	30	15.7	0.94	1.07	1.29	0.178	0.129	Youd & Bennett (1983), Bennett et al (1984), Seed et al (1984), Cetin et al (2000)
<i>1980 M=6.0 Mid-Chiba earthquake - Sept 24 (UTC)</i>																						
Owi-1	6.0	0.095	No	6.1	0.9	108	57	5.0	7.1	1	1.09	1.36	0.95	1	13	9.6	0.89	1.05	1.48	0.104	0.067	Ishihara et al (1981), Seed et al (1984), Cetin et al (2000)
Owi-2	6.0	0.095	No	14.3	0.9	254	123	4.0	3.9	1	1.09	0.90	1.00	1	27	9.1	0.69	0.98	1.48	0.089	0.061	Ishihara et al (1981), Seed et al (1984), Cetin et al (2000)

Earthquake & site	M	a _{max} (g)	Liq ?	Avg depth (m)	Depth GWT (m)	σ_v (kPa)	σ'_v (kPa)	Avg N _m	(N ₁) ₆₀	C _B	C _E	C _N	C _R	C _S	FC (%)	(N ₁) _{60cs}	r _d	K _{σ}	MSF	CSR	CSR for M=7.5, $\sigma'_v=1$	Primary source of data
<i>1981 M=5.9 WestMorland earthquake - April 26</i>																						
Kornbloom B	5.9	0.32	Yes	4.3	2.7	77	62	5.0	6.2	1	1.13	1.29	0.85	1	92	11.7	0.93	1.05	1.52	0.240	0.151	Bennett et al (1984), Seed et al (1984), Cetin et al (2000)
McKim Ranch A	5.9	0.09	No	2.1	1.5	38	32	3.0	4.6	1	1.13	1.70	0.80	1	31	10.0	0.97	1.10	1.52	0.068	0.040	Bennett et al (1984), Seed et al (1984), Cetin et al (2000)
Radio Tower B1	5.9	0.20	Yes	3.4	2.1	62	50	2.0	2.9	1	1.13	1.49	0.85	1	64	8.5	0.95	1.06	1.52	0.152	0.094	Bennett et al (1984), Seed et al (1984), Cetin et al (2000)
Radio Tower B2	5.9	0.20	No	2.3	2.1	40	38	11.0	15.2	1	1.13	1.53	0.80	1	30	20.6	0.97	1.10	1.52	0.131	0.078	Bennett et al (1984), Seed et al (1984), Cetin et al (2000)
River Park A	5.9	0.21	No	1.8	0.3	35	20	3.0	4.6	1	1.13	1.70	0.80	1	80	10.2	0.98	1.10	1.52	0.231	0.138	Bennett et al (1981), Youd & Bennett (1983), Seed et al (1984), Cetin et al (2000)
River Park C	5.9	0.21	No	4.3	0.3	83	45	11.0	15.2	1	1.13	1.44	0.85	1	18	19.3	0.93	1.10	1.52	0.237	0.142	Bennett et al (1981), Youd & Bennett (1983), Seed et al (1984), Cetin et al (2000)
Wildlife B	5.9	0.26	Yes	4.6	1.2	87	54	7.1	10.3	1	1.13	1.36	0.95	1	30	15.7	0.92	1.07	1.52	0.267	0.164	Youd & Bennett (1983), Bennett et al (1984), Seed et al (1984), Cetin et al (2000)
<i>1982 M=6.9 Urakawa-Oki earthquake - Mar 21</i>																						
Tokachi	6.90	0.168	No	2.4	1.6	42	35	10.0	17.0	1	1.22	1.64	0.85	1	5	17.0	0.98	1.10	1.17	0.129	0.100	Iai et al (1989)
<i>1983 M=6.8 Nihonkai-Chubu earthquake - June 21</i>																						
Arayamotomachi	6.8	0.15	No	4.3	1.0	69	37	2.6	5.1	1	1.22	1.70	0.95	1	5	5.1	0.95	1.08	1.20	0.172	0.133	Yasuda & Tohno (1988), Cetin et al (2000)
Arayamotomachi Coarse Sand	6.8	0.15	No	9.2	1.0	158	77	13.1	18.1	1	1.22	1.13	1.00	1	0	18.1	0.86	1.03	1.20	0.172	0.139	Yasuda & Tohno (1988), Cetin et al (2000)
Takeda Elementary Sch.	6.8	0.111	Yes	4.3	0.35	81	42	7.4	13.3	1	1.22	1.56	0.95	1	0	13.3	0.95	1.09	1.20	0.132	0.101	Yasuda & Tohno (1988), Cetin et al (2000)
<i>1983 M=7.7 Nihonkai-Chubu earthquake - May 26</i>																						
Aomori Station	7.7	0.116	Yes	5.7	0.0	95	38	9.0	16.5	1	1.22	1.58	0.95	1	3	16.5	0.96	1.10	0.95	0.178	0.171	Yasuda & Tohno (1988), Cetin et al (2000)
Arayamotomachi	7.7	0.20	Yes	4.3	1.0	69	37	2.6	5.1	1	1.22	1.70	0.95	1	5	5.1	0.97	1.08	0.95	0.234	0.230	Yasuda & Tohno (1988), Cetin et al (2000)
Gaiko Wharf B-2	7.7	0.227	Yes	7.5	0.4	123	53	7.7	12.4	1	1.22	1.39	0.95	1	1	12.4	0.94	1.06	0.95	0.320	0.317	Hamada (1992), Cetin et al (2000)
Noshiro Section N-7	7.7	0.25	yes	3.5	1.7	55	38	9.8	16.2	1	1.22	1.60	0.85	1	1	16.2	0.98	1.10	0.95	0.232	0.222	Hamada (1992), Cetin et al (2000)
Takeda Elementary Sch.	7.7	0.283	Yes	4.3	0.4	81	42	7.4	13.3	1	1.22	1.56	0.95	1	0	13.3	0.97	1.10	0.95	0.397	0.381	Yasuda & Tohno (1988), Cetin et al (2000)
Akita station (1)	7.7	0.205	No	2.865	1.75	52	41	12.0	18.7	1	1.22	1.50	0.85	1	3	18.7	0.99	1.10	0.95	0.166	0.159	Iai et al (1989)
Akita station (2)	7.7	0.205	No	2.895	1.75	53	41	8.5	13.8	1	1.22	1.56	0.85	1	3	13.8	0.99	1.09	0.95	0.167	0.161	Iai et al (1989)
Aomori Port	7.7	0.116	No	3.338	1.14	63	41	8.0	13.1	1	1.22	1.58	0.85	1	5	13.1	0.98	1.09	0.95	0.113	0.109	Iai et al (1989)
Gaiko 1	7.7	0.205	Yes	6.9125	1.5	132	79	6.6	8.7	1	1.22	1.15	0.95	1	3	8.7	0.95	1.02	0.95	0.211	0.218	Iai et al (1989)

Earthquake & site	M	a _{max} (g)	Liq ?	Avg depth (m)	Depth GWT (m)	σ _v (kPa)	σ' _v (kPa)	Avg N _m	(N ₁) ₆₀	C _B	C _E	C _N	C _R	C _S	FC (%)	(N ₁) _{60cs}	r _d	K _σ	MSF	CSR	CSR for M=7.5, σ' _v =1	Primary source of data
Gaiko 2	7.7	0.205	Yes	9.7986	1.47	189	107	5.9	6.9	1	1.22	0.97	1.00	1	4	6.9	0.91	1.00	0.95	0.214	0.227	Iai et al (1989)
Hakodate	7.7	0.052	No	4.295	1.6	81	54	2.6	4.2	1	1.22	1.41	0.95	1	66	9.8	0.97	1.06	0.95	0.049	0.049	Iai et al (1989)
Nakajima No. 1 (5)	7.7	0.205	Yes	6.47	1.46	124	74	7.3	9.9	1	1.22	1.18	0.95	1	8	10.4	0.95	1.03	0.95	0.210	0.216	Iai et al (1989)
Nakajima No. 2 (1)	7.7	0.205	Yes	7.1314	1.45	136	81	10.4	13.5	1	1.22	1.12	0.95	1	3	13.5	0.94	1.02	0.95	0.213	0.219	Iai et al (1989)
Nakajima No. 2 (2)	7.7	0.205	Yes	3.7825	1.5	71	48	6.0	9.3	1	1.22	1.50	0.85	1	7	9.4	0.98	1.07	0.95	0.191	0.189	Iai et al (1989)
Nakajima No. 3(3)	7.7	0.205	Yes	6.0356	1.58	115	71	7.3	10.2	1	1.22	1.21	0.95	1	2	10.2	0.96	1.03	0.95	0.205	0.210	Iai et al (1989)
Nakajima No. 3(4)	7.7	0.205	Yes	5.7443	1.51	109	68	8.0	11.5	1	1.22	1.24	0.95	1	2	11.5	0.96	1.04	0.95	0.206	0.209	Iai et al (1989)
Ohama No. 1(1)	7.7	0.205	No	3.905	1.2	74	47	13.0	18.9	1	1.22	1.41	0.85	1	3	18.9	0.98	1.10	0.95	0.203	0.195	Iai et al (1989)
Ohama No. 1(2)	7.7	0.205	No	3.42	1.2	64	42	15.9	23.5	1	1.22	1.43	0.85	1	2	23.5	0.98	1.10	0.95	0.198	0.190	Iai et al (1989)
Ohama No. 1(3)	7.7	0.205	No	2.5833	1.2	48	34	14.1	23.0	1	1.22	1.57	0.85	1	1	23.0	0.99	1.10	0.95	0.184	0.176	Iai et al (1989)
Ohama No. 1(4)	7.7	0.205	No	5.1767	1.2	99	60	25.0	34.6	1	1.22	1.19	0.95	1	3	34.6	0.96	1.10	0.95	0.213	0.204	Iai et al (1989)
Ohama No. 1(5)	7.7	0.205	No	2.2167	1.2	41	31	24.7	37.3	1	1.22	1.46	0.85	1	1	37.3	0.99	1.10	0.95	0.175	0.168	Iai et al (1989)
Ohama No. 1(58-22)	7.7	0.205	No	4.48	1.2	85	53	13.2	20.3	1	1.22	1.33	0.95	1	2	20.3	0.97	1.09	0.95	0.208	0.202	Iai et al (1989)
Ohama No. 2 (2)	7.7	0.205	Yes	5.21	0.72	100	56	3.3	5.4	1	1.22	1.43	0.95	1	2	5.4	0.96	1.05	0.95	0.229	0.231	Iai et al (1989)
Ohama No. 3 (1)	7.7	0.205	Yes	5.41	1.37	103	63	4.8	7.4	1	1.22	1.31	0.95	1	2	7.4	0.96	1.04	0.95	0.209	0.212	Iai et al (1989)
Ohama No. 3 (3)	7.7	0.205	Yes	5.48	1.35	104	64	3.7	5.6	1	1.22	1.32	0.95	1	2	5.6	0.96	1.04	0.95	0.210	0.213	Iai et al (1989)
Ohama No. 3 (4)	7.7	0.205	Yes	3.91	1.46	73	49	5.2	8.1	1	1.22	1.50	0.85	1	2	8.1	0.98	1.06	0.95	0.194	0.192	Iai et al (1989)
Ohama No. Rvt (1)	7.7	0.205	No	4.5425	1.45	86	55	15.8	23.5	1	1.22	1.28	0.95	1	2	23.5	0.97	1.09	0.95	0.200	0.193	Iai et al (1989)
Ohama No. Rvt (2)	7.7	0.205	No	6.67	1.6	127	77	17.3	22.5	1	1.22	1.12	0.95	1	4	22.5	0.95	1.04	0.95	0.208	0.211	Iai et al (1989)
Ohama No. Rvt (3)	7.7	0.205	No	3.5667	1.45	67	46	18.3	25.9	1	1.22	1.37	0.85	1	0	25.9	0.98	1.10	0.95	0.190	0.182	Iai et al (1989)
<i>1984 M=6.9 earthquake - Aug 7</i>																						
Hososhima	6.9	0.268	No	2.895	2	53	45	8.0	12.1	1	1.22	1.46	0.85	1	36	17.6	0.97	1.10	1.17	0.203	0.158	Iai et al (1989)

Earthquake & site	M	a _{max} (g)	Liq ?	Avg depth (m)	Depth GWT (m)	σ _v (kPa)	σ' _v (kPa)	Avg N _m	(N ₁) ₆₀	C _B	C _E	C _N	C _R	C _S	FC (%)	(N ₁) _{60cs}	r _d	K _σ	MSF	CSR	CSR for M=7.5, σ' _v =1	Primary source of data
<i>1987 M=6.2 and M=6.5 Superstition Hills earthquakes - 01 & 02 - Nov 24</i>																						
Radio Tower B1	6.22	0.09	No	3.4	2.1	62	50	2.0	2.9	1	1.13	1.49	0.85	1	64	8.5	0.96	1.06	1.40	0.069	0.046	Seed et al (1984)
Wildlife B	6.22	0.133	No	4.6	1.2	87	54	7.1	10.3	1	1.13	1.36	0.95	1	30	15.7	0.93	1.07	1.40	0.138	0.092	Seed et al (1984)
Heber Road A1	6.54	0.156	No	2.9	1.8	53	42	30.4	37.8	1	1.13	1.30	0.85	1	12	40.0	0.97	1.10	1.29	0.124	0.088	Bennett et al (1981), Youd & Bennett (1983), Seed et al (1984), Cetin et al (2000)
Heber Road A2	6.54	0.15	No	3.7	1.8	68	50	2.0	2.9	1	1.13	1.51	0.85	1	18	7.0	0.96	1.06	1.29	0.127	0.093	Bennett et al (1981), Youd & Bennett (1983), Seed et al (1984), Cetin et al (2000)
Heber Road A3	6.54	0.13	No	4.0	1.8	79	56	13.0	16.2	1	1.13	1.29	0.85	1	25	21.2	0.95	1.08	1.29	0.115	0.082	Bennett et al (1981), Youd & Bennett (1983), Seed et al (1984), Cetin et al (2000)
Kornbloom B	6.54	0.174	No	4.3	2.7	77	62	5.0	6.2	1	1.13	1.29	0.85	1	92	11.7	0.95	1.05	1.29	0.132	0.098	Bennett et al (1984), Seed et al (1984), Cetin et al (2000)
McKim Ranch A	6.54	0.16	No	2.1	1.5	38	32	3.0	4.6	1	1.13	1.70	0.80	1	31	10.0	0.98	1.10	1.29	0.121	0.085	Bennett et al (1984), Seed et al (1984), Cetin et al (2000)
Radio Tower B1	6.54	0.20	No	3.4	2.1	62	50	2.0	2.9	1	1.13	1.49	0.85	1	64	8.5	0.96	1.06	1.29	0.154	0.113	Bennett et al (1984), Seed et al (1984), Cetin et al (2000)
Radio Tower B2	6.54	0.18	No	2.3	2.1	40	38	11.0	15.2	1	1.13	1.53	0.80	1	30	20.6	0.98	1.10	1.29	0.119	0.084	Bennett et al (1984), Seed et al (1984), Cetin et al (2000)
River Park A	6.54	0.19	No	1.8	0.3	35	20	3.0	4.6	1	1.13	1.70	0.80	1	80	10.2	0.98	1.10	1.29	0.210	0.149	Youd & Bennett (1983), Seed et al (1984), Cetin et al (2000)
River Park C	6.54	0.19	No	4.3	0.3	83	45	11.0	15.2	1	1.13	1.44	0.85	1	18	19.3	0.95	1.10	1.29	0.218	0.154	Youd & Bennett (1983), Seed et al (1984), Cetin et al (2000)
Wildlife B	6.54	0.206	Yes	4.6	1.2	87	54	7.1	10.3	1	1.13	1.36	0.95	1	30	15.7	0.94	1.07	1.29	0.216	0.157	Youd & Bennett (1983), Seed et al (1984), Cetin et al (2000), Bennett (2010 p.c.)
<i>1989 M=6.9 Loma Prieta earthquake - Oct 18</i>																						
Alameda Bay Farm Dike	6.93	0.24	No	6.5	3.0	125	91	37.0	43.3	1	0.92	1.03	0.95	1.3	7	43.4	0.92	1.03	1.16	0.198	0.165	Cetin et al (2000)
Farris Farm	6.93	0.37	Yes	6.0	4.5	106	92	9.0	10.2	1	1.13	1.05	0.95	1	8	10.6	0.93	1.01	1.16	0.259	0.221	Cetin et al (2000)
General Fish	6.93	0.28	No	2.5	1.4	45	35	16.9	21.4	1	1.00	1.58	0.80	1	5	21.4	0.98	1.10	1.16	0.232	0.182	Boulanger et al (1995, 1997)
Hall Avenue	6.93	0.14	No	4.6	3.5	75	64	4.6	5.7	1	0.92	1.28	0.95	1.1	30	11.0	0.95	1.04	1.16	0.102	0.084	Cetin et al (2000)
Marine Laboratory B1	6.93	0.28	Yes	4.6	2.4	87	65	11.0	13.1	1	1.00	1.25	0.95	1	3	13.1	0.95	1.05	1.16	0.230	0.189	Boulanger et al (1995, 1997), Cetin et al (2000)
Marine Laboratory B2	6.93	0.28	Yes	3.5	2.5	65	55	13.0	14.9	1	1.00	1.35	0.85	1	3	14.9	0.97	1.07	1.16	0.207	0.167	Boulanger et al (1995, 1997), Cetin et al (2000)
Marine Laboratory UCB-6-12 & F1-F6	6.93	0.28	Yes	5.3	1.5	102	64	12.0	17.6	1	1.25	1.23	0.95	1	3	17.6	0.94	1.06	1.16	0.270	0.220	Boulanger et al (1995, 1997)
MBARI No. 3: EB-1	6.93	0.28	No	2.0	2.0	35	35	18.0	22.6	1	1.00	1.57	0.80	1	1	22.6	0.99	1.10	1.16	0.179	0.140	Boulanger et al (1995, 1997), Cetin et al (2000)
MBARI No. 3: EB-5	6.93	0.28	No	3.4	1.8	63	47	12.0	14.9	1	1.00	1.46	0.85	1	1	14.9	0.97	1.09	1.16	0.235	0.187	Boulanger et al (1995, 1997), Cetin et al (2000)

Earthquake & site	M	a _{max} (g)	Liq ?	Avg depth (m)	Depth GWT (m)	σ _v (kPa)	σ' _v (kPa)	Avg N _m	(N ₁) ₆₀	C _B	C _E	C _N	C _R	C _S	FC (%)	(N ₁) _{60cs}	r _d	K _σ	MSF	CSR	CSR for M=7.5, σ' _v =1	Primary source of data
MBARI No. 4 [B4/B5/EB2/EB3]	6.93	0.28	No	3.4	1.9	62	48	18.0	21.2	1	1.00	1.38	0.85	1	5	21.2	0.97	1.10	1.16	0.231	0.180	Boulanger et al (1995, 1997)
MBARI Technology	6.93	0.28	No	3.4	2.0	62	48	12.0	14.7	1	1.00	1.44	0.85	1	4	14.7	0.97	1.08	1.16	0.226	0.180	Boulanger et al (1995, 1997)
Miller Farm CMF 3	6.93	0.39	Yes	6.2	4.9	114	101	9.2	9.9	1	1.13	1.00	0.95	1	32	15.3	0.92	0.99	1.16	0.252	0.219	Holzer et al (1994), Bennett & Tinsley (1995)
Miller Farm CMF 5	6.93	0.39	Yes	7.0	4.7	130	108	20.0	20.9	1	1.13	0.97	0.95	1	13	23.4	0.91	0.99	1.16	0.280	0.243	Holzer et al (1994), Bennett & Tinsley (1995)
Miller Farm CMF 8	6.93	0.39	Yes	6.0	4.4	111	95	8.8	9.8	1	1.13	1.03	0.95	1	25	14.9	0.93	1.01	1.16	0.274	0.234	Holzer et al (1994), Bennett & Tinsley (1995)
Miller Farm CMF10	6.93	0.39	No	8.4	3.0	158	105	19.0	20.2	1	1.13	0.99	0.95	1	20	24.6	0.89	0.99	1.16	0.338	0.292	Holzer et al (1994), Bennett & Tinsley (1995)
POO7-2	6.93	0.28	Yes	6.3	3.0	121	89	14.4	15.4	1	0.92	1.11	0.95	1.1	3	15.4	0.92	1.01	1.16	0.229	0.194	Mitchell et al (1994), Kayen et al (1998), Cetin et al (2000)
POO7-3	6.93	0.28	Mar- ginal	6.3	3.0	121	89	16.0	17.0	1	0.92	1.10	0.95	1.1	3	17.0	0.92	1.02	1.16	0.229	0.194	Mitchell et al (1994), Kayen et al (1998), Cetin et al (2000)
POR-2&3&4	6.93	0.18	Yes	5.9	3.5	97	73	4.3	5.1	1	0.92	1.27	0.95	1.1	50	10.7	0.93	1.03	1.16	0.142	0.119	Mitchell et al (1994), Kayen et al (1998), Cetin et al (2000)
Sandholdt UC-B10	6.93	0.28	Yes	3.0	1.8	55	43	9.5	15.3	1	1.25	1.52	0.85	1	2	15.3	0.97	1.10	1.16	0.226	0.177	Boulanger et al (1995,1997), Cetin et al (2000)
Sandholdt UC-B10	6.93	0.28	No	6.1	1.8	115	73	26.0	34.4	1	1.25	1.11	0.95	1	5	34.4	0.93	1.08	1.16	0.266	0.211	Boulanger et al (1995,1997), Cetin et al (2000)
SFOBB-1&2	6.93	0.27	Yes	6.3	3.0	118	86	7.5	8.6	1	0.92	1.10	0.95	1.2	8	9.0	0.92	1.01	1.16	0.222	0.189	Mitchell et al (1994), Kayen et al (1998), Cetin et al (2000)
State Beach UC-B1	6.93	0.28	Yes	3.4	1.8	61	46	6.3	10.3	1	1.25	1.53	0.85	1	1	10.3	0.97	1.07	1.16	0.234	0.187	Boulanger et al (1995,1997), Cetin et al (2000)
State Beach UC-B2	6.93	0.28	Yes	4.9	2.6	90	67	12.8	18.4	1	1.25	1.20	0.95	1	1	18.4	0.95	1.05	1.16	0.229	0.188	Boulanger et al (1995,1997), Cetin et al (2000)
Treasure Island	6.93	0.16	Yes	6.5	1.5	116	67	4.3	6.4	1	1.13	1.24	0.95	1.1	20	10.8	0.92	1.04	1.16	0.165	0.137	Pass (1994), Youd & Shakal (1994), Cetin et al (2000)
WoodMarine UC-B4	6.93	0.28	Yes	1.8	1.0	32	25	6.7	9.1	1	1.00	1.70	0.80	1	35	14.6	0.99	1.10	1.16	0.233	0.183	Boulanger et al (1995,1997), Cetin et al (2000)
<i>1990 M=7.7 Luzon earthquake - July 16</i>																						
Cereenan St. B-12	7.7	0.25	No	5.0	2.3	94	68	34.7	24.9	1	0.65	1.16	0.95	1	19	29.2	0.97	1.08	0.95	0.218	0.213	Wakamatsu (1992), Cetin et al (2000)
Perez B1v. B-11	7.7	0.25	Yes	7.2	2.3	139	90	19.9	13.0	1	0.65	1.06	0.95	1	19	17.3	0.94	1.01	0.95	0.236	0.245	Wakamatsu (1992), Cetin et al (2000)
<i>1993 M=7.6 Kushiro-Oki earthquake - Jan 15</i>																						
Kushiro Port Quay Wall Site A	7.6	0.40	Yes	5.2	2.0	100	68	11.7	16.4	1	1.22	1.21	0.95	1	2	16.4	0.96	1.05	0.97	0.366	0.359	Iai et al (1994), Cetin et al (2000)
Kushiro Port Quay Wall Site D	7.6	0.40	No	10.8	1.6	208	118	26.8	30.9	1	1.22	0.95	1.00	1	0	30.9	0.89	0.97	0.97	0.408	0.434	Iai et al (1994), Cetin et al (2000)
Kushiro Port Seismo St.	7.6	0.47	Yes	3.8	2.0	65	47	17.4	25.9	1	1.30	1.35	0.85	1	5	25.9	0.98	1.10	0.97	0.410	0.383	Iai et al. (1995)

Earthquake & site	M	a _{max} (g)	Liq ?	Avg depth (m)	Depth GWT (m)	σ _v (kPa)	σ' _v (kPa)	Avg N _m	(N ₁) ₆₀	C _B	C _E	C _N	C _R	C _S	FC (%)	(N ₁) _{60cs}	r _d	K _σ	MSF	CSR	CSR for M=7.5, σ' _v =1	Primary source of data
<i>1994 M=6.7 Northridge earthquake - Jan 17</i>																						
Balboa B1v. Unit C	6.69	0.84	Yes	8.5	7.2	156	143	13.6	13.1	1	1.13	0.86	1.00	1	50	18.7	0.87	0.96	1.24	0.428	0.362	Bennett et al (1998), Holzer et al (1998), Cetin et al (2000)
Malden Street Unit D	6.69	0.51	No	9.3	3.9	154	101	24.1	27.2	1	1.13	1.00	1.00	1	25	32.3	0.86	1.00	1.24	0.431	0.349	Bennett et al (1998), Holzer et al (1998), Cetin et al (2000)
Potrero Canyon C1	6.69	0.43	Yes	7.1	2.0	139	88	7.4	8.5	1	1.13	1.07	0.95	1	64	14.1	0.91	1.02	1.24	0.320	0.254	Bennett et al (1998), Holzer et al (1998), Cetin et al (2000)
Wynne Ave. Unit C1	6.69	0.51	Yes	6.7	4.3	129	105	11.0	11.6	1	1.13	0.98	0.95	1	33	17.0	0.91	1.00	1.24	0.390	0.317	Bennett et al (1998), Holzer et al (1998), Cetin et al (2000)
<i>1995 M=6.9 Hyogoken-Nambu (Kobe) earthquake - Jan 16</i>																						
1	6.9	0.40	No	5.8	2.4	113	80	42.1	52.0	1	1.22	1.07	0.95	1	3	52.0	0.93	1.07	1.17	0.345	0.275	Tokimatsu (2010 pers. comm.)
2	6.9	0.40	No	8.0	2.9	152	103	34.2	39.5	1	1.22	1.00	0.95	1	15	42.7	0.89	1.00	1.17	0.345	0.296	Tokimatsu (2010 pers. comm.)
3	6.9	0.40	No	5.8	2.5	109	77	40.0	49.8	1	1.22	1.08	0.95	1	3	49.8	0.93	1.08	1.17	0.344	0.271	Tokimatsu (2010 pers. comm.)
4	6.9	0.40	No	4.3	2.1	76	54	25.8	36.6	1	1.22	1.23	0.95	1	1	36.6	0.95	1.10	1.17	0.350	0.272	Tokimatsu (2010 pers. comm.)
5	6.9	0.35	Yes	8.9	3.0	173	116	5.4	6.1	1	1.22	0.92	1.00	1	1	6.1	0.88	0.99	1.17	0.298	0.258	Tokimatsu (2010 pers. comm.)
6	6.9	0.40	No	5.9	2.3	107	72	13.4	17.8	1	1.22	1.15	0.95	1	21	22.5	0.93	1.05	1.17	0.360	0.293	Tokimatsu (2010 pers. comm.)
7	6.9	0.40	Yes	3.3	3.2	62	60	8.0	10.9	1	1.22	1.32	0.85	1	0	10.9	0.93	1.02	1.17	0.314	0.262	Tokimatsu (2010 pers. comm.)
8	6.9	0.50	Yes	5.0	3.0	85	65	17.4	24.1	1	1.22	1.20	0.95	1	0	24.1	0.94	1.07	1.17	0.402	0.321	Tokimatsu (2010 pers. comm.)
9	6.9	0.50	Yes	4.3	2.8	79	64	8.3	12.2	1	1.22	1.27	0.95	1	2	12.2	0.95	1.05	1.17	0.383	0.313	Tokimatsu (2010 pers. comm.)
10	6.9	0.60	No	7.5	4.5	137	107	24.1	27.4	1	1.22	0.98	0.95	1	9	28.0	0.90	0.99	1.17	0.450	0.388	Tokimatsu (2010 pers. comm.)
11	6.9	0.50	Yes	6.8	1.5	114	62	5.6	8.5	1	1.22	1.31	0.95	1	5	8.5	0.91	1.04	1.17	0.546	0.447	Tokimatsu (2010 pers. comm.)
12	6.9	0.50	No	5.3	3.2	92	72	18.6	24.7	1	1.22	1.14	0.95	1	14	27.6	0.94	1.06	1.17	0.393	0.316	Tokimatsu (2010 pers. comm.)
13	6.9	0.50	Yes	6.5	2.3	116	74	9.5	12.7	1	1.22	1.16	0.95	1	15	16.0	0.92	1.04	1.17	0.464	0.383	Tokimatsu (2010 pers. comm.)
14	6.9	0.50	No	4.8	3.1	86	69	15.0	20.3	1	1.22	1.17	0.95	1	19	24.5	0.95	1.06	1.17	0.382	0.307	Tokimatsu (2010 pers. comm.)
15	6.9	0.50	Yes	5.7	3.7	102	82	15.1	19.2	1	1.22	1.10	0.95	1	5	19.2	0.93	1.03	1.17	0.375	0.312	Tokimatsu (2010 pers. comm.)
16	6.9	0.60	No	4.5	2.5	80	60	17.5	25.0	1	1.22	1.23	0.95	1	5	25.0	0.95	1.09	1.17	0.495	0.390	Tokimatsu (2010 pers. comm.)
17	6.9	0.50	Yes	4.5	0.8	80	43	12.6	21.1	1	1.22	1.45	0.95	1	5	21.1	0.95	1.10	1.17	0.574	0.446	Tokimatsu (2010 pers. comm.)
18	6.9	0.70	No	10.5	7.7	199	171	40.5	42.6	1	1.22	0.86	1.00	1	0	42.6	0.85	0.85	1.17	0.448	0.452	Tokimatsu (2010 pers. comm.)
19	6.9	0.60	No	7.5	6.1	137	124	20.0	21.3	1	1.22	0.92	0.95	1	10	22.5	0.90	0.97	1.17	0.391	0.344	Tokimatsu (2010 pers. comm.)

Earthquake & site	M	a _{max} (g)	Liq ?	Avg depth (m)	Depth GWT (m)	σ_v (kPa)	σ'_v (kPa)	Avg N _m	(N ₁) ₆₀	C _B	C _E	C _N	C _R	C _S	FC (%)	(N ₁) _{60cs}	r _d	K _{σ}	MSF	CSR	CSR for M=7.5, $\sigma'_v=1$	Primary source of data
20	6.9	0.55	No	6.0	2.0	114	75	50.8	63.7	1	1.22	1.08	0.95	1	0	63.7	0.93	1.09	1.17	0.505	0.396	Tokimatsu (2010 pers. comm.)
21	6.9	0.60	No	3.5	1.7	62	44	24.4	33.5	1	1.22	1.32	0.85	1	0	33.5	0.97	1.10	1.17	0.531	0.412	Tokimatsu (2010 pers. comm.)
22	6.9	0.60	No	6.0	2.4	114	79	30.8	38.6	1	1.22	1.08	0.95	1	6	38.6	0.93	1.07	1.17	0.524	0.416	Tokimatsu (2010 pers. comm.)
23	6.9	0.60	No	5.0	3.0	92	72	18.1	24.0	1	1.22	1.15	0.95	1	10	25.1	0.94	1.06	1.17	0.468	0.379	Tokimatsu (2010 pers. comm.)
24	6.9	0.50	Yes	3.5	2.4	63	51	18.0	24.6	1	1.22	1.32	0.85	1	0	24.6	0.97	1.10	1.17	0.383	0.297	Tokimatsu (2010 pers. comm.)
25	6.9	0.70	No	3.5	2.2	64	50	27.5	35.8	1	1.22	1.25	0.85	1	3	35.8	0.97	1.10	1.17	0.555	0.431	Tokimatsu (2010 pers. comm.)
26	6.9	0.60	No	3.5	0.9	63	37	26.0	37.0	1	1.22	1.37	0.85	1	0	37.0	0.97	1.10	1.17	0.633	0.491	Tokimatsu (2010 pers. comm.)
27	6.9	0.60	No	2.5	1.1	43	29	27.6	40.8	1	1.22	1.43	0.85	1	10	42.0	0.98	1.10	1.17	0.568	0.441	Tokimatsu (2010 pers. comm.)
28	6.9	0.40	Yes	3.5	1.8	62	44	14.3	21.1	1	1.22	1.42	0.85	1	8	21.4	0.97	1.10	1.17	0.348	0.270	Tokimatsu (2010 pers. comm.)
29	6.9	0.40	Yes	3.8	2.0	67	49	12.4	17.9	1	1.22	1.39	0.85	1	0	17.9	0.96	1.09	1.17	0.337	0.264	Tokimatsu (2010 pers. comm.)
30	6.9	0.60	No	8.5	1.5	146	78	30.5	40.1	1	1.22	1.08	1.00	1	10	41.3	0.88	1.08	1.17	0.649	0.514	Tokimatsu (2010 pers. comm.)
31	6.9	0.60	No	4.0	1.2	73	46	34.8	49.7	1	1.22	1.23	0.95	1	0	49.7	0.96	1.10	1.17	0.599	0.465	Tokimatsu (2010 pers. comm.)
32	6.9	0.50	No	3.5	1.4	61	41	20.1	29.1	1	1.22	1.40	0.85	1	6	29.2	0.97	1.10	1.17	0.472	0.367	Tokimatsu (2010 pers. comm.)
33	6.9	0.50	No	8.0	2.0	142	83	21.3	27.9	1	1.22	1.07	1.00	1	50	33.5	0.89	1.05	1.17	0.496	0.404	Tokimatsu (2010 pers. comm.)
34	6.9	0.40	Yes	7.0	1.8	124	73	18.3	24.2	1	1.22	1.14	0.95	1	9	25.0	0.91	1.05	1.17	0.403	0.326	Tokimatsu (2010 pers. comm.)
35	6.9	0.50	Yes	4.5	2.1	79	55	12.3	18.9	1	1.22	1.32	0.95	1	6	18.9	0.95	1.08	1.17	0.445	0.352	Tokimatsu (2010 pers. comm.)
36	6.9	0.60	No	3.5	0.9	61	36	21.2	31.6	1	1.22	1.44	0.85	1	3	31.6	0.97	1.10	1.17	0.639	0.496	Tokimatsu (2010 pers. comm.)
37	6.9	0.35	Yes	5.0	4.0	89	79	15.0	19.3	1	1.22	1.12	0.95	1	0	19.3	0.94	1.03	1.17	0.241	0.200	Tokimatsu (2010 pers. comm.)
38	6.9	0.50	Yes	8.0	3.0	143	94	15.1	19.1	1	1.22	1.03	1.00	1	5	19.1	0.89	1.01	1.17	0.441	0.373	Tokimatsu (2010 pers. comm.)
39	6.9	0.60	No	4.5	2.6	84	66	47.0	61.0	1	1.22	1.12	0.95	1	0	61.0	0.95	1.10	1.17	0.476	0.370	Tokimatsu (2010 pers. comm.)
40	6.9	0.60	No	3.5	2.8	66	59	32.5	39.7	1	1.22	1.18	0.85	1	0	39.7	0.97	1.10	1.17	0.421	0.326	Tokimatsu (2010 pers. comm.)
41	6.9	0.40	Yes	4.1	2.0	71	50	9.2	15.0	1	1.22	1.41	0.95	1	0	15.0	0.96	1.08	1.17	0.352	0.279	Tokimatsu (2010 pers. comm.)
42	6.9	0.40	Yes	5.0	1.2	84	46	7.0	12.1	1	1.22	1.48	0.95	1	10	13.2	0.94	1.08	1.17	0.445	0.352	Tokimatsu (2010 pers. comm.)
43	6.9	0.35	Yes	4.7	2.2	80	55	10.0	15.2	1	1.22	1.31	0.95	1	20	19.6	0.95	1.08	1.17	0.311	0.246	Tokimatsu (2010 pers. comm.)
44	6.9	0.40	Yes	4.0	1.6	67	43	4.4	8.3	1	1.22	1.61	0.95	1	5	8.3	0.96	1.07	1.17	0.388	0.308	Tokimatsu (2010 pers. comm.)

Earthquake & site	M	a _{max} (g)	Liq ?	Avg depth (m)	Depth GWT (m)	σ _v (kPa)	σ' _v (kPa)	Avg N _m	(N ₁) ₆₀	C _B	C _E	C _N	C _R	C _S	FC (%)	(N ₁) _{60cs}	r _d	K _σ	MSF	CSR	CSR for M=7.5, σ' _v =1	Primary source of data
Ashiyama A (Mntn Sand 1)	6.9	0.40	No	5.2	3.5	97	80	16.6	21.1	1	1.22	1.10	0.95	1	18	25.2	0.94	1.04	1.17	0.295	0.243	Shibata et al (1996), Cetin et al (2000)
Ashiyama C-D-E (Marine Sand)	6.9	0.40	Yes	8.8	3.5	166	115	10.9	12.5	1	1.22	0.94	1.00	1	2	12.5	0.88	0.99	1.17	0.331	0.286	Shibata et al (1996), Cetin et al (2000)
Port Island Borehole Array Station	6.9	0.34	Yes	7.8	2.4	149	96	5.7	6.8	1	1.22	1.03	0.95	1	20	11.3	0.90	1.01	1.17	0.307	0.260	Shibata et al (1996), Cetin et al (2000)
Port Island Improved Site (Ikegaya)	6.9	0.40	No	8.5	5.0	159	125	20.2	22.7	1	1.22	0.92	1.00	1	20	27.2	0.88	0.96	1.17	0.293	0.260	Yasuda et al (1996; data from Ikegaya 1980), Cetin et al (2000)
Port Island Improved Site (Tanahashi)	6.9	0.40	No	10.0	5.0	189	140	18.2	19.5	1	1.22	0.88	1.00	1	20	24.0	0.86	0.95	1.17	0.301	0.270	Yasuda et al (1996; data from Tanahashi et al 1987), Cetin et al (2000)
Port Island Improved Site (Watanabe)	6.9	0.40	No	9.5	5.0	179	135	30.9	34.6	1	1.22	0.92	1.00	1	20	39.1	0.87	0.92	1.17	0.299	0.278	Yasuda et al (1996; data from Watanabe 1981), Cetin et al (2000)
Port Island Site I	6.9	0.34	Yes	10.0	3.0	192	123	9.7	10.8	1	1.22	0.91	1.00	1	20	15.3	0.86	0.98	1.17	0.295	0.258	Tokimatsu et al (1996), Cetin et al (2000)
Rokko Island Building D	6.9	0.40	Yes	7.5	4.0	141	107	14.8	16.8	1	1.22	0.98	0.95	1	25	21.9	0.90	0.99	1.17	0.310	0.267	Tokimatsu et al (1996), Cetin et al (2000)
Rokko Island Site G	6.9	0.34	Yes	11.5	4.0	219	146	12.0	12.3	1	1.22	0.84	1.00	1	20	16.8	0.83	0.96	1.17	0.275	0.246	Tokimatsu et al (1996), Cetin et al (2000)
Torishima Dike	6.9	0.25	Yes	4.7	0.0	93	46	8.5	14.0	1	1.22	1.42	0.95	1	20	18.5	0.95	1.10	1.17	0.308	0.240	Matsuo (1996), Cetin et al (2000)

3.2. Earthquake magnitudes and peak accelerations

Moment magnitudes (M or M_w) are used for all earthquakes in the updated liquefaction database (Tables 3.1 and 3.2). The liquefaction databases compiled by Seed et al. (1984) and Cetin et al. (2004) often referenced the earthquake magnitudes that had been quoted in the original case history reference. These original references, however, often used other scales for the earthquake magnitude. For the updated database, we obtained moment magnitudes from the Next Generation Attenuation (NGA) project flatfile (Chiou et al. 2008) and the USGS Centennial Earthquake Catalog (Engdahl and Villasenor 2002, and online catalog 2010). Preference was given to the NGA values if the two sources gave different estimates of M .

Table 3.2. Earthquake magnitudes in the liquefaction triggering database

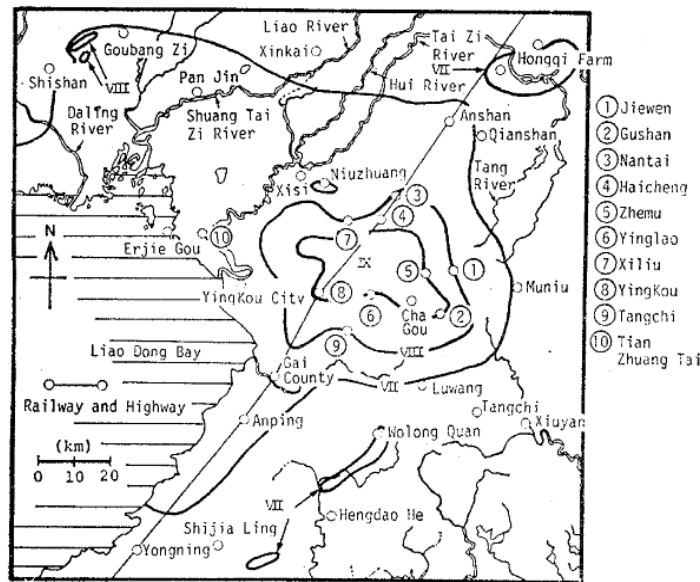
Earthquake	Magnitude in Seed et al. (1984)	Magnitude in Cetin et al. (2004)	Magnitude in Idriss and Boulanger (2004)	Moment magnitude (M) adopted in this study
1944 Tohankai	8.0	8.0	8.0	8.1
1948 Fukui	7.3	7.3	7.3	7.3
1964 Niigata	7.5	7.5	7.5	7.6
1968 Tokachi-Oki	7.9	7.9 & 7.8	7.9	8.3
1971 San Fernando	6.6	6.6	6.6	6.6
1975 Haicheng	7.3	7.3	7.3	7.0
1976 Guatemala	7.5	7.5	7.5	7.5
1976 Tangshan	7.6	8	8.0	7.6
1977 Argentina	7.4	7.4	7.4	7.5
1978 Miyagiken-Oki – Feb. 20	6.7	6.7	6.7	6.5
1978 Miyagiken-Oki – June 12	7.4	7.4	7.4	7.7
1979 Imperial Valley	6.6	6.5	6.5	6.5
1981 Westmoreland	5.6	5.9	5.9	5.9
1982 Urakawa-Oki	--	--	--	6.9
1983 Nihonkai-Chubu – June 21	--	7.1	7.1	6.8
1983 Nihonkai-Chubu – May 26	--	7.7	7.7	7.7
1987 Superstition Hills	--	6.7 & 6.6	6.5	6.5
1989 Loma Prieta	--	7.0	6.9	6.9
1990 Luzon	--	7.6	7.6	7.7
1993 Kushiro-Oki	--	8.0	8.0	7.6
1994 Northridge	--	6.7	6.7	6.7
1995 Hyogoken-Nambu (Kobe)	--	6.9	6.9	6.9

Estimates of peak horizontal ground accelerations (PGA or a_{max}) are listed for each site in Table 3.1. PGA estimates by the original site investigators or from the Seed et al. (1984) database were used in almost all cases.

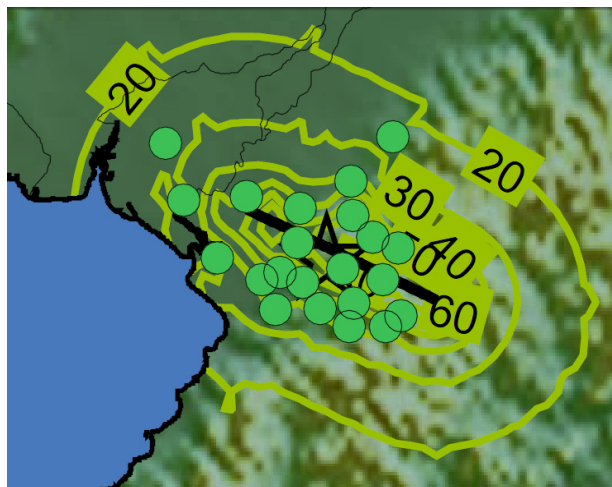
USGS ShakeMaps (Worden et al. 2010), when available, were used to check PGA estimates for a number of sites with no nearby recordings. The new ShakeMaps incorporate a weighted-average approach for combining different types of data (e.g., recordings, intensities, ground motion prediction equations) to arrive at best estimates of peak ground motion parameters. With one exception, the ShakeMaps

confirmed that existing estimates of PGA were reasonable, such that no changes to these estimates were warranted.

The ShakeMap for the 1975 Haicheng earthquake, however, indicated that significant changes to PGA estimates were warranted for some sites affected by the earthquake. The ShakeMap showing contours of PGA (in percentages) for the 1975 Haicheng earthquake is shown in Figure 3.1, along with the original reference's map of seismic intensities. Seed et al. (1984) had estimated values of PGA of 0.10, 0.13, 0.20, and 0.20 for the Shuang Tai Zi River Sluice Gate, Panjin Chemical Fertilizer Plant, Ying Kou Glass Fibre Plant, and Ying Kou Paper Plant, respectively, based on a correlation between seismic intensity and PGA. The USGS ShakeMap for this earthquake indicates best estimates of PGA would be at least 0.20, 0.20, 0.30, and 0.30 for these four sites, respectively.



(a) Contours of seismic intensity used by Shengcong and Tatsuoka (1984) and Seed et al. (1984) to estimate PGA at case history sites



(b) Contours of PGA in percent from USGS ShakeMap (2010)

Figure 3.1. Ground motion estimates for the 1975 Haicheng earthquake

3.3. Selection and computation of $(N_1)_{60cs}$ values

The selected critical depth intervals and the associated calculation of representative $(N_1)_{60cs}$ values are presented in Appendix C. Selections and calculations are shown for the 44 Kobe proprietary case sites, the added case sites from Iai et al. (1989), and 31 additional sites that plot close to the liquefaction correlation boundary curve. The remaining cases plot well above (for liquefaction sites) or well below (for no-liquefaction sites) the liquefaction boundary correlation; for those cases the selections of representative N values by either Seed et al. (1984) or Cetin et al. (2004) were adopted.

A number of case histories are discussed in detail in this section to illustrate aspects of how the individual case histories were interpreted.

Moss Landing State Beach

Liquefaction occurred along the access road to the Moss Landing State Beach during the 1989 M = 6.9 Loma Prieta earthquake (Boulanger et al. 1997). The estimated PGA at the site is 0.28 g. A profile along the access road is shown in Figure 3.2. Ground surface displacements ranged from about 30-60 cm at the Entrance Kiosk to about 10-30 cm at the Beach Path. Ground displacements were not observed farther up the road (near CPT sounding UC-18).

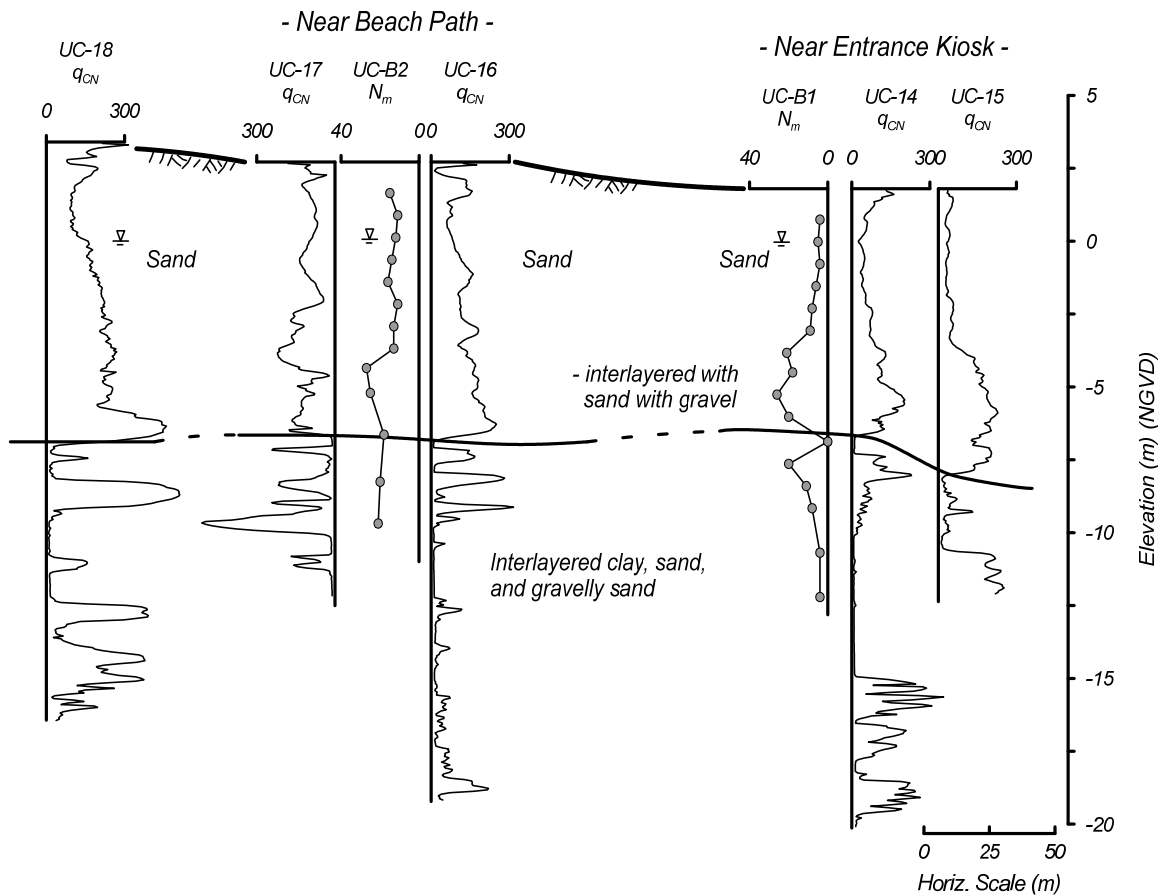


Figure 3.2: Profile at the Moss Landing State Beach (Boulanger et al. 1997)

At the Beach Path, the first five measured SPT N_m values below the water table in boring UC-B2 were 14, 16, 11, 13, and 13, after which they increased to over 20. The computations of $(N_1)_{60cs}$ values for the first five N_m values are summarized in Table 3.3. The average of the lower three $(N_1)_{60cs}$ values is 16.9, whereas the average of the five $(N_1)_{60cs}$ values is 18.4. The lateral spreading displacement of 10-30 cm would represent a shear strain of about 4-13% across a 2.3-m thick zone, or 3-8% across a 3.8-m-thick zone. While either of these average $(N_1)_{60cs}$ values could be an acceptable choice for representing this site, the value of 18.4 was adopted as representative of this stratum. For forward evaluations, however, the choice of $(N_1)_{60cs} = 16.9$ would be more conservative.

Table 3.3. Computation of the representative $(N_1)_{60cs}$ value for UC-B2 at Moss Landing

Depth (m)	Depth to GWT (m)	σ_{vc} (kPa)	σ'_{vc} (kPa)	(N_m)	$(N_1)_{60}$	C_B	C_E	C_N	C_R	C_S	FC (%)	$(N_1)_{60cs}$	$\Delta(N_1)_{60cs}$	
3.4	2.6	60	52	14	19.9	1	1.25	1.34	0.85	1	1	19.9		
4.1	2.6	75	60	16	21.3	1	1.25	1.25	0.85	1	1	21.3		
4.9	2.6	90	67	11	15.9	1	1.25	1.22	0.95	1	1	15.9		
5.6	2.6	105	75	13	17.8	1	1.25	1.15	0.95	1	1	17.8		
6.4	2.6	120	82	13	17.0	1	1.25	1.10	0.95	1	1	17.0		
Average values:														
	4.9			13.4	18.4						1	18.4		
Representative values given the above averages:														
	4.9	2.60	90	67	12.8	18.4	1	1.25	1.20	0.95	1	1	18.4	0.0

The above table also illustrates a bookkeeping detail about reporting representative values for all the other parameters. The issue is that computing representative values for $(N_1)_{60}$ and $(N_1)_{60cs}$ using the average values for depth, N_m , and FC, does not produce values equal to those obtained by directly averaging $(N_1)_{60}$ and $(N_1)_{60cs}$. Alternatively, the representative value of N_m can be back-calculated based on the average values for depth and FC along with the averaged values of $(N_1)_{60}$ and $(N_1)_{60cs}$. In the above table, the back-calculated representative N_m value is 12.8, which is only 5% less than the average N_m of 13.4. This difference can be positive or negative, but is almost always less than a few percent (see Appendix C). The advantage of the latter approach (bottom row in the above table) is that the reported values are internally consistent, which has its advantage for others who wish to use the database for sensitivity analyses.

At the Entrance Kiosk, the first five N_m values below the water table in boring UC-B1 were 5, 4, 6, 8, and 9, after which they increased markedly. The first three N values represent a 2-m thick interval of the upper clean sand strata, for which the average of the corresponding three $(N_1)_{60cs}$ values is 8.5. If the first five N values, representing a 3.5-m thick interval, are assumed to have liquefied, then the average $(N_1)_{60cs}$ value is 10.3. The value of 10.3 was adopted as representative of this stratum for this case history. For forward evaluations, however, the choice of $(N_1)_{60cs} = 8.5$ would be more conservative.

Consider the forward analysis of these two sites based on this method for selecting representative $(N_1)_{60cs}$ values. If there was an earthquake that was just strong enough to produce a computed $FS_{liq} = 1.0$ for the representative $(N_1)_{60cs}$ value of 18.4 at the Beach Path, then the FS_{liq} would be less than 1.0 for three of the five SPT tests in the looser strata. Since ground deformations may develop over thinner intervals within the identified strata, this approach for selecting representative $(N_1)_{60cs}$ values should result in the liquefaction correlation (which generally bounds the bulk of the data) being conservative for forward applications in practice. In fact, in many instances it may prove most effective to treat each blow count separately in forward applications, rather than using an average value. In other instances, such as

applications involving earthfill dams, use of an average $(N_1)_{60cs}$ for a stratum may be more appropriate if the potential failure surfaces are extensive relative to the stratum's dimensions. In general, the appropriateness of any averaging of $(N_1)_{60cs}$ values for a specific stratum in forward analyses or case history interpretations depends on the spatial characteristics of the stratum (e.g., thickness, lateral extent, continuity), the mode of deformation (e.g., reconsolidation settlement, lateral spreading, slope instability), and the spatial dimensions of the potential deformation mechanisms relative to the strata of concern.

Wildlife Liquefaction Array

Liquefaction occurred at the Wildlife Liquefaction Array in the 1981 Westmoreland and in the 1987 Superstition Hills earthquakes. A cross-section of the site is shown in Figure 3.3. Results of CPT, SPT, and laboratory index tests were obtained from Youd and Bennett (1983), Holzer and Youd (2007), and Bennett (2010, personal communication). Liquefaction was triggered in the silty sand layer between depths of about 2.5 and 6.5 m, as evidenced by the pore pressure transducer records and inclinometer readings. The upper 1 m of this layer is predominantly sandy silt and silt with an average fines content of about 78%, whereas the lower portion is predominantly silty sand with an average fines content of about 30%. Twenty-one N values obtained in six borings that span a distance of about 30 m in the area of liquefaction (boils and modest lateral spreading) are summarized in Table 3.4. Only some of the FC values come directly from the SPT samples; therefore, FC for other SPT N values were estimated based on data for parallel samples or average FC values for the same sample descriptions. The $(N_1)_{60cs}$ values ranged from about 10 to 22 (excluding one value of 28), and had a trend of increasing with depth.

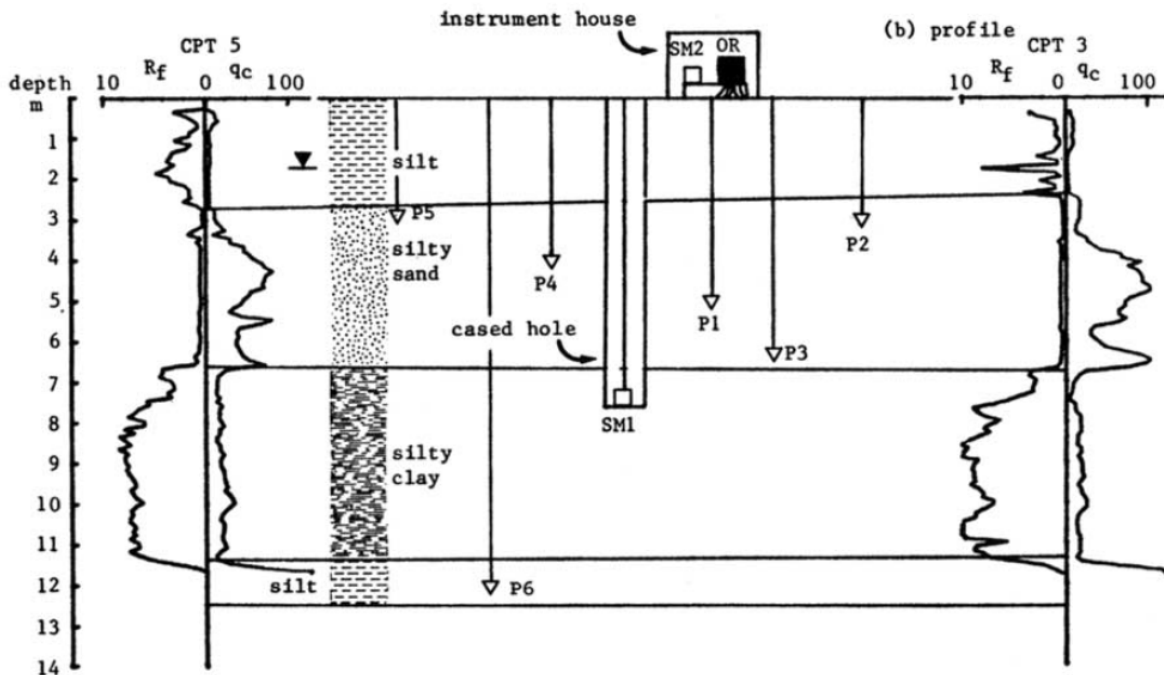


Figure 3.3: Profile at the Wildlife Liquefaction Array (Bennett et al. 1984)

Table 3.4. Computation of the representative $(N_1)_{60cs}$ value for Wildlife Liquefaction Array site

Depth (m)	Depth to GWT (m)	σ_{vc} (kPa)	σ'_{vc} (kPa)	(N_m)	$(N_1)_{60}$	C_B	C_E	C_N	C_R	C_S	FC (%)	$(N_1)_{60,cs}$	$\Delta(N_1)_{60,cs}$
2.3	1.2	43	32	4	6.1	1	1.13	1.70	0.8	1	69	11.7	
3.0	1.2	57	39	6	9.2	1	1.13	1.59	0.85	1	33	14.6	
3.0	1.2	57	39	5	7.8	1	1.13	1.63	0.85	1	20	12.3	
3.4	1.2	63	42	3	4.6	1	1.13	1.60	0.85	1	33	10.1	
3.4	1.2	63	42	5	7.6	1	1.13	1.58	0.85	1	17	11.5	
3.4	1.2	63	42	10	14.2	1	1.13	1.48	0.85	1	25	19.3	
3.7	1.2	69	45	6	8.6	1	1.13	1.49	0.85	1	33	14.1	
3.8	1.2	72	46	13	17.4	1	1.13	1.39	0.85	1	20	21.9	
4.3	1.2	81	51	5	6.9	1	1.13	1.43	0.85	1	33	12.3	
4.3	1.2	81	51	11	14.4	1	1.13	1.37	0.85	1	20	18.9	
4.3	1.2	81	51	7	9.4	1	1.13	1.40	0.85	1	33	14.9	
4.3	1.2	81	51	9	11.9	1	1.13	1.38	0.85	1	25	17.0	
4.6	1.2	87	54	10	14.3	1	1.13	1.33	0.95	1	20	18.8	
4.9	1.2	92	56	4	5.8	1	1.13	1.36	0.95	1	33	11.3	
5.2	1.2	98	59	4	5.7	1	1.13	1.33	0.95	1	33	11.2	
5.2	1.2	98	59	17	22.4	1	1.13	1.23	0.95	1	25	27.5	
5.3	1.2	101	61	6	8.3	1	1.13	1.29	0.95	1	33	13.8	
5.5	1.2	104	62	10	13.4	1	1.13	1.25	0.95	1	33	18.9	
6.1	1.2	116	68	9	11.7	1	1.13	1.21	0.95	1	33	17.1	
6.1	1.2	116	68	12	15.3	1	1.13	1.19	0.95	1	33	20.8	
6.1	1.20	116	68	12	15.4	1	1.13	1.19	0.95	1	25	20.4	
7.0	1.2	133	76	6.0	7.5	1	1.13	1.16	0.95	1	18	11.6	
7.0	1.2	133	76	14.0	16.9	1	1.13	1.13	0.95	1	33	22.4	
Average values:													
4.6				7.8	10.6					Average=	30	15.7	
Representative values given the above averages:													
4.6	1.2	87	54	7.1	10.3	1	1.13	1.36	0.95	1	30	15.7	5.4

The data in Table 3.4 can be used to illustrate the uncertainty associated with determining a representative value of $(N_1)_{60cs}$ for a case history. The average $(N_1)_{60cs}$ values for each of the six borings are 12.7, 14.0, 15.4, 15.7, 17.7, and 18.9. Thus, if only one of these six borings had been drilled, then the average $(N_1)_{60cs}$ value for this site might have ranged from 12.7 to 18.9. Using all six borings, the average and median $(N_1)_{60cs}$ values for the entire layer are 15.7 and 14.8, respectively, which are reasonably close together. Thus, as the number of borings and SPT data points increases, it becomes easier to evaluate the distribution of the $(N_1)_{60cs}$ values and hence select a representative value. For this case, $(N_1)_{60cs} = 15.7$, was selected as representative because the critical stratum is well defined and the borings are located relatively close together.

Miller and Farris Farms

Liquefaction and ground failure developed along the Pajaro River between the Miller and Farris Farms during the 1989 Loma Prieta earthquake. A cross-section across the zone of ground failure is shown in Figure 3.4. Exploration data from the site are described in Bennett and Tinsley (1995) and discussed in Holzer et al. (1994) and Holzer and Bennett (2007). They concluded that the zone of ground failure was restricted to the areas underlain by the younger (Q_{yf}) floodplain deposit, which fills an old river channel that was incised into the older (Q_{of}) floodplain deposit. Thus, boring CMF-10 (left side of Figure 3.4), with its relatively thick surface deposit of high-plasticity silt, is in an area of no liquefaction, whereas boring CMF-8, with its relatively thick interval of Q_{yf} , is in an area of liquefaction. Holzer et al. (1994) reported that the liquefied layer (Q_{yf}) had $(N_1)_{60}$ values of 14 ± 7 with an average FC = 22% based on a

total of 15 blow counts from several borings. The variation in average $(N_1)_{60}$ values for the liquefied layer from individual borings is illustrated by considering borings CMF-3, -5, and -8 which spanned a distance of about 550 m within the failure zone parallel to the river; these borings had 3, 1, and 3 blow counts in the liquefied layer, respectively, from which representative $(N_1)_{60}$ values of 9.9, 20.9, and 9.8 with FC of 27%, 13%, and 25% were obtained, respectively. Some of the variability in these average $(N_1)_{60}$ values is likely due to the small sample sizes (i.e., one to three blow counts cannot be expected to provide an accurate indication of the true average blow count in the vicinity of a boring), while some of it could be due to systematic variations in the average $(N_1)_{60}$ value across the site. These three borings are listed separately in Table 3.4 because of the relatively large distances between any two borings. For the nonliquefied layer (Q_{of}), a representative $(N_1)_{60}$ value of 20.2 for boring CMF-10 was obtained by averaging the two lower blow counts (12 and 25) with FC = 20%, which resulted in a representative $(N_1)_{60cs} = 24.6$.

This site is one of several examples used by Holzer and Bennett (2007) to illustrate how the boundaries of a lateral spread are often controlled by changes in geologic facies. It also illustrates how borings located short distances outside of a ground failure zone may, or may not, be representative of the soils that have liquefied. For this reason, the interpretation of liquefaction case histories using borings located outside the failure zone have the potential to be misinterpreted unless the geologic conditions are fully understood and taken into consideration. It also emphasizes the need for investigators to incorporate and include the geologic conditions in the description of the case histories investigated.

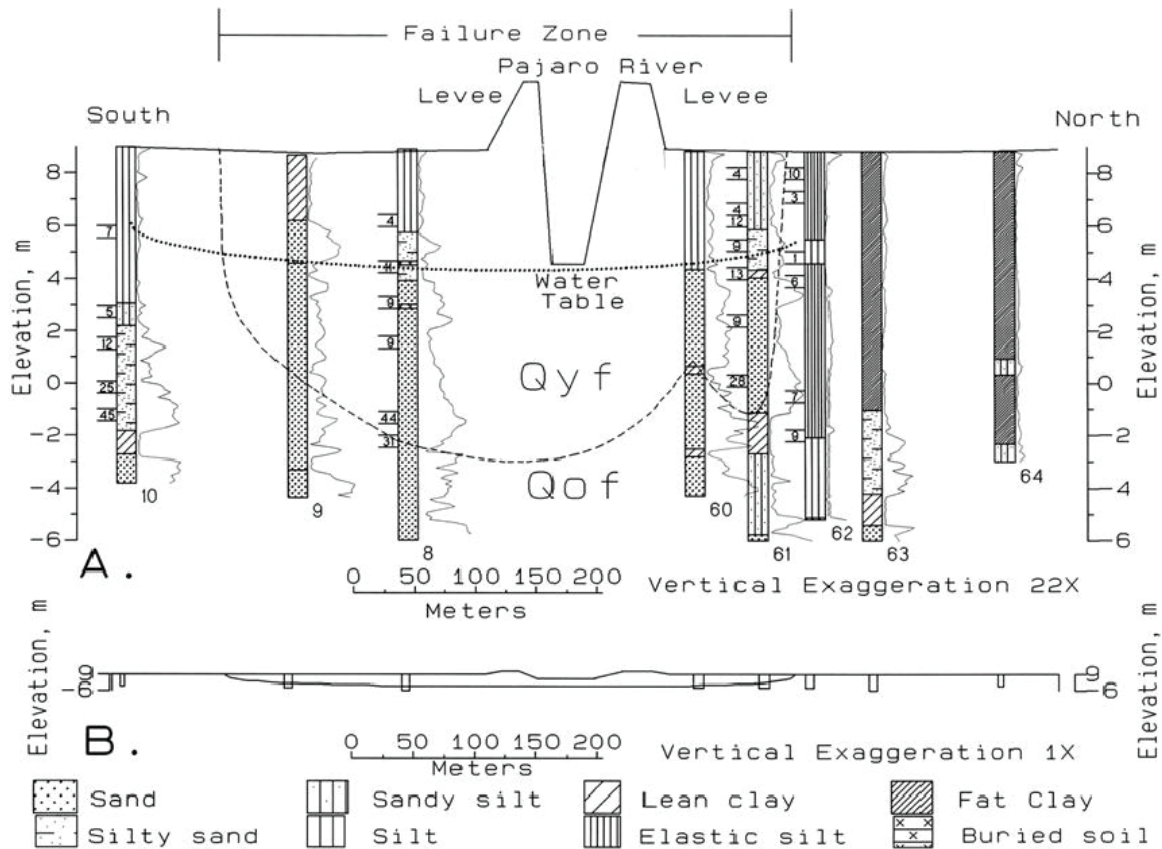


Figure 3.4. Profile across the failure zone at the Miller (south side of Pajaro River) and Farris Farms (north side of Pajaro River) during the 1989 Loma Prieta Earthquake (Holzer et al. 1994)

Balboa Boulevard

Liquefaction and ground failure developed along Balboa Boulevard during the 1994 Northridge earthquake. The estimated PGA at the site was about 0.84 g (Holzer et al. 1999). A cross-section across the zone of ground failure is shown in Figure 3.5. Exploration data from the site and interpretations of the behavior are presented by Holzer et al. (1999) and discussed by O'Rourke (1998). The site is underlain by an 8- to 10-m-thick stratum of Holocene silty sand and lean clay with sand; the upper 1-m-thick unit is fill (Unit A), underlain by sheet flood and debris flow deposits (Unit B), and then fluvial deposits (Unit C). These Holocene deposits are underlain by Pleistocene silty sand (Unit D), which was identified as the Saugus formation. Holzer et al. (1999) calculated average $(N_1)_{60cs}$ values for Units C and D using the procedures described in Youd et al. (2001), which had been initially published in an NCEER report in 1997 (NCEER 1997). For Unit C, 8 SPT blow counts were obtained, of which 4 were in clayey sands and 4 were in silty sands; the average of the 4 tests in silty sands gave an $(N_1)_{60cs}$ value of 21 with FC = 42%. For Unit D, 44 SPT N values were obtained, of which 15 were in clayey sands and 29 were in silty sands; the average of the 29 tests in silty sands gave an $(N_1)_{60cs}$ value of 59 with FC = 36%. Permanent ground deformations were limited to the area where the water table is within the Holocene sediments, such that the silty sand soils within Unit C were identified as the material that liquefied during the earthquake. The procedures described in this report produce a representative $(N_1)_{60cs}$ value of 18.7 for Unit C based on the average of the 4 SPT blow counts obtained in the silty sands of this stratum, as outlined in Appendix C.

Holzer et al. (1999) and Holzer and Bennett (2007) noted that the Balboa Boulevard site is an example of how the location of lateral spreading and ground failure can be controlled by the position of the ground water table relative to the geologic strata. As shown in Figure 3.5, ground failure along Balboa Boulevard was limited to the area where the ground water table was within the Holocene sediments, while no ground failure was observed where the ground water table was within the underlying, denser Pleistocene sediments. This case history also illustrates how the identification of the major geologic facies can be essential for understanding or predicting the extent and location of ground failure during earthquakes.

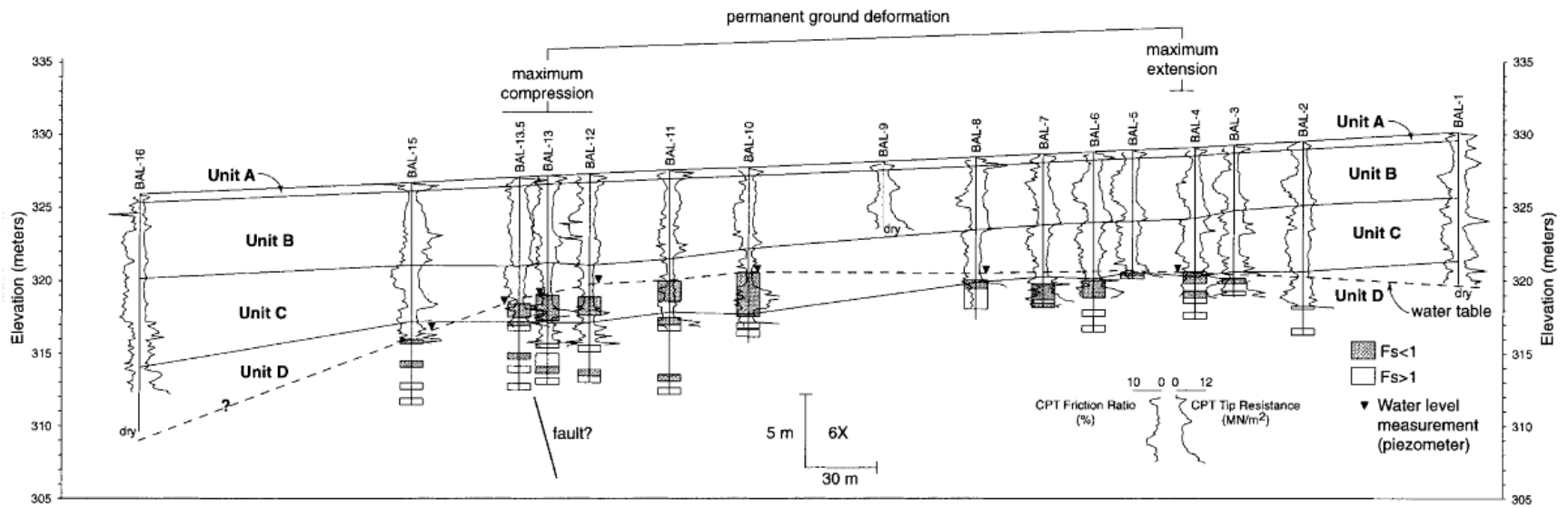


Figure 3.5: Profile across the failure zone at the Balboa Boulevard site during the 1994 Northridge Earthquake (Holzer et al. 1999)

Malden Street

Ground failure along Malden Street during the 1994 Northridge earthquake is an example of ground failure due to lurching in soft clays (O'Rourke 1998, Holzer et al. 1999). The estimated PGA at this location was 0.51 g. A cross-section across the ground failure zone is shown in Figure 3.6. The failure zone is underlain by an 8.5-m-thick stratum of Holocene lean to sandy lean clay (Units A and B), which is underlain by Pleistocene silty sand (Unit D). The ground water table in the failure zone was at a depth of 3.9 m, and no Holocene sands were encountered below the water table. The fine grained soils of Unit B typically had FC > 70% with an average PI of 18. Undrained shear strengths (s_u) for Units A and B were determined from field vane shear tests and CPT data. The s_u in Unit B was generally less than 50 kPa, compared to about 120 kPa for Unit A, and it decreased to an average value of $s_u = 26$ kPa in the 1.5-m-thick interval between depths 4.3 and 5.8 m in the area of ground failure. Holzer et al. (1999) computed peak dynamic shear stresses, based on the estimated PGA of 0.51 g that were about twice the soil's undrained shear strength. For the underlying Pleistocene sediment (Unit D), Holzer et al. (1999) obtained 8 SPT blow counts, of which 2 were in silty sands and 6 were in clayey sands; they reported an average $(N_1)_{60cs}$ value of 43 (using the procedures from Youd et al. 2001) with an average FC = 27% based on the two tests in silty sands. Holzer et al. (1999) and O'Rourke (1998) both concluded that cyclic softening/failure of the soft clay along Malden Street caused the observed ground deformations. In fact, O'Rourke used this site as a key example of ground failure due to lurching in soft clays, and not liquefaction of a cohesionless deposit.

This case history illustrates the importance of recognizing that ground failures can develop in soft clays under strong earthquake shaking, which is important to the interpretation of ground failure case histories and to the forward prediction of ground failures in practice. Additional case histories from the 1999 Chi-Chi and Kocaeli earthquakes have provided several examples regarding the behavior of low-plasticity fine grained soils, including cases of ground failure attributed to cyclic softening of silty clays beneath strongly loaded foundations (e.g., Chu et al. 2008) and cases where the low but measurable plasticity of the fines fraction was identified as one of the characteristics associated with lateral spreading displacements being significantly smaller than would be predicted by the application of current liquefaction analysis procedures (e.g., Chu et al. 2006, Youd et al. 2009).

3.4. Classification of site performance

Site performance during an earthquake is classified as a "liquefaction", "no liquefaction", or a "marginal" case; some databases designate these cases as "yes", "no", or "no/yes", respectively. In this report, the classification of site performance was based on the classification assigned by the original investigator, except for the Seventh Street Wharf site at the Port of Oakland (discussed below). Cases described as "liquefaction" were generally accompanied with reports of sand boils and/or visible ground surface settlements, cracks, or lateral spreading movements. Cases described as "no liquefaction" were either accompanied with reports of no visible surface manifestations (i.e., no sand boils, ground surface settlements, cracks, or lateral movements) or can be inferred as having corresponded to such conditions when not explicitly stated.

A case is described as "marginal" if the available information suggests that conditions at the site are likely at, or very near, the boundary of conditions that separate the occurrence of liquefaction from nonliquefaction. Only three cases are classified as marginal in the database because it is very difficult to define a marginal case in most field conditions. Areas of liquefaction and nonliquefaction in the field are often separated by distinct geologic boundaries (e.g., Holzer and Bennett 2007) such that borehole data can be used to describe liquefaction and no liquefaction cases, but not the marginal condition. Thus

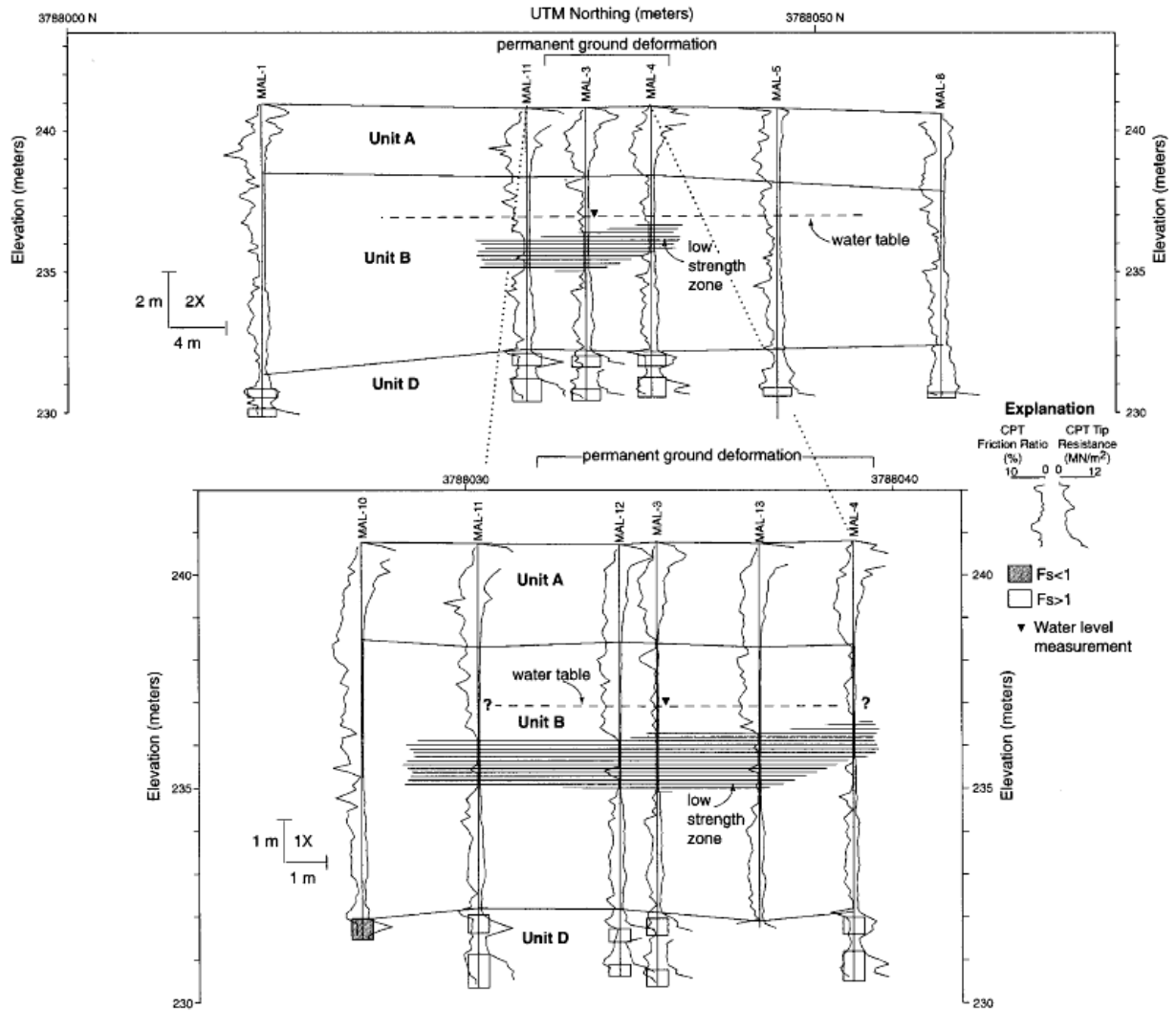


Figure 3.6. Profile across the failure zone at the Malden Street site during the 1994 Northridge Earthquake (Holzer et al. 1999)

explicit information is typically not available for marginal conditions. The three marginal cases in the database are, therefore, discussed below.

The Seventh Street Wharf site at the Port of Oakland and its performance in the 1989 Loma Prieta earthquake are described in Kayen et al. (1998) and Kayen and Mitchell (1998). Boring POO7-2 was intentionally located in an area with surface manifestations of liquefaction, whereas boring POO7-3 was in an area with no surface manifestations. The two borings, POO7-2 and POO7-3, were characterized as "liquefaction" and "no liquefaction" sites, respectively, in Kayen et al. (1998). The following additional information and updated interpretation of the performance of these sites was provided by Kayen (2010, personal communication).

The two borings, POO7-2 and POO7-3, were separated by 70-100 m. At the location of POO7-3, there were no sand boils in the immediate 15-20 meters. This site was at the back of the park (now converted to container yard) at the farthest distance from the dike. In the zone along the bay margin, perhaps 20 m

wide, there were ample fissures and sand boils, deformations toward the free-face, and a small lateral spread into the bay. The distance from this zone to POO7-3 was about 20-30 m. Kayen (2010, personal communication) indicated that, at this time, he would classify the location at POO7-3 as a liquefaction site because it was too close to the park perimeter deformations to be classified as a non-liquefaction site based on surface observations alone. This site was listed as a "marginal" case in the database presented herein because the soil conditions at POO7-3 had similar stratigraphy but slightly denser conditions than at POO7-2.

Two other sites are listed as marginal cases in the database. Seed et al. listed the Rail Road 2 case as a "no/yes" case and assigned it a representative N value that corresponds to the value Koizumi (1966) considered to have been the critical value that separated cases of liquefaction from cases of no liquefaction in the Niigata earthquake. Thus, the N value assigned to the Rail Road 2 case was explicitly derived as a point that should fall on the triggering curve. The Amatitlan B-1, B-2, B-3, and B-4 cases from the 1976 Guatemala earthquake are described by Seed et al. (1979). Boring B-2 was intentionally located in a nonliquefied zone, but very close to the boundary between the areas of liquefaction and non-liquefaction. Seed et al. listed boring B-2 case as a "no/yes" case because they concluded that it probably represented the limiting conditions at which liquefaction would just occur or just not occur for the ground conditions and ground motions experienced at this site in the Guatemala earthquake.

3.5. Distribution of data

The distributions of $(N_1)_{60}$, $CSR_{M=7.5, \sigma=1}$, M , and FC from the database are plotted versus the average depths for the critical zones in Figure 3.7 for "liquefaction", "marginal", and "no liquefaction" cases. These figures indicate that the database is limited to average critical depths less than 12 m and has very few data points for M greater than 7.7 or less than 6.4 or for FC greater than 40%.

The distributions of the data are further illustrated in Figure 3.8 showing a_{max} versus M (two parameters which enter the calculation of $CSR_{M=7.5, \sigma=1}$) and FC versus $(N_1)_{60}$ (two parameters which enter the calculation of $(N_1)_{60cs}$). The plot of FC versus $(N_1)_{60}$ indicates that the data points for FC greater than about 25% are largely limited to $(N_1)_{60}$ values less than about 15.

The distributions of σ'_v , C_N , C_R , K_σ , r_d , and MSF are plotted versus average depth in Figure 3.9. The computed values for σ'_v are generally less than about 140 kPa, the C_N factors are generally between 0.8 and 1.7 (cutoff value), the K_σ values are generally between 0.9 and 1.1 (cutoff value), and r_d values are generally greater than 0.8.

The maximum depth and average depth for the critical zones are compared in Figure 3.10; for example, if the critical zone for a site extended between depths of 6 m and 10 m, the average depth would be 8 m while the maximum depth would be 10 m. This figure includes all the cases (liquefaction or no liquefaction) for which a detailed calculation of the average $(N_1)_{60cs}$ value was performed (Appendix C). This figure shows that there were a significant number of cases for which the critical zone extended to maximum depths of about 12 to 13 m, whereas Figures 3.7 and 3.9 indicate that there are relatively few cases for which the average depth of the critical zone was close to 12 m.

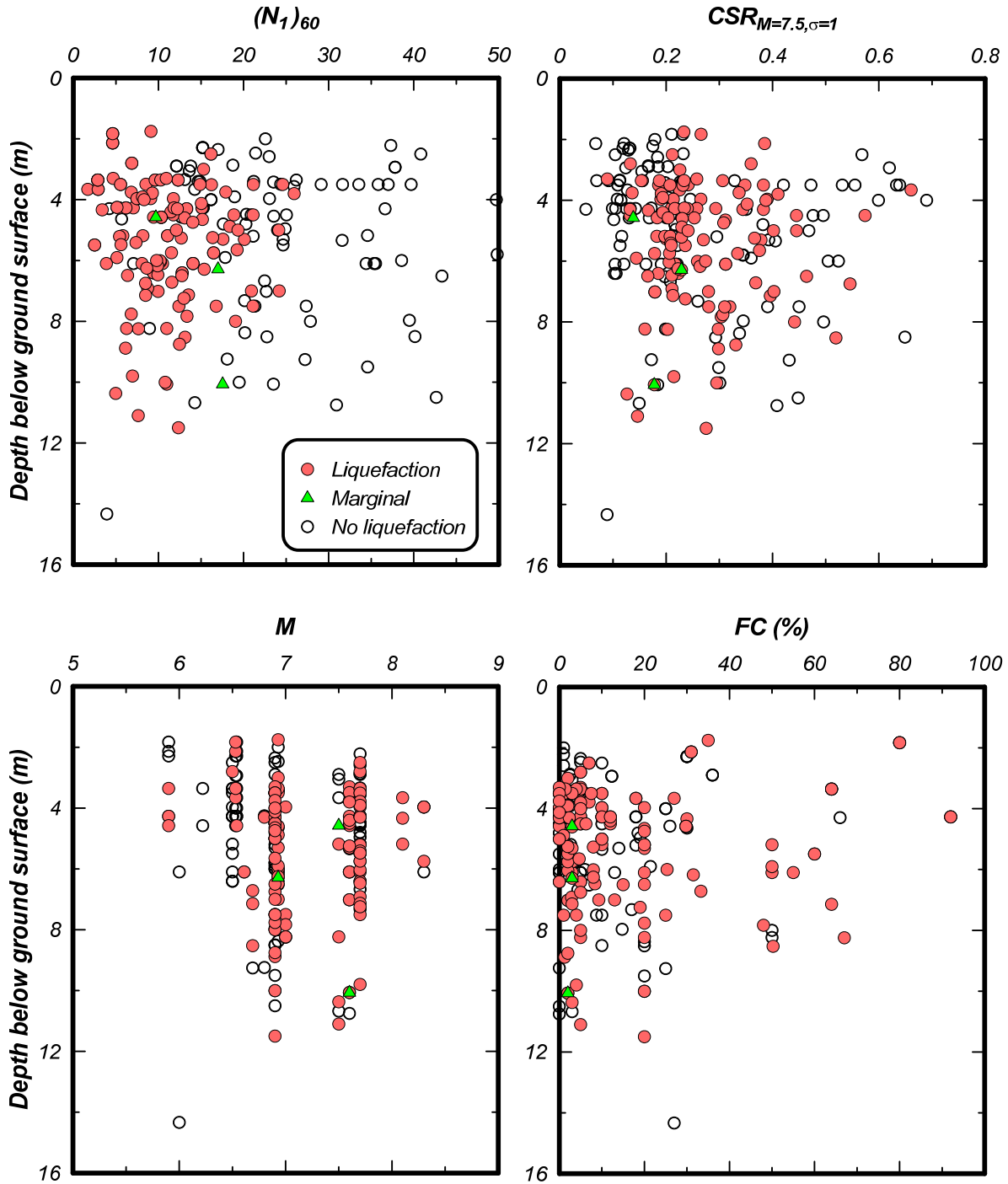


Figure 3.7. Distribution versus depth of the case history parameters $(N_1)_{60cs}$, $CSR_{M=7.5, \sigma=1}$, M , and FC .

Explicit statements regarding the plasticity of the fines fraction [e.g., a plasticity index (PI) or statement that the fines are nonplastic] are not provided for most case histories. For example, consider the 25 case history data points for $FC > 35\%$. These 25 case histories come from only 16 different sites since several of the sites were shaken by more than one earthquake event. No explicit statement regarding the plasticity index or nonplastic nature of the fines fraction was provided for 12 of these sites, although the

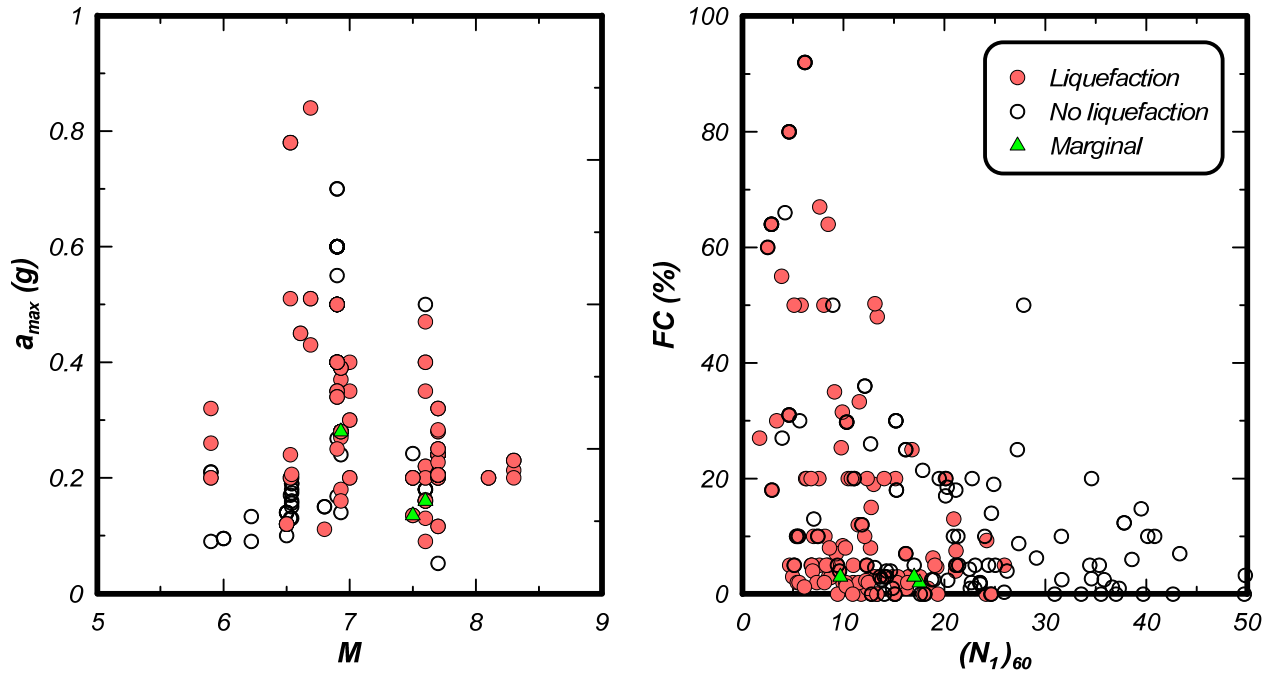


Figure 3.8. Distributions of a_{max} versus M and FC versus $(N_1)_{60}$. Note that it appears that there are fewer data points in the graph of a_{max} versus M because many of the points plot on top of each other.

visual descriptions and classifications of the soils (e.g., SM, ML) implied either nonplastic or low-plasticity fines. For the critical layers at Van Norman and Juvenile Hall, Cetin et al. (2000) suggest PI values of 3-10 were representative of the fines fraction. For Unit C1 at Potrero Canyon (Bennett et al. 1998), the data from the SPT samples used to represent the liquefiable lenses (Appendix C) indicate an average FC = 64%, classifications as SM or ML, and PI values of 2-3 for three of the 9 samples (PI values not reported for the other samples); note that the summary in Holzer et al. (1999) suggests an average PI = 5 for the range of silt and silty sand in the C1 unit. For the saturated portion of Unit C at Balboa Boulevard (Bennett et al. 1998), the data from the four SPT samples in the sandy silt and silty sand portions of this stratum indicated an average FC = 50%, classifications as SM or ML, and no indication of plasticity; note that the summary in Holzer et al. (1999) suggests an average PI = 11 for the heterogeneous range of clays to silty sands in this stratum. While explicit information of fines plasticity is lacking throughout the case history database, it is believed that the database presented herein corresponds primarily to soils with essentially nonplastic or very low plasticity fines.

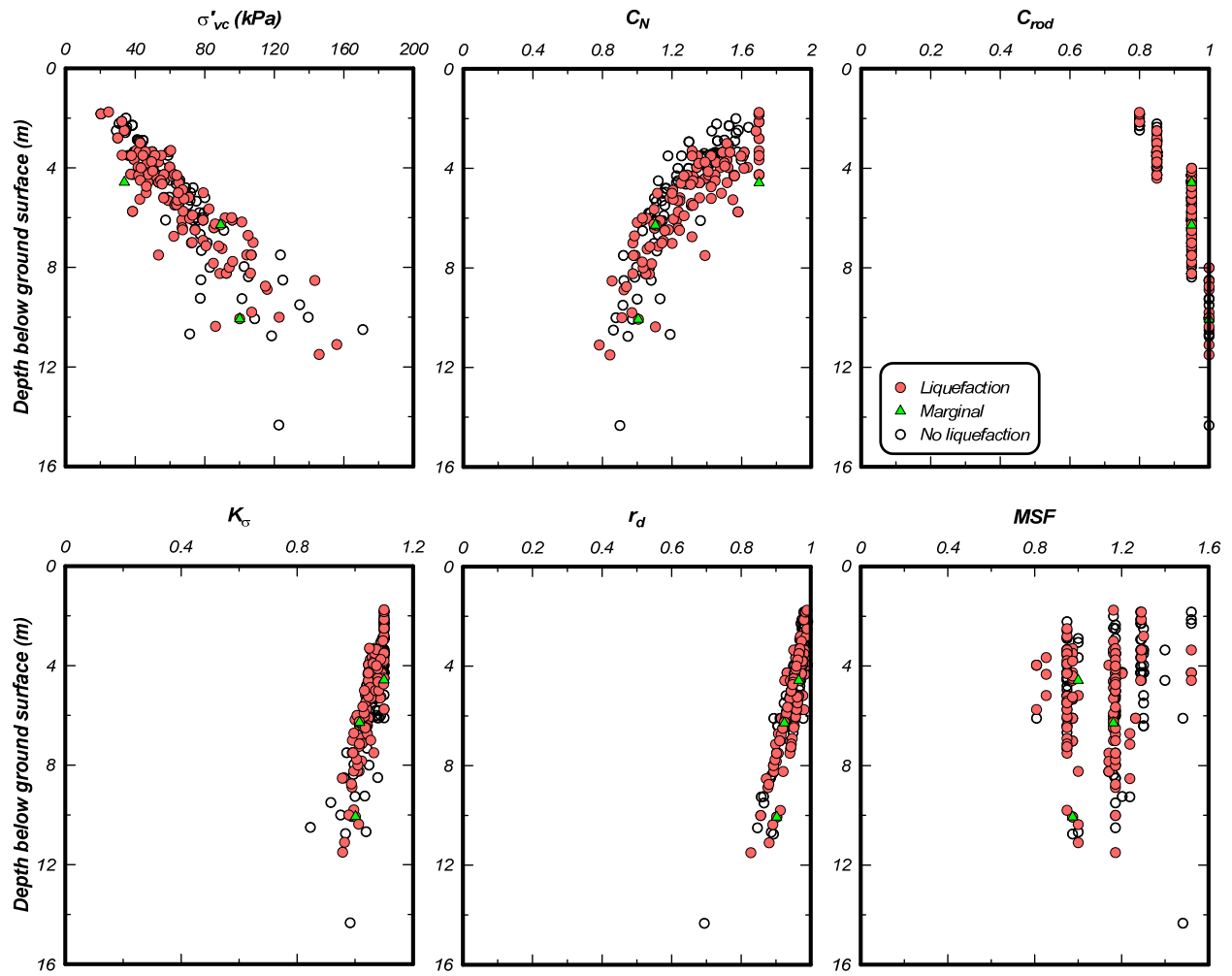


Figure 3.9. Distribution versus depth of the case history analysis parameters σ'_v , C_N , C_R , K_σ , r_d , and MSF.

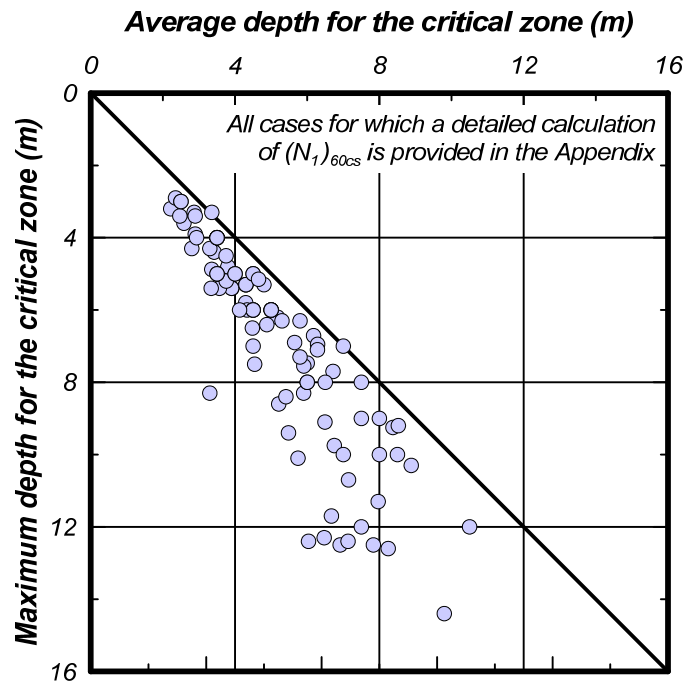


Figure 3.10. Maximum depth for the critical zone versus the average depth for the critical zone.

4. EXAMINATION OF THE LIQUEFACTION TRIGGERING CORRELATION

4.1. Case history data

This section contains an examination of the updated case history data, as described in Section 3 and listed in Table 3.1, for evidence of trends or biases relative to the liquefaction triggering correlation by Idriss and Boulanger (2004, 2008). The full, updated database is shown with the Idriss-Boulanger triggering correlation in terms of equivalent $CSR_{M=7.5, \sigma_v=1}$ versus equivalent clean sand $(N_1)_{60cs}$ in Figure 4.1. For comparison, the database previously used by Idriss and Boulanger (2004, 2008) is shown in Figure 4.2. Comparison of Figure 4.1 with Figure 4.2 indicates that the updated database includes considerably more case histories and that the updated database continues to support the previously derived triggering correlation.

The uncertainties in the measured or estimated $(N_1)_{60cs}$ and $CSR_{M=7.5, \sigma_v=1}$ values for each case history should be considered when evaluating the preferred position of a liquefaction triggering correlation relative to the case history data points. Specifically, the consequence of these measurement (or parameter) uncertainties is that a reasonably conservative, deterministic liquefaction triggering curve should not be expected to fully envelop all of the liquefaction case histories. Heuristically, a deterministic liquefaction triggering curve can be expected to be positioned so that the number of liquefaction case histories falling below the curve is relatively small compared to the number of no-liquefaction case histories falling above the curve. More formally, statistical methods can be used to address the influence of measurement uncertainties and evaluate the uncertainty in liquefaction triggering correlations. In this regard, the probabilistic analyses of the case history database presented in Section 6 of this report indicates that the deterministic liquefaction triggering curve by Idriss and Boulanger (2004, 2008) corresponds to a probability of liquefaction of about 16% based on model uncertainty alone [i.e., if the $(N_1)_{60cs}$ and $CSR_{M=7.5, \sigma_v=1}$ values are known perfectly] and to a probability of liquefaction of about 35% with the inclusion of measurement uncertainties [i.e., allowing for the uncertainty in the $(N_1)_{60cs}$ and $CSR_{M=7.5, \sigma_v=1}$ values for each case history].

Examination of the updated case history data (Table 3.1) included sorting the data into various parameter bins (e.g., soil characteristics, earthquake magnitudes, data sources, and individual earthquakes) and comparing the binned data to the Idriss-Boulanger triggering correlation. These comparisons are presented in terms of $(N_1)_{60cs}$ so that the entire data (clean sands, silty sands and nonplastic sandy silts) can be combined in different data bins.

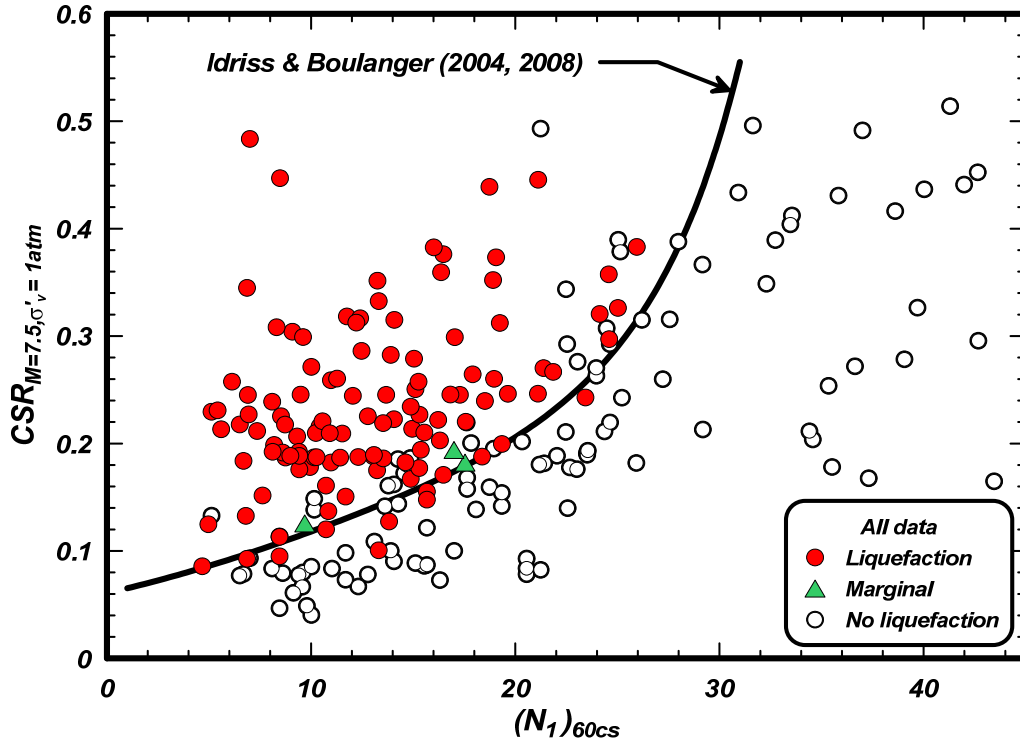


Figure 4.1. Updated SPT case history database of liquefaction in cohesionless soils with various fines contents in terms of equivalent CSR for $M = 7.5$ and $\sigma'_v = 1 \text{ atm}$ and equivalent clean sand $(N_1)_{60cs}$

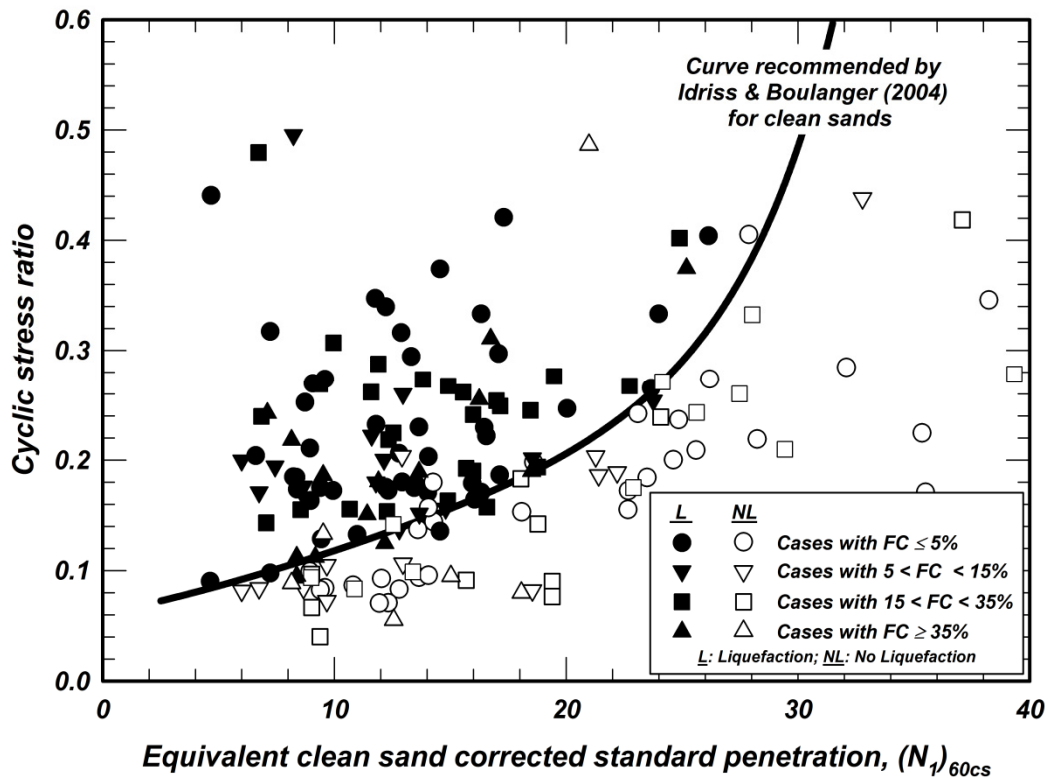


Figure 4.2. SPT case history database used previously by Idriss and Boulanger (2004, 2008)

4.1.1. Variation with fines content

The data for clean sands ($FC \leq 5\%$) are shown in the plot of $CSR_{M=7.5, \sigma'_v=1}$ versus $(N_1)_{60cs}$ in Figure 4.3a. There are 2 liquefaction points that are below the Idriss-Boulanger triggering correlation and 8 no-liquefaction points above it.

The Nakamura Dyke N-4 site in the February 20, 1978 Miyagiken-Oki earthquake is one of the liquefaction points with $FC \leq 5\%$ that plots below the triggering curve. This case had a $PGA = 0.12$ g, a critical depth = 2.8 m, $\sigma'_v = 30$ kPa, $(N_1)_{60} = 6.9$, and $FC = 5\%$. The representative $(N_1)_{60cs}$ value of 6.9 is based on the average of 4 N values (5, 3, 5, and 6) from a single boring.

The Takeda Elementary School site in the June 21st aftershock of the 1983 Nihonkai-Chubu earthquake is the other liquefaction point with $FC \leq 5\%$ that plots below the triggering curve. This case had an estimated $PGA = 0.11$ g, critical depth = 4.3 m, $\sigma'_v = 42$ kPa, $(N_1)_{60} = 13.3$, and $FC = 0\%$. The representative $(N_1)_{60cs}$ value of 13.3 is based on the average of 3 N values (8, 7, & 8) from a single boring provided by the Nakazato Town Office to Yasuda and Tohno (1988). Yasuda and Tohno (1988) reported that this site liquefied during both the May 26th main shock and the June 21st aftershock (26 days later); they estimated the PGA as being 0.283 g and 0.111 g during the main shock and aftershock, respectively, based on recordings at a station 6 km away.

The data for sands with $5\% \leq FC \leq 15\%$ are shown in the plot of $CSR_{M=7.5, \sigma=1}$ versus $(N_1)_{60cs}$ in Figure 4.3b. There are 2 liquefaction points that are below the Idriss-Boulanger triggering correlation and 2 no-liquefaction points above it.

The Coastal region site in the 1976 Tangshan earthquake is one of the liquefaction points with $5\% \leq FC \leq 15\%$ that plots below the triggering curve. This case had $PGA = 0.13$ g, critical depth = 4.5 m, $\sigma'_v = 54$ kPa, $(N_1)_{60} = 11.7$, and $FC = 12\%$. The representative $(N_1)_{60cs}$ value of 13.8 is based on the average of 4 N values (7, 8, 13, and 10) from a single boring. Had only the first two N values been used, then the resulting data point would be $(N_1)_{60cs} = 9.7$, which would be positioned just to the left (i.e. above) the triggering curve.

The Miller Farm CMF-5 site in the 1989 Loma Prieta earthquake is the second liquefaction point with $5\% \leq FC \leq 15\%$ that plots below the triggering curve. This case corresponds to one of several borings within an area of liquefaction parallel to a river, as discussed in more detail in Section 3.3. The data for CMF-5 was $PGA = 0.39$ g, critical depth = 7.0 m, $\sigma'_v = 108$ kPa, $(N_1)_{60} = 20.9$, and $FC = 13\%$. The representative $(N_1)_{60cs}$ value of 23.4 is based on a single N value from this boring. Two other borings within the failure zone, CMF-3 and CMF-8, each had three N values in the liquefied layer and had representative $(N_1)_{60cs}$ values of 15.3 and 14.9, respectively. If an average $(N_1)_{60cs}$ value had been adopted for the entire failure zone (i.e., averaging the data across these borings), the resulting data points would plot above the triggering curve. The data for these three borings were, however, plotted separately because they span a relatively large distance (about 550 m), and thus they may reflect spatial variability as well as the effect of small sample sizes.

The data with $15\% \leq FC \leq 35\%$ are shown in Figure 4.3c. Two liquefaction data points, corresponding to the same site in two different earthquakes, fall just below the triggering curve and 4 no-liquefaction points are above it.

The Wildlife B site in the 1981 M = 5.9 Westmoreland and 1987 M = 6.5 Superstition Hills earthquakes represents the two data points with $15\% \leq FC \leq 35\%$ that plot below the triggering curve. This site was well characterized with 21 SPT N values from six borings, as described previously in Section 3.3.

The data with $FC \geq 35\%$ are shown in Figure 4.3d. There is 1 liquefaction data point that is just below the triggering curve and 3 no-liquefaction points that are above it.

The Radio Tower B-1 site in the 1981 Westmoreland earthquake is the one liquefaction case with $FC \geq 35\%$ that plots just below the triggering curve. This case had a PGA = 0.20 g, critical depth = 3.3 m, $\sigma'_v = 49$ kPa, $(N_1)_{60} = 2.9$, and $FC = 75\%$. The representative $(N_1)_{60cs}$ value of 8.4 is based on a single N value from a single boring.

The full dataset, including all fines contents, has a total of 7 points that fall below the triggering curve and 18 nonliquefaction points that are above it. The 3 marginal data points fall very close to, or slightly above, the triggering curve. The 7 points that fall below the triggering curve for the liquefaction cases are listed below:

Table 4.1. Aspects of the seven data points falling below the Idriss-Boulanger triggering curve

Case	$(N_1)_{60cs}$	FC (%)	$CSR_{M=7.5, \sigma'_v=1 \text{ atm}}^*$	$CRR_{M=7.5, \sigma'_v=1 \text{ atm}}^{**}$	Increment below triggering curve
Nakamura Dyke N-4 site (1978 M = 6.4 Miyagiken-Oki earthquake)	6.9	5	0.093	0.097	0.004
Takeda Elementary School site (June 21 st M = 6.8 aftershock, 1983 Nihonkai-Chubu earthquake)	13.3	0	0.101	0.142	0.041
Coastal region site (1976 M = 7.6 Tangshan earthquake)	13.8	12	0.127	0.146	0.019
Miller Farm CMF-5 site (1989 M = 6.9 Loma Prieta earthquake)	23.4	13	0.243	0.257	0.014
Wildlife B site (1981 M = 5.9 Westmoreland earthquake)	15.7	30	0.155	0.162	0.007
Wildlife B site (1987 M = 6.5 Superstition Hills earthquake)	15.7	30	0.148	0.162	0.014
Radio Tower B-1 site (1981 M = 5.9 Westmoreland earthquake)	8.4	75	0.094	0.107	0.013

* Value of $CSR_{M=7.5, \sigma'_v=1 \text{ atm}}$ for the case history.

** Value of $CRR_{M=7.5, \sigma'_v=1 \text{ atm}}$ from the triggering curve at $(N_1)_{60cs}$ for the case history.

Except for the Takeda Elementary School site, these are minor differences and do not warrant changing the triggering curve. Obviously, the liquefaction triggering correlation should not be controlled by a single case history, particularly given the potential effects of measurement uncertainties in the case history database.

Therefore, the position of the triggering curve appears to be relatively unbiased with respect to fines content, and to be reasonably conservatively positioned.

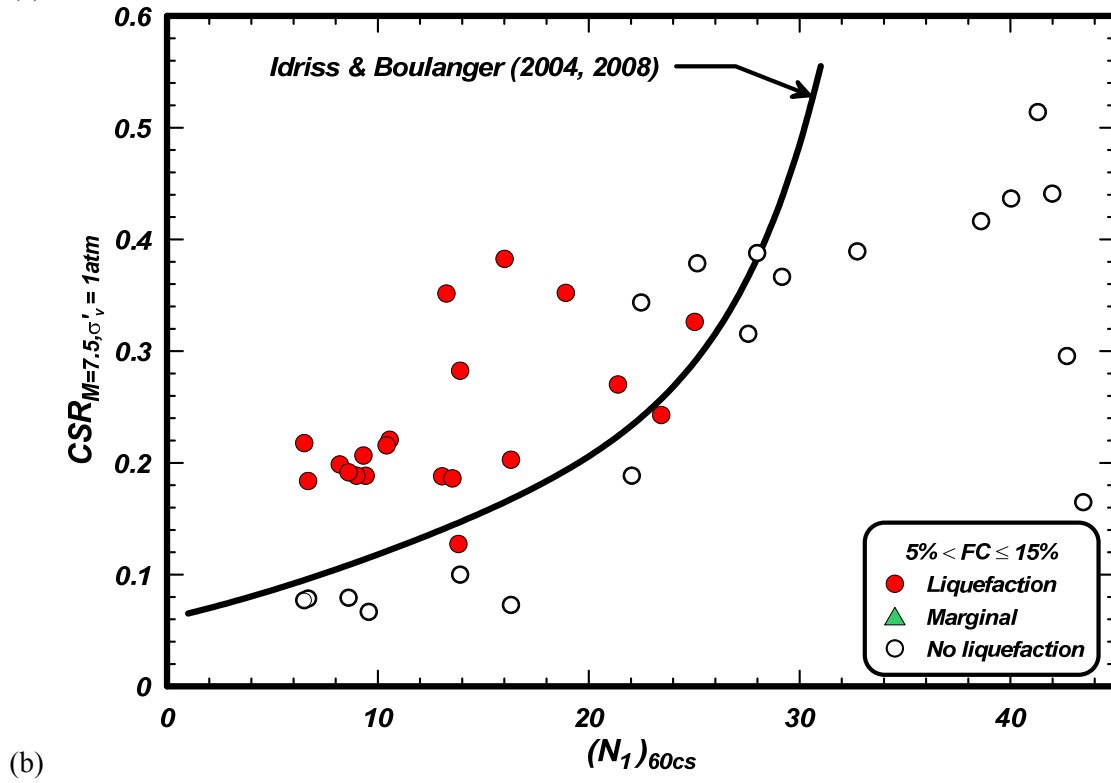
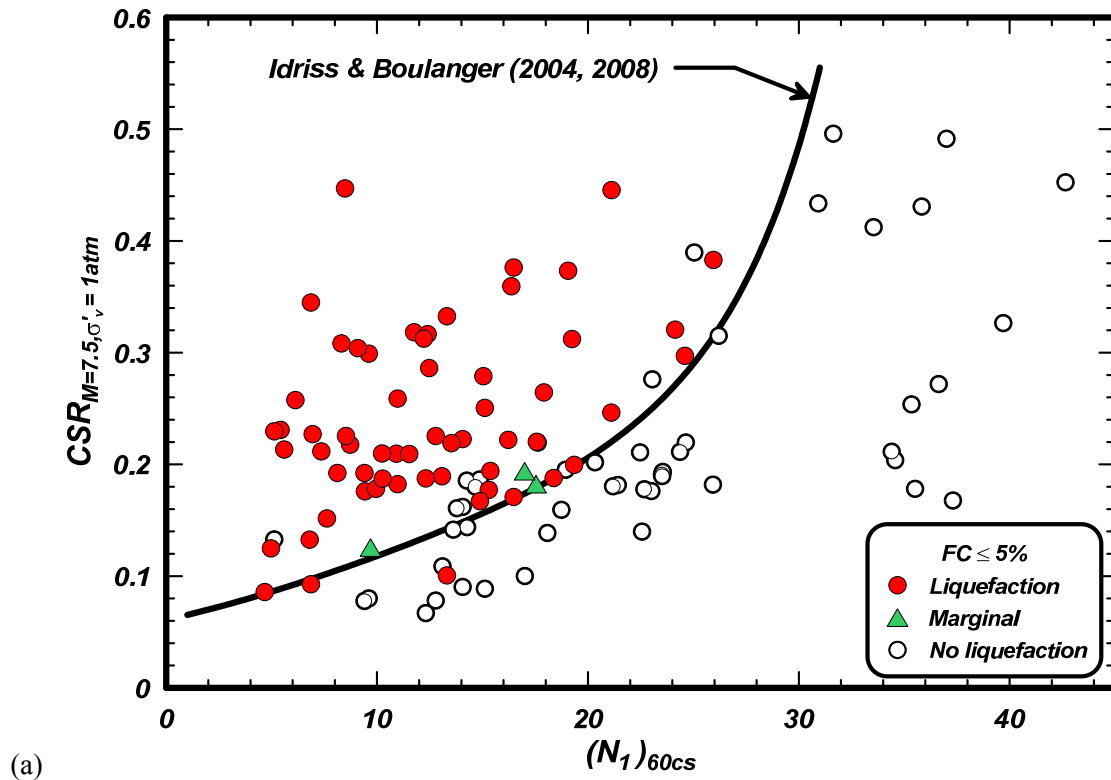
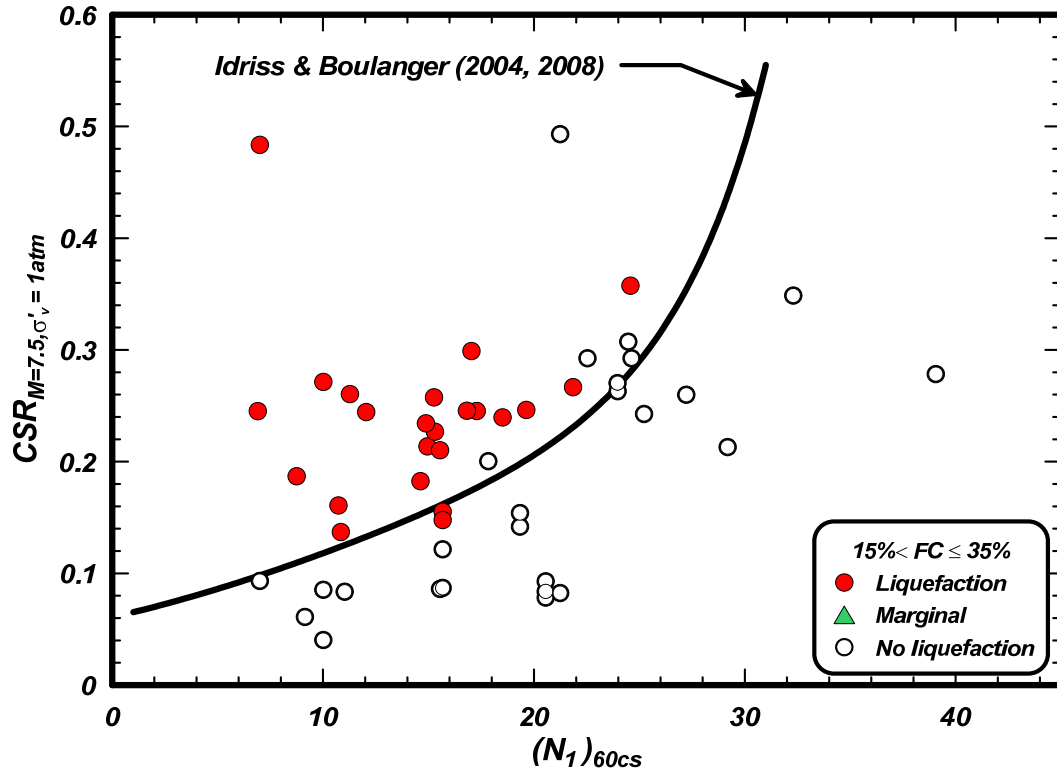
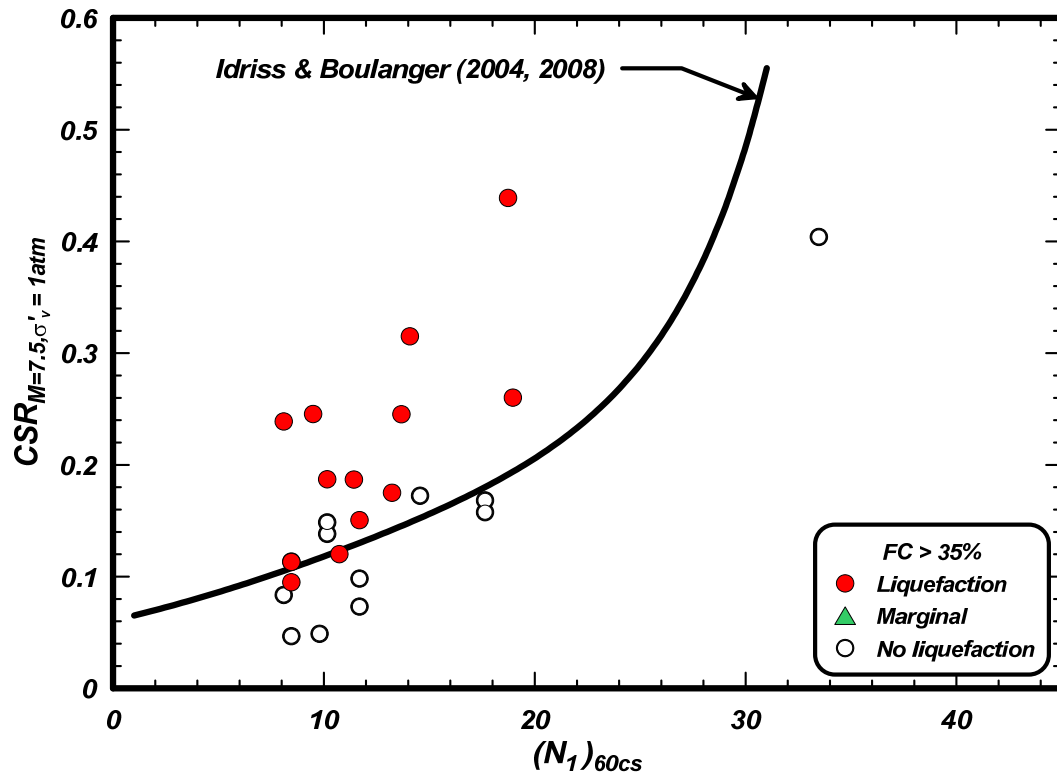


Figure 4.3a-b. Distribution of case history data with different fines contents



(c)



(d)

Figure 4.3c-d. Distribution of case history data with different fines contents

4.1.2. Variation with effective overburden stress

The distribution of data points for different vertical effective stresses is presented in Figures 4.4a through 4.4e showing the data for cases with σ'_v binned between 0-0.4 atm, 0.4-0.6 atm, 0.6-0.8 atm, 0.8-1.2 atm, and >1.2 atm, respectively. There are 1, 5, 0, 1, and 0 liquefaction points below the triggering curve in these five bins, respectively, and there are 4, 6, 5, 2, and 1 no-liquefaction points above the triggering curve, respectively. The bins with σ'_v between 0.4-0.6 atm and 0.6-0.8 atm have the most data, including the majority of the liquefaction cases that lie close to and along the liquefaction triggering curve. The bin with σ'_v between 0.0-0.4 atm has fewer data points, but their positioning relative to the triggering curve is consistent with the data at σ'_v between 0.4-0.8 atm. For the bin with σ'_v between 0.8-1.2 atm, one liquefaction point is slightly below the triggering curve while the other liquefaction points are at least 10-20% above the triggering curve. The bin with $\sigma'_v > 1.2$ atm has the fewest data and has only three liquefaction points, all of which plot well above the triggering curve. Thus, the case histories do not constrain the triggering curve equally well across these stress bins. Nonetheless, the overall distribution of both the liquefaction and no-liquefaction data points relative to the triggering curve across these stress bins appears reasonably balanced.

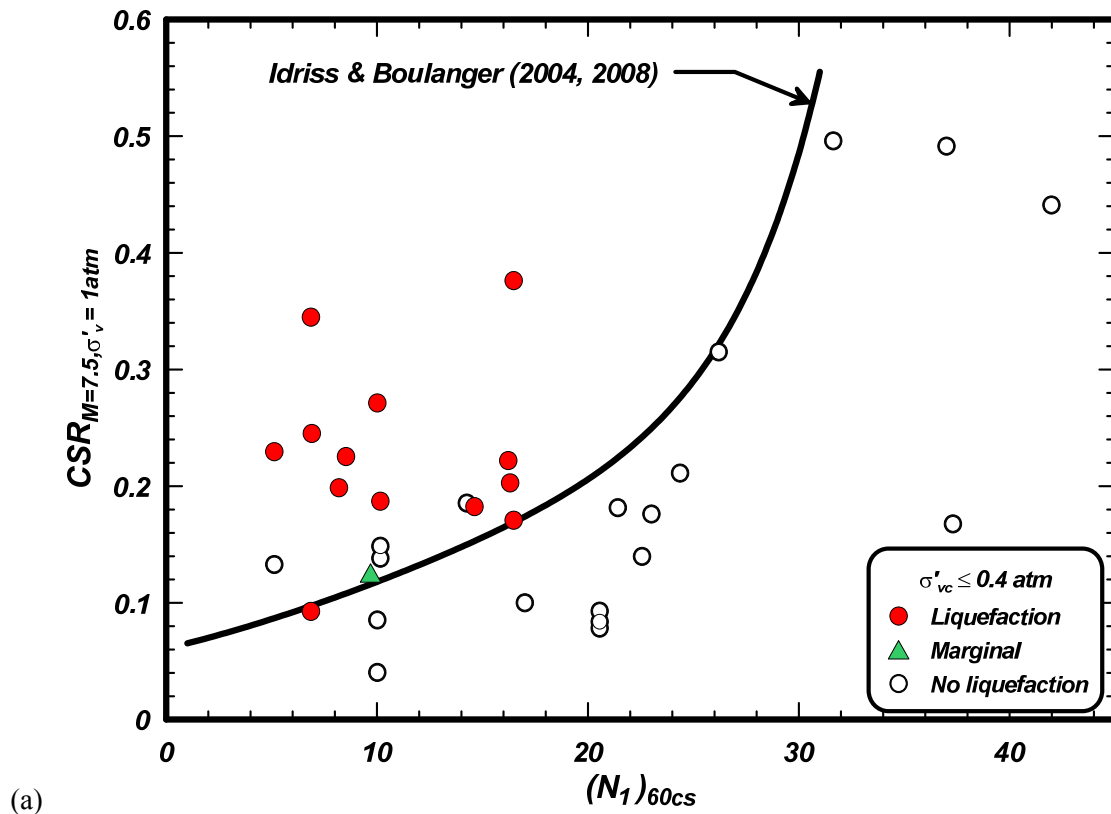
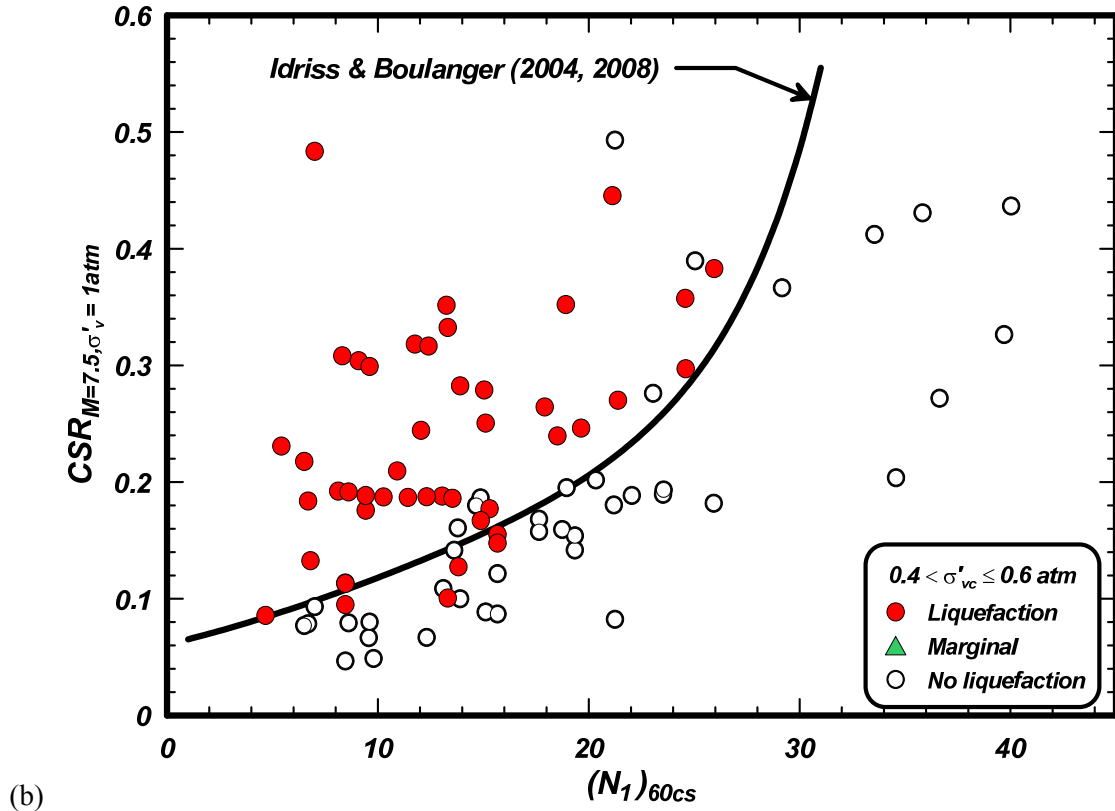
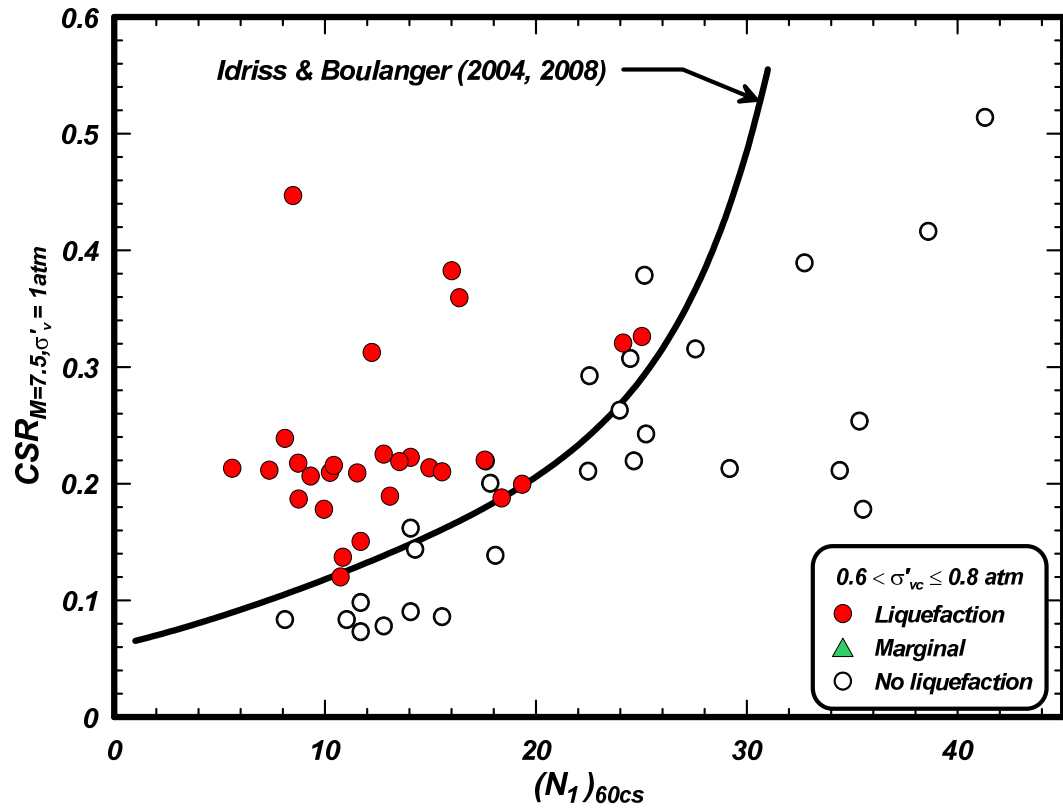


Figure 4.4a. Distribution of case history data with different effective overburden stresses



(b)



(c)

Figure 4.4b-c. Distribution of case history data with different effective overburden stresses

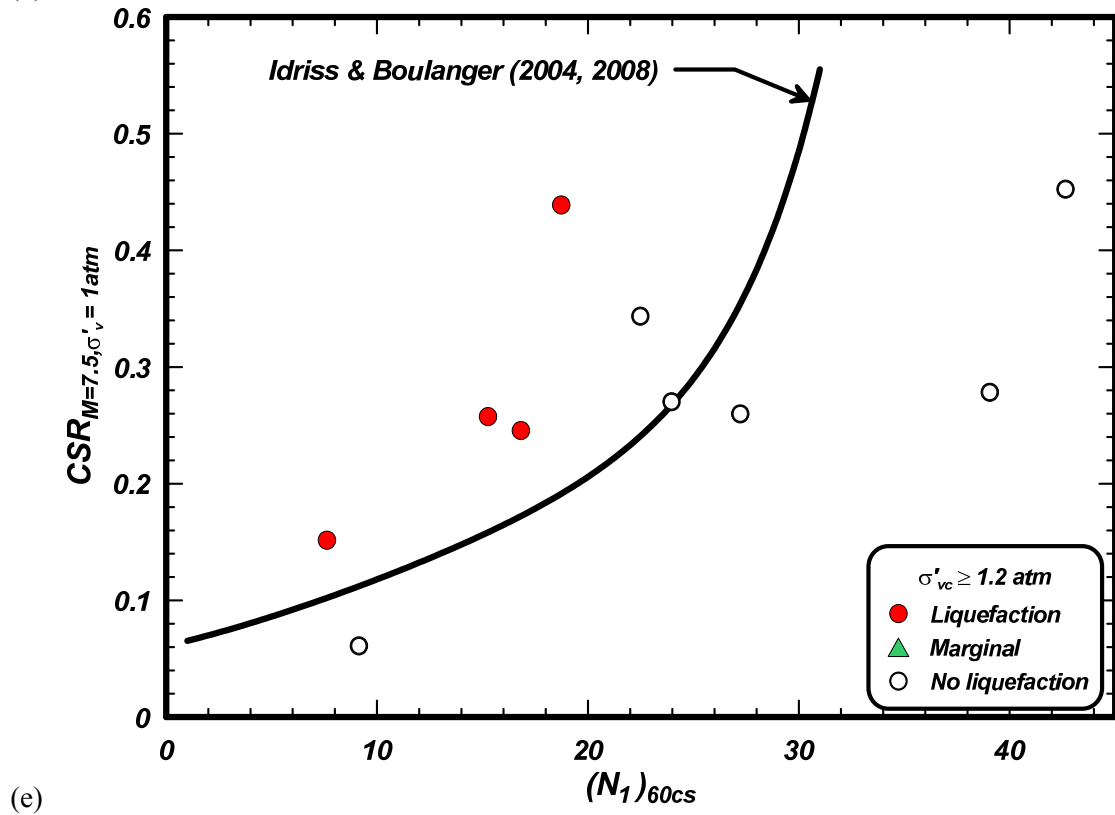
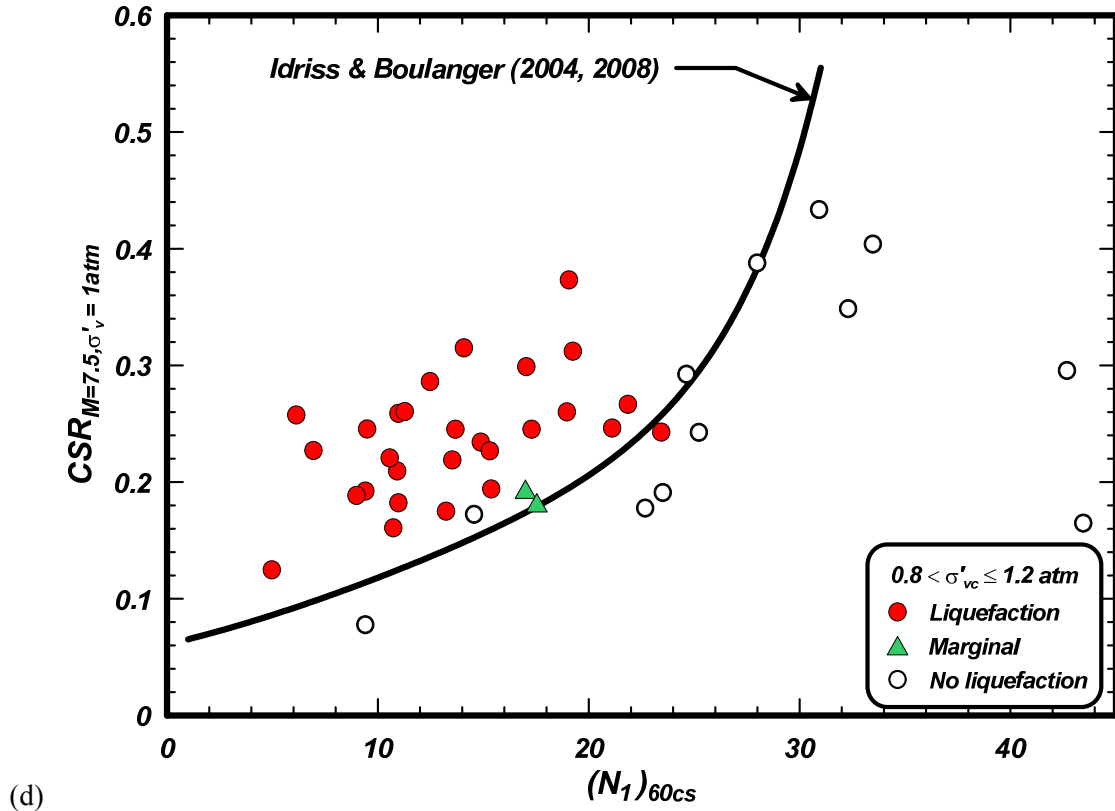


Figure 4.4d-e. Distribution of case history data with different effective overburden stresses

4.1.3. Variation with earthquake magnitude

The distribution of data points for different earthquake magnitudes is presented in Figures 4.5a through 4.5e showing the data for cases with M binned for the ranges of $M < 6.25$, $6.25-6.75$, $6.75-7.25$, $7.25-7.75$, and $M > 7.75$, respectively. There are 2, 2, 2, 1, and 0 liquefaction points below the triggering curve in these five bins, and 1, 2, 10, 5, and 1 no-liquefaction points above the triggering curve, respectively. The liquefaction and no-liquefaction data points show no apparent bias with respect to M in the first four bins (i.e., M up to values of 7.75). The few data points for $M > 7.75$ are also consistent with the triggering curve, but they are not close enough to the curve to constrain it.

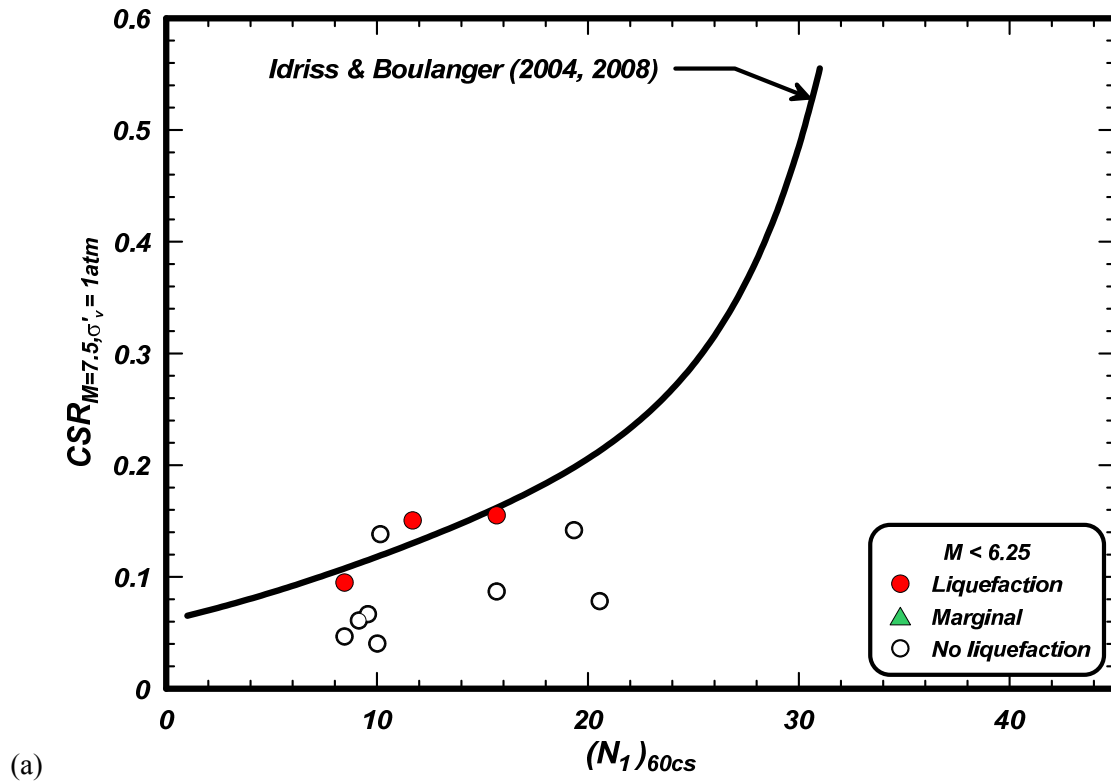


Figure 4.5a. Distribution of case history data with different earthquake magnitudes

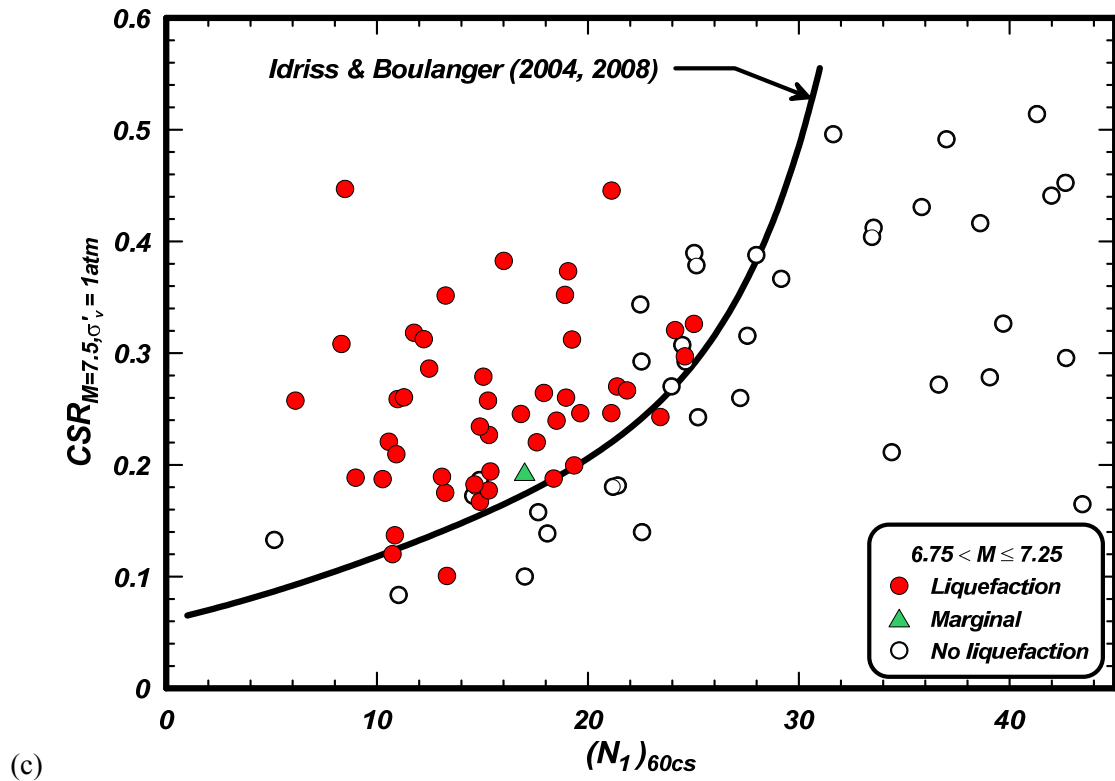
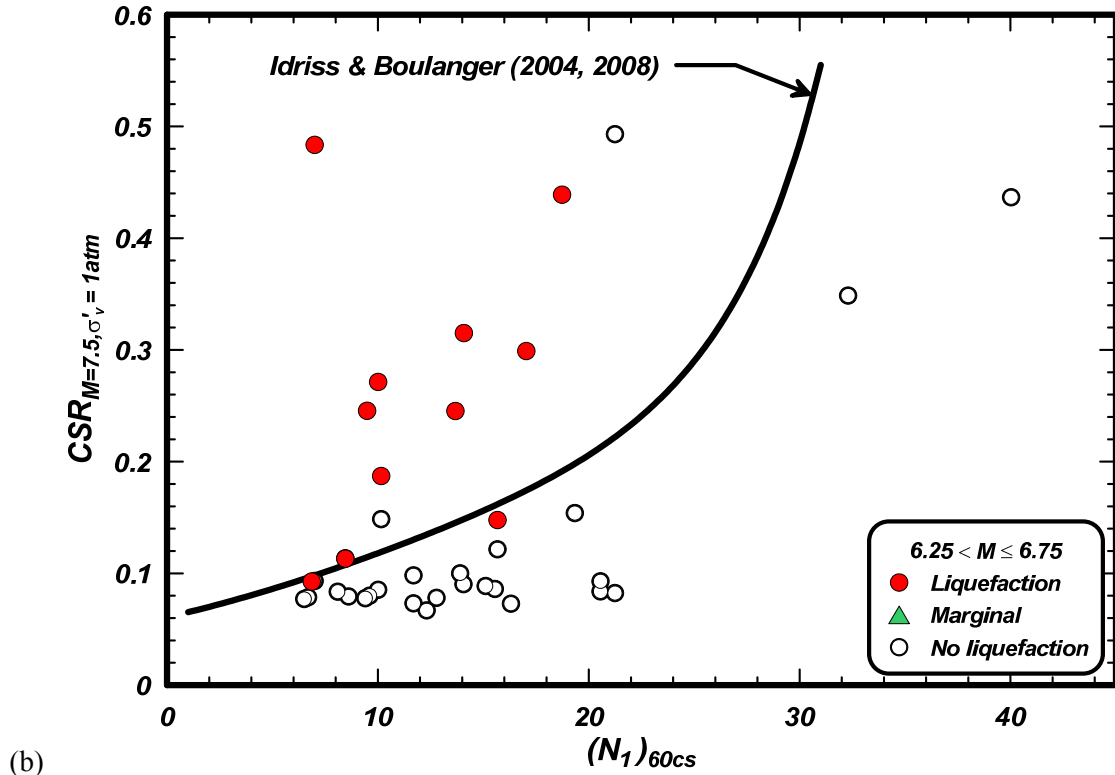


Figure 4.5b-c. Distribution of case history data with different earthquake magnitudes

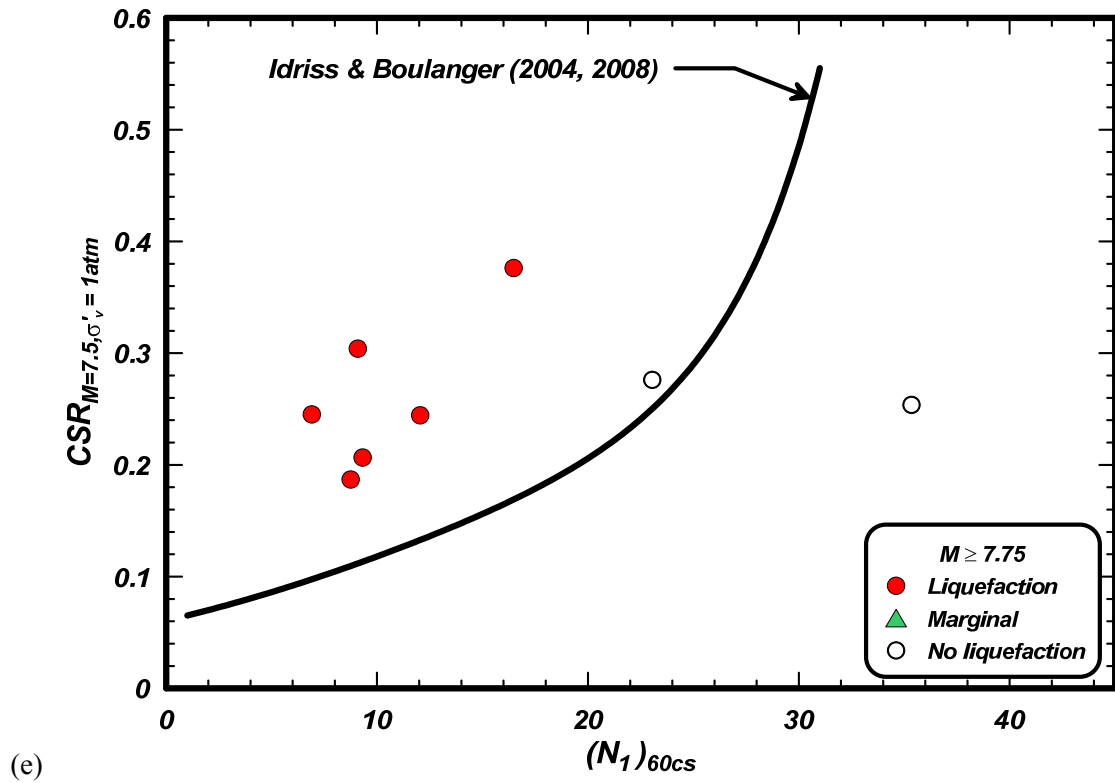
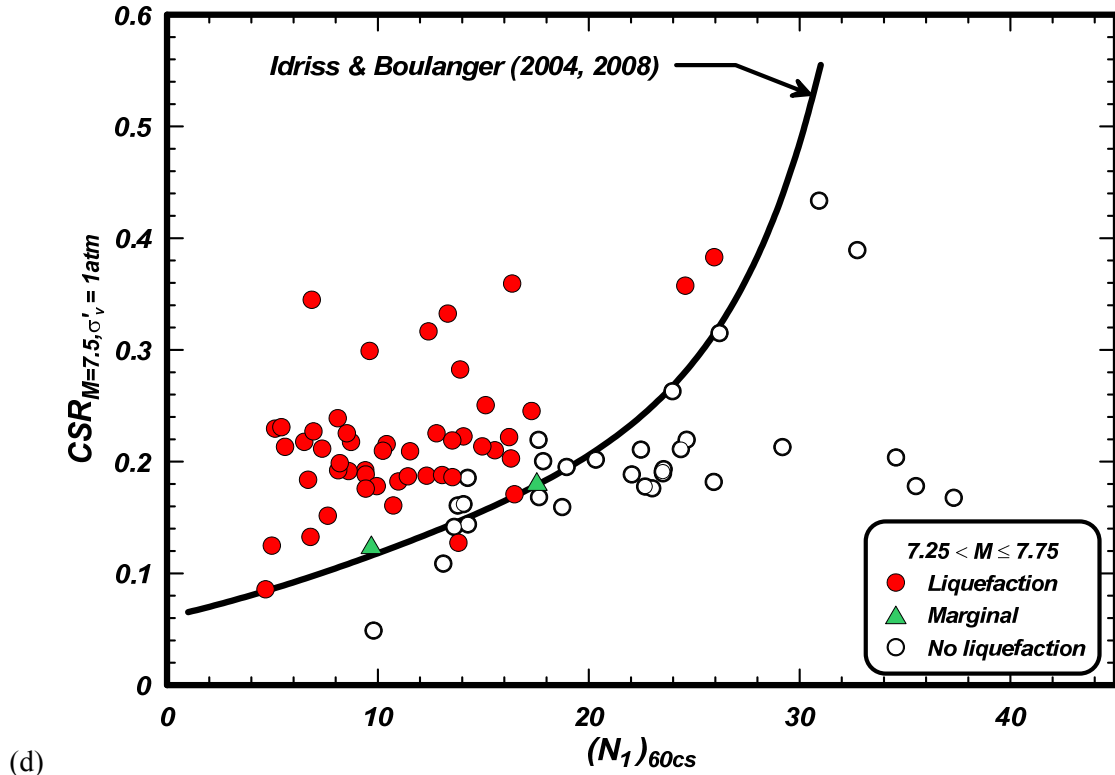


Figure 4.5d-e. Distribution of case history data with different earthquake magnitudes

4.1.4. Variation with SPT procedures

Data from the US and Japan are plotted separately because of the systematic differences in SPT test procedures. The data from U.S. are shown in Figure 4.6a, and the data from Japan are shown in Figure 4.6b. There does not appear to be any differences in the distribution of data from either country, which suggests that the various correction factors of SPT N values are reasonable.

The effects of SPT testing procedures became more widely understood in the 1980s. Accordingly, the data from earthquakes occurring pre-1986 and post-1986 are plotted separately in Figures 4.7a and 4.7b, respectively. Five of the seven liquefaction points that fall below the triggering curve are for pre-1986 events, while the other two are from post-1986 events.

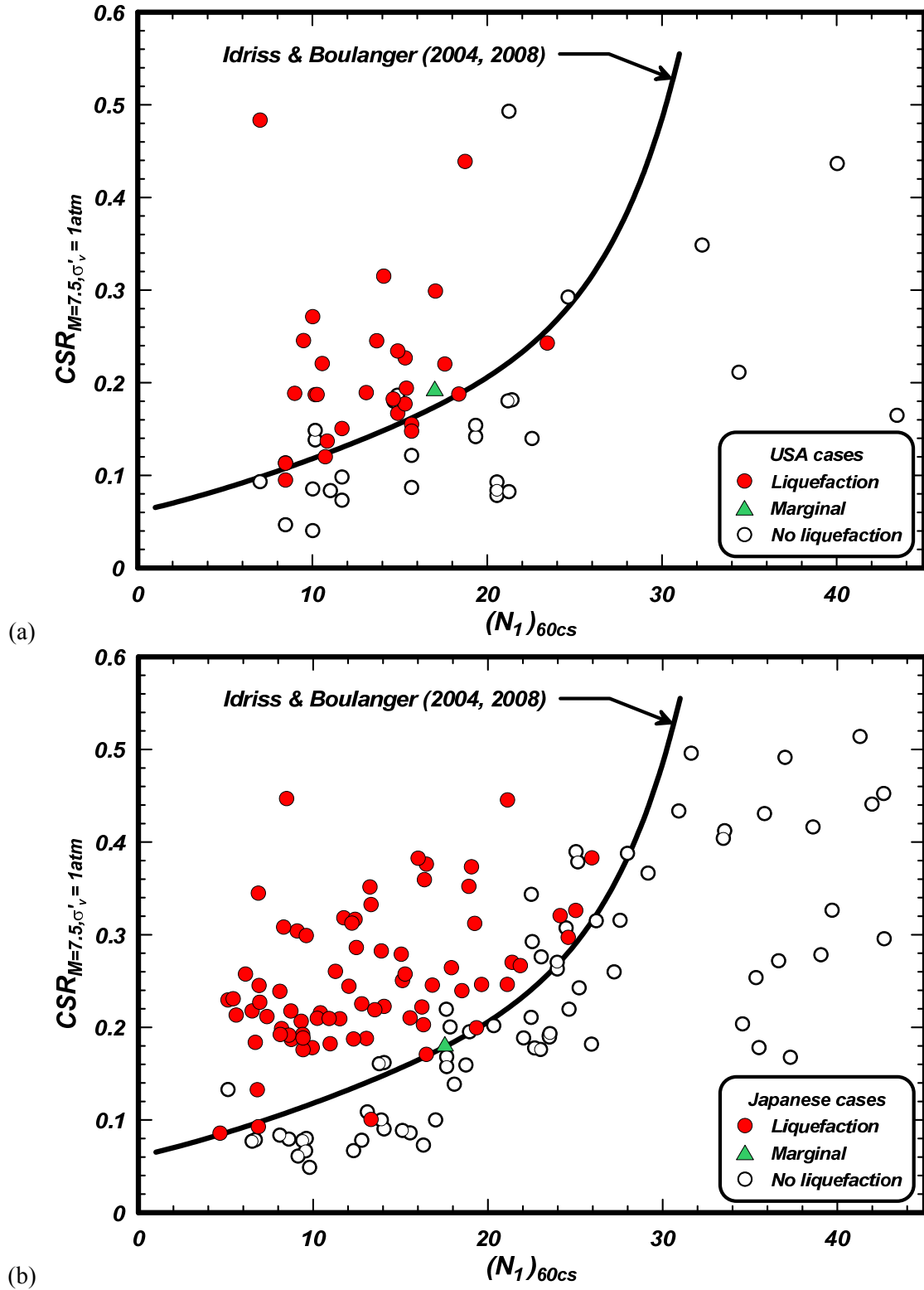
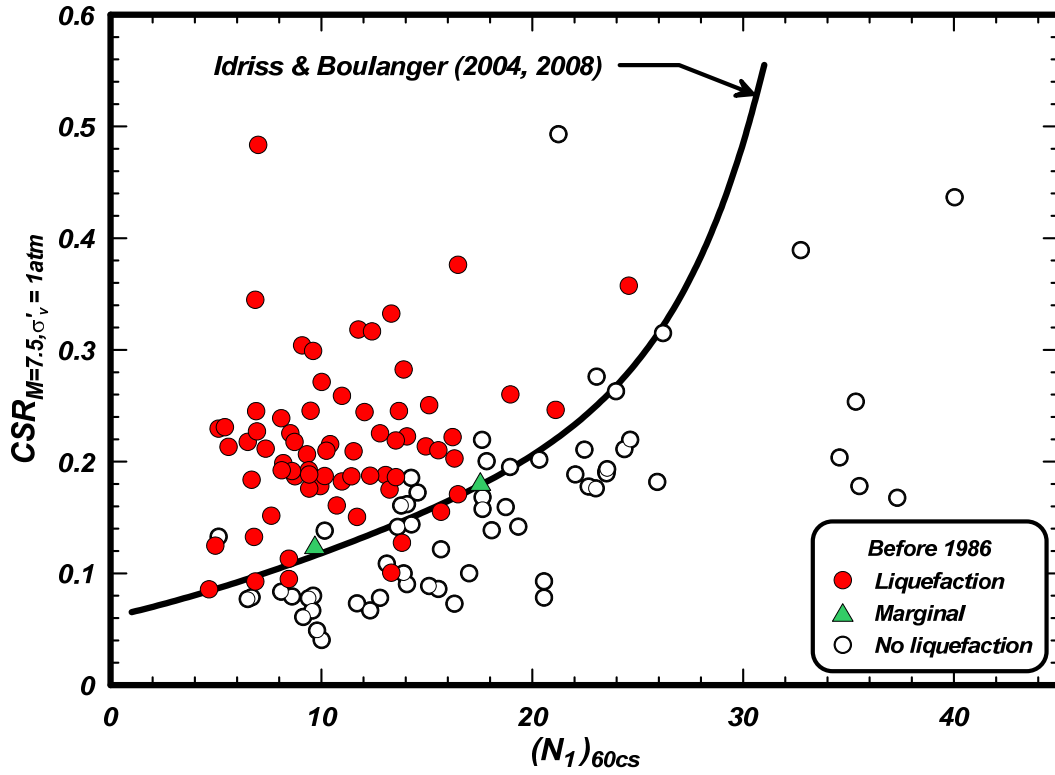
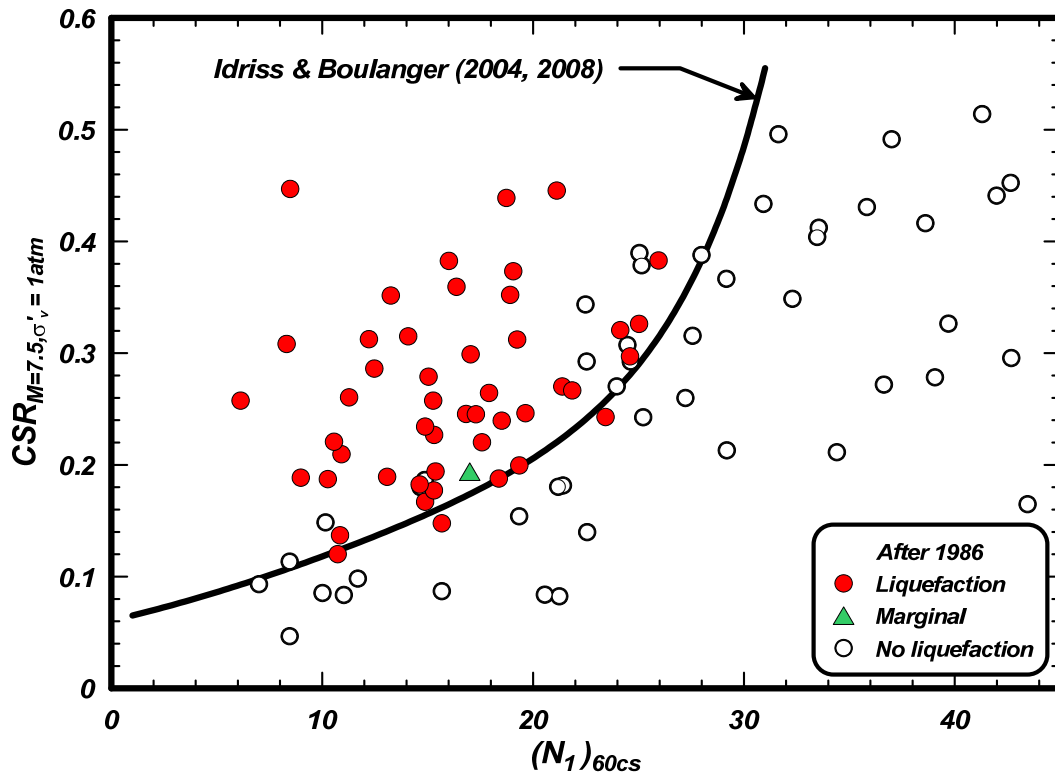


Figure 4.6. Distribution of case history data from the USA and Japan



(a)



(b)

Figure 4.7. Distribution of case history data for earthquakes occurring before and after 1986

4.1.5. Case histories at strong ground motion recording stations

Data from sites at strong ground motion recordings are shown in Figure 4.8; the sites at recording stations include the Akita station, Kawagishi-cho, Kushiro Port, Owi, Port Island, Treasure Island, and the Wildlife B sites. One liquefaction case (Wildlife B in the 1987 Superstition Hills earthquake) is below the triggering curve and one no-liquefaction case (Akita Port station in the 1983 Nihonkai-Chubu earthquake) is above it.

Sites that have a factor of safety against liquefaction of 1.0 for a given earthquake loading would be expected to develop liquefaction near the end of strong shaking and to plot very close to the triggering curve. For example, consider the data points for the Treasure Island, Kushiro Port, and Wildlife B cases identified in Figure 4.8. The Treasure Island (Youd and Carter 2005) and Kushiro Port Seismic Station (Iai et al. 1995) sites are two sites where surface manifestation of liquefaction was not evident, but the characteristics of the strong ground motion recording at the site showed evidence of significant soil softening or liquefaction during or near the end of strong shaking. The pore pressure transducer and accelerometer recordings at Wildlife B indicate that liquefaction developed near the end of strong shaking. The fact the triggering curve passes close to these data points, as shown in Figure 4.8, is consistent with the observations at these sites; e.g., if the true triggering curve was significantly lower than the data points, then liquefaction would have been expected to develop early in shaking.

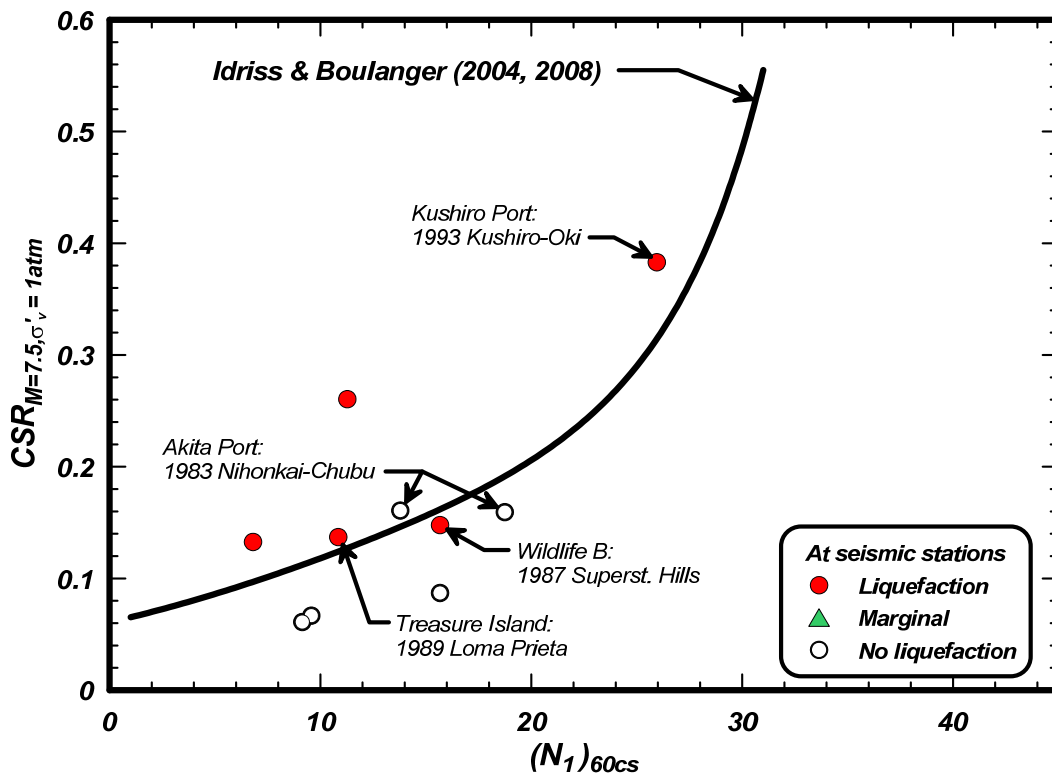


Figure 4.8. Case history data for sites at strong ground motion recording stations

4.1.6. Data from the 1995 Kobe earthquake

Data from sites affected by the 1995 Kobe earthquake, including the proprietary data set provided by Professor Tokimatsu (2010, personal communication), are shown in Figure 4.9. These include 19 cases of "liquefaction" and 25 cases of "no-liquefaction".

These data represent the largest set of cases involving liquefaction and no-liquefaction of higher-blow-count soils under strong shaking (0.35 to 0.7 g). There were no cases of liquefaction for $(N_1)_{60cs}$ greater than 25, which provides some constraint on the upward bend of the liquefaction triggering curve near $(N_1)_{60cs} = 30$. As shown in Figure 4.9, none of the liquefaction cases are below the triggering curve and five no-liquefaction cases are above it.

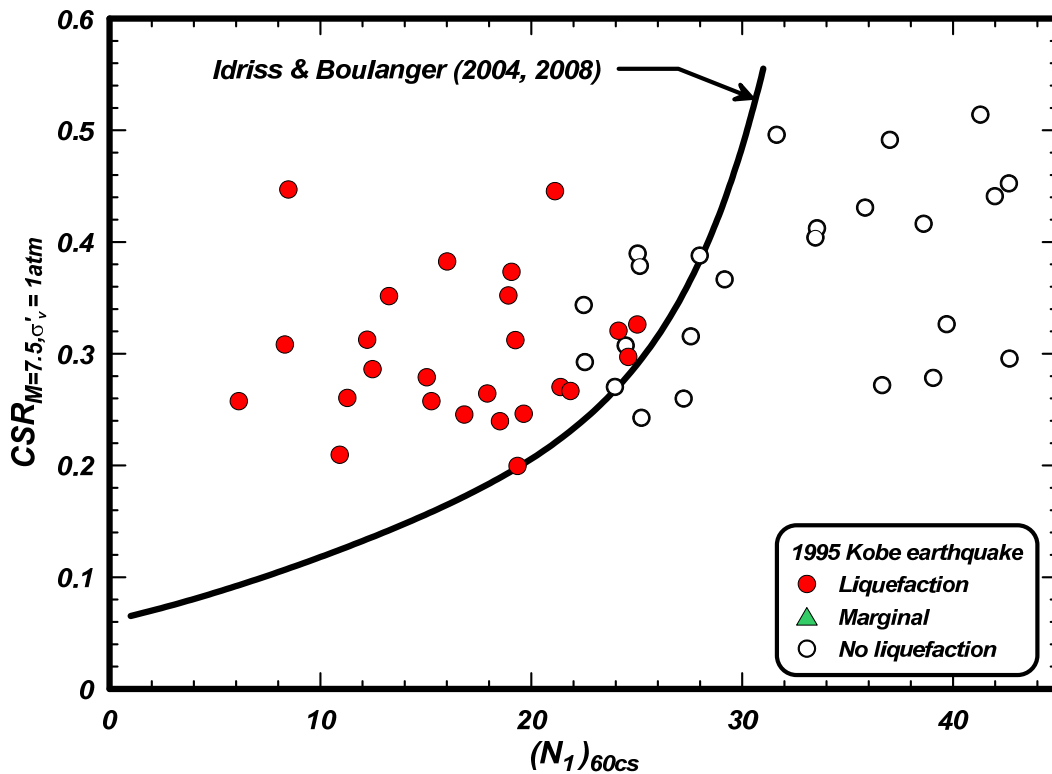


Figure 4.9. Case history data for sites from the 1995 Kobe earthquake

4.2. Sensitivity of case history data points to components of the analysis framework

The sensitivity of the case history data points to the components of the analysis framework is investigated by varying different components of the framework and observing the resulting changes in the case history data points.

4.2.1. Overburden correction factor for penetration resistance, C_N

The case histories were reprocessed using the Liao and Whitman (1986) expression for C_N with a limit of 1.7 as adopted in the NCEER workshop (Youd et al. 2001), i.e.,

$$C_N = \left(\frac{P_a}{\sigma'_{vc}} \right)^{0.5} \leq 1.7 \quad (4.1)$$

The C_N values calculated using this expression are equal to those computed using the Idriss-Boulanger expression for $(N_1)_{60cs} = 13.7$ (i.e., the exponent is equal to 0.5 for this condition). For vertical effective stresses less than 1 atm, the Liao-Whitman expression moves data points with an $(N_1)_{60cs} > 14$ to the right and data points with an $(N_1)_{60cs} < 13$ to the left. The movements in the data points, however, do not affect the overall fit of the data with the liquefaction triggering curve as shown in Figure 4.10.

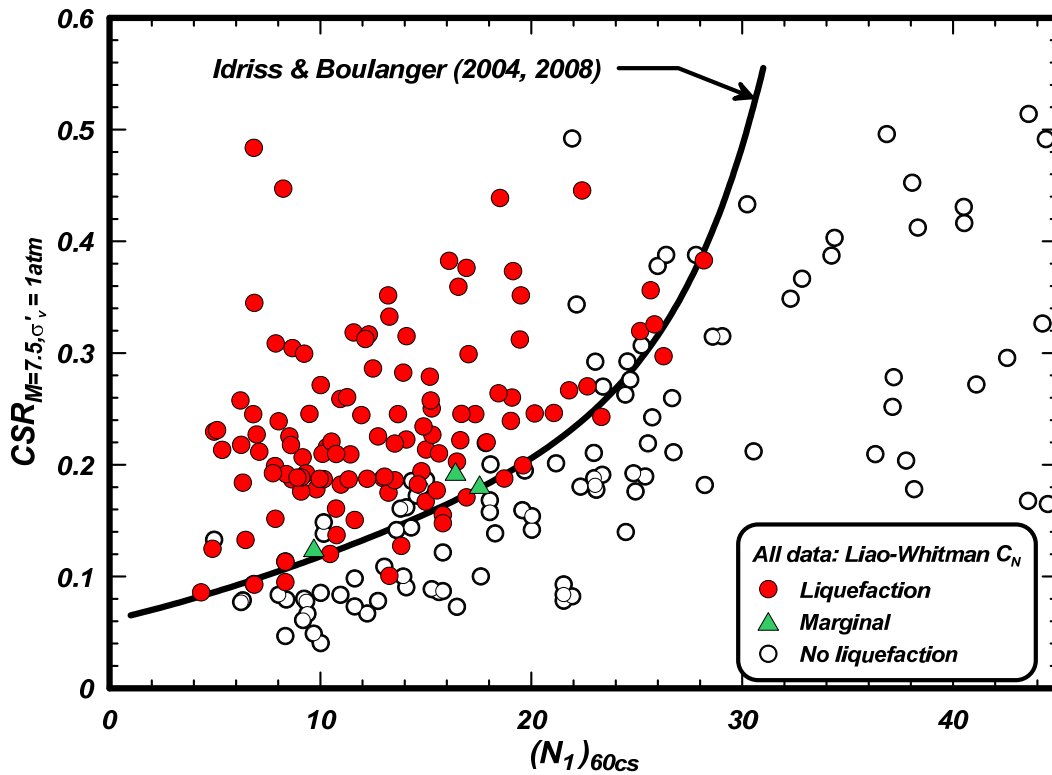


Figure 4.10. Case history data processed using the Liao-Whitman (1986) expression for C_N

4.2.2. Overburden correction factor for cyclic strength, K_σ

The effect of not limiting the overburden correction factor, K_σ , to a maximum value of 1.1 was evaluated by reprocessing the database with no limit. Without any limit, the relationships in the Idriss-Boulanger framework produced 47 cases with K_σ values greater than 1.1, of which only 8 were greater than 1.2 and only 2 were greater than 1.3 (largest value was 1.37). The larger K_σ values caused the corresponding data points to move downward, as shown in Figure 4.11. The reprocessed data are, however, still in good agreement with the liquefaction triggering curve. The higher K_σ values did not affect the fit between the data and the triggering correlation because: (1) the case histories which were most affected were those corresponding to denser soils at the shallowest depths; and (2) the triggering correlation was already reasonably conservatively positioned relative to the case histories with larger $(N_1)_{60cs}$ values at the shallowest depths, as previously shown by the plot for effective overburden stresses, $\sigma'_v < 0.4$ atm, in Figure 4.4a.

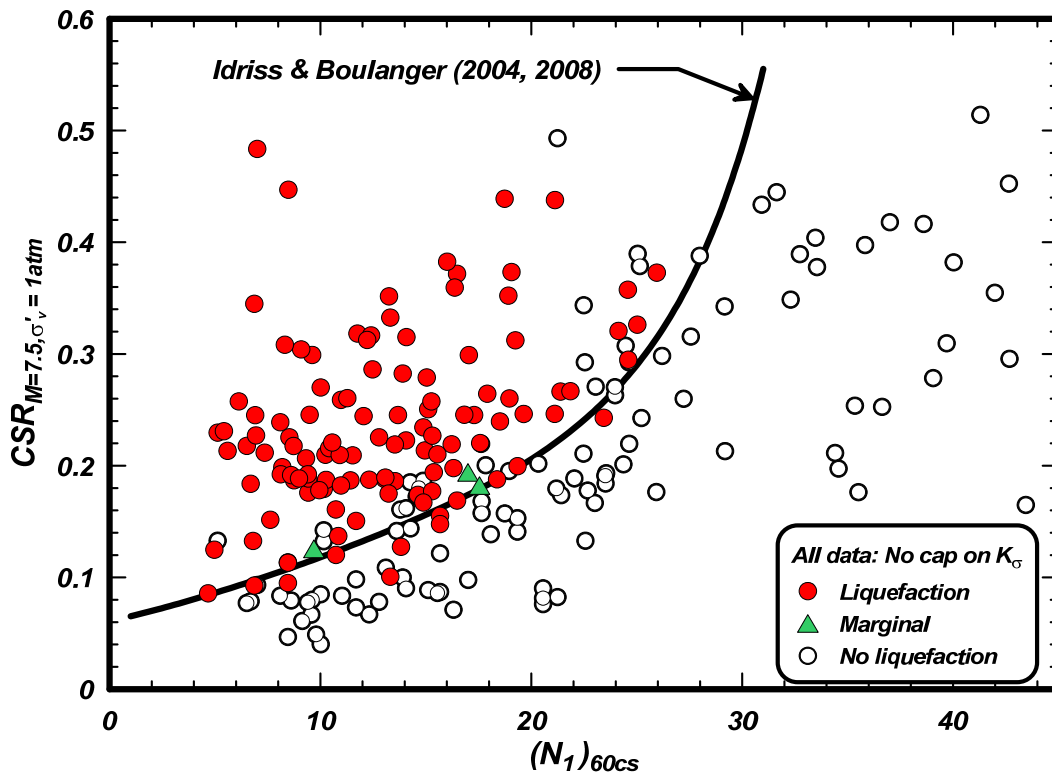


Figure 4.11. Case history data processed with no cap on the maximum value of K_σ

4.2.3. Short rod correction factor, C_R

The short rod correction factor (C_R) is affected by the selection of rod stick-up lengths (i.e., rod length is equal to the stick-up length plus the depth to the SPT test) and the method used to represent the short-rod correction effect (e.g., smooth curve or discrete steps in C_R values). The rod stick-up lengths were taken as 2.0 m for all cases from Japan and 1.5 m for all other cases in the current examination of the case history database. The effect of alternative rod stick-up lengths is illustrated in Figure 4.12 where a value of 2.5 m was assumed for all cases in the database. Use of the longer rod length results in slightly greater $(N_1)_{60cs}$ values at the shallower depths, but the reprocessed data are still in good agreement with the liquefaction triggering curve.

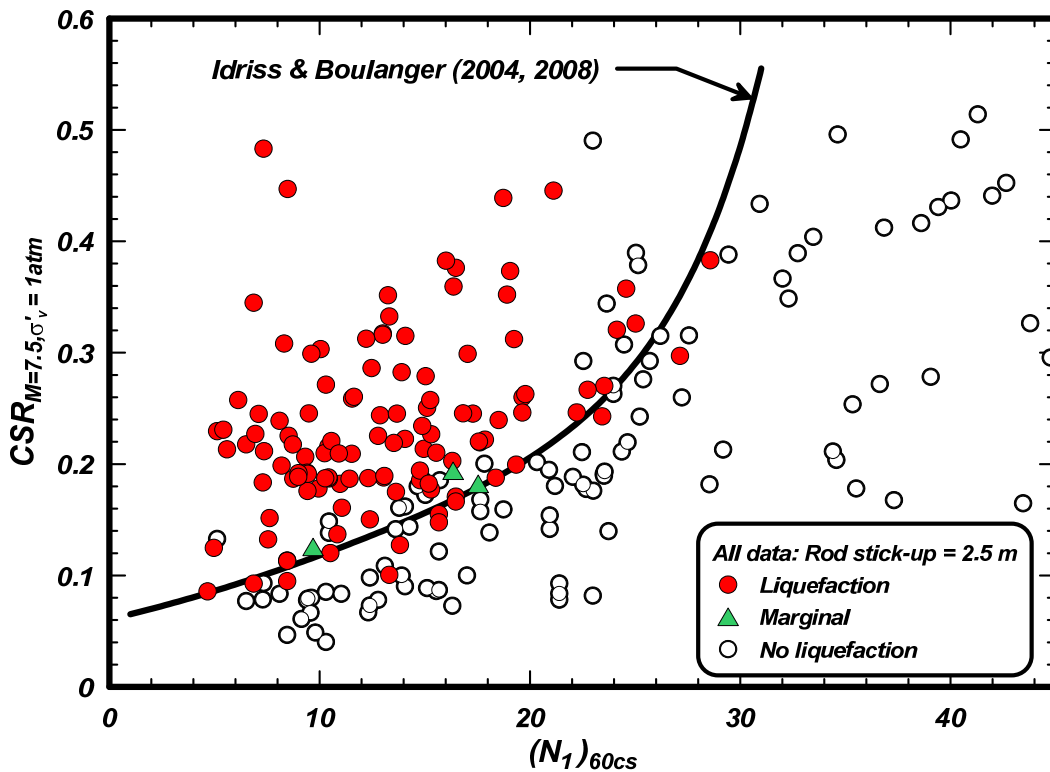


Figure 4.12. Case history data processed with rod stick-up length of 2.5 m

4.2.4. Shear stress reduction factor, r_d

The earthquake-induced cyclic stress ratio for each case history is dependent on the PGA, the shear stress reduction factor (r_d), and the ratio of total to effective vertical overburden stresses. The effect of different r_d relationships on the interpretation of the case history database is evaluated in this section, after providing some necessary background on the Idriss (1999) and Kishida et al. (2009b) relationships.

Idriss (1999) r_d relationship

The r_d relationship developed by Idriss (1999) utilized results from six different soil profiles with a set of about 60 motions, as described in Appendix B. The relationships proposed by Idriss (1999) corresponded to about the 67th percentile r_d values from these analyses, with this percentile chosen so that the curve for $M = 7.5$ was consistent with the earlier Seed and Idriss (1971) r_d curve (i.e., Figure 2.1). The median r_d values were, however, only slightly lower than the 67th percentile values, as shown by the comparison in Figure 4.13. The differences between the 50th percentile and 67th percentile curves progressively increases from 0% at the ground surface to about 5% at a depth of 10 m for all M .

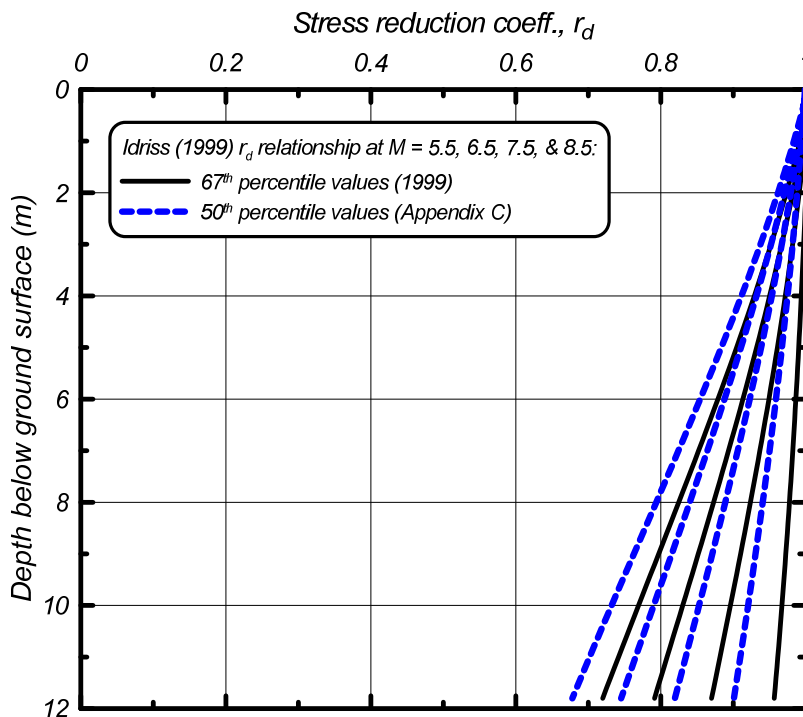


Figure 4.13. Idriss (1999) r_d relationship and the median values from those analyses for $M = 5.5$ to 8.5

Kishida et al. (2009) r_d relationship

Kishida et al. (2009a, 2009b) developed an r_d relationship based on regression of results of one-dimensional equivalent-linear site response analyses for a wide range of soil profiles, motions, and realizations of soil properties using Monte Carlo simulations. Eighteen soil profiles with five different realizations of soil properties were shaken with 264 ground motions, for a total of about 23,000 analyses. Input parameters for their r_d relationship were the PGA, the average shear wave velocity, and the spectral

ratio parameter [$S_1 = Sa(1.0s)/Sa(0.2s)$, where $Sa(1.0s)$ is the 5%-damped spectral acceleration for a period of 1 sec and $Sa(0.2s)$ is the 5%-damped spectral acceleration for a period of 0.2 sec]. More details of the development of this r_d relationship are provided in Kishida et al. (2009a, 2009b).

The regression model for r_d was based on superimposing the response of the soil column (with an average shear wave velocity \bar{V}_s and fundamental period T'_s above the depth z of interest) to the largely-independent frequencies of 1 Hz and 5 Hz, with the relative strengths of these two frequencies described by the spectral ratio parameter S_1 . The resulting model was,

$$r_d = \left[\frac{1}{2} \left(\frac{\sin\left(\frac{\pi T'_s}{2 \cdot 0.2}\right)}{\frac{\pi T'_s}{2 \cdot 0.2}} + \frac{\sin\left(\frac{\pi T'_s}{2 \cdot 1.0}\right)}{\frac{\pi T'_s}{2 \cdot 1.0}} \right) \right]^a + \frac{0.833}{2} \left(\frac{1 - S_1}{1 + S_1} \right) \left(\frac{\sin\left(\frac{\pi T'_s}{2 \cdot 0.2}\right)}{\frac{\pi T'_s}{2 \cdot 0.2}} - \frac{\sin\left(\frac{\pi T'_s}{2 \cdot 1.0}\right)}{\frac{\pi T'_s}{2 \cdot 1.0}} \right) \quad (4.2)$$

where

$$T'_s = \min\left(\frac{4z}{\bar{V}_s}, 0.6s\right) \quad (4.3)$$

$$a = 0.651 \cdot PGA^{0.0473} \quad (4.4)$$

$$S_1 = \frac{Sa(1.0s)}{Sa(0.2s)} \quad (4.5)$$

The variations of S_1 with earthquake magnitude, estimated using the NGA relationships developed for lower velocity sites (Abrahamson and Silva 2008, Boore and Atkinson 2008, Campbell and Bozorgnia 2008, Chiou and Youngs 2008), are shown in Figure 4.14 for $V_{S30} = 150, 200, \text{ and } 250 \text{ m/s}$ and $PGA = 0.1, 0.2, \text{ and } 0.3 \text{ g}$. The parameter S_1 depends most strongly on M , and can be reasonably approximated using the expression,

$$S_1 = \frac{M^{2.36}}{155} \quad (4.6)$$

The dependence of S_1 on other factors, such as V_{S30} , PGA , and earthquake source characteristics, were of lesser importance to the computation of r_d , such that the above expression is a reasonable approximation for the purpose of computing r_d .

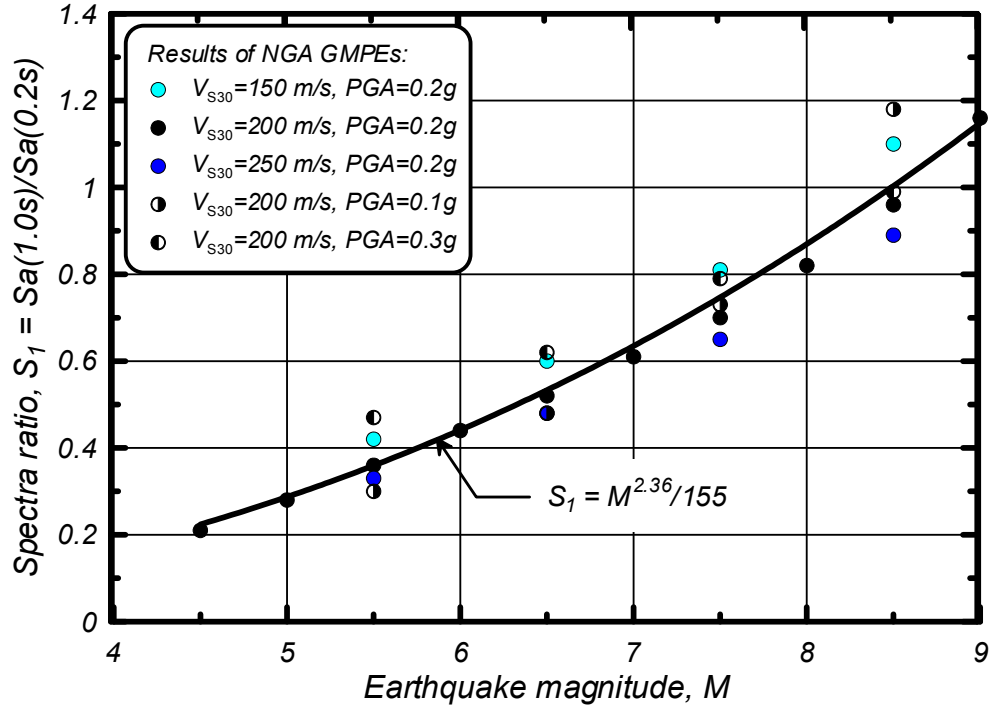


Figure 4.14. Variation of spectral ratio S_1 with M based on NGA relationships

Comparison of r_d values

Differences between the r_d values computed using the Kishida et al. (2009b), Idriss (1999), and Cetin et al. (2004) relationships are illustrated for depths less than 12 m in Figures 4.15 through 4.17. The focus of these comparisons is on depths less than 12 m because this is the depth range of importance to the interpretation of the liquefaction case histories.

The Kishida et al. relationship is first compared to the Idriss relationship in Figure 4.15 for $M = 5.5$ to 8.5 , a $PGA = 0.2$ g, an average V_s of 160 m/s, and depths up to 12 m. The Kishida et al. curves show a smaller spread with M and are generally lower than the Idriss relationship, which is consistent with the fact that the Idriss relationship was developed to represent about the 67th percentile values, whereas the results shown for the Kishida et al. relationship are the expected values ($\approx 50^{\text{th}}$ percentile).

The three r_d relationships are then compared in Figure 4.16 showing results for $M = 6.5$ and 7.5 with a $PGA = 0.2$ g and average V_s of 160 m/s. The average V_s value of 160 m/s is also the value recommended by Cetin et al. for use with their relationships when detailed information on the V_s profile is not available. As shown in these figures, the curves produced using the Kishida et al. relationship are similar to those produced using the Idriss relationship at shallow depths and become more intermediate to the curves produced by the Idriss and Cetin et al. relationships at larger depths.

The Kishida et al., Cetin et al., and Idriss relationships are also compared in Figure 4.17 for softer soil conditions (V_s of 120 m/s), with the results showing that the Kishida et al. r_d values remains intermediate to the other two relationships. These figures also illustrate how the Cetin et al. relationship predicts a much more rapid reduction in r_d values in the upper 2-3 m than is obtained with the other relationships. A rapid drop in r_d near the ground surface implies that the Cetin et al. analyses have produced much shorter wave lengths near the ground surface than were obtained in either of the other studies. Alternatively,

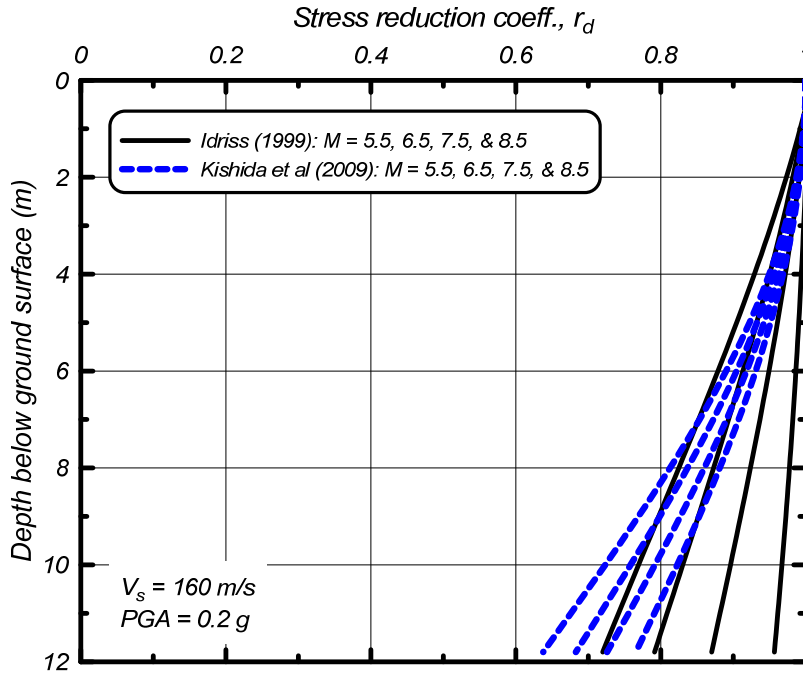


Figure 4.15. Idriss (1999) and Kishida et al. (2009b) r_d relationships compared for $M = 5.5$ to 8.5 with an average $V_s = 160 \text{ m/s}$ and $\text{PGA} = 0.2 \text{ g}$

some functional forms for the regression models may produce a bias at shallow depths because the equation must start with $r_d = 1.0$ at the ground surface, and then drop to the lower r_d values at larger depths. Wave propagation theory suggests that the r_d curve should be vertical at the ground surface, and the functional form in the Cetin et al. relationship deviates from that expectation the most. The plots of residuals from the regression model development presented in Kishida et al. (2009b) show no significant bias at shallow depths. Cetin et al. do not present residuals for their model; therefore, the potential for bias in their model at these shallow depths cannot be assessed from their results.

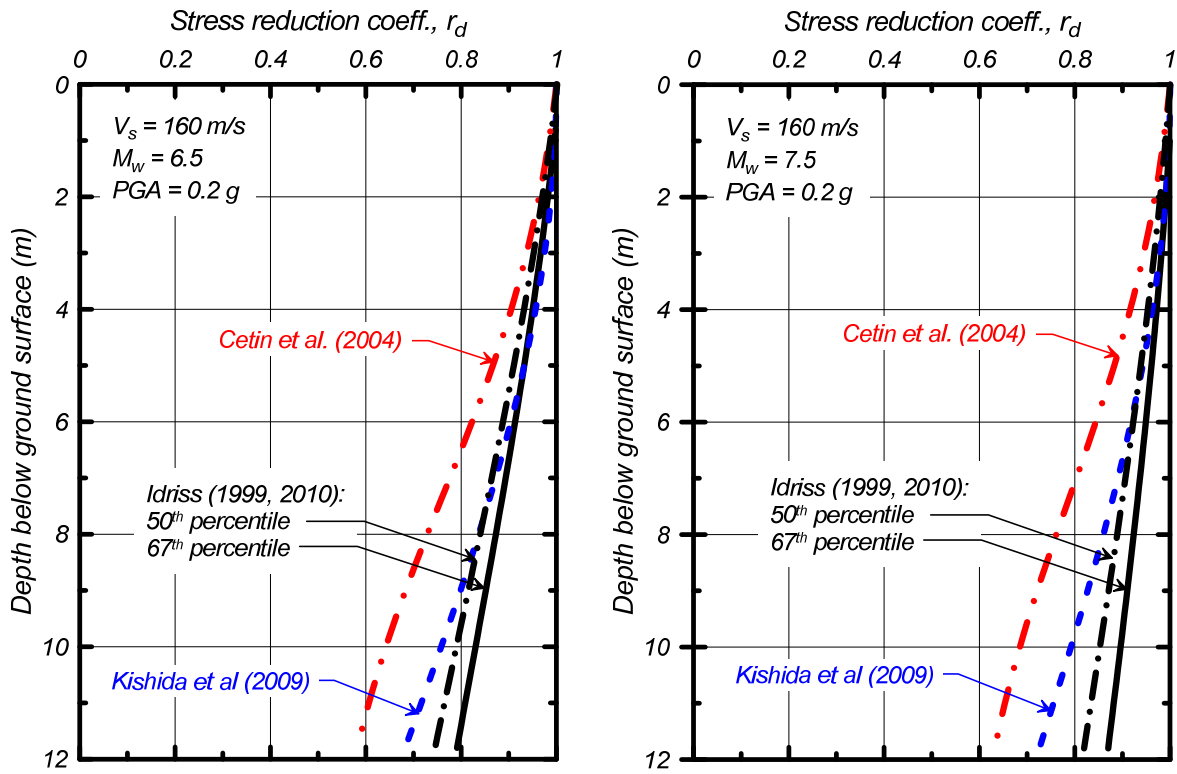


Figure 4.16. Different r_d relationships compared for $M = 6.5$ and 7.5 and average $V_s = 160$ m/s

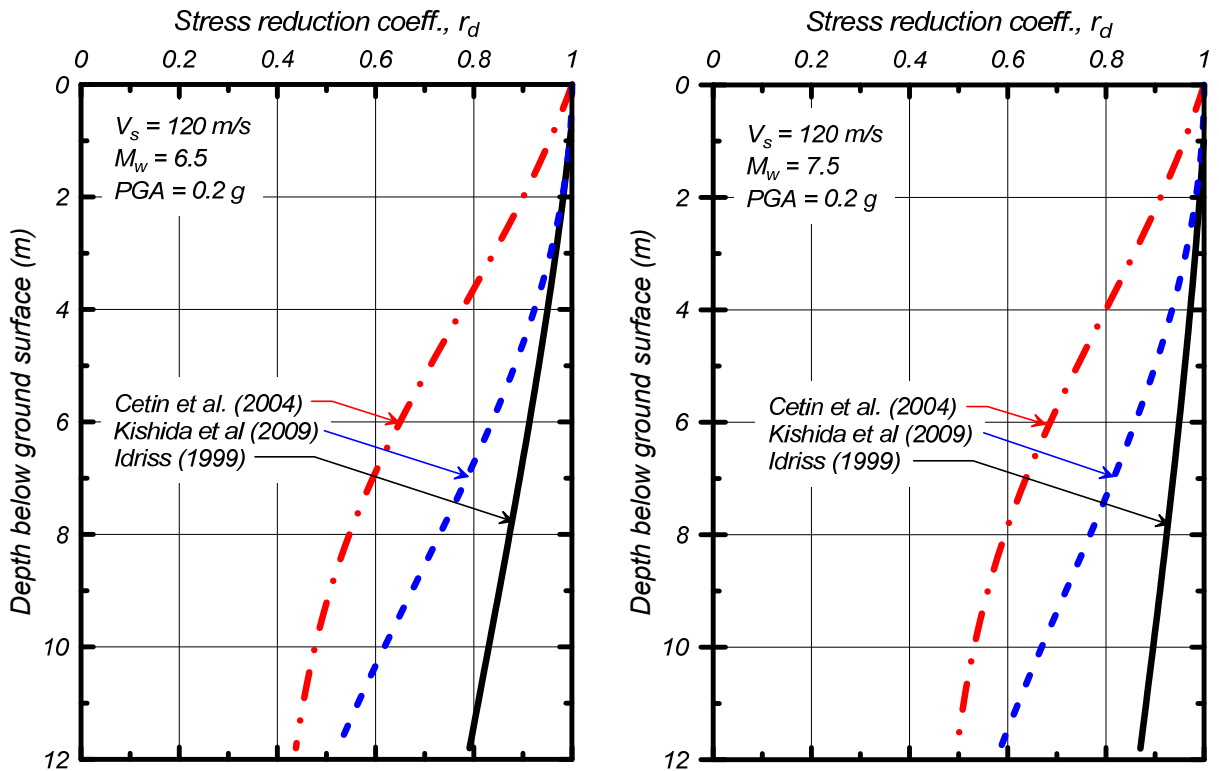


Figure 4.17. Different r_d relationships compared for $M = 6.5$ and 7.5 and average $V_s = 120$ m/s

Effect of r_d on case history interpretations

The effect of the r_d relationship on the case history interpretations was evaluated using the Kishida et al. (2009b) relationship with the above expression for S_1 and an average V_s of 160 m/s. The r_d values computed using Kishida et al.'s relationship are lower than the values computed using the Idriss (1999) relationship, but these differences did not significantly affect the fit between the case histories and the triggering correlations as shown in Figure 4.18. The reasons for the lower r_d curves having only a small effect are: (1) the case histories which were most affected by the lower r_d curves are those that correspond to the larger depths, and (2) the triggering correlation was already reasonably conservatively positioned relative to the case histories at these depths, as previously shown by the plots for effective overburden stresses, $\sigma'_v = 0.8-1.2$ atm and $\sigma'_v > 1.2$ atm, in Figures 4.4(c) and 4.4(d), respectively.

The effects of using the median r_d values from the Idriss (1999) analyses (Appendix B) are evaluated in Section 6 as part of the development of a probabilistic relationship. Using the median r_d values caused the probabilistic liquefaction triggering curves to shift lower by only 2% relative to those derived using the Idriss (1999) relationship.

The effect of using the r_d relationship by Cetin et al. (2004) with their recommended default average V_s of 160 m/s is illustrated in Figure 4.19. The number of points falling below the Idriss-Boulanger triggering curve increased. The lower data points would be consistent with a triggering curve that is about 10% lower than the Idriss-Boulanger triggering curve.

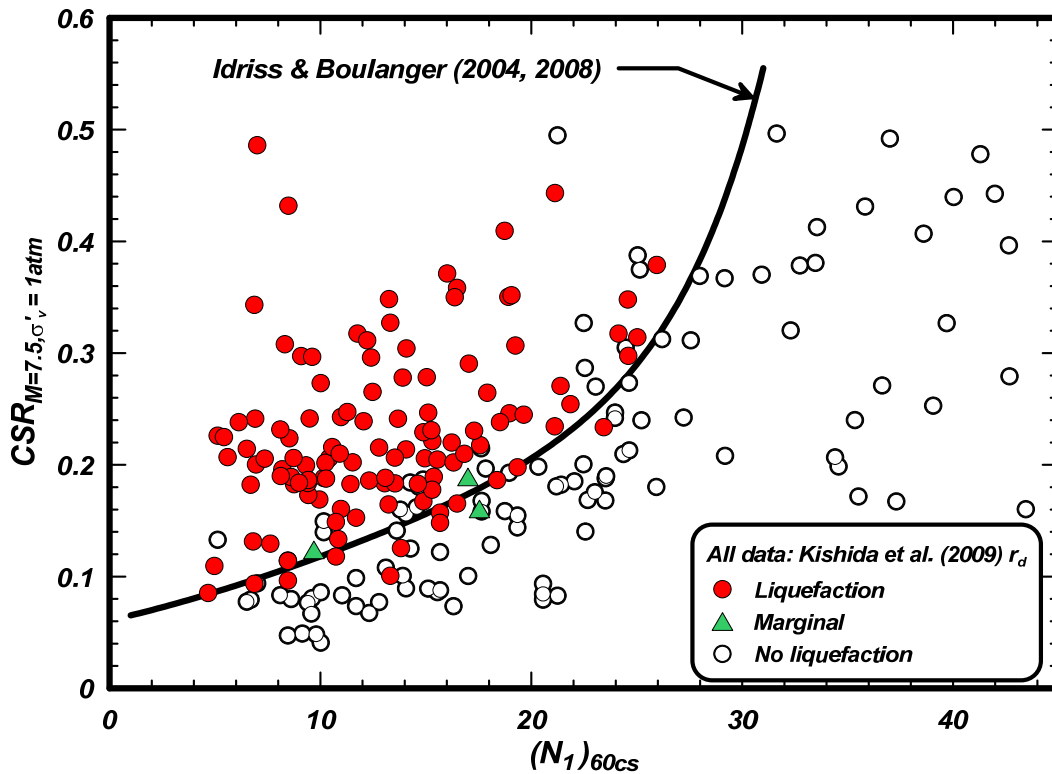


Figure 4.18. Case history data processed with the r_d relationship by Kishida et al. (2009b)

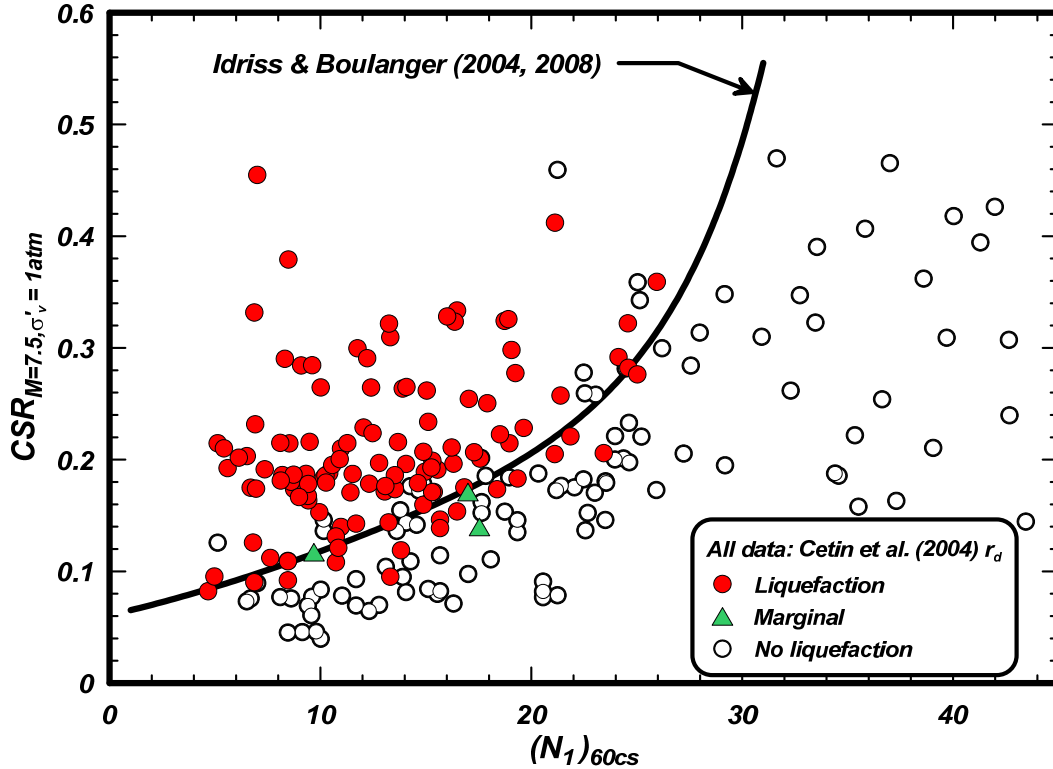


Figure 4.19. Case history data processed with the r_d relationship by Cetin et al. (2004)

4.2.5. Equivalent clean sand adjustment, $\Delta(N_1)_{60}$

The effect of using the equivalent clean sand adjustment, $\Delta(N_1)_{60}$, from the Youd et al. (2001) procedure versus the Idriss and Boulanger (2004, 2008) procedure is illustrated in Figure 4.20 for all sands with FC greater than 15%. The effect was relatively small except for a few data points. In particular, there are two liquefaction data points with $(N_1)_{60cs}$ values of about 16 which fall below the liquefaction triggering curve with either adjustment procedure, but fall slightly farther below the triggering curve when using the Youd et al. adjustment.

The reason for this relatively small effect on the data points can be understood by considering the differences in the two adjustment procedures (Figure 2.5) and the distribution of case history data versus fines content (Figures 3.8 and 4.3). The equivalent clean sand adjustments by these two procedures are almost equal for $FC < 15\%$, as shown in Figure 2.5, and thus the data points for $FC < 15\%$ are essentially unaffected by the choice of adjustments. This is why the data points for $FC < 15\%$ are omitted from Figure 4.20. For $FC > 15\%$, the difference in the two adjustments depends on the $(N_1)_{60}$ values. For sands with $(N_1)_{60}$ values of about 5, the two adjustments are almost equal over the full range of FC. For sands with $(N_1)_{60} \approx 10$, the $\Delta(N_1)_{60}$ by the Youd et al. (2001) procedure is somewhat greater than that obtained using the Idriss-Boulanger procedure as FC increases; e.g., at $FC > 35\%$, the $\Delta(N_1)_{60}$ values would be 7.0 and 5.6, respectively. For sands with $(N_1)_{60}$ values of about 20, the differences in the $\Delta(N_1)_{60}$ by the two procedures increases; e.g., at $FC > 35\%$, the $\Delta(N_1)_{60}$ values would now be 9.0 and 5.6, respectively. Thus, the differences in the equivalent clean sand adjustments only become significant when the FC is greater than about 20% and the $(N_1)_{60}$ values are greater than about 10.

The case history database, however, includes very few data points with FC greater than 25% and $(N_1)_{60}$ values greater than 15, as previously shown by the plot of FC versus $(N_1)_{60}$ in Figure 3.8. In combination

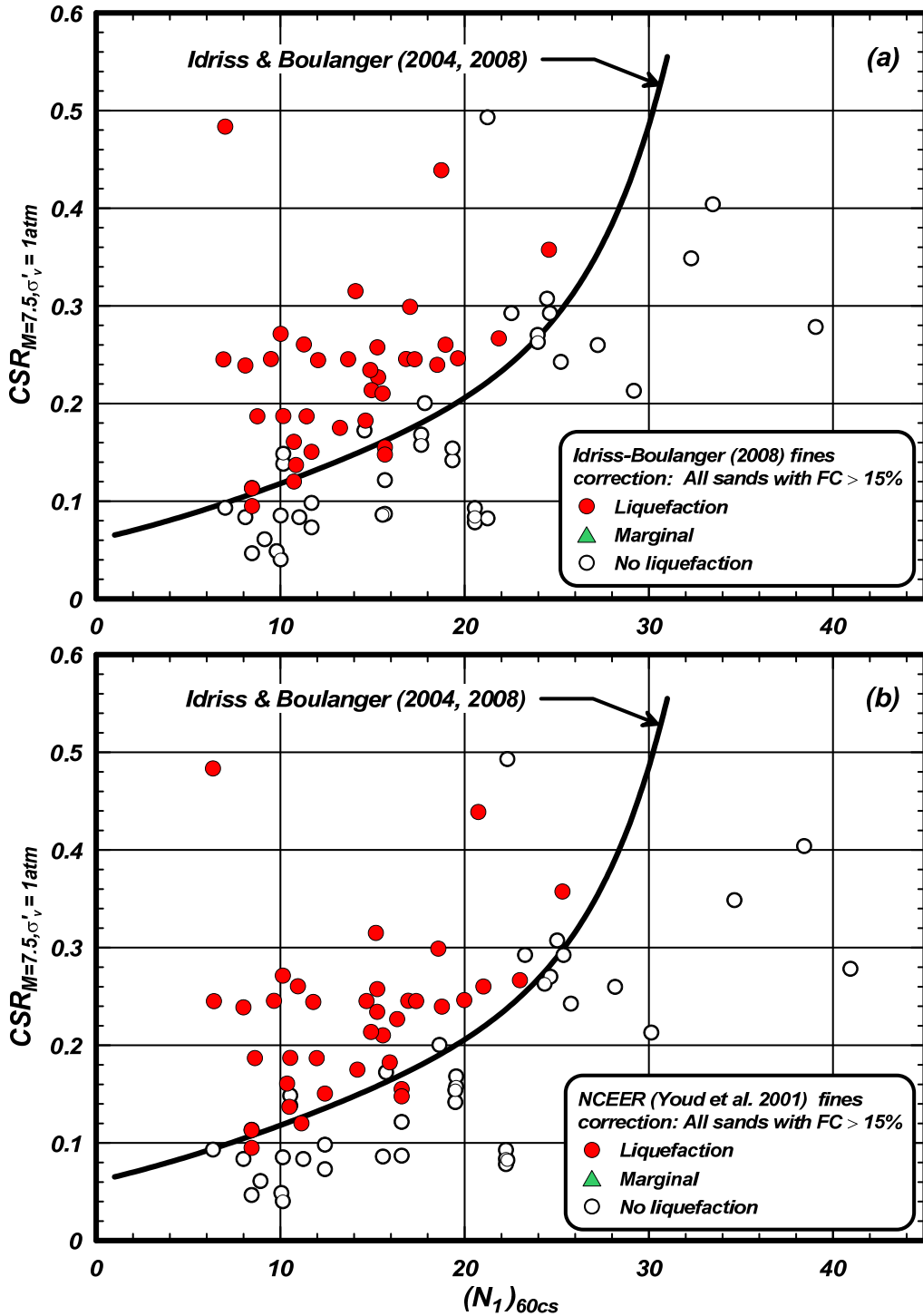


Figure 4.20. Case history data for sands with $FC > 15\%$ processed with the fines content correction $\Delta(N_1)_{60}$ of: (a) Idriss-Boulanger (2004, 2008) and (b) NCEER (Youd et al. 2001)

with the distribution of these data points about the triggering curve, as previously shown in Figure 4.3, the case history data do not provide definitive constraints on the empirically-derived equivalent clean sand adjustments at high FC and high $(N_1)_{60}$ values.

In summary, the equivalent clean sand adjustment by Idriss and Boulanger (2004, 2008) provides a slightly more conservative interpretation of the case history database (Figure 4.20) along with more conservative guidance on extrapolating this effect to sands with high FC and high $(N_1)_{60}$ values (Figure 2.5) than is provided by the Seed et al. (1984)/Youd et al. (2001) adjustment.

4.3. Summary of re-examination of case history database

The updated SPT-based liquefaction triggering database was first examined relative to the SPT-based liquefaction triggering curve by Idriss and Boulanger (2004, 2008). The distributions of the data relative to the triggering curves are shown to be reasonably consistent across the range of case history conditions (e.g., fines content, overburden stress, earthquake magnitude) and data sources (e.g., U.S. versus Japanese case histories, data for sites at strong ground motion recording stations, data from the 1995 Kobe earthquake). No biases in the distributions were identified, suggesting that the functional forms used in the Idriss-Boulanger procedure continue to be reasonable.

The interpretation of the database was also shown to be relatively insensitive to reasonable variations in the components of the analysis framework. For example, the position of the triggering curve would not be affected by switching to the Liao and Whitman (1986) C_N relationship, by omitting a cap on the K_σ relationship, by increasing the estimated rod stick up length to 2.5 m for all cases, or by using the r_d relationship by Kishida et al. (2009b). The effect of using the Cetin et al. r_d relationship would increase the number of liquefaction cases below the triggering curve, but the differences would represent a relatively small contribution to the differences between the liquefaction triggering curves by Idriss and Boulanger (2004, 2008) and Cetin et al. (2004). The effect of using the equivalent clean sand adjustment by Seed et al. (1984)/Youd et al. (2001) was shown to move a couple of liquefaction points slightly farther below the triggering curve, but to otherwise have had a small effect on the interpretation of the case history database.

It is important, however, to note that the differences in the components (e.g., C_N , K_σ , r_d , MSF, $\Delta(N_1)_{60}$) of liquefaction analysis procedures recommended by various investigators become more important when the procedures are used to extrapolate outside the range of the case history data (e.g., depths greater than 12 m). These issues are discussed in greater detail in Section 7.

5. COMPARISON WITH RESULTS OF TESTS ON FROZEN SAND SAMPLES

SPT-based relationships for evaluating the cyclic resistance ratio of clean sands have also been developed from the results of cyclic laboratory tests on specimens obtained using frozen sampling techniques (e.g., Yoshimi et al. 1994, Pillai et al. 1994). This section contains a re-examination of available data for frozen sand samples, a comparison of those data to the Idriss and Boulanger (2004, 2008) liquefaction triggering correlation, and a detailed examination of the unique set of data for large overburden stresses at Duncan Dam.

5.1. Examination of data from tests on frozen sand samples

5.1.1. Test data and published correlations

Frozen sampling techniques have been shown to produce high-quality samples of loose to dense clean sands when properly implemented (e.g., Singh et al. 1982; Goto and Nishio 1988; Yoshimi et al. 1989, 1994). The volumetric expansion of saturated clean sand during one-dimensional freezing has been shown to depend on the confining (or surcharge) pressure on the sand, as illustrated in Figure 5.1 (Yoshimi et al. 1978). At low confining stresses, the freezing process can produce significant volumetric expansion, which loosens the sand and reduces sample quality. As confining stress increases, the volumetric expansion during one-dimensional freezing progressively decreases. For the sands shown in Figure 5.1, the volumetric expansion becomes negligible for confining stresses greater than about 10 to 50 kPa, with the critical value of confining stress being different for the three sands. Specimens that have been one-dimensionally frozen under sufficient confinement, and hence have developed very small net volumetric strains, have been shown to retain the memory of prior stress and strain loading histories throughout the sampling, handling, and mounting processes (e.g., Singh et al. 1982; Goto and Nishio 1988; Yoshimi et al. 1989, 1994).

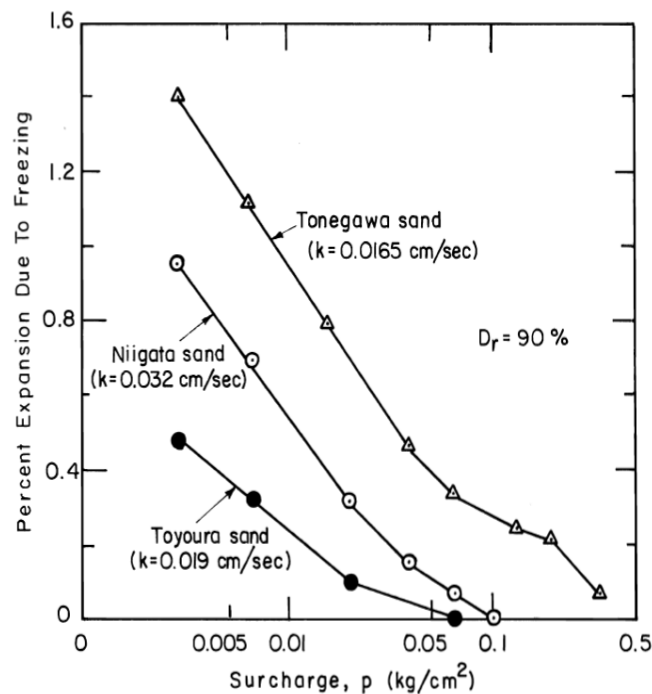


Figure 5.1. Effect of surcharge pressure on expansive strains in sands during one-dimensional freezing (after Yoshimi et al. 1978; redrawn in Singh et al. 1979)

Results of field and laboratory test programs using frozen sand sampling techniques are summarized in Tables 5.1 and 5.2. The results by Yoshimi et al. (1989), Tokimatsu et al. (1990), Iai and Kurato (1991), and Iai et al. (1995) involving cyclic triaxial tests (TX) are summarized in Table 5.1. The cyclic strengths from these studies correspond to 15 uniform loading cycles to cause double-amplitude axial strains of 5%; this failure criterion is comparable to a single-amplitude shear strain of 3.75% assuming that cyclic strains were reasonably symmetric (i.e., single-amplitude axial strains were 2.5%) and Poisson's ratio is 0.5 for undrained conditions. The results by Pillai and Stewart (1994) for Duncan Dam, involving both cyclic triaxial and cyclic simple shear (DSS) tests, are summarized in Table 5.2. The failure criteria from this study correspond to a single-amplitude axial strain of 2.5% for TX tests and a single-amplitude shear strain of 4% for DSS tests. The cyclic resistance ratios from the isotropically-consolidated undrained (ICU) triaxial tests are converted to equivalent DSS strengths using the relationship,

$$CRR_{DSS} = \left(\frac{1 + 2K_o}{3} \right) CRR_{ICU-TX} \quad (5.1)$$

where K_o is the coefficient of lateral earth pressure at rest. The value of K_o was taken as possibly ranging from 0.5 to 1.0 in-situ, as was suggested by Yoshimi et al. (1989, 1994). The data by Pillai and Stewart (1994) for Duncan Dam involved cyclic DSS and TX tests, from which the correction of TX to DSS conditions was established directly. The data by Pillai and Stewart (1994) also included tests on specimens at consolidation stresses ranging from 2 to 12 atm; these data are re-examined in greater detail in Section 5.2 in this report. The DSS and equivalent DSS strengths from all studies are multiplied by a factor of 0.9 to account for the effects of two-directional shaking in-situ. The cyclic strengths are further corrected to an equivalent effective confining stress of 1 atm by dividing each by the K_o factor determined using the relationships by Boulanger and Idriss (2004); this final correction was very small for most of the available data because they were performed at effective consolidation stresses close to 1 atm, with the exception of the Duncan Dam tests which had been conducted at stresses up to 12 atm.

The effects of volumetric expansion during in-situ radial freezing are expected to be small for the majority of the studies summarized in Tables 5.1 and 5.2 because the effective overburden stresses were greater than 50 kPa for all but one site (Yamanashi Prefecture site in Table 5.1). Nonetheless, there is always a concern that some expansion could develop due to adverse freezing conditions in-situ. If volumetric expansion does occur during freezing, the specimen can be expected to also develop volumetric contraction strains during thawing under confinement in the laboratory. The anticipated net effect of any disturbance induced by volumetric expansion during in-situ freezing would be an increase in cyclic strengths for very loose sands and a decrease in cyclic strengths for dense sands.

Table 5.1. Summary of SPT and triaxial test data from studies using frozen sand sampling

Site	Soil	Depth (m)	σ'_v (kPa)	FC (%)	SPT data					TX tests	Conversion to in-situ with $\sigma'_v = 1$ atm		
					N_m	C_R	C_N	$(N_1)_{60}$	$(N_1)_{60cs}$	$CRR_{N=15}$	K_σ	$CRR_{M=7.5, \sigma=1}$ if $K_o = 0.5$	$CRR_{M=7.5, \sigma=1}$ if $K_o = 1.0$
Yamanashi Pref. ¹	Fill	4.0	36	1	1	0.86	1.70	2	2	0.13	1.07	0.07	0.11
Showa Bridge ¹	Natural soil	9.8	98	0	18	1	1.01	24	24	0.27	1.00	0.16	0.24
Meike ¹	Natural soil	6.9	78	0	16	0.96	1.12	22	22	0.26	1.04	0.15	0.23
"	Natural soil	7.9	88	0	24	0.98	1.05	32	32	0.39	1.03	0.23	0.34
"	Natural soil	9.0	98	0	26	1	1.01	34	34	0.37	1.01	0.22	0.33
Niigata Station ¹	Natural soil	9.7	106	0	32	1	0.99	41	41	0.91	0.99	0.55	0.83
Higashi-Ohgishima 1 ²	Densified soil	8.6	77	3	25	1	1.09	36	36	0.85	1.07	0.48	0.71
"	Densified soil	9.3	83	6	24	1	1.07	33	33	0.45	1.05	0.26	0.39
"	Densified soil	10.0	90	4	20	1	1.05	27	27	0.43	1.02	0.25	0.38
Higashi-Ohgishima 2 ³	Fill	8.0	92	1	3	0.99	1.06	4	4	0.13	1.01	0.08	0.12
Kushiro Port ⁴	Natural soil	4.5	51	5	14	0.95	1.33	23	23	0.247	1.10	0.13	0.20
"	Natural soil	5.5	61	5	36	0.95	1.14	51	51	>1.0	1.15	>0.8	>0.8
"	Natural soil	6.6	72	5	34	0.95	1.09	46	46	0.446	1.10	0.24	0.36

Notes:

- (1) Yoshimi et al. (1994)
- (2) Tokimatsu et al. (1990)
- (3) Iai and Kurata (1991)
- (4) Iai et al. (1995)
- (5) C_R values from Yoshimi (1994) for first nine cases; and based on Youd et al. (2001) for last four cases.
- (6) Idriss and Boulanger (2008) relationships for C_N , FC correction, and K_σ .

Table 5.2. Summary of SPT and laboratory test data for Duncan Dam

σ'_v (kPa)	SPT data				DSS tests		Triaxial tests		Conversion to $\sigma'_v = 1 \text{ atm}$		
	C_N	N_{60}	$(N_1)_{60}$	$(N_1)_{60cs}$	Lab $CRR_{N=10}$	Field $CRR_{M=7.5}$	Lab $CRR_{N=10}$	Field $CRR_{M=7.5}$	In-situ $CRR_{M=7.5}$	K_σ	In-situ $CRR_{M=7.5, \sigma=1}$
200	0.70	16.4	11.5	11.6	0.14	0.118	0.169	0.121	0.120	0.93	0.128
400	0.50	26.5	13.3	13.4	0.149	0.126	0.171	0.123	0.124	0.86	0.145
600	0.42	34.0	14.1	14.2	0.143	0.121	0.168	0.120	0.120	0.81	0.149
1200	0.30	49.1	14.7	14.8	--	--	0.170	0.122	0.122	0.73	0.168

Notes:

- (1) Original data from Pillai and Byrne (1994).
- (2) Average ratio of $CRR_{DSS}/CRR_{TX} = 0.85$ is used to convert triaxial test results to field simple shear conditions.
- (3) Cyclic strengths multiplied by 0.937 to convert from 10 to 15 equivalent uniform cycles (based on slope of CRR versus number of uniform cycles curves).
- (4) Cyclic strengths multiplied by 0.90 to convert from 1D to 2D cyclic loading conditions.
- (5) Final value for in-situ $CRR_{M=7.5}$ taken as average of strengths from DSS and Triaxial tests.

The CRR values for 15 uniform loading cycles to cause $\approx 3.8\%$ shear strain in undrained cyclic loading are plotted versus the corrected SPT $(N_1)_{60cs}$ values in Figure 5.2, along with the proposed relationships by Tokimatsu and Yoshimi (1983) and Yoshimi et al. (1994). The results of the cyclic triaxial tests are shown with the range of equivalent field CRR values that were computed using the estimated range of in-situ K_σ values of 0.5 and 1.0. The DSS and TX data from Pillai and Stewart (1994) were not included in the data set used by Yoshimi et al. (1994), but they are in excellent agreement with the Tokimatsu and Yoshimi (1983) and Yoshimi et al. relationships for the range of $(N_1)_{60cs}$ applicable to the Duncan Dam data. The data points from Kushiro Port (Iai et al. 1995) were also not included in the data set used by Yoshimi et al. (1994), but they are in reasonable agreement with the other frozen sand test data with the exception of the data point for samples from depths of about 6.5 m. The samples from 6.5 m depth at Kushiro Port produced a CRR of 0.24-0.36 and corresponded to an in-situ SPT $(N_1)_{60cs}$ of 46; the resulting point plots outside the limits of this graph and well below the other frozen sand data points. Iai et al. (1995) noted that this one data point was inconsistent with other observations and that possible reasons for this inconsistency were not specifically known.

The upper part of Figure 5.2 shows the "limiting shear strain" as described in Seed et al. (1984), which essentially corresponds to the value of shear strain that can be expected to develop in 15 uniform loading cycles under very high CSR values. The concept of a limiting shear strain is related to the observed cyclic loading responses of dense sand specimens. For example, consider the cyclic loading response of the dense Niigata sand (Yoshimi et al. 1984) with an $(N_1)_{60cs}$ of about 41 as shown in Figure 5.3. The cyclic stress-strain response shows a very slow, progressive accumulation of shear strains with each cycle of loading, despite the extremely large cyclic stress ratio of about 1.25 (Figure 5.3a). The resistance to accumulation of axial strains is also illustrated in the plot of cyclic stress ratio versus number of uniform loading cycles to different double-amplitude axial strain levels (Figure 5.3b), wherein the cyclic resistances increase significantly with increasing values of the axial shear strain used to define failure. Seed et al. (1984) used the concept of limiting shear strains to derive triggering curves for different levels of peak shear strains, as are shown for peak shear strains of 1%, 3%, and 10% in the lower part of Figure 5.2.

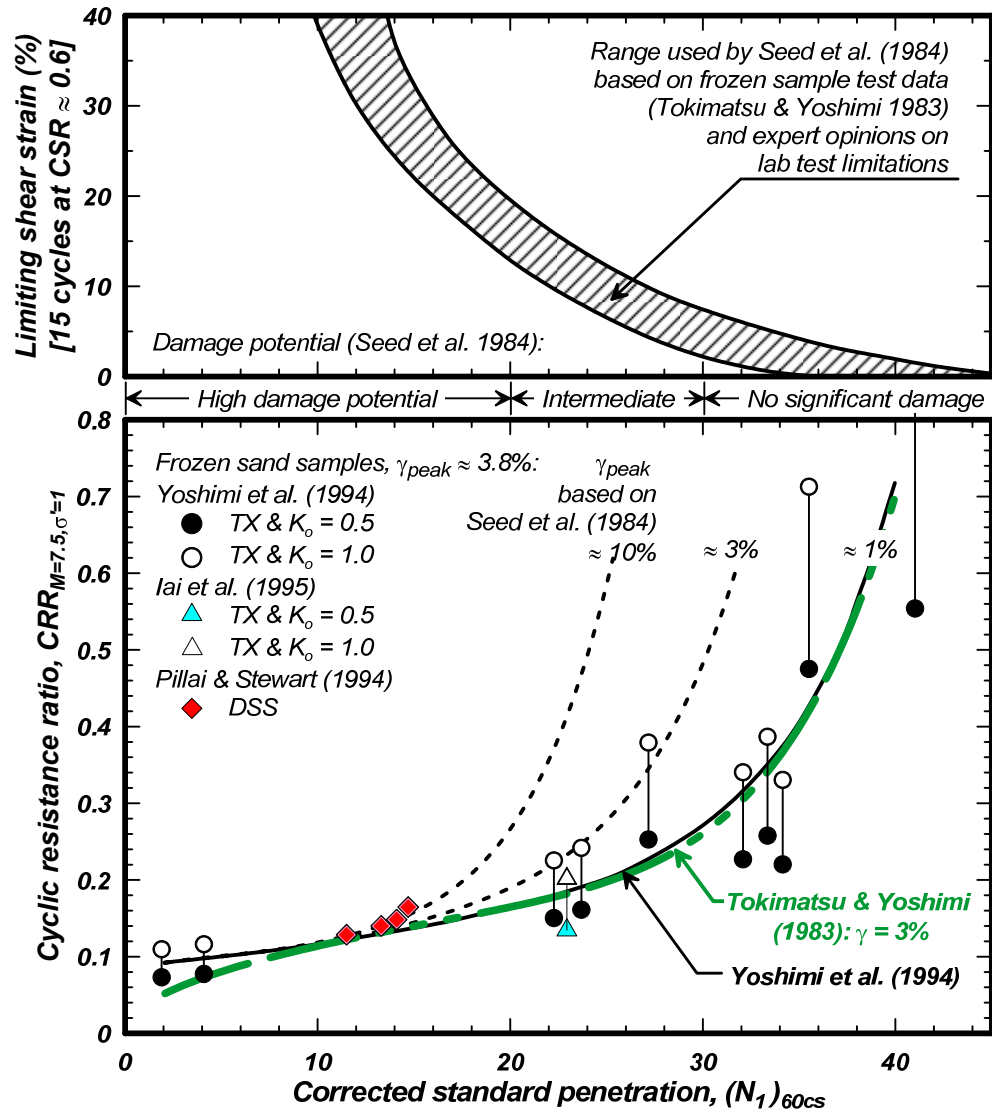


Figure 5.2. $CRR_{M=7.5, \sigma=1}$ versus $(N_1)_{60cs}$ based on results from frozen sand samples and considering the practical limits on peak shear strains

The usefulness of cyclic laboratory tests for providing reasonable approximations of in-situ cyclic strengths was discussed by Castro (1975), Peck (1979), Seed (1979), and Casagrande (1980). Castro (1975) and Casagrande (1980) expressed the belief that the stress and strain concentrations that develop at the top and bottom caps in a cyclic triaxial test enable the accumulation of strains faster than would develop in-situ. The effects of stress and strain concentrations in a cyclic triaxial or DSS test can be expected to reduce cyclic strengths by an amount that varies with the relative density of the sand. For loose sands with low SPT blow counts, the triggering of high excess pore pressures is quickly followed by the development of large shear strains; it seems unlikely that the boundary conditions can significantly reduce the strengths of these looser specimens, and thus the cyclic strengths are likely reasonable. For dense sands, the accumulation of shear strains is much more gradual as illustrated by the data in Figure 5.3; for this reason, it seems reasonable to suspect that the boundary conditions would have the greatest effect on strain accumulation for dense sands under large cyclic loads.

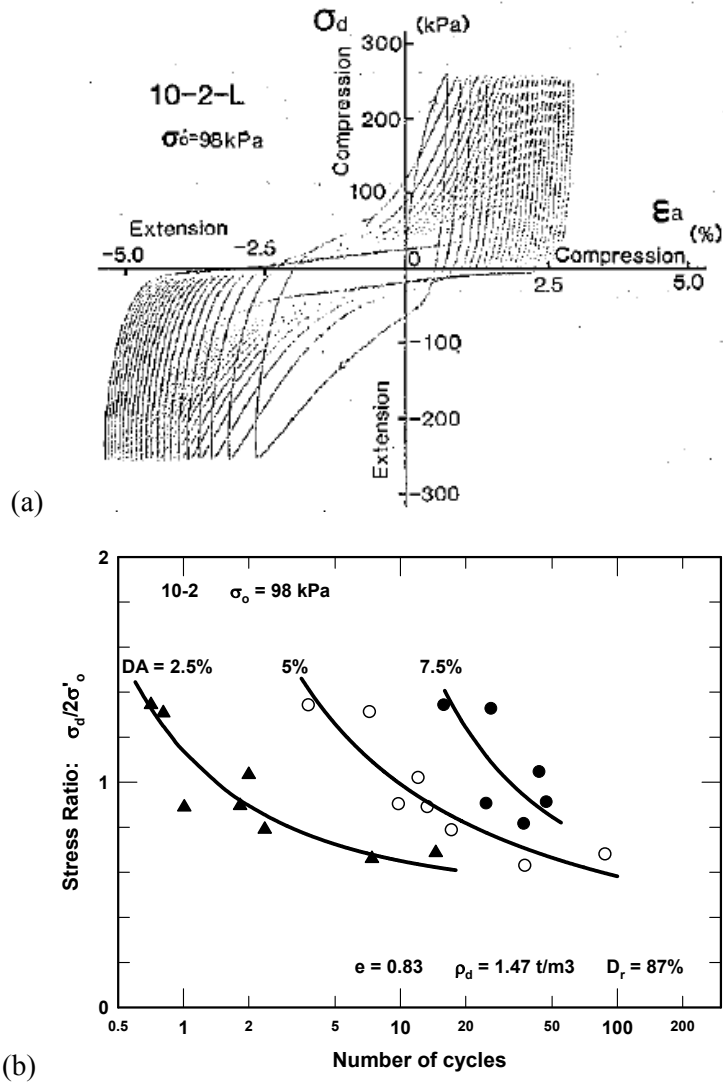


Figure 5.3. Results of undrained cyclic triaxial tests on frozen sand samples of a dense Niigata sand (Yoshimi et al. 1984): (a) cyclic stress-strain response, and (b) cyclic stress ratio versus number of uniform loading cycles to different double-amplitude axial strains.

The issues associated with measuring cyclic strengths and cyclic strain accumulation for dense sands in the laboratory were considered by Seed et al. (1985) in deriving their SPT-based liquefaction triggering correlation. They referenced the existing data from frozen sand samples, and used them to develop the limiting strain relationship shown in the upper part of Figure 5.2. They concluded that clean sands with $(N_1)_{60} \approx 30$ would develop only relatively small shear strains under even the largest earthquake-induced cyclic stress ratios, and that the associated ground deformations would be small. This conclusion led to their liquefaction triggering correlation curving sharply upward at $(N_1)_{60} \approx 30$, even though the existing frozen sand data at that time showed that it was possible to generate excess pore pressure ratios of 100% in even denser sands.

5.1.2. Comparison to the Idriss-Boulanger liquefaction triggering correlation

The case history-based liquefaction triggering correlation by Idriss and Boulanger (2004, 2008) is compared in Figure 5.4 to the cyclic test results for frozen sand samples and the correlations that Tokimatsu and Yoshimi (1983) and Yoshimi et al. (1994) developed based on cyclic triaxial test data for frozen sand samples. These three correlations are in good agreement with the frozen sand test data for $(N_1)_{60cs}$ values less than about 15. At greater $(N_1)_{60cs}$ values, the Tokimatsu and Yoshimi (1983) and Yoshimi et al. (1994) curves follow the results of the frozen sand test data in curving sharply upward near $(N_1)_{60cs}$ of about 40, whereas the Idriss and Boulanger (2004, 2008) relationship and the similar Seed et al. (1984)/Youd et al. 2001 relationship curve sharply upward near $(N_1)_{60cs}$ of about 30.

The liquefaction triggering relationships by Idriss and Boulanger (2004, 2008), Tokimatsu and Yoshimi (1983) and Yoshimi et al. (1994) are compared in Figure 5.5 to the updated case history data compiled herein. For values of $(N_1)_{60cs}$ less than about 15, these three correlations are consistent with the case history data. For $(N_1)_{60cs}$ values greater than about 15, the Idriss and Boulanger correlation more closely follows the case history data, whereas the Tokimatsu and Yoshimi (1983) and Yoshimi et al. (1994) correlations increasingly fall below the liquefaction case history points with an increasing number of no-liquefaction cases above it. The case history database contains no cases of liquefaction for $(N_1)_{60cs}$ values greater than 26 despite the very strong shaking levels and numerous sites with representative $(N_1)_{60cs}$ in the range of 25 to 40. There were also 10 no-liquefaction cases with values of $(N_1)_{60cs}$ between 21 and 28 that plotted above the Idriss-Boulanger triggering curve.

There are a number of influencing factors to consider when examining the differences in liquefaction triggering relationships at high $(N_1)_{60cs}$ values shown in Figures 5.4 and 5.5. One consideration is that for very dense sands, the peak cyclic strains, and hence any permanent shear or reconsolidation strains, may be sufficiently small that the resulting ground deformations cause no observable settlement, movements, boils, or damage. If the permanent shear strains in the field are only a fraction of the peak shear strains for dense sands, then the triggering curve based on field observations of permanent ground deformations would be expected to plot to the left of a triggering curve based on laboratory measurements of peak shear strains or peak excess pore pressure ratios. A second consideration is whether volumetric strains during in-situ freezing were truly negligible; the effects of even minor disturbance for dense sands would be expected to cause the laboratory-based triggering curve to plot lower than the in-situ triggering curve. The third consideration, as discussed by Castro (1975), Peck (1979), Seed (1979), and Casagrande (1976, 1980), is whether measurements of cyclic strengths and cyclic strain accumulation for dense sands in the laboratory are reasonable approximations of in-situ cyclic strengths, or whether stress and strain concentrations that develop at the top and bottom caps in a cyclic triaxial test enable the accumulation of strains faster than would develop in-situ. Regardless of the possible reasons, the case history data suggest that sites with $(N_1)_{60cs}$ values greater than about 30 can be expected to develop no significant damage even in cases of strong shaking.

5.1.3. Summary of comparisons

The cyclic laboratory test results for frozen sand samples, with the exception of the data from Duncan Dam discussed in the following section correspond to vertical effective stresses of 36 to 106 kPa and $(N_1)_{60cs}$ values of 2 to 51.

At $(N_1)_{60cs}$ values less than about 15, the cyclic resistances obtained from laboratory tests on frozen sand samples and from analyses of the field case history data are in good agreement. Specifically, the liquefaction triggering curve by Idriss and Boulanger (2004, 2008) was shown to be in good agreement

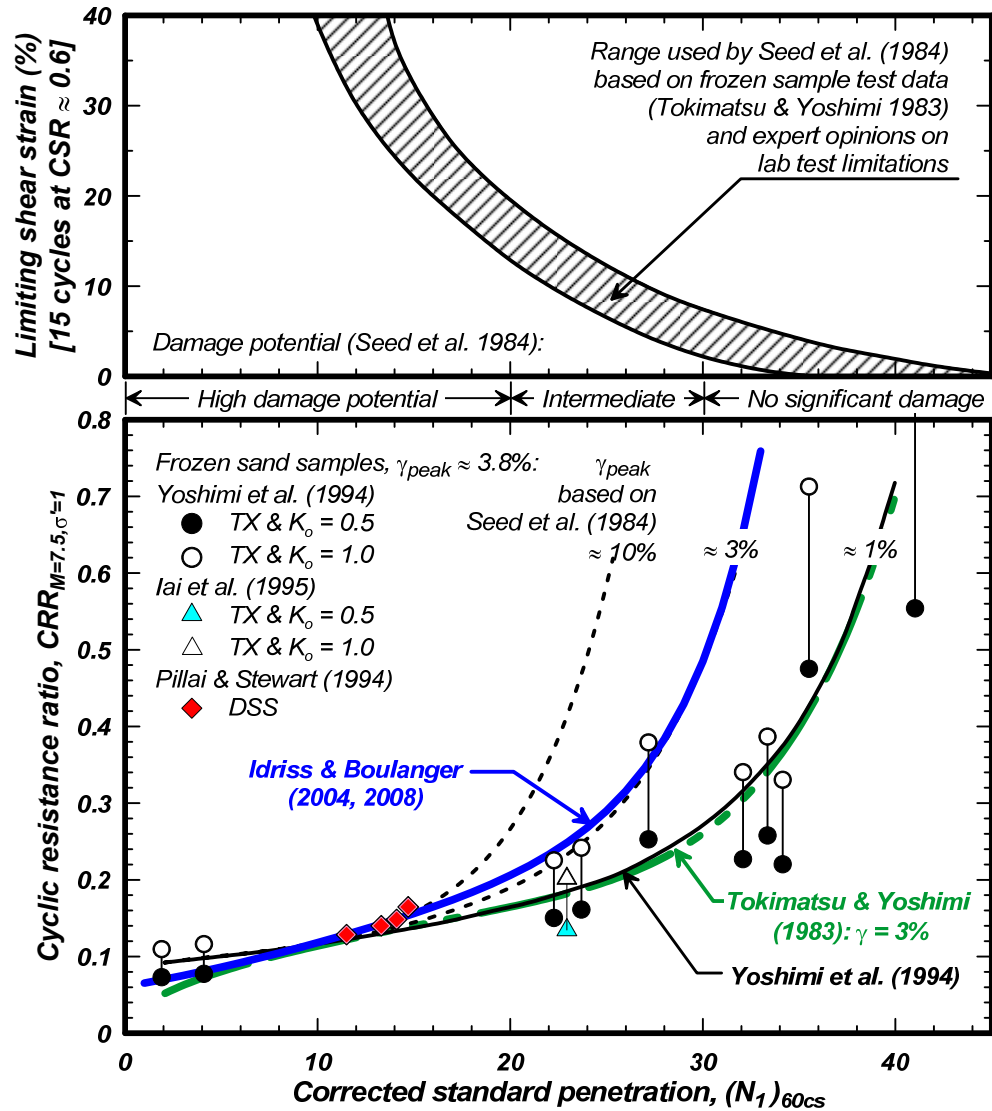


Figure 5.4. Comparison of the Idriss-Boulanger (2004, 2008) liquefaction triggering correlation with the frozen sand sample test data and the Tokimatsu and Yoshimi (1983) and Yoshimi et al. (1994) correlations.

with the results of the cyclic laboratory test on frozen sand samples and the associated correlations by Tokimatsu and Yoshimi (1983) and Yoshimi et al. (1994) for this range of $(N_1)_{60cs}$ values.

At $(N_1)_{60cs}$ values greater than about 15, the cyclic resistances obtained from laboratory tests on frozen sand samples are smaller than obtained from analyses of the field case history data. Specifically, the liquefaction triggering curve by Idriss and Boulanger (2004, 2008) and the similar Seed et al. (1984)/Youd et al. (2001) curve turn sharply upward near $(N_1)_{60cs}$ values of about 30, whereas the curves based on cyclic tests of frozen sand samples (Tokimatsu and Yoshimi 1983; Yoshimi et al. 1994) turn sharply upward near $(N_1)_{60cs}$ values of about 40.

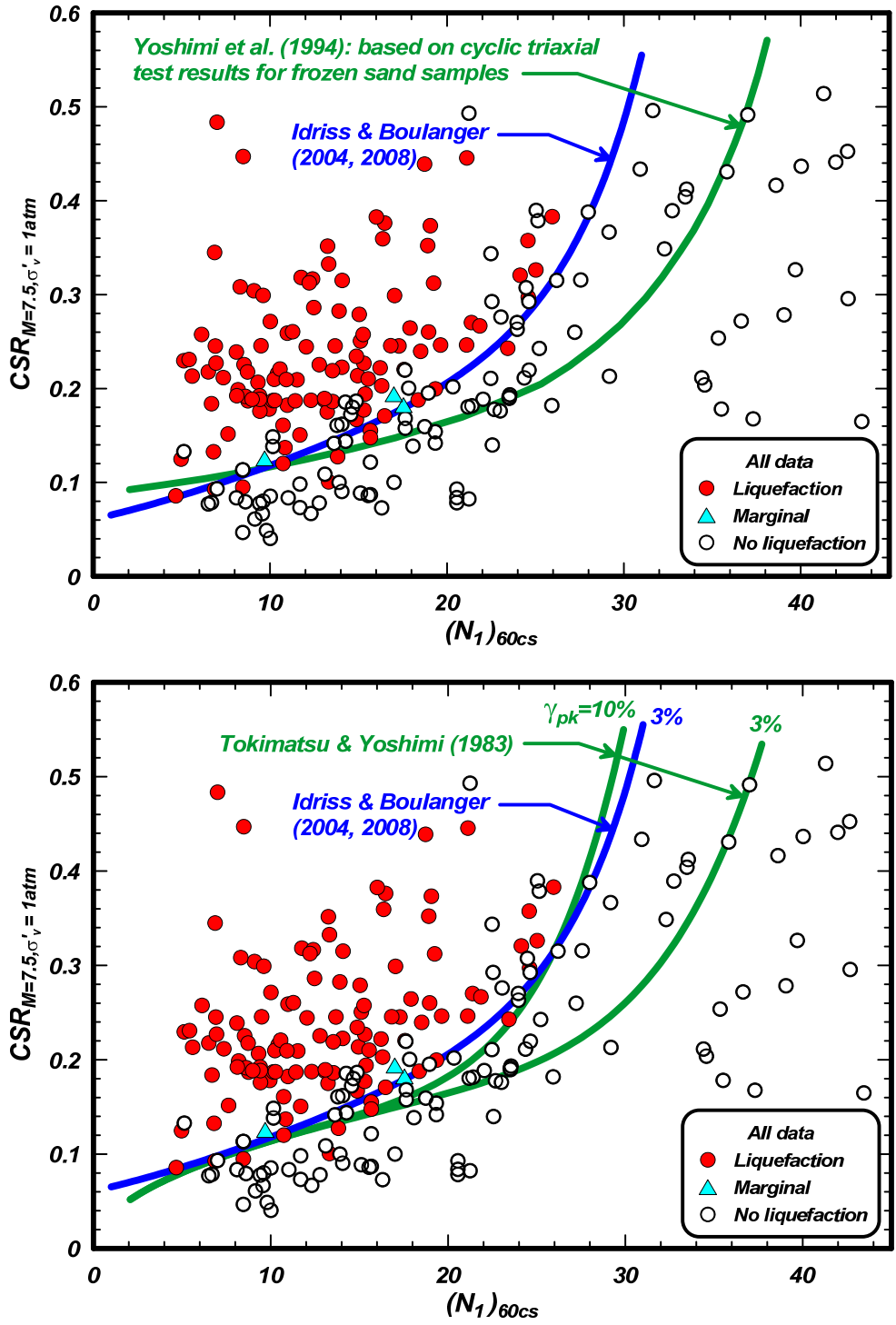


Figure 5.5. Comparison of the frozen sample-based Yoshimi et al. (1994) and Tokimatsu and Yoshimi (1983) correlations to the case history data and case history-based correlation by Idriss-Boulanger (2004, 2008).

For predicting field performance in practice, it is recommended that the position of the liquefaction triggering curve at high $(N_1)_{60cs}$ values be guided more closely toward the field case history data than to the results of the cyclic tests on frozen sand samples. The cyclic tests on frozen sand samples show that it may be possible to generate peak excess pore pressure ratios of 100% in very dense sands under very strong cyclic triaxial loads, but that the associated shear strains will generally be small. The field case history data suggest that no significant damage may be expected in sands with $(N_1)_{60cs}$ values greater than about 25 to 30, which may be because the in-situ permanent shear and volumetric strains are small enough that they are not manifested at the ground surface in most situations. For practice, the current position of the Idriss and Boulanger (2004, 2008) liquefaction triggering curve at high $(N_1)_{60cs}$ values is considered appropriate for predicting the conditions required to trigger the onset of visible consequences of liquefaction.

5.2. Duncan Dam – prediction of CRR at large overburden stresses

5.2.1 Background

The cyclic resistance of a sand unit at Duncan Dam in British Columbia was evaluated using cyclic undrained direct simple shear (DSS) and cyclic undrained triaxial testing of samples obtained using frozen sampling techniques (Pillai and Byrne 1994, Pillai and Stewart 1994). The in-situ SPT and laboratory testing data cover effective confining stresses up to 12 atm, and hence provide a unique set of data for evaluating how the effects of effective overburden stress are accounted for in liquefaction evaluation procedures.

The focus of the investigations was the loose sand strata identified as "unit 3c" in the cross-section shown in Figure 5.6 (Pillai and Byrne 1994). This sand unit was geologically interpreted as being of relatively uniform density before construction of the dam, and is comprised of predominantly fine sand with fines contents of 5-10% (7% as a reasonable average). The relatively loose condition of the sand and the high overburden stresses imposed by the dam suggest that the sand in this unit is essentially normally consolidated under the dam.

Frozen sampling techniques were used to obtain samples from a boring drilled near the toe of the dam at the location shown in Figure 5.6. The samples were used in cyclic undrained DSS tests at effective vertical consolidation stresses of 2, 4, and 6 atm and in cyclic undrained triaxial tests at effective isotropic consolidation stresses of 2, 4, 6, and 12 atm.

SPTs were performed in unit 3c from different locations on the dam, such that N values were obtained at confining stresses ranging from about 1 to 12 atm. An energy ratio of 43% was selected based on energy measurements during calibration tests for the same rig and operator (Plewes et al. 1984).

The sand from unit 3c was found to compress (densify) with increasing confining stress (Plewes et al. 1994). The in-situ relative density of the sand was determined to be about 30-35% beneath the dam toe and about 55-60% beneath the dam crest based on the frozen sand sample test results, borehole density logging with a gamma-gamma density tool, and correlations with in-situ penetration test data. Oedometer tests on sand samples produced increases in relative density with increasing confining stress that were consistent with the field studies.

The effect of increasing density with increasing confining stress in the laboratory did not, however, result in a significant change in the cyclic resistance ratios (CRR) measured in either the DSS or triaxial tests. The fact that CRR was almost constant for all confining stresses was attributed to the increasing density (e.g., D_R increased from about 30-35% at $\sigma'_v \approx 150$ kPa to about 55-60% at $\sigma'_v \approx 800$ kPa) offsetting the

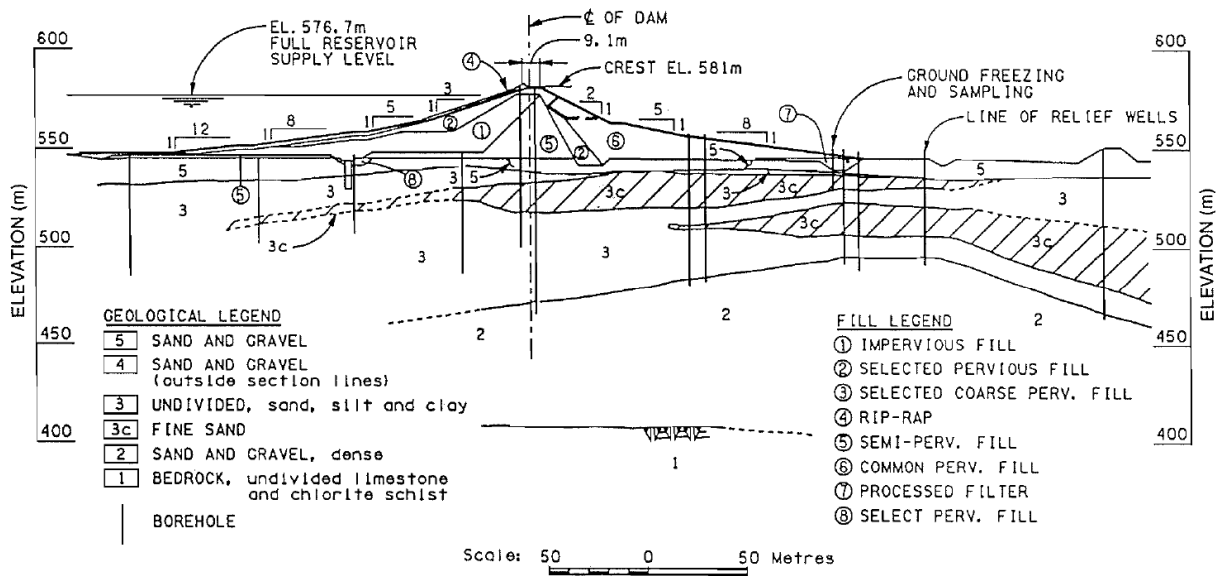


Figure 5.6. Typical section through Duncan Dam showing the unit 3c sand layer (Pillai and Byrne 1994)

normally observed decrease in CRR with increasing confining stress for sand at a constant value of relative density (i.e., the K_σ effect).

The present study re-examines the field and laboratory test data from Duncan Dam relative to the site-specific procedures developed by Pillai and Byrne (1994) and the liquefaction evaluation procedures by Idriss and Boulanger (2004, 2008), NCEER/NSF (Youd et al. 2001), and Cetin et al. (2004). The Duncan Dam data were also used to develop points for the $CRR-(N_1)_{60cs}$ correlation, as presented in Section 5.1.

5.2.2. Laboratory test data

The results of the cyclic undrained DSS and triaxial tests are summarized in Table 5.2 (Section 5.1). The cyclic resistance ratios, as reported for 10 equivalent uniform loading cycles and single-amplitude axial strains of 2.5% for triaxial and 4.0% shear strain for the DSS tests, are listed in the table. The CRR values were almost constant, independent of confining stress, for both types of tests. The average ratio of the DSS strength to the triaxial strength was 0.85.

The laboratory strengths were converted to CRR for in-situ loading conditions and an earthquake magnitude of $M = 7.5$ as follows. CRR values for triaxial tests were multiplied by 0.85 to arrive at equivalent DSS strengths, which are believed to better approximate the loading conditions in-situ. CRR values were multiplied by a factor of 0.937 to convert them from 10 equivalent uniform loading cycles to 15 equivalent uniform loading cycles; this conversion was based on the slopes of the CRR versus number of equivalent uniform loading cycles plot shown in Pillai and Byrne (1994). A total of 15 uniform loading cycles is considered approximately equivalent to an $M = 7.5$ earthquake event when using the Seed-Idriss (1971) Simplified Procedure for estimating cyclic stress ratios (i.e., at 65% of the peak seismic shear stress ratio). CRR values were further multiplied by a factor of 0.9 to convert them from 1-

D to 2-D shaking conditions. The values obtained from the DSS and triaxial tests were then averaged to arrive at an estimate of the in-situ $CRR_{M=7.5}$.

5.2.3. Predicting the variation of CRR with depth based on SPT-based correlations

The SPT data were used to predict the variation of CRR with depth using four different SPT-based liquefaction evaluation procedures.

1. The site-specific C_N and K_σ relations developed by Pillai and Byrne (1994) in combination with the Seed et al. (1984) liquefaction triggering correlation that Pillai and Byrne had used in deriving their relations.
2. The liquefaction evaluation procedures by Idriss and Boulanger (2004, 2008).
3. The liquefaction evaluation procedures by NCEER/NSF (Youd et al. 2001).
4. The liquefaction evaluation procedures by Cetin et al. (2004) with their recommendation that deterministic analyses could use a curve that was equal to their curve for a probability of liquefaction (P_L) equal to 15% for $(N_1)_{60cs}$ values less than or equal to 32 and a slightly steeper curve at greater $(N_1)_{60cs}$ values. The $(N_1)_{60cs}$ values at Duncan Dam are well below 32; thus, the comparisons shown herein are based on the Cetin et al. (2004) $P_L = 15\%$ curve.

The three liquefaction triggering correlations used in these four comparisons are shown in Figure 5.7.

The C_N and K_σ relationships used in these four comparisons are shown in Figure 5.8. The Liao and Whitman (1986) C_N relationship,

$$C_N = \left(\frac{P_a}{\sigma'_{vc}} \right)^{0.5} \quad (5.2)$$

is used in both the NCEER/NSF (Youd et al. 2001) and Cetin et al. procedures. Youd et al. indicated that the alternative expression by Kayen et al. (1992),

$$C_N = \frac{2.2}{1.2 + \frac{\sigma'_v}{P_a}} \quad (5.3)$$

provided a slightly better fit to the original C_N curves specified by Seed and Idriss (1982) and could be used in routine practice. The Kayen et al. expression, however, produces considerably smaller values of C_N at large overburden stresses as shown in Figure 5.8. The C_N values produced by the Kayen et al. expression at overburden stresses greater than about 4 atm are lower than supported by available calibration chamber test data and penetration theories. For this reason, the Liao-Whitman expression is used in the NCEER/NSF procedures for the analysis of the Duncan Dam data. The Hynes and Olson (1998) K_σ relationship,

$$K_\sigma = \left(\frac{P_a}{\sigma'_{vc}} \right)^{1-f} \quad (5.4)$$

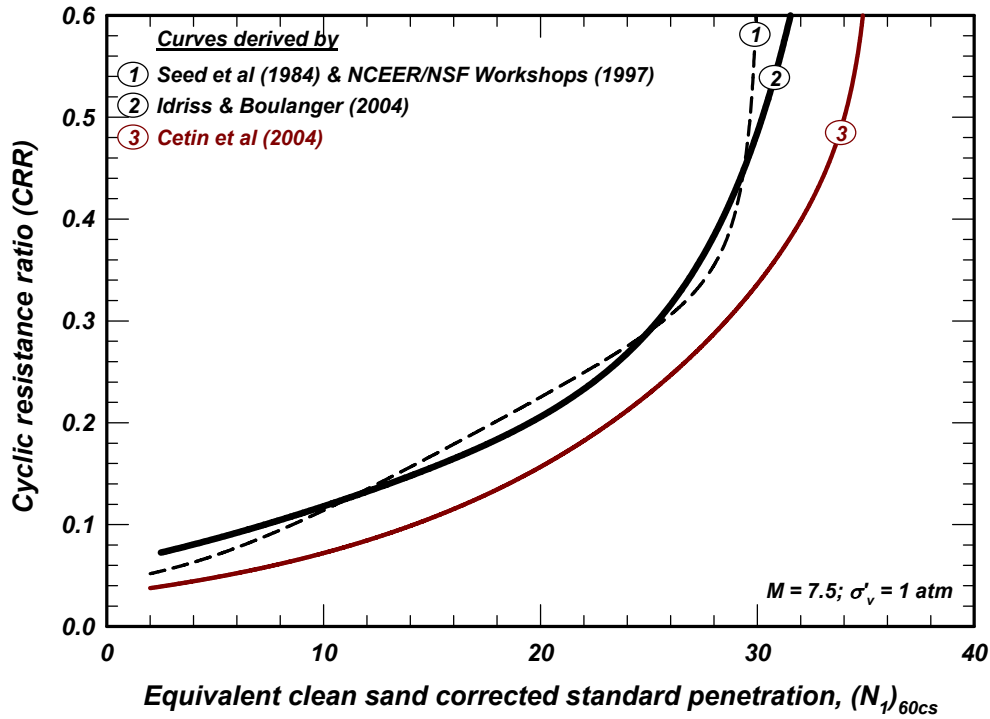


Figure 5.7. Liquefaction triggering correlations used in the analyses of the Duncan Dam data

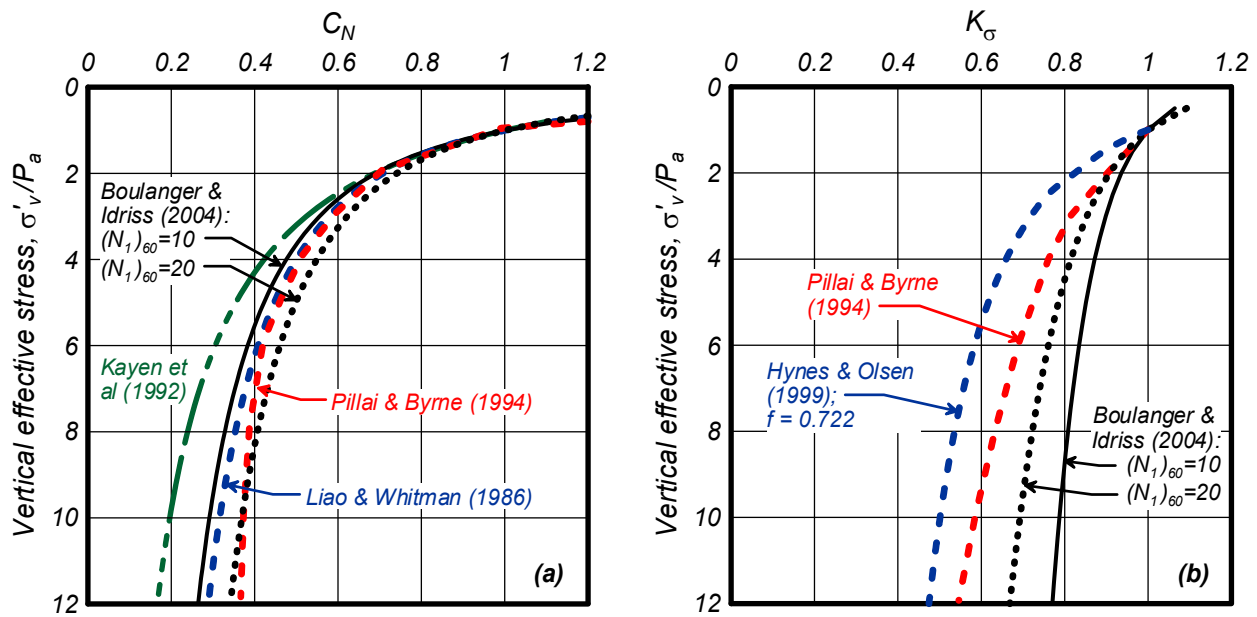


Figure 5.8. Comparison of relationships for C_N and K_σ

with $f = 0.722$ is used with both the NCEER/NSF and Cetin et al. procedures for the analyses of Duncan Dam for the following reasons. Cetin et al. recommended using the NCEER K_σ relations when the confining stress was greater than about 2 atm. The $(N_1)_{60}$ values are in the range of 15 (slightly increasing with depth), for which the in-situ relative density would be about 50-60% range; an average D_R of 56% would result in a stress exponent from the NCEER relations which exactly matches the value embodied in

the Cetin et al. (2004) relationships. Thus, for this site, the same expression would apply for confining stresses greater than 1 atm for both the Cetin et al. and NCEER/NSF procedures.

The first evaluation of the SPT data using the site-specific C_N and K_σ relations developed by Pillai and Byrne (1994) in combination with the Seed et al. (1984) / NCEER (1997) liquefaction triggering correlation is summarized in Figure 5.9. The measured N values, after correcting from their equivalent energy ratio of 43%, are plotted versus effective overburden stress in Figure 5.9. The N_{60} values were then corrected to an equivalent overburden stress of 1 atm using the C_N relation; the resulting $(N_1)_{60}$ values are shown to increase with increasing confining stress. These $(N_1)_{60}$ values are then used with the liquefaction triggering correlation to obtain $CRR_{M=7.5, \sigma'_v=1 \text{ atm}}$ values, which are then multiplied by the K_σ value to obtain the $CRR_{M=7.5}$ values shown in the figure. The predicted $CRR_{M=7.5}$ values are approximately constant with increasing confining stress and reasonably consistent with, but slightly lower than, the results of the laboratory tests, which is expected given the site-specific K_σ relation was developed to achieve the observed independence of CRR with depth.

The second evaluation of the SPT data using the procedures by Idriss and Boulanger (2004, 2008) is summarized in Figure 5.10. The $(N_1)_{60}$ values are seen to increase slightly with increasing confining stress. The predicted $CRR_{M=7.5}$ values are approximately constant with increasing confining stress and are reasonably consistent with the results of the laboratory tests.

The third evaluation of the SPT data using the procedures by NCEER/NSF (Youd et al. 2001) is summarized in Figure 5.11. The $(N_1)_{60}$ values are again seen to increase slightly with increasing confining stress. However, the predicted $CRR_{M=7.5}$ values progressively decrease with increasing confining stress; they also begin as slightly lower than the laboratory test results at the lower confining stresses, and become increasingly smaller than the laboratory test results as the overburden stress increases.

The fourth evaluation of the SPT data using the procedures by Cetin et al. (2004) is summarized in Figure 5.12. The $(N_1)_{60}$ values increase with increasing confining stress in the same way as the NCEER/NSF procedures because both use the Liao-Whitman C_N relationship. The predicted $CRR_{M=7.5}$ values progressively decrease with increasing confining stress in the same way as the NCEER/NSF procedures because they use the same K_σ relationship for $\sigma'_v > 1 \text{ atm}$. The $CRR_{M=7.5}$ values from the Cetin et al. procedures are, however, smaller than those obtained with the NCEER/NSF procedure because the Cetin et al. liquefaction triggering curve is lower.

The $CRR_{M=7.5}$ values from the Cetin et al. procedures are substantially smaller (especially at the larger depths) than the laboratory test results or the values obtained using the site-specific relationships of Pillai and Byrne (1994) or the procedures by Idriss and Boulanger (2004, 2008). The differences between the results obtained using the Cetin et al, Pillai and Byrne, and Idriss and Boulanger relationships are due to the combined effects of the differences in their liquefaction triggering curves and K_σ and C_N relationships.

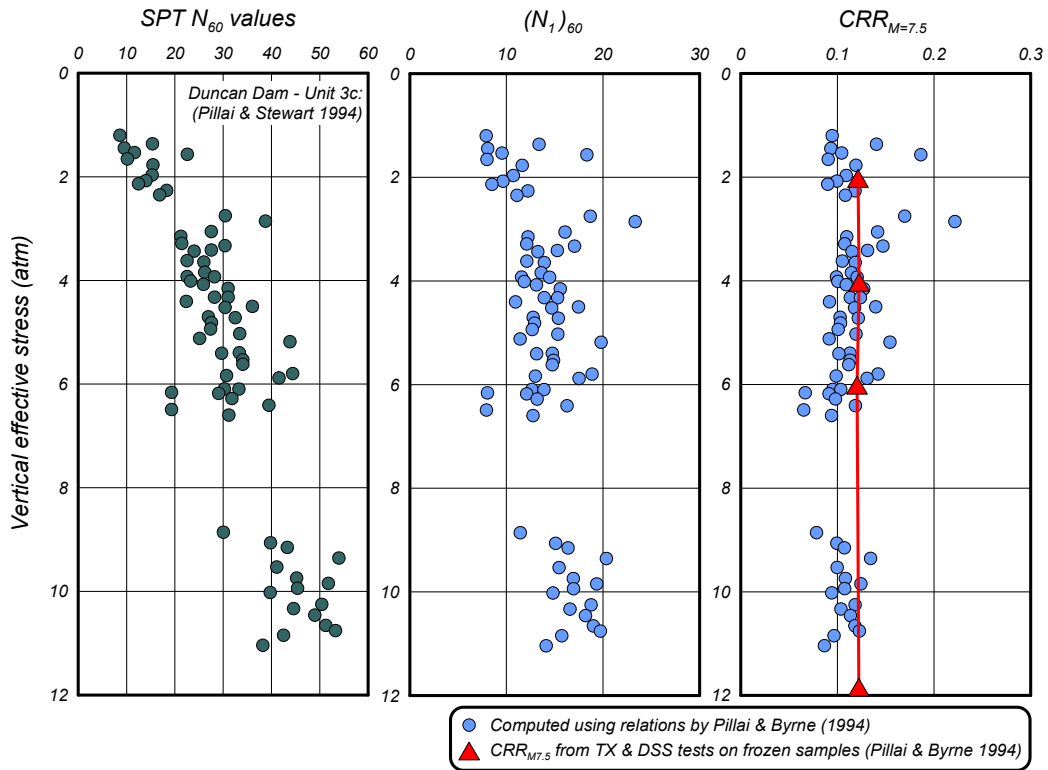


Figure 5.9. Computed $CRR_{M7.5}$ values using the relations by Pillai and Byrne (1994) with the SPT-based liquefaction correlation from NCEER (1997).

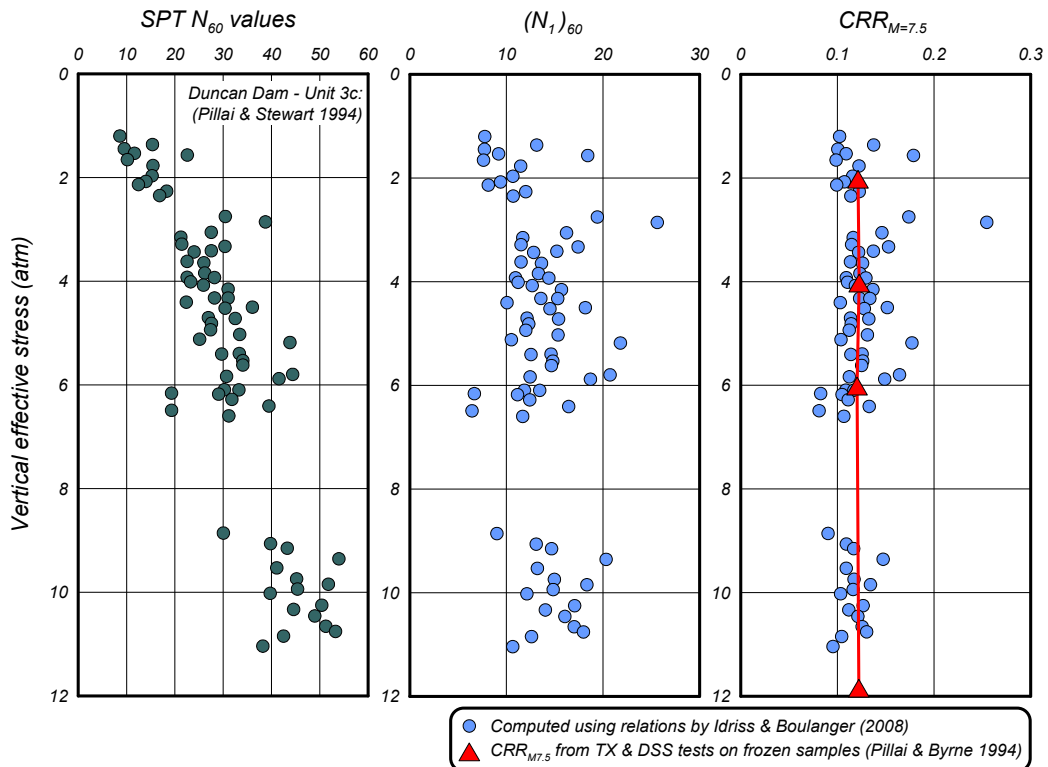


Figure 5.10. Computed $CRR_{M7.5}$ values using the relations by Idriss and Boulanger (2008).

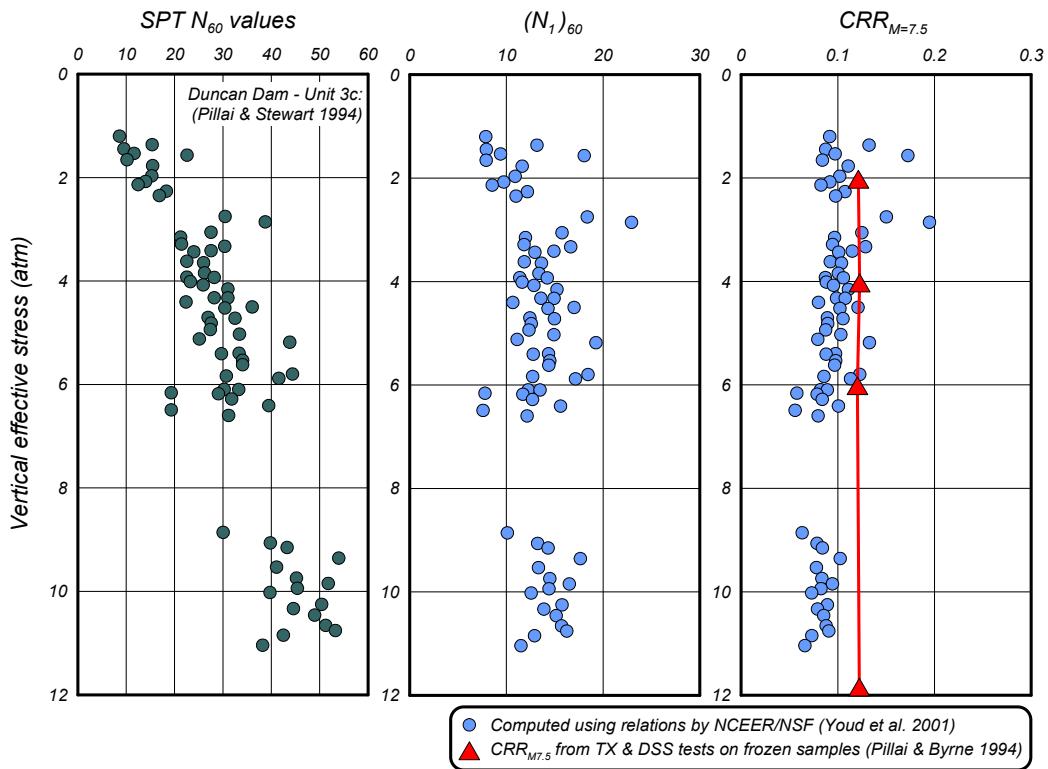


Figure 5.11. Computed $CRR_{M7.5}$ values using the relations by NCEER/NSF (Youd et al. 2001).

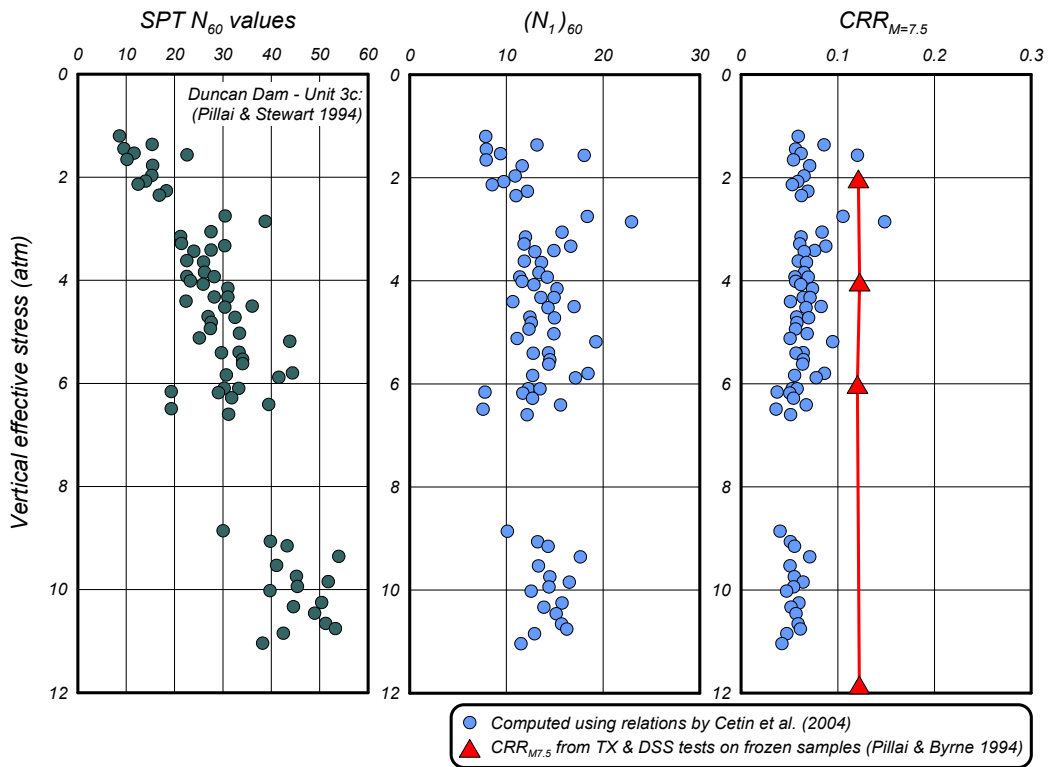


Figure 5.12. Computed $CRR_{M7.5}$ values using the relations by Cetin et al. (2004).

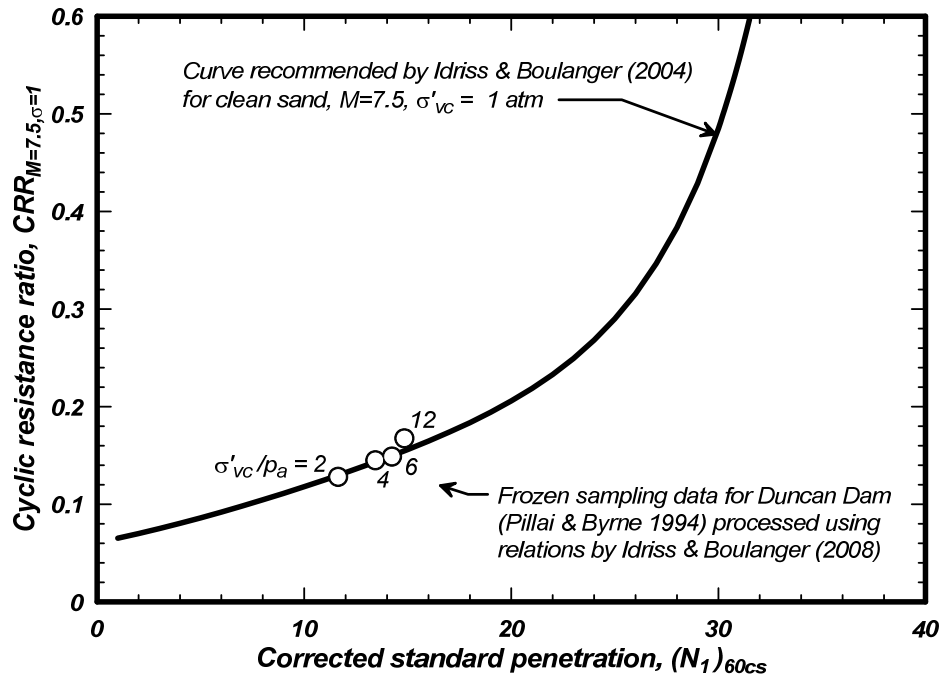


Figure 5.13. $CRR_{M=7.5, \sigma=1}$ versus $(N_1)_{60cs}$ values derived from Duncan Dam using the C_N and K_σ relations by Idriss and Boulanger (2008).

5.2.4. Values of CRR and $(N_1)_{60cs}$ for Duncan Dam

The SPT and laboratory test data from Duncan Dam were used to generate the four pairs of $CRR_{M=7.5, \sigma=1}$ and $(N_1)_{60cs}$ values listed in Table 5.2 and plotted versus the liquefaction correlation of Idriss and Boulanger (2004, 2008) in Figure 5.13. The C_N and K_σ relations by Idriss and Boulanger were used in the computation of $(N_1)_{60cs}$ values and the conversion of the $CRR_{M=7.5}$ values to $CRR_{M=7.5, \sigma=1}$ values. The cyclic strength data from these frozen sampling test results are in excellent agreement with the liquefaction triggering correlation developed by Idriss and Boulanger based on field case histories.

5.2.5. Summary of comparisons

The cyclic laboratory test results for frozen sampling specimens from unit 3c at Duncan Dam provide a direct assessment of the sand's in-situ strength for effective confining stresses of 2 to 12 atm. The SPT and laboratory test data showed the sand increased in density with increasing confining stress, but that the combination of increasing density and confining stress produced CRR values that did not change significantly with increasing confining stress.

The site-specific C_N and K_σ relationships developed by Pillai and Byrne (1994) were shown to be consistent with the field and laboratory test data for Duncan Dam.

The liquefaction evaluation procedure by Idriss and Boulanger (2004, 2008) was shown to be in good agreement with the in-situ and laboratory test data over the full range of confining stresses for Duncan Dam. The good agreement obtained with both the Idriss-Boulanger and Pillai-Byrne procedures, despite

their use of different C_N and K_σ relationships, illustrates how these two relationships can have compensating effects on the computation of CRR values at large depths.

The liquefaction evaluation procedure by NCEER/NSF (Youd et al. 2001) increasingly under-predicted the laboratory-derived strengths with increasing confining stress. This under-prediction of cyclic strengths is caused by the combined effects of the adopted C_N and K_σ relationships.

The liquefaction evaluation procedure by Cetin et al. (2004) predicted substantially lower cyclic strengths at all depths compared to those obtained from the laboratory tests on frozen sand samples or those obtained using the other three liquefaction triggering procedures. The under-prediction of cyclic strengths is caused by the combined effects of their lower liquefaction triggering correlation and the adopted C_N and K_σ relationships.

6. PROBABILISTIC RELATIONSHIP FOR LIQUEFACTION TRIGGERING

6.1. Probabilistic relationships for liquefaction triggering

SPT- and CPT-based probabilistic correlations for the triggering of liquefaction in sands and silty sands have been developed by a number of investigators, including Christian and Swiger (1975), Liao et al. (1988), Liao and Lum (1998), Youd and Nobel (1997), Toprak et al. (1999), Juang et al. (2002), Cetin et al. (2002, 2004), and Moss et al. (2006). For example, the SPT-based relationships by Toprak et al. (1999) and Cetin et al. (2004) are presented in Figures 6.1a and 6.1b, respectively, which show curves of $CSR_{M=7.5, \sigma'=1atm}$ versus $(N_1)_{60cs}$ corresponding to probabilities of liquefaction (P_L) of 5 to 95%. The spread between the contours for $P_L = 5\%$ and $P_L = 95\%$ are very different for the two relationships shown in Figure 6.1 because they are actually representing two different results. The relationship by Toprak et al. (1999) represents the total uncertainty in the evaluation of the case history database; i.e., it includes the uncertainty in the triggering relationship (model uncertainty) and the uncertainty in the $(N_1)_{60}$ and CSR values determined for the case histories (measurement or parameter uncertainty). The relationship by Cetin et al. (2002, 2004) was developed using a statistical approach that allowed a separate accounting of the model and measurement uncertainties. The curves in Figure 6.1b represent Cetin et al.'s relationship with the model uncertainty alone, and since the model uncertainty is smaller than the total uncertainty, the spread in the contours for $P_L = 5\%$ and $P_L = 95\%$ is much narrower. For applications, the total uncertainty will include contributions from the liquefaction triggering model and the input parameters $(N_1)_{60}$ and CSR. The parameter uncertainties in an application are not the same as the measurement uncertainties in the case history database, and thus it is important to have separately quantified the model uncertainty so that it can be more rationally combined with the parameter uncertainties in a full probabilistic liquefaction evaluation.

A probabilistic version of the Idriss and Boulanger (2004, 2008) liquefaction triggering correlation is developed using the updated case history database and a maximum likelihood method that utilizes the forms of the limit state and likelihood functions used by Cetin et al. (2002). Measurement or estimation uncertainties in CSR and $(N_1)_{60cs}$ for the case histories, and choice-based sampling bias, are accounted for. Sensitivity of the maximum likelihood solution to the assumptions regarding uncertainties in CSR and $(N_1)_{60cs}$ and the correction for sampling bias are examined.

6.2. Methodology

6.2.1. Limit state function

The model for the limit state function (g) was taken as the difference between the natural logs of the $CRR_{M=7.5, \sigma'=1atm}$ and $CSR_{M=7.5, \sigma'=1atm}$ values, such that liquefaction is assumed to have occurred if $g \leq 0$ and to have not occurred if $g > 0$. The $CRR_{M=7.5, \sigma'=1atm}$ value was estimated using the following form of the Idriss and Boulanger (2004, 2008) relationship,

$$CRR_{M=7.5, \sigma'=1atm} = \exp \left(\frac{(N_1)_{60cs}}{14.1} + \left(\frac{(N_1)_{60cs}}{126} \right)^2 - \left(\frac{(N_1)_{60cs}}{23.6} \right)^3 + \left(\frac{(N_1)_{60cs}}{25.4} \right)^4 - C_o \right) \quad (6.1)$$

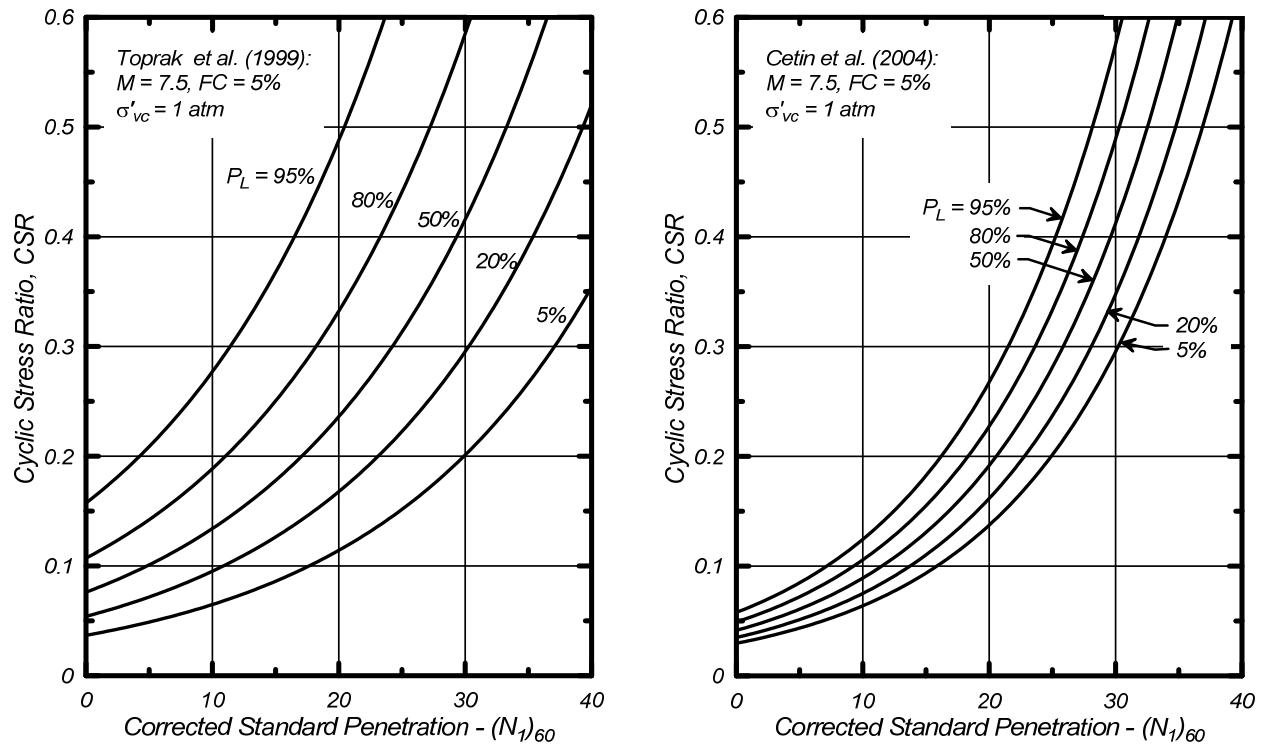


Figure 6.1. SPT-based probabilistic correlations for the CRR of clean sands for $M = 7.5$: (a) Toprak et al. (1999), and (b) Cetin et al. (2004)

where C_o is an unknown fitting parameter that serves to scale the Idriss-Boulanger relationship while maintaining its shape; note that the Idriss-Boulanger deterministic relationship corresponds to $C_o = 2.8$. The use of a single fitting parameter provides the means for examining the uncertainty in the Idriss-Boulanger relationship; the effect of including additional fitting parameters that modify the shape of the Idriss-Boulanger relationship is evaluated later. The $CSR_{M=7.5, \sigma'_v=1atm}$ value represents the loading that would be expected to be induced by the shaking, and it was also estimated using the Seed-Idriss (1971) simplified procedure with the updated relationships from Idriss and Boulanger (2004, 2008).

$$CSR_{M=7.5, \sigma'_v=1atm} = 0.65 \frac{\sigma_v}{\sigma'_v} \frac{a_{max}}{g} r_d \frac{1}{MSF} \frac{1}{K_\sigma} \quad (6.2)$$

The limit state function can then be written as,

$$\hat{g} \left((N_1)_{60cs}, C_o, CSR_{M=7.5, \sigma'_v=1atm} \right) = \ln \left(CRR_{M=7.5, \sigma'_v=1atm} \right) - \ln \left(CSR_{M=7.5, \sigma'_v=1atm} \right) \quad (6.3)$$

where the hat on g indicates that the limit state function is imperfect in its prediction of liquefaction behavior. This form is similar to that used by Cetin et al. (2002), although it is considerably simpler because most of the liquefaction triggering analysis components considered herein are based on experimental and theoretical considerations in lieu of including some of them as unknown fitting parameters.

The uncertainties in the limit state function are represented by three contributors. Measurement or estimation uncertainties in the case history data points are assumed to be adequately represented by including uncertainties in the $(N_1)_{60cs}$ and $CSR_{M=7.5, \sigma'=1atm}$ values. The uncertainty in $(N_1)_{60cs}$ is assumed to be normally distributed with a constant coefficient of variation (COV_N) (e.g., Orchard et al. 1988). The uncertainty in $CSR_{M=7.5, \sigma'=1atm}$ is assumed to be log-normally distributed, which is consistent with log-normal distributions for the uncertainty in predictions of peak ground accelerations (e.g., Abrahamson et al. 2008). Uncertainty in the $CRR_{M=7.5, \sigma'=1atm}$ expression is represented by inclusion of a random model error term, which is also assumed to be log normally distributed with mean of zero.

The uncertainty in the representative $(N_1)_{60cs}$ value assigned to any case history includes contributions from two major sources. One source of uncertainty is variability in the SPT equipment and procedures used at different case history sites. The second major source of uncertainty is the degree to which the available SPT data are truly representative of the critical strata, which depends on the degree to which the geologic conditions are understood, the heterogeneity of the deposits, the number of borings, and the placement of the borings relative to the strata of concern. Either of these sources of uncertainty can dominate the total uncertainty in the selection of a representative $(N_1)_{60cs}$ value for a given site. Furthermore, the large majority of the liquefaction case histories lack sufficient information to justify attempting to develop site-specific estimates of these uncertainties for each case history. For this reason, the value of COV_N was taken as being the same for all case histories.

The uncertainty in the $CSR_{M=7.5, \sigma'=1atm}$ values estimated for any case history similarly depends on numerous factors, including the proximity of strong ground motion recordings, potential variability in site responses, and availability and quality of indirect measures of shaking levels (e.g., eye witness reports, damage to structures, disruption of nonstructural contents). The estimates of a_{max} at liquefaction and non-liquefaction sites by various researchers are often based on a combination of these types of information, and can be expected to have smaller variances than estimates obtained from ground motion prediction equations alone. The uncertainty in estimates of a_{max} for each case history depends on the quality of information available, but it was found that quantifying these uncertainties on a case-history specific basis was generally not justified, except for those few cases that had a strong ground motion recording directly at the site. For this reason, the standard deviation in $\log(CSR_{M=7.5, \sigma'=1atm})$ was set to one of two values; a relatively small value for the seven sites that had strong ground motion recordings directly at the site and a relatively greater value for all other sites.

It is convenient to simplify the notation as follows,

$$N = (N_1)_{60cs} \quad (6.4)$$

$$S = CSR_{M=7.5, \sigma'=1atm} \quad (6.5)$$

$$R = CRR_{M=7.5, \sigma'=1atm} \quad (6.6)$$

The limit state function can be written using a total error term ε_T , to account for both the inability of \hat{g} to predict liquefaction perfectly and the uncertainty in the parameters used to compute \hat{g} .

$$g(N, S, C_o, \varepsilon_{\ln(R)}) = \hat{g}(N, S, C_o) + \varepsilon_T \quad (6.7)$$

The ε_T is normally distributed with a mean value of zero, and it includes the effects of uncertainty in the parameters, which can be expressed as,

$$N = \hat{N} + \varepsilon_N \quad (6.8)$$

$$\sigma_N = COV_N \cdot N \quad (6.9)$$

$$\ln(S) = \ln(\hat{S}) + \varepsilon_{\ln(S)} \quad (6.10)$$

$$\ln(R) = \ln(\hat{R}) + \varepsilon_{\ln(R)} \quad (6.11)$$

The corrected limit state function with inclusion of the uncertainties can then be written as,

$$g(N, S, C_o, \varepsilon_{\ln(R)}) = \ln(R) - \ln(S) \quad (6.12)$$

$$g(N, S, C_o, \varepsilon_{\ln(R)}) = \left(\frac{N + \varepsilon_N}{14.1} + \left(\frac{N + \varepsilon_N}{126} \right)^2 - \left(\frac{N + \varepsilon_N}{23.6} \right)^3 + \left(\frac{N + \varepsilon_N}{25.4} \right)^4 - C_o \right) + \varepsilon_{\ln(R)} - \ln(\hat{S}) - \varepsilon_{\ln(S)} \quad (6.13)$$

This expression can be simplified by multiplying out the polynomial terms and then neglecting the higher order terms with ε_N squared or cubed. The resulting expression is,

$$g(N, S, C_o, \varepsilon_{\ln(R)}) = \left(\frac{N}{14.1} + \left(\frac{N}{126} \right)^2 - \left(\frac{N}{23.6} \right)^3 + \left(\frac{N}{25.4} \right)^4 - C_o \right) + \left(\frac{1}{14.1} + \frac{2N}{126^2} - \frac{3N^2}{23.6^3} + \frac{4N^3}{25.4^4} \right) \varepsilon_N + \varepsilon_{\ln(R)} - \ln(\hat{S}) - \varepsilon_{\ln(S)} \quad (6.14)$$

$$g(N, S, C_o, \varepsilon_{\ln(R)}) = \hat{g}(N, S, C_o) + \left(\frac{1}{14.1} + \frac{2N}{126^2} - \frac{3N^2}{23.6^3} + \frac{4N^3}{25.4^4} \right) \varepsilon_N + \varepsilon_{\ln(R)} - \varepsilon_{\ln(S)} \quad (6.15)$$

The standard deviation in ε_T can be expressed as,

$$(\sigma_T)^2 = \left(\frac{1}{14.1} + \frac{2N}{126^2} - \frac{3N^2}{23.6^3} + \frac{4N^3}{25.4^4} \right)^2 (\sigma_N)^2 + (\sigma_{\ln(R)})^2 + (\sigma_{\ln(S)})^2 \quad (6.16)$$

6.2.2. Likelihood function

The likelihood function is the product of the probabilities of the individual case history observations, assuming that the case history observations are statistically independent. For a liquefaction case ($g \leq 0$), the probability of having observed liquefaction can be expressed as,

$$P\left[g\left(N, S, C_o, \varepsilon_{\ln(R)}\right) \leq 0\right] = \Phi\left[-\frac{\hat{g}\left(\hat{N}, \hat{S}, C_o\right)}{\sigma_T}\right] \quad (6.17)$$

where Φ is the standard normal cumulative probability function. For example, the probability of having observed liquefaction becomes greater than 0.84 if the case history data point plots more than one σ_T above the triggering curve. In this regard, it is important to recognize that case history data points are plotted at the $CSR_{M=7.5, \sigma'=1atm}$ value expected in the absence of liquefaction, and that this $CSR_{M=7.5, \sigma'=1atm}$ value may be significantly greater than the value which developed if liquefaction was triggered early in strong shaking. For this reason, the case history data points that fall well above the triggering curve have probabilities close to unity, and thus they have very little influence on the overall likelihood function. The reverse is true for the no-liquefaction cases. The likelihood function can now be written as,

$$L\left(C_o, \varepsilon_{\ln(R)}\right) = \prod_{Liquefied\ sites} P\left[g\left(N, S, C_o, \varepsilon_{\ln(R)}\right) \leq 0\right] \prod_{Nonliquefied\ sites} P\left[g\left(N, S, C_o, \varepsilon_{\ln(R)}\right) > 0\right] \quad (6.18)$$

$$L\left(C_o, \varepsilon_{\ln(R)}\right) = \prod_{Liquefied\ sites} \Phi\left[-\frac{\hat{g}\left(\hat{N}, \hat{S}, C_o\right)}{\sigma_T}\right] \prod_{Nonliquefied\ sites} \Phi\left[\frac{\hat{g}\left(\hat{N}, \hat{S}, C_o\right)}{\sigma_T}\right] \quad (6.19)$$

The case history database is, however, believed to contain an uneven sampling of liquefaction and no-liquefaction case histories because researchers more often have chosen to investigate liquefaction sites. Manski and Leman (1977) suggest that the bias from an uneven choice-based sampling process can be corrected for by weighting the observations to better represent the actual population. Cetin et al. (2002) noted that this amounted to rewriting the likelihood function as,

$$L\left(C_o, \varepsilon_{\ln(R)}\right) = \prod_{Liquefied\ sites} \Phi\left[-\frac{\hat{g}\left(\hat{N}, \hat{S}, C_o\right)}{\sigma_T}\right]^{w_{liquefied}} \prod_{Nonliquefied\ sites} \Phi\left[\frac{\hat{g}\left(\hat{N}, \hat{S}, C_o\right)}{\sigma_T}\right]^{w_{nonliquefied}} \quad (6.20)$$

where the exponents $w_{liquefied}$ and $w_{nonliquefied}$ used to weight the observations are computed as,

$$w_{liquefied} = \frac{Q_{liq,true}}{Q_{liq,sample}} \quad (6.21)$$

$$w_{nonliquefied} = \frac{1 - Q_{liq,true}}{1 - Q_{liq,sample}} \quad (6.22)$$

where $Q_{liq,true}$ is the true proportion of the occurrences of liquefaction in the population, and $Q_{liq,sample}$ is the proportion of occurrences of liquefaction in the sample set. Cetin et al. (2002) reported that a panel of eight experts agreed that the ratio $w_{liquefied}/w_{nonliquefied}$ should be greater than 1.0 and less than 3.0, with the most common estimate being between 1.5 and 2.0. They further allowed this ratio to be a parameter in the Bayesian updating analyses, and found that a ratio of 1.5 minimized their overall model variance. Accordingly, they adopted weighting values of $w_{liquefied} = 1.2$ and $w_{nonliquefied} = 0.8$, producing the ratio $w_{liquefied}/w_{nonliquefied} = 1.5$.

6.3. Results of parameter estimation

6.3.1. Results and sensitivity to assumed parameter estimation errors

There are five parameters that can be either estimated or left as fitting parameters in determining the maximum likelihood solution: C_o , $\sigma_{\ln(R)}$, $\sigma_{\ln(S)}$, COV_N , and $w_{\text{liquefied}}/w_{\text{nonliquefied}}$. Cetin et al. (2002) estimated uncertainties in S and N for the individual case histories that were used in their Bayesian analyses, and then suggested that $\sigma_{\ln(S)}$ would be about 0.2 and COV_N would be about 0.15 in applications with good practices. Orchant et al. (1988) suggested that COV_N can range from 0.15 to 0.45 depending on the quality of the data. Ground motion prediction equations have standard deviations of about 0.45-0.55 in the natural log of the peak ground acceleration (Abrahamson et al. 2008), which suggest that $\sigma_{\ln(S)}$ could be around 0.45-0.55 if it was estimated solely on the basis of a ground motion prediction equation; smaller values of $\sigma_{\ln(S)}$ would be expected for most case histories given the additional information provided by strong ground motion recordings and site-specific observations (e.g., eye witness reports, damage to structures, disruption of nonstructural contents). As previously discussed, the data available for most sites in the liquefaction database are inadequate to quantify the site-specific uncertainty in N or S, and thus the approach adopted in this study was to solve for C_o and $\sigma_{\ln(R)}$ using a range of estimated values for $\sigma_{\ln(S)}$, COV_N , and $w_{\text{liquefied}}/w_{\text{nonliquefied}}$.

Maximum likelihood solutions for C_o and $\sigma_{\ln(R)}$ are listed in Table 6.1 for six cases with different assumptions regarding the values for $\sigma_{\ln(S)}$, COV_N , and $w_{\text{liquefied}}/w_{\text{nonliquefied}}$. The first four cases involve varying the values for $\sigma_{\ln(S)}$ from 0.15 to 0.25 and COV_N from 0.15 to 0.20 while keeping $w_{\text{liquefied}}/w_{\text{nonliquefied}} = 1.5$. For the seven sites that had strong ground motion recordings at the site (as shown in Figure 4.8), a reduced value for $\sigma_{\ln(S)}$ of 0.05 was used. The value of σ_T obtained from the solution for these first four cases is plotted versus N in Figure 6.2; the results show that the rate at which σ_T increases with N is dependent on the assumed value of COV_N , but that the overall values for σ_T are relatively similar for all four cases. As the assumed values for the uncertainties in S and N are increased, the most likely value for the uncertainty in R is decreased. For the fourth case, the values of $\sigma_{\ln(S)} = 0.25$ and $COV_N = 0.20$ are sufficiently large that the most likely solution is a unique relationship for R (i.e., $\sigma_{\ln(R)} = 0.0$). In addition, the differences in the values of the likelihood function for these first three cases were not significant, such that the maximum likelihood solution does not provide strong support for one case over another. These results illustrate how the maximum likelihood analysis of the case history data provides insight on the total uncertainty, but does not provide clear guidance on the appropriate partitioning of that uncertainty into the components of N, S, and R. The four cases, however, give very similar values for the fitting parameter C_o (i.e., 2.66-2.67) such that the most likely position of the triggering curve is well constrained (the minor shift in position of the triggering curve for these different C_o values is illustrated in later figures).

Table 6.1. Results of parameter estimations for liquefaction triggering relationship

Parameters	Case 1	Case 2	Case 3	Case 4	Case 5	Case 6
$\sigma_{\ln(S)}$	0.15	0.20	0.20	0.25	0.20	0.20
COV_N	0.15	0.15	0.20	0.20	0.15	0.15
$w_{\text{liquefied}}/w_{\text{nonliquefied}}$	1.5	1.5	1.5	1.5	1.2	1.8
C_o	2.66	2.67	2.67	2.67	2.70	2.64
$\sigma_{\ln(R)}$	0.19	0.15	0.11	0.0	0.14	0.15

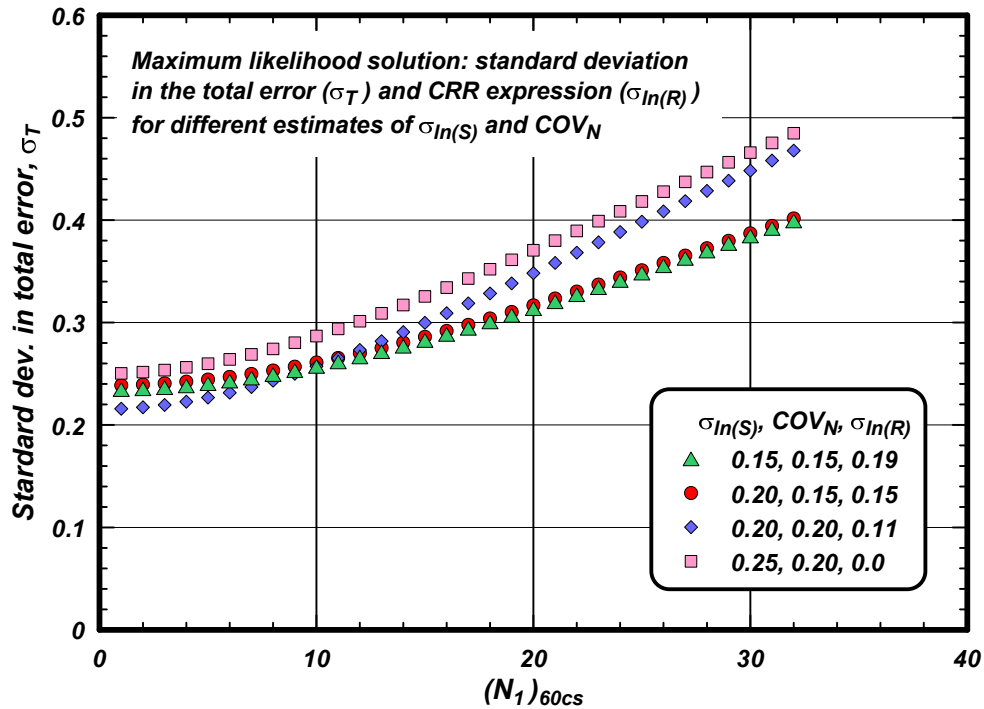


Figure 6.2. Standard deviation in the total error term (σ_T) and CRR relationship ($\sigma_{\ln(R)}$) from the maximum likelihood solution for different estimates of $\sigma_{\ln(S)}$ and COV_N .

The last two cases listed in Table 6.1 vary the ratio $w_{\text{liquefied}}/w_{\text{nonliquefied}}$ from 1.2 to 1.8, while keeping $\sigma_{\ln(S)}$ and COV_N constant. The smaller weighting ratio causes the solution for the most likely triggering curve to shift slightly downward (i.e., C_0 increases from 2.66 to 2.70), while the greater weighting ratio causes the most likely triggering curve to shift slightly upward (i.e., C_0 decreases to 2.64). The solution for $\sigma_{\ln(R)}$ is relatively unaffected by the choice of weighting function.

Curves for probabilities of liquefaction [P_L] equal to 15% and 50%, with inclusion of the estimation errors in $CSR_{M=7.5, \sigma=1atm}$ and $(N_1)_{60cs}$, for the six cases listed in Table 6.1 are plotted together with the case history data in Figure 6.3. This figure illustrates how the median curves (i.e., $P_L = 50\%$) from the six solution cases listed in Table 6.1 are almost identical. In addition, the $P_L = 15\%$ curves are also very similar because all six solution cases have similar total error terms, as illustrated in Figure 6.2.

The triggering curves for a probability of liquefaction [P_L] equal to 15% based on model uncertainty alone [i.e., including only the uncertainty in $CRR_{M=7.5, \sigma=1atm}$] for the six solution cases listed in Table 6.1 are plotted together with the case history data in Figure 6.4. These curves do not include the estimation errors in S or N, and thus are located higher than the $P_L = 15\%$ curves in Figure 6.3. The highest $P_L = 15\%$ curve in Figure 6.4 is from case 4, primarily because it had the smallest uncertainty in R. The other $P_L = 15\%$ curves in Figure 6.4 are closely spaced together. The deterministic triggering correlation recommended by Idriss and Boulanger (2004, 2008) overlies the $P_L = 15\%$ curves for these five cases.

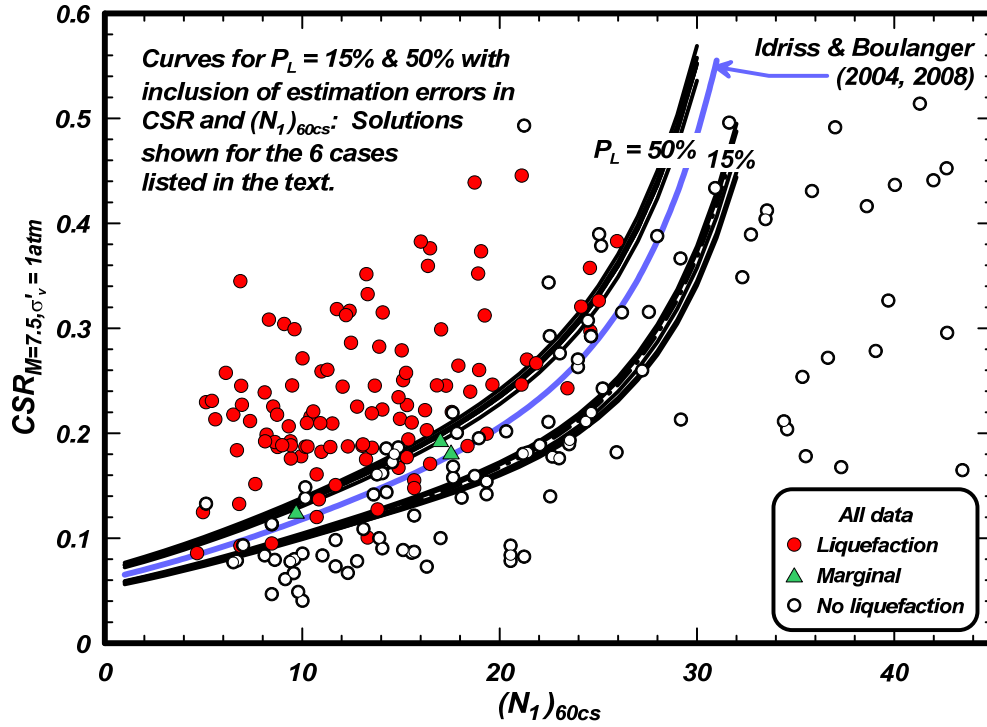


Figure 6.3. Curves of $CRR_{M=7.5, \sigma'_v=1atm}$ versus $(N_1)_{60cs}$ for probabilities of liquefaction of 15% and 50% with inclusion of estimation errors in CSR and $(N_1)_{60cs}$: Solutions for the six cases listed in Table 6.1.

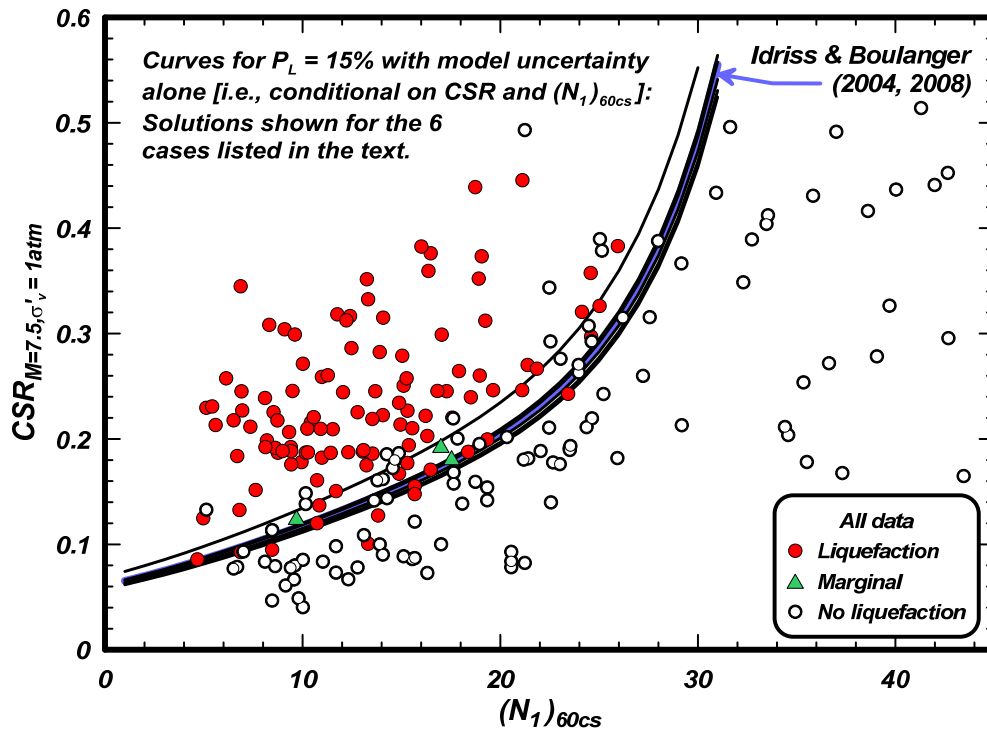


Figure 6.4. Curves of $CRR_{M=7.5, \sigma'_v=1atm}$ versus $(N_1)_{60cs}$ for probabilities of liquefaction of 15% excluding uncertainties in CSR and $(N_1)_{60cs}$: Solutions for the six cases listed in Table 6.1.

6.3.2. Additional sensitivity studies

Sensitivity of the results to the form of the liquefaction triggering equation was evaluated by introducing additional flexibility into the expression for $CRR_{M=7.5, \sigma'_v=1atm}$ as,

$$CRR_{M=7.5, \sigma'_v=1atm} = \exp \left(\frac{(N_1)_{60cs}}{14.1} + \left(\frac{(N_1)_{60cs}}{126} \right)^2 - \left(\frac{(N_1)_{60cs}}{23.6} \right)^3 + \left(\frac{(N_1)_{60cs}}{C_4} \right)^4 - C_o \right) \quad (6.23)$$

where the additional fitting parameter C_4 controls the sharpness with which the liquefaction triggering relationship curves upward at higher $(N_1)_{60cs}$ values. The median triggering curve was found to be relatively insensitive to the assumed values for the uncertainties in S and N or to the weighting factors, as was demonstrated for the original form of the liquefaction triggering equation in the previous section. Triggering curves for $P_L = 15\%$, 50% , and 85% are shown in Figure 6.5 for the case where $\sigma_{ln(S)} = 0.2$, $COV_N = 0.15$, and $w_{liquefied}/w_{nonliquefied} = 1.5$ (i.e., same assumptions as for Case 2 in Table 6.1). The median triggering curve is almost equal to the Idriss-Boulanger (2004, 2008) deterministic curve at $(N_1)_{60cs}$ values less than 10, and becomes increasingly higher than the Idriss-Boulanger deterministic curve with increasing values of $(N_1)_{60cs}$. This result indicates that the case history data would, on its own, support a triggering curve that turns sharply upward at values of $(N_1)_{60cs}$ smaller than does the Idriss-Boulanger (2004, 2008) deterministic curve.

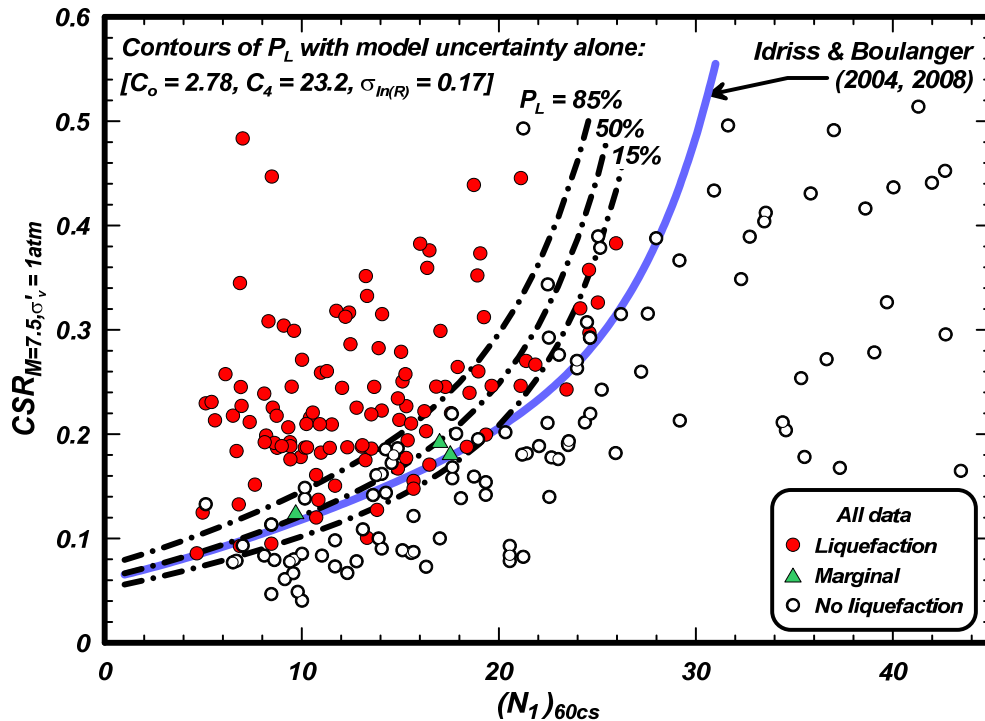


Figure 6.5. Curves of $CRR_{M=7.5, \sigma'_v=1atm}$ versus $(N_1)_{60cs}$ for probabilities of liquefaction of 15%, 50%, and 85% using the expression for $CRR_{M=7.5, \sigma'_v=1atm}$ with two fitting parameters.

The results obtained with the original form of the liquefaction triggering equation were also checked for their sensitivity to the use of the 50th percentile rather than 67th percentile r_d values from the Idriss (1999) relationship (Appendix B). The relationships originally proposed by Idriss (1999) corresponded to about the 67th percentile r_d values from those analyses, with this percentile chosen so that the curve for $M = 7.5$ was consistent with the earlier Seed and Idriss (1971) r_d curve (i.e., Figure 2.1). The median r_d values were slightly lower, with the difference progressively increasing from 0% at the ground surface to about 5% at a depth of 10 m for all M . The case histories were reprocessed with the median r_d values, and the probabilistic triggering relationships recomputed. The median triggering curve was again relatively insensitive to the assumed values for the uncertainties in S and N or to the weighting factors, as was demonstrated in the previous section. Furthermore, the median triggering curve was found to be only slightly lowered by the use of median r_d values, as expected. For example, using $\sigma_{\ln(S)} = 0.2$, $COV_N = 0.15$, and $w_{\text{liquefied}}/w_{\text{nonliquefied}} = 1.5$ (i.e., the same assumptions as for Case 2 in Table 6.1), the derived fitting parameter C_o was increased from 2.67 to 2.69 and the $\sigma_{\ln(R)}$ was unchanged at 0.15. This change in C_o lowers the triggering curves by 2% [i.e., $\exp(2.67-2.69) = 0.98$].

6.3.3. Recommended relationships

Selecting the most appropriate values for C_o and $\sigma_{\ln(R)}$ from the results of these maximum likelihood solutions involves subjective evaluation of the most appropriate partitioning of the total uncertainty in the liquefaction case history database. This evaluation must also consider the limitations of the statistical models and case history database, including uncertainties that are not explicitly accounted for, and the other available information regarding cyclic loading behavior of sands (e.g., the results of tests on frozen sand samples as discussed in Section 5). Taking these factors into consideration, the results in Table 6.1 are considered reasonable bounds of different interpretations, from which values of $C_o = 2.67$ and $\sigma_{\ln(R)} = 0.13$ are recommended as reasonable for use in practice.

The liquefaction triggering correlation derived from the maximum likelihood solution can then be expressed as,

$$CRR_{M=7.5, \sigma'_v=1atm} = \exp \left(\frac{(N_1)_{60cs}}{14.1} + \left(\frac{(N_1)_{60cs}}{126} \right)^2 - \left(\frac{(N_1)_{60cs}}{23.6} \right)^3 + \left(\frac{(N_1)_{60cs}}{25.4} \right)^4 - 2.67 + \varepsilon_{\ln(R)} \right) \quad (6.24)$$

where $\varepsilon_{\ln(R)}$ is normally distributed with a mean of 0.0 and a standard deviation of $\sigma_{\ln(R)} = 0.13$. This expression can also be written as,

$$CRR_{M=7.5, \sigma'_v=1atm} = \exp \left(\frac{(N_1)_{60cs}}{14.1} + \left(\frac{(N_1)_{60cs}}{126} \right)^2 - \left(\frac{(N_1)_{60cs}}{23.6} \right)^3 + \left(\frac{(N_1)_{60cs}}{25.4} \right)^4 - 2.67 + \sigma_{\ln(R)} \cdot \Phi^{-1}(P_L) \right) \quad (6.25)$$

where Φ^{-1} is the inverse of the standard cumulative normal distribution, and P_L is the probability of liquefaction. Alternatively, the conditional probability of liquefaction for known values of $CSR_{M=7.5, \sigma'_v=1atm}$ and $(N_1)_{60cs}$ can be computed as,

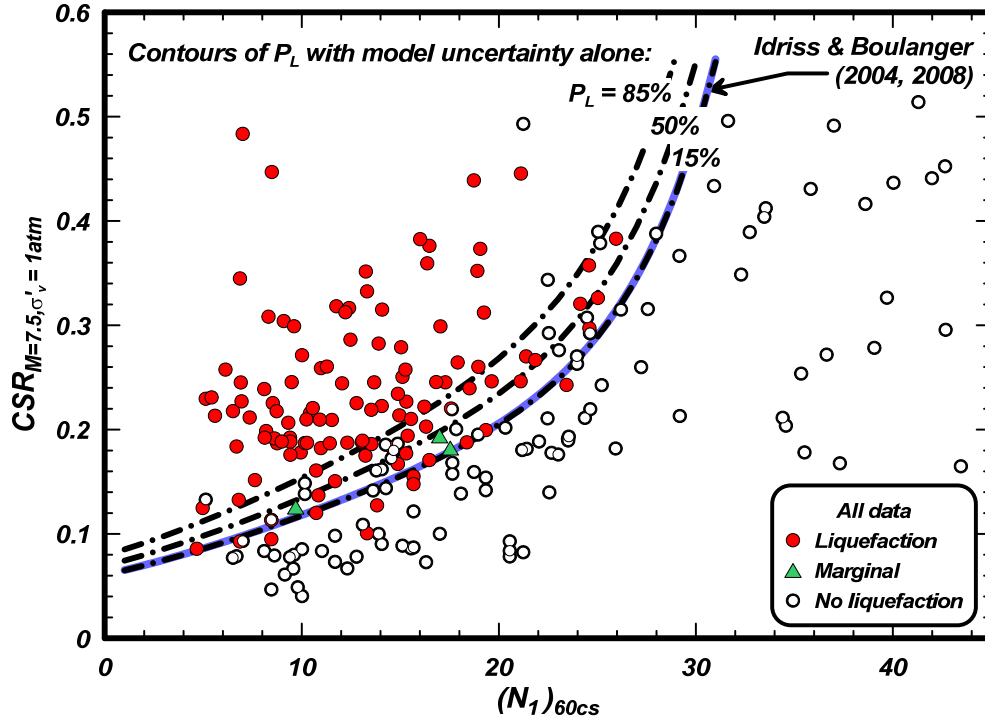


Figure 6.6. Curves of $CRR_{M=7.5, \sigma'_v=1atm}$ versus $(N_1)_{60cs}$ for probabilities of liquefaction of 15%, 50%, and 85%.

$$P_L \left((N_1)_{60cs}, CSR_{M=7.5, \sigma'_v=1atm} \right) = \Phi \left[\frac{\left(\frac{(N_1)_{60cs}}{14.1} + \left(\frac{(N_1)_{60cs}}{126} \right)^2 - \left(\frac{(N_1)_{60cs}}{23.6} \right)^3 + \left(\frac{(N_1)_{60cs}}{25.4} \right)^4 - 2.67 - \ln \left(CSR_{M=7.5, \sigma'_v=1atm} \right)}{\sigma_{\ln(R)}} \right] \quad (6.26)$$

The recommended triggering curves for probabilities of liquefaction [P_L] equal to 15%, 50%, and 85% with model uncertainty alone [i.e., conditional on known values of $CSR_{M=7.5, \sigma'_v=1atm}$ and $(N_1)_{60cs}$] are plotted together with the case history data in Figure 6.6. The above probabilistic triggering relationship (equation 6.24) is equal to the deterministic triggering correlation recommended by Idriss and Boulanger (2004, 2008) when $\varepsilon_{\ln(R)} = -0.13$. The deterministic relationship is therefore 1 standard deviation below the expected triggering curve and accordingly corresponds to a probability of liquefaction of about 16% as illustrated in Figures 6.4 and 6.6.

The probabilistic triggering curves by Cetin et al. (2002, 2004), as shown in Figure 6.1b, are located significantly lower than the curves derived herein (Figure 6.6). The reasons for these differences are examined in detail in Appendix A, where it is shown that the lower position of the Cetin et al. curves are primarily due to the misclassification of some key case histories and numerical errors in the processing of

their case history database. It is believed that the differences in the probabilistic models will be greatly reduced once their case history interpretations and numerical errors have been resolved and corrected.

The probabilistic triggering relationship expressed in Equations 6.23-6.25 must be recognized as being conditional on known values for $CSR_{M=7.5, \sigma'=1atm}$ and $(N_1)_{60cs}$ values; i.e., these equations only include the model uncertainty. To assess the probability of liquefaction in a liquefaction hazard evaluation, the conditional probability of liquefaction provided by these equations needs to be combined with the probabilities of the $CSR_{M=7.5, \sigma'=1atm}$ and $(N_1)_{60cs}$ values; i.e., the parameter uncertainties. In most situations, the uncertainties in estimating the latter parameters are much greater than the uncertainty in the liquefaction triggering model. For this reason, the formal treatment of uncertainties in the seismic hazard analysis and a detailed site characterization effort are generally more important to a liquefaction evaluation analysis than the uncertainty in the liquefaction triggering model.

Similarly, probabilistic relationships similar to that of Toprak et al. (1999) shown in Figure 6.1a must be recognized as already including some uncertainty in the input parameters (i.e., the measurement uncertainties in the case history database). For example, a probabilistic liquefaction hazard analysis can be structured so that it sequentially branches through a range of seismic hazards (which would account for the majority of the uncertainty in the $CSR_{M=7.5, \sigma'=1atm}$ values) and a range of site characterizations (which should account for the majority of the uncertainty in the $(N_1)_{60cs}$ values) before it gets to the liquefaction triggering analysis. In that scenario, it may be reasonable to only include model uncertainty in the liquefaction triggering analysis because the parameter uncertainties were already accounted for in the previous branches of the analysis. If instead, a probabilistic liquefaction triggering relationship such as that by Toprak et al. (1999) is used, then the inclusion of the model and measurement uncertainties in addition to the parameter uncertainties can be unnecessarily conservative.

6.4. Summary

A probabilistic version of the Idriss and Boulanger (2004, 2008) liquefaction triggering correlation was developed using the updated case history database and a maximum likelihood approach. Measurement and estimation uncertainties in CSR and $(N_1)_{60cs}$ and the effects of the choice-based sampling bias in the case history database are accounted for. The results of sensitivity analyses showed that the position of the most likely triggering curve was well constrained by the data and that the magnitude of the total error term was also reasonably constrained. The most likely value for the standard deviation of the error term in the triggering correlation was, however, found to be dependent on the uncertainties assigned to CSR and $(N_1)_{60cs}$. Despite this and other limitations, the results of the sensitivity study appear to provide reasonable bounds on the effects of different interpretations on the positions of the triggering curves for various probabilities of liquefaction. The probabilistic relationship for liquefaction triggering proposed herein is considered a reasonable approximation in view of these various findings.

The deterministic liquefaction triggering correlation by Idriss and Boulanger (2004, 2008) was shown to correspond to a probability of liquefaction of 16% based on the probabilistic liquefaction triggering relationship developed herein and considering model uncertainty alone.

A full probabilistic liquefaction hazard analysis will need to consider the uncertainties in the seismic hazard, the site characterization, and the liquefaction triggering model. The uncertainty in the liquefaction triggering model is much smaller than the uncertainty in the seismic hazard, and will often also be smaller than the uncertainty in the site characterization. For this reason, the seismic hazard analysis and the site characterization efforts are often the most important components of any probabilistic assessment of liquefaction hazards.

7. COMPARISON TO OTHER LIQUEFACTION TRIGGERING PROCEDURES

This section contains an examination of the differences between the liquefaction triggering correlations recommended by Idriss and Boulanger (2004, 2008), Youd et al. (2001), and Cetin et al. (2004). These three liquefaction triggering correlations, normalized to $M = 7.5$ and $\sigma'_v = 1$ atm, are compared in Figure 7.1. The CRR values obtained using these three correlations under different conditions are first compared in Section 7.1 to illustrate the magnitude of the differences for: (1) the range of depths and conditions represented in the case history database, and (2) depths and other conditions that require extrapolation outside the range of the case history data. This is followed by a summary of the primary reasons for the differences between these liquefaction triggering correlations in Section 7.2, with the more detailed examination and explanation for these differences presented in Appendix A. Lastly, Section 7.3 describes a few new findings and comments regarding the liquefaction analysis components C_N , K_σ , MSF, and r_d and their importance for guiding the application of liquefaction analysis procedures to conditions outside the range of the case history data.

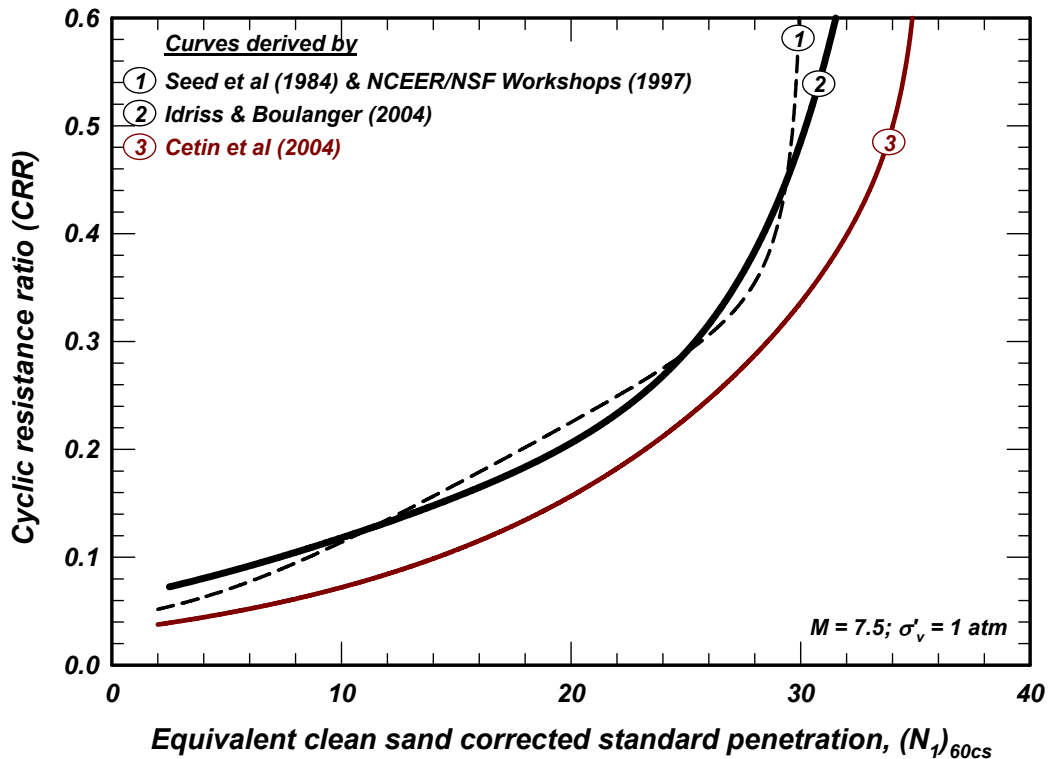


Figure 7.1. Liquefaction triggering correlations for $M = 7.5$ and $\sigma'_v = 1$ atm developed by: (1) Seed et al. (1984), as modified by the NCEER/NSF Workshops (1997) and published in Youd et al. (2001); (2) Idriss and Boulanger (2004, 2008); and (3) Cetin et al. (2004)

7.1. Comparison of CRR values obtained using different triggering correlations

The CRR values obtained using three different liquefaction triggering correlations are compared in this section. The first is the consensus correlation from the NCEER/NSF workshop (Youd et al. 2001) which is only slightly modified at low SPT blow counts relative to the relationship developed by the late Professor H. Bolton Seed and colleagues (Seed et al. 1985). Youd et al. indicated that the C_N expressions by Liao and Whitman (1986) and Kayen et al. (1992) were both acceptable for conventional practice and effective overburden stresses less than 2 atm and 3 atm, respectively. The C_N values produced by the Kayen et al. expression at overburden stresses greater than about 4 atm, however, are lower than supported by available calibration chamber test data and penetration theories. For this reason, the Liao-Whitman C_N expression is used in the NCEER/NSF procedures.

The K_σ relationship in the NCEER/NSF procedure requires an estimate of the in-situ D_R , which was obtained using,

$$D_R = \sqrt{\frac{(N_1)_{60cs}}{46}} \quad (7.1)$$

The following expression was then used to interpolate values for the exponent term in the NCEER/NSF K_σ relationship,

$$\begin{aligned} f &= 0.8 \quad \text{if } D_R \leq 0.4 \\ f &= 1 - \frac{D_R}{2} \quad \text{if } 0.4 \leq D_R \leq 0.8 \\ f &= 0.6 \quad \text{if } D_R \geq 0.8 \end{aligned}$$

$$K_\sigma = \left(\frac{P_a}{\sigma'_v} \right)^{1-f} \quad (7.2)$$

The second liquefaction triggering procedure compared in this section is that proposed by Cetin et al. (2004). Note that Cetin et al. developed their procedures probabilistically, after which they recommended that deterministic analyses could use a curve that was equal to their curve for a probability of liquefaction (P_L) equal to 15% for $(N_1)_{60cs}$ values less than or equal to 32, and then becomes slightly higher than the $P_L = 15\%$ curve as the $(N_1)_{60cs}$ values exceed 32. For simplicity, the comparisons shown herein are based on their $P_L = 15\%$ curve.

The third liquefaction procedure compared in this section is that developed by Idriss and Boulanger (2004, 2008).

The CRR values obtained using the three liquefaction procedures for clean sand ($FC = 5\%$) to depths of 20 m are compared in Figure 7.2. This figure shows contours of the ratio of the CRR values obtained using the Idriss-Boulanger or Cetin et al. procedures to the CRR value obtained using the NCEER/NSF procedure (e.g., CRR_{IB}/CRR_{NCEER} and $CRR_{Cetin \text{ et al.}}/CRR_{NCEER}$) for a range of SPT N_{60} values versus depth. These comparisons are for a water table depth of 1 m and an earthquake magnitude, $M = 7.5$.

The comparisons in Figure 7.2 serve to illustrate: (1) the differences over the range of depths for which there are case history data, and (2) the differences as the procedures are extrapolated to greater depths. The case history data are largely limited to depths less than about 12 m. For this range of depths, the

Idriss-Boulanger correlation gives CRR values that are generally within $\pm 10\%$ of the results obtained using the NCEER/NSF procedures. The Cetin et al. procedure gives CRR values that are generally within $\pm 10\%$ of those obtained by the NCEER/NSF procedures at depths close to 4 m, but then gives CRR values that are generally 10-40% smaller than the NCEER/NSF values at depths of 6-12 m. Thus, the primary difference between the three correlations in the depth range constrained by case history data is that the Cetin et al. procedures give significantly lower CRR values at the lower range of depths covered by the case history data (i.e., 6-12 m).

The differences in the procedures become more significant as they are extrapolated beyond the range of the case history data. For this range of depths, the Idriss-Boulanger correlation gives CRR values that are generally 10-40% larger than the CRR_{NCEER} values, and even larger for N_{60} values greater than 35 at depths greater than 16 m. In contrast, the Cetin et al. procedures give CRR values that are generally 10-40% smaller than the NCEER/NSF values at depths close to 20 m. The greatest contributors to these differences in the CRR values obtained by these three procedures are the baseline triggering correlation and the C_N and K_σ relationships. For depths less than about 4 m, however, the higher values of K_σ obtained with the Cetin et al.'s equation for K_σ result in CRR values much closer to the NCEER/NSF and the Idriss and Boulanger values.

The CRR values obtained using the three liquefaction procedures for silty sand ($FC = 35\%$) to depths of 20 m are compared in Figure 7.3. The Idriss-Boulanger procedure tends to give lower cyclic strengths than the NCEER/NSF procedure, reflecting the influence of their different equivalent clean sand adjustments as described in Section 2.2. The Cetin et al. procedure, however, produces CRR values that are significantly smaller than those obtained using the other two procedures for almost all depths.

The CRR values obtained using the three different procedures for clean sand ($FC = 5\%$) to the greater depth of 60 m are illustrated in Figure 7.4. This figure shows contours of the CRR values directly (and not as the ratios of CRR values) for this range of measured N_{60} values and depths. The contours show that the CRR values at depths of 20-40 m tend to be largest for the Idriss-Boulanger procedure, intermediate for the NCEER/NSF procedure, and significantly smaller for the Cetin et al. procedure. The greatest contributors to the differences in these CRR values are the differences in the baseline triggering correlations and the C_N and K_σ relationships, as was demonstrated previously for the Duncan Dam case study in Section 5.2.

Section 7.2 examines the reasons for the differences between these three correlations over the range of depths for which there are case history data, and Section 7.3 examines the issues with extrapolation to other conditions and depths.

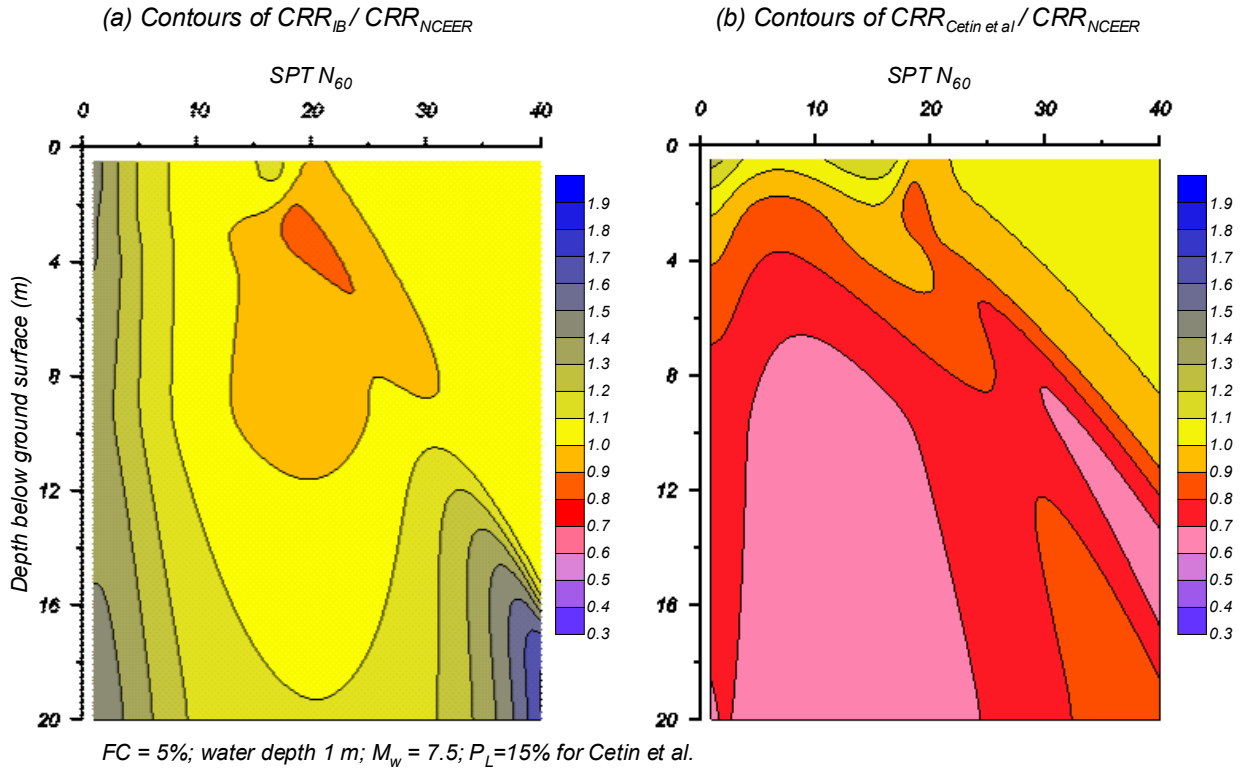


Figure 7.2. Comparison of liquefaction analysis procedures Idriss and Boulanger (2004, 2008), Cetin et al. (2004), and NCEER/NSF (Youd et al. 2001) for clean sand

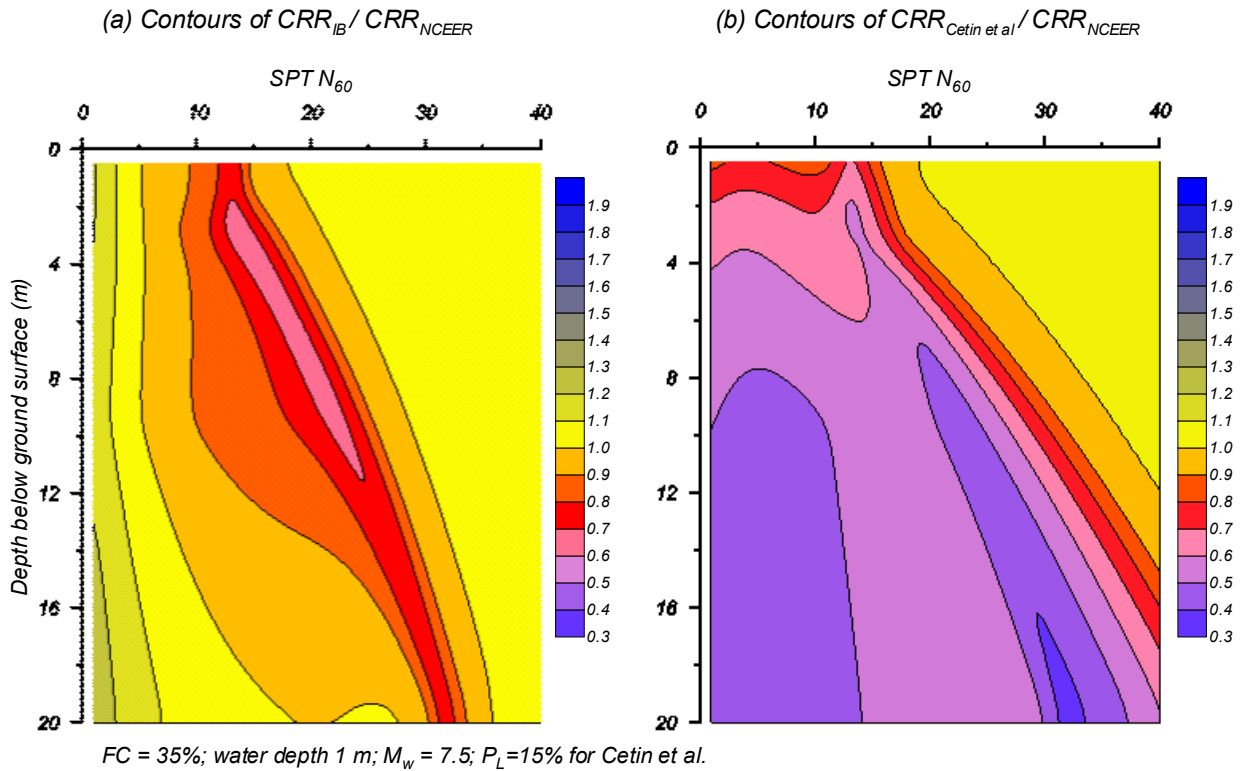


Figure 7.3. Comparison of liquefaction analysis procedures by Idriss and Boulanger (2004, 2008), Cetin et al. (2004), and NCEER/NSF (Youd et al. 2001) for silty sand with FC = 35%

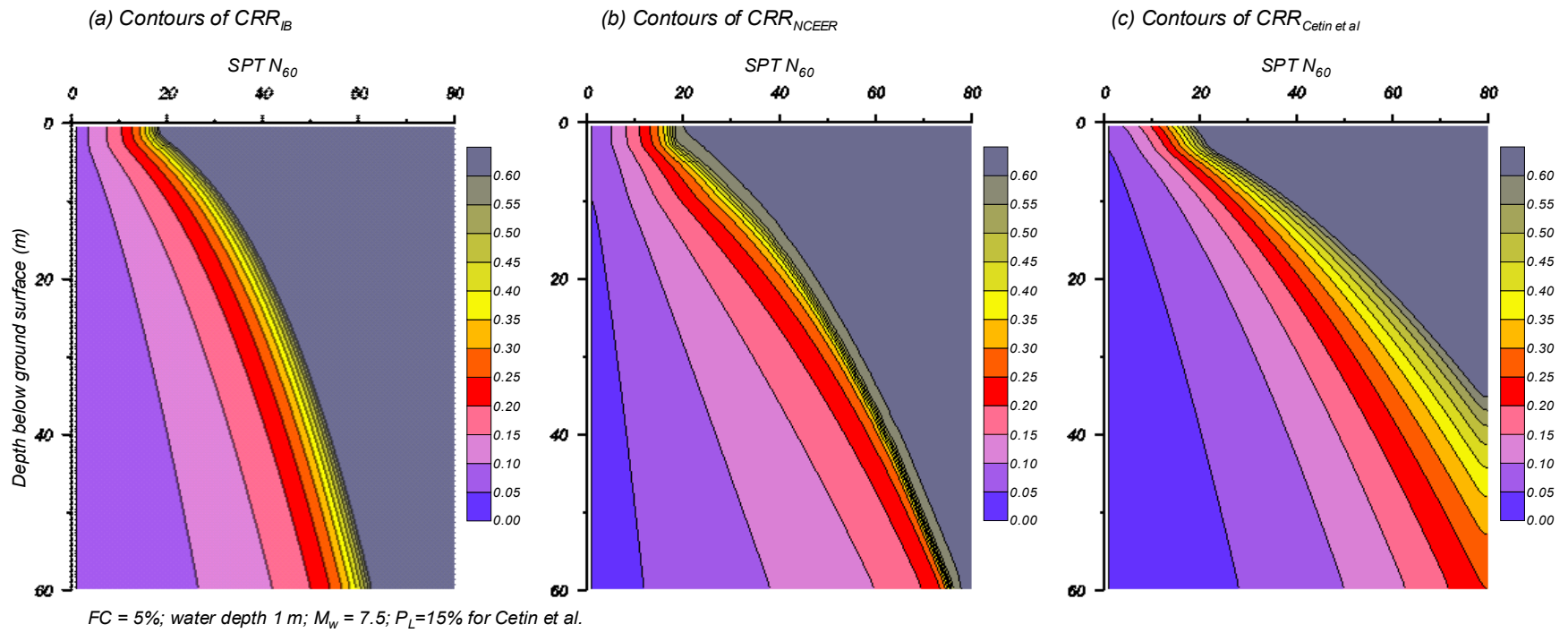


Figure 7.4. Contours of CRR values obtained using the procedures by Idriss and Boulanger (2004, 2008), NCEER/NSF (Youd et al. 2001), and Cetin et al. (2004) for clean sand for depths up to 60 m.

7.2. Reasons for the differences in the triggering correlations

The case history databases and analysis frameworks used by Seed et al. (1984), Youd et al. (2001), Cetin et al. (2004), and Idriss and Boulanger (2004, 2008) were examined and compared to identify the primary causes for the resulting differences in these liquefaction triggering correlations. It had been suspected that the differences in the liquefaction analysis components (r_d , K_σ , and C_N) may have played a significant role, but it was found that their effects were of secondary importance. Instead, the primary cause of the differences in the liquefaction triggering correlations was found to be the interpretations and treatment of 11 key case histories in the Cetin et al. (2000, 2004) database. Accordingly, a detailed examination of the Cetin et al. (2000, 2004) liquefaction procedure and the 11 key case histories is presented in Appendix A.

This section provides a brief summary of the findings presented in Appendix A regarding the Cetin et al. (2000, 2004) liquefaction triggering correlation and database. This examination was necessitated by the unfortunate events listed in Section 1 of this report. The results of this examination were communicated to Professor Onder Cetin in the summer of 2010, but there has been no indication from him or his co-authors that these issues will be addressed.

The key to finding what caused the difference among these liquefaction triggering correlations was assessing how well the case histories with σ'_v close to 1 atm supported any given correlation. The case histories that control the position of the different correlations (i.e., the data points that plot close to the triggering curve) with σ'_v close to 1 atm were identified and examined in detail. This examination showed that the case history interpretations by Seed et al. (1984) (which are also the basis for Youd et al. 2001) and Idriss and Boulanger (2004, 2008) provide rational support for their respective correlations. The case history interpretations by Cetin et al. (2004) were also found to support their correlation, but that support was found to hinge on a number of significant discrepancies and problems in the case history interpretations.

The primary cause for the differences in the three liquefaction triggering curves was found to be the interpretations by Cetin et al. (2000, 2004) for 11 key case histories for which the effective vertical stresses range from $\sigma'_v = 0.65$ to 1.5 atm in their database. The differences in the r_d , K_σ , and C_N relationships used in developing these three liquefaction triggering correlations were found to be lesser contributors to the differences in the triggering curves. In particular, the differences in the K_σ and C_N relationships are generally small near $\sigma'_v = 1$ atm, such that they have even smaller effects on the interpretations of the 11 key case histories discussed subsequently.

The case histories interpreted by, and listed in, Cetin et al. (2004) with σ'_v ranging from 0.65 to 1.5 atm are shown in Figure 7.5. The values of CSR adjusted for $M = 7.5$ and $\sigma'_v = 1$ atm are plotted versus the corresponding $(N_1)_{60cs}$, which shows that the case histories interpreted using the parameters listed by Cetin et al. (2004) support their liquefaction triggering curve for $M = 7.5$ and $\sigma'_v = 1$ atm.

The eleven case history points that appear to control the position of the Cetin et al. (2004) liquefaction triggering curve (for $\sigma'_v = 1$ atm and $M = 7.5$) were found to require the following significant adjustments. For ease of reference, these points are numbered 1 through 11 in Figure 7.5.

- Four cases (points 1, 2, 3, & 10) were identified and interpreted by the original investigators as "no liquefaction" sites, but were listed and used as "liquefaction" sites by Cetin et al. (2004). These sites are:
 - Point 1: Miller Farm CMF-10, 1989 Loma Prieta earthquake, $M = 6.9$ (Holzer et al. 1994, Holzer and Bennett 2007)

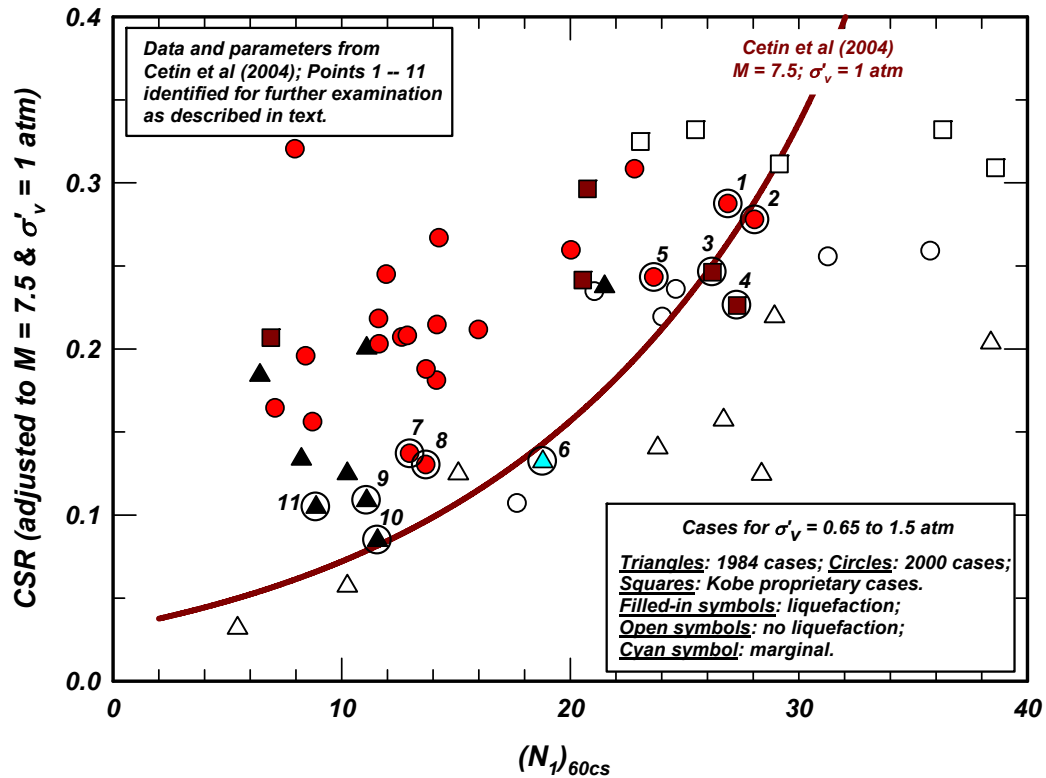


Figure 7.5. Case histories for $\sigma'_v = 0.65$ to 1.5 atm published by Cetin et al. (2004) with eleven points (cases) identified for further examination.

- Point 2: Malden Street, Unit D, 1994 Northridge earthquake, $M = 6.7$ (Holzer et al. 1999, O'Rourke 1998)
- Point 3: Kobe #6, 1995 Kobe earthquake, $M = 6.9$ (Tokimatsu 2010, pers. comm.)
- Point 10: Shuang Tai Zi River, 1975 Haicheng earthquake, $M = 7.0$ (Shengcong and Tatsuoka 1984, Seed et al. 1985).

The observations and interpretations provided by the original investigators regarding each site are well supported as summarized in Appendix A, and thus these four points should be re-classified as "no liquefaction" cases.

- Six of the key cases were affected by a discrepancy in the r_d values listed in the Cetin et al. (2004) database. For cases where Cetin et al. (2004) report using their regression equation for computing r_d , the values of r_d listed and used in their database do not agree with the values computed using their r_d regression equation. The differences between the computed and listed r_d values for the Cetin et al. database increase with depth, as shown in Figure 7.6. The key sites affected by this discrepancy are:
 - Point 3: Kobe #6, 1995 Kobe earthquake, $M = 6.9$, critical depth = 5.8 m
 - Point 4: Kobe #7, 1995 Kobe earthquake, $M = 6.9$, critical depth = 6.3 m
 - Point 6: Rail Road #2, 1964 Niigata earthquake, $M = 7.6$, critical depth = 10 m

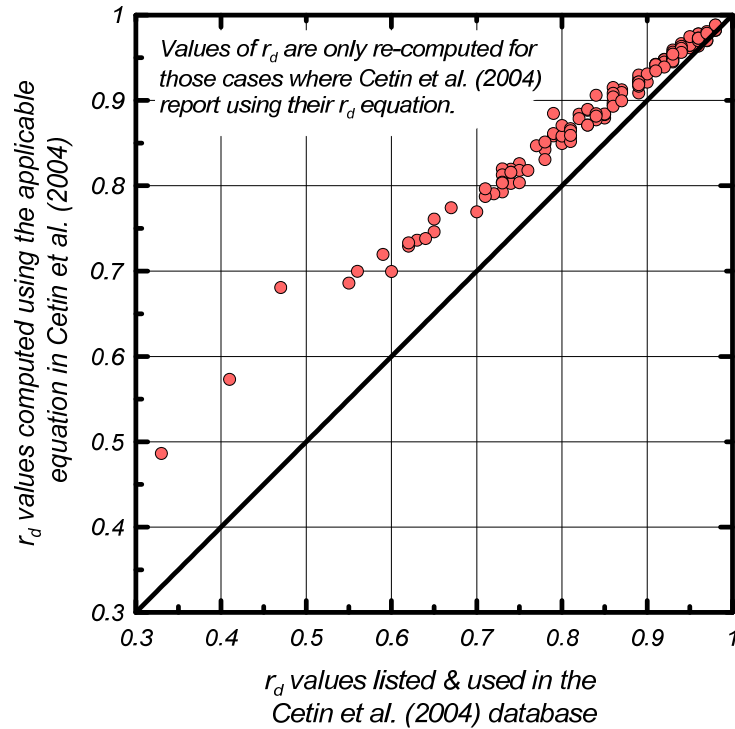


Figure 7.6. Discrepancy between r_d values computed using the Cetin et al. (2004) equation and the values listed and used in their database

- Point 9: Panjin Chemical Fertilizer Plant, 1975 Haicheng earthquake, $M = 7.0$, critical depth = 8 m
- Point 10: Shuang Tai Zi River, 1975 Haicheng earthquake, $M = 7.0$, critical depth = 8.5 m
- Point 11: San Juan B-3, 1974 Argentina earthquake, $M = 7.4$, critical depth = 11.7 m

The values of r_d were recalculated for these sites using the Cetin et al. (2004) r_d equation, as the authors indicated that the equation was correct (Cetin 2010, personal communication). This increased the CSR by 5% to 25%, which resulted in these case histories plotting farther above Cetin et al.'s liquefaction triggering curve.

- The boring data obtained at Kobe site No. 7 (Point 4) included a measured $N = 8$ value in the sand below the water table, but this N value was not utilized by Cetin et al. (2004) in assigning a representative $(N_1)_{60} = 27.3$ for this site. If the shallower $N = 8$ zone had been considered the critical zone by itself (as adopted in the updated database for this report), then the resulting $(N_1)_{60} = 11.0$ (using the Cetin et al. procedures) would be far above the Cetin et al. triggering curve. If the $N = 8$ blow count is at least included with the other blow counts used by Cetin et al., the computation gives an average $(N_1)_{60} = 23.2$ (using their procedures), which still results in locating the point considerably above the Cetin et al. (2004) liquefaction triggering curve for $M = 7.5$ and $\sigma'_v = 1$ atm.
- The Rail Road #2 site in the 1964 Niigata earthquake (Point 6), which is a marginal case, is the only point that remained close to the Cetin et al. (2004) triggering curve. Cetin et al. plotted this point considerably lower than did other investigators, with one contributing reason being that Cetin

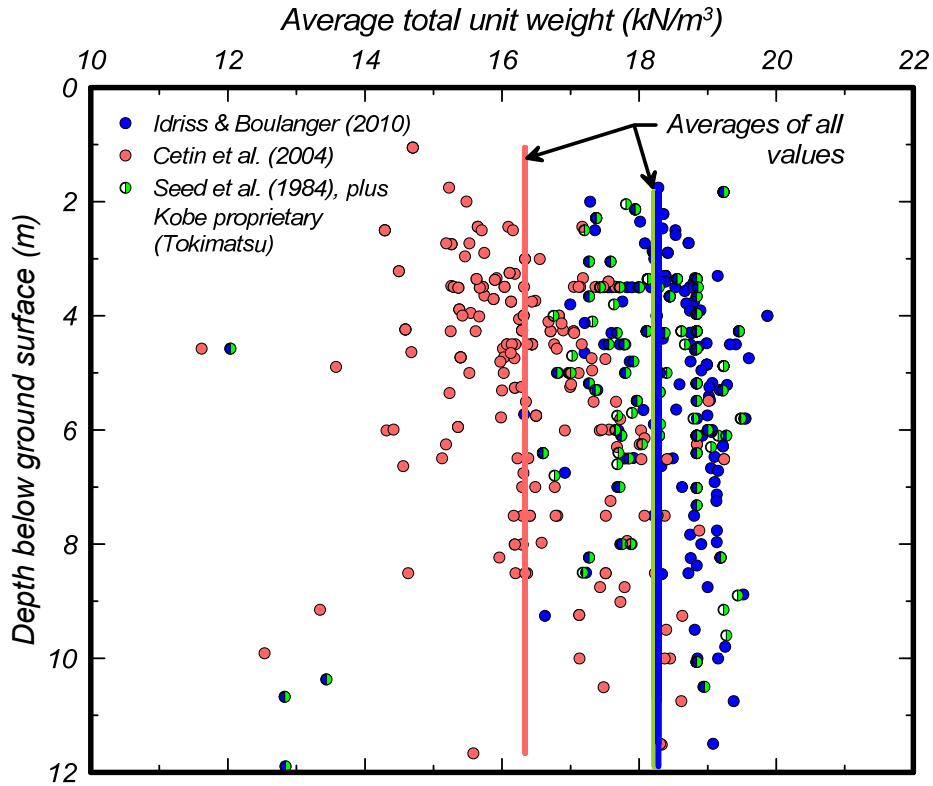


Figure 7.7. Comparison of average total unit weights used by different researchers in developing their liquefaction correlations

et al. used considerably smaller unit weights than did other investigators (Figure 7.7). Using more realistic total unit weights for this site, the point moves farther away from the Cetin et al. liquefaction triggering curve for $M = 7.5$ and $\sigma'_v = 1$ atm.

The case histories interpreted by, and listed in, Cetin et al. (2004) with σ'_v ranging from about 0.65 to 1.5 atm are shown in Figure 7.8 with the above-described adjustments to 8 of the 11 key points. The Cetin et al. database, with the above adjustments, no longer supports the Cetin et al. (2004) liquefaction correlation for $M = 7.5$ and $\sigma'_v = 1$ atm. Instead, the adjusted data points, which still utilize the Cetin et al. analysis framework, are now in better agreement with the liquefaction triggering curves proposed by the late Professor H. Bolton Seed and colleagues (Seed et al. 1985, Youd et al. 2001) and Idriss and Boulanger (2004, 2008).

The Cetin et al. (2004) triggering correlation, if it were updated after correcting the above issues, would be expected to move close to the Idriss-Boulanger and Seed et al. (1985)/Youd et al. (2001) correlations at effective vertical stresses ranging from about 0.65 to 1.5 atm. This would also cause the Cetin et al. K_σ relationship to become flatter because it is regressed as part of their analyses, and higher CRR values at higher confining stresses would dictate a flatter K_σ relationship. The combination of these changes would be expected to reduce the degree to which the Cetin et al. procedure predicts significantly smaller CRR values than the other liquefaction triggering correlations as depth increases.

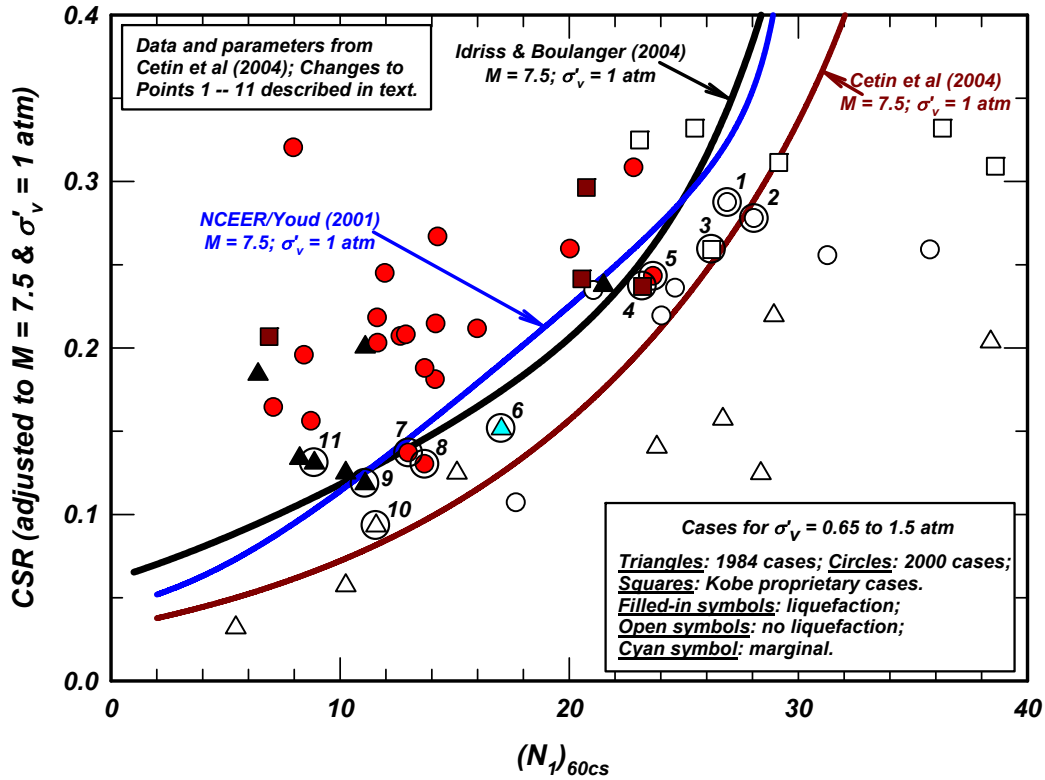


Figure 7.8. Case histories for $\sigma'_v = 0.65$ to 1.5 atm published by Cetin et al. (2004) with the corrections to the eleven points as described in the text

The above findings indicate that the lower position of the Cetin et al. (2004) triggering correlation, particularly at $(N_1)_{60cs}$ values less than 20, does not represent epistemic uncertainty, but rather is the result of case history interpretations and numerical errors that can be resolved and corrected.

7.3. Components affecting extrapolation outside the range of the case history data

Extrapolation of liquefaction triggering procedures beyond the range of conditions covered by the case histories (e.g., Figures 3.7 to 3.9) depends on the functional relationships for C_N , K_σ , MSF, and r_d in the analysis framework. Some recent findings and comments related to these analysis components are discussed in this section.

7.3.1. Role of C_N relationship

The effect of C_N relationships on the interpretation of the liquefaction case histories, with overburden stresses less than about 1.4 atm, was illustrated earlier in Figure 4.10. The use of the C_N expression recommended by Liao and Whitman (1986) versus the expression developed by Boulanger and Idriss (2004) shifts the data points, particularly at higher or lower N values, but the differences would not have affected the final liquefaction correlation.

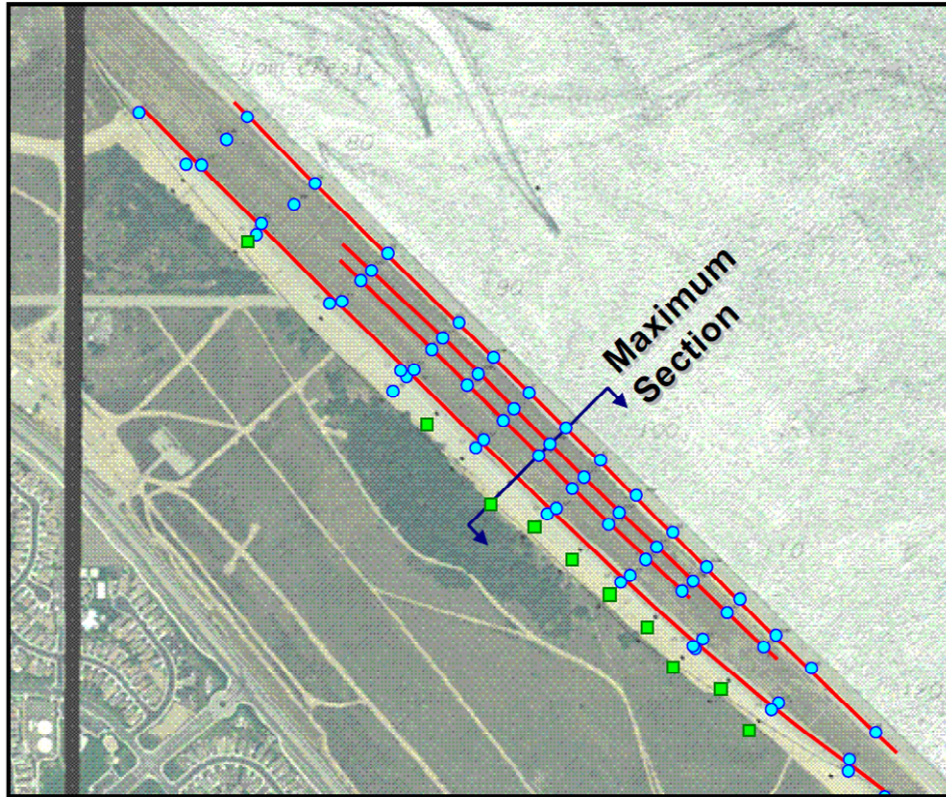


Figure 7.9. Aerial photo and boring locations at Perris Dam (Wehling and Rennie 2008)

The effect of different C_N expressions does, however, become very important for σ'_v greater than about 2 atm. It is often necessary in high dams to estimate C_N for σ'_v up to 12 atm, in which case the differences between the Liao-Whitman and Boulanger-Idriss relationships can be extremely important (Figures 5.8 and 7.4). Note that the Liao and Whitman (1986) relationship was based on an average fitting of the SPT data available at that time (primarily chamber test data with σ'_v up to 5.4 atm); the average fitting intentionally neglected the effect of D_R on C_N to keep the relationship simple. The Boulanger (2003) relationship was based on a combination of an updated regression analysis of the SPT chamber test data and the cone penetration theory of Salgado et al. (1997a,b) calibrated to the results of over 400 CPT calibration chamber tests with σ'_v up to about 7 atm. Boulanger included the effect of D_R on C_N because of its potential importance at large depths.

Recent extensive field studies by the California Department of Water Resources for Perris Dam enabled the development of a site-specific, field-based C_N relationship for the foundation silty and clayey sands with typical fines contents of 30-45% and σ'_v of 0.2 to 8.5 atm (CDWR 2005, Wehling and Rennie 2008). The locations of borings along the dam are shown on the plan view in Figure 7.9. The site-specific correlation was based on 316 SPT values from the upper 8 m of the foundation alluvium over a reach where these foundation soils were thickest and the depositional environment was judged to exhibit the highest degree of continuity in the upstream-downstream direction (CDWR 2005). The SPT data from the foundation alluvium beneath the toe, lower bench, upper bench, and crest are plotted versus vertical overburden stress in Figure 7.10. About 25% of the samples classified as nonplastic silty sand (SM), about 27% as low-plasticity clayey silty sand (SC-SM), about 34% as low-plasticity clayey sand (SC), and about 13% as low-plasticity clays (CL). The majority of these samples were considered susceptible to liquefaction due to the high sand content and the low-plasticity of the fines. Since these SPT data were

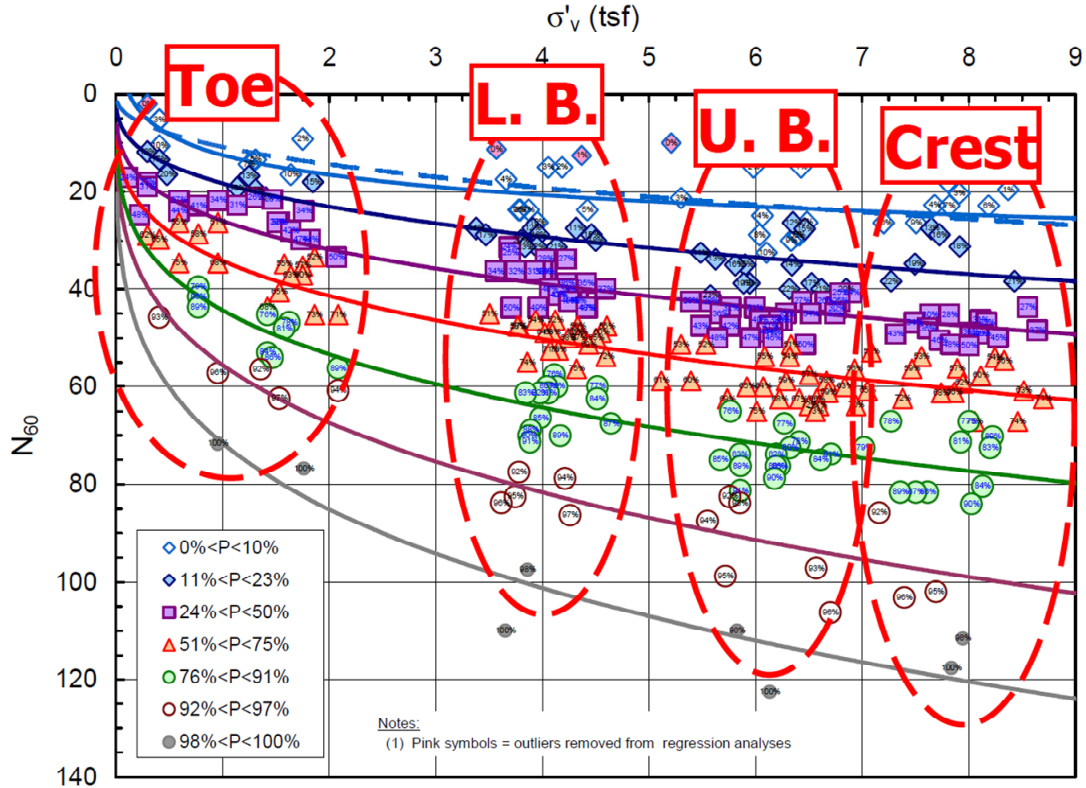


Figure 7.10. SPT data by location and percentile groupings (Wehling and Rennie 2008)

selected from a reach where the geologic conditions were interpreted as being relatively uniform in the upstream-downstream direction, it was assumed that the distribution of computed $(N_1)_{60}$ values should be approximately the same at the different locations beneath the dam. This assumption may be considered reasonable if the increase in stress caused by construction of the dam does not cause significant densification of the foundation soils [would increase the $(N_1)_{60}$ value], significant breakdown in cementation or ageing effects [would decrease the value of $(N_1)_{60}$], or significantly reduce the overconsolidation ratio or K_0 condition [would reduce the $(N_1)_{60}$ value]. Wehling and Rennie (2008) divided the N_{60} data into percentile bins, and fit each percentile bin with a regression of the form,

$$N_{60} = (N_1)_{60} \left(\frac{\sigma'_v}{P_a} \right)^m \quad (7.3)$$

where the $(N_1)_{60}$ and exponent "m" are parameters determined from the regression analysis. The corresponding site-specific C_N relationship is then,

$$C_N = \left(\frac{P_a}{\sigma'_v} \right)^m \quad (7.4)$$

Wehling and Rennie (2008) obtained values for the exponent m that decreased from 0.42 to 0.25 as the denseness of the soil increased (Figure 7.11).

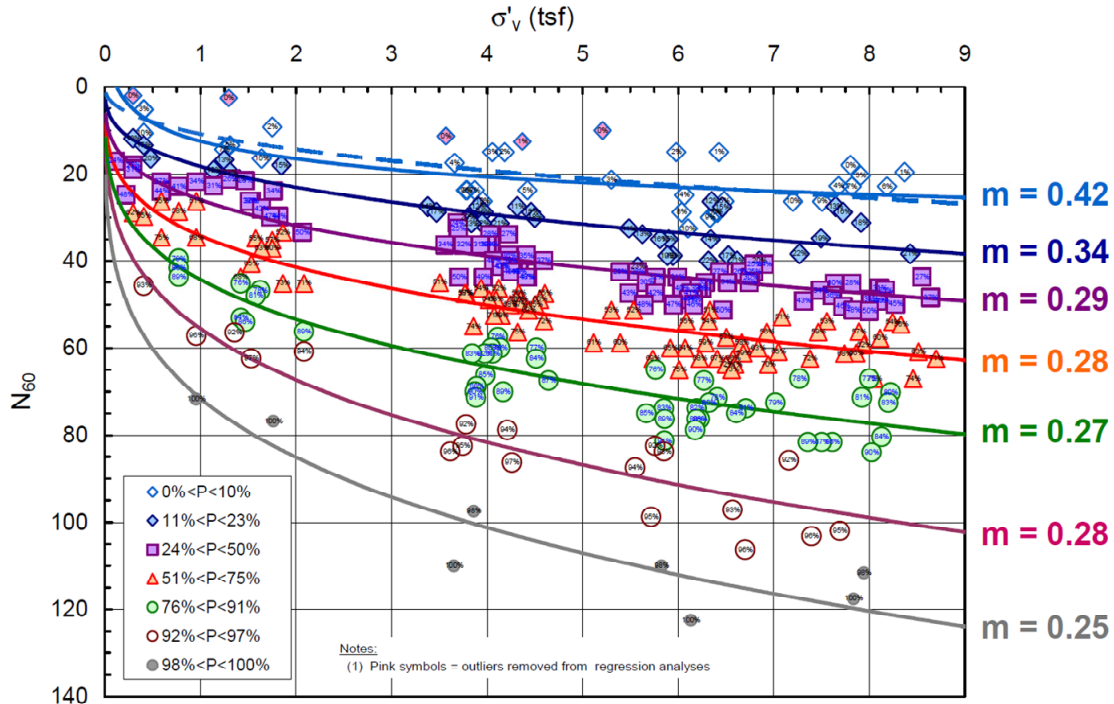


Figure 7.11. Regression on percentile bins of SPT data (Wehling and Rennie 2008)

The results that Wehling and Rennie (2008) obtained for Perris dam are compared to the C_N relationship used by Idriss and Boulanger (2008) in Figure 7.12 showing the exponent m versus the corresponding $(N_1)_{60}$ value (upper plot) and $(N_1)_{60cs}$ value (lower plot) for each of the data bins. The results from Perris Dam by Wehling and Rennie (2008) are in good agreement with the C_N relationship in the Idriss and Boulanger procedure, including the recommendation to relate the exponent m to $(N_1)_{60cs}$ rather than to $(N_1)_{60}$ for silty sands.

The Perris Dam data also illustrate how the use of $m = 0.5$, as in the Liao-Whitman relationship, would greatly underestimate C_N , and hence $(N_1)_{60}$, for these denser silty and clayey sands at high overburden stresses. For example, for $N_{60} = 60$, measured in the foundation layer under the crest of the dam, where $\sigma'_v \approx 8$ atm, the computed values of $(N_1)_{60}$ would be about 21 and 31 using the Liao-Whitman and Idriss-Boulanger relationships, respectively.

The above results by Wehling and Rennie (2008) assume that construction of the dam did not cause significant densification of the foundation soils, significant breakdown in cementation or ageing effects, or change the in-situ OCR sufficiently to alter the SPT blow counts. The potential significance of these assumptions is illustrated by the following numerical examples for evaluating how densification and changes in OCR might have affected the back-calculation of the exponent m in the C_N relationship.

The numerical example for evaluating the potential effects of densification on the interpretation of SPT data from beneath a dam, with conditions similar to those at Perris Dam, was developed based on the following assumptions.

- The dam is founded on a uniform layer of clean sand that had an $(N_1)_{60} = 22$ before construction of the dam.

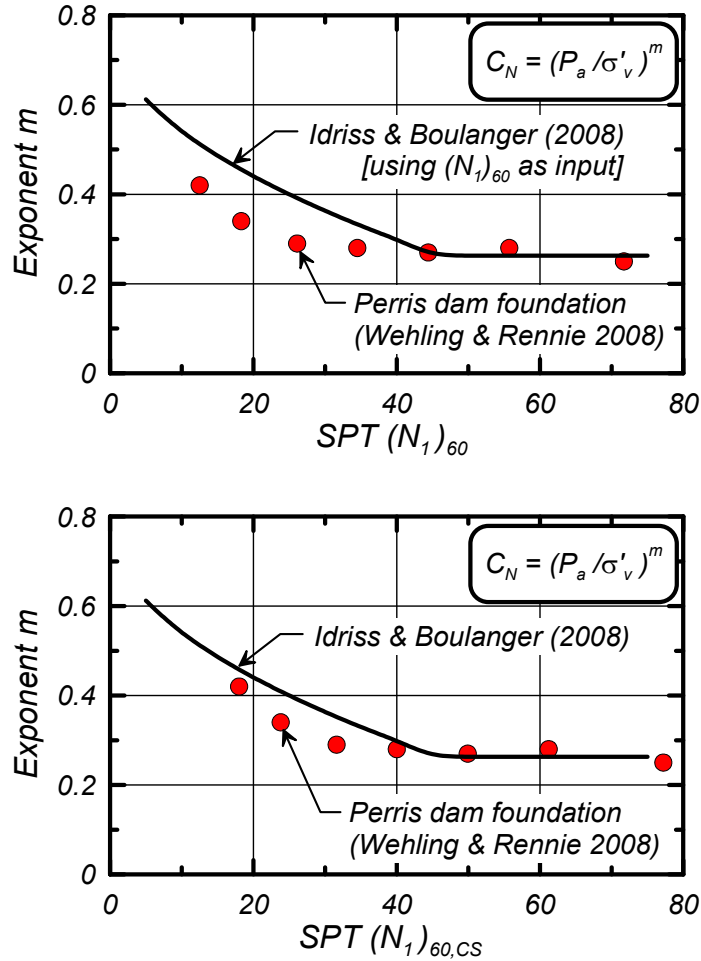


Figure 7.12. Comparison of the site-specific, field-based C_N data from Perris Dam (Wehling and Rennie 2008) with the relationship used by Idriss and Boulanger (2008).

- The variation of N_{60} with D_R and σ'_v in the sand is expressed by combining equations 7.1 and 7.4 as follows:

$$N_{60} = \frac{(N_1)_{60}}{C_N} = \left[46(D_R)^2 \right] \left(\frac{\sigma'_v}{P_a} \right)^m \quad (7.5)$$

This expression produces $D_R = 69\%$ for the $(N_1)_{60} = 22$ before construction of the dam.

- The stress exponent m in equation 7.5 is equal to 0.34 and is independent of D_R ; this value for m is comparable to those obtained for Perris Dam by Wehling and Rennie (2008), and the assumption that it is independent of D_R simplifies the example.
- The stress increases imposed by construction of the dam increase the relative density, D_R , by 1% per atm of stress increase; this compressibility is about 40% of the compressibility observed at Duncan Dam (Section 5), which is consistent with the soils being denser at Perris dam than at Duncan Dam. The assumed compressibility results in the D_R increasing from $D_R = 69\%$ at an effective overburden stress of 1 atm (i.e., beneath the toe) to $D_R = 76\%$ at an effective overburden stress 8 atm (i.e., beneath the crest).

These assumptions provide a complete description of how the D_R and SPT N_{60} values would theoretically vary with location beneath the dam. The computed variations in N_{60} versus σ'_v for $D_R = 69\%$ and $D_R =$

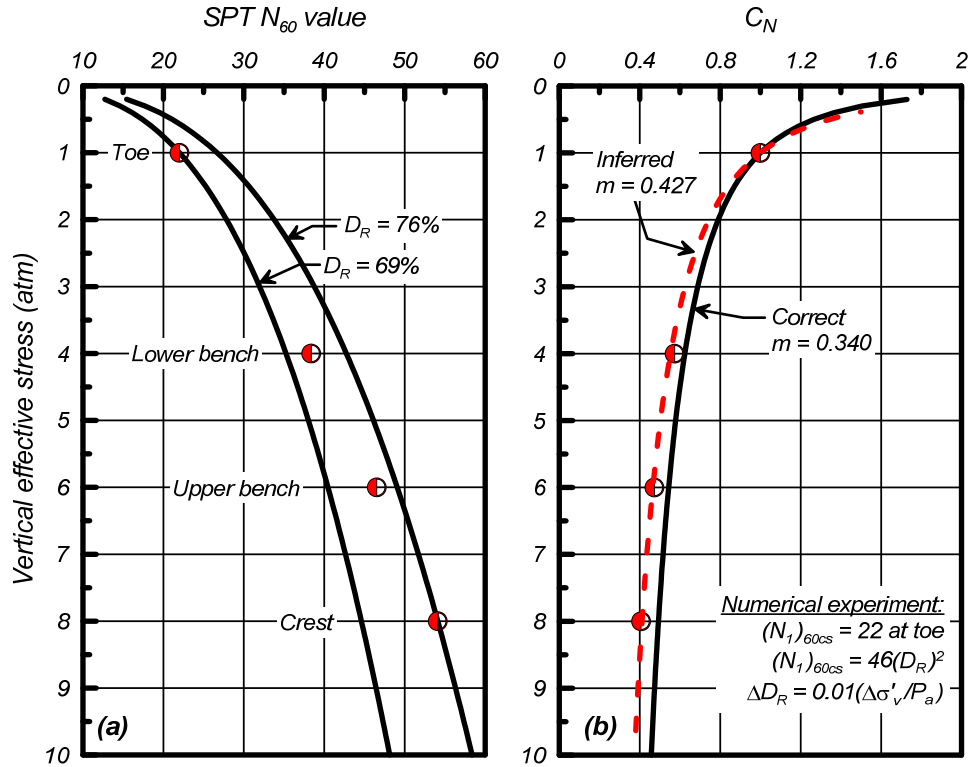


Figure 7.13. Numerical experiment to illustrate how densification of soils under the weight of the dam may have affected the back-calculated C_N relationship

76% are shown in Figure 7.13a. Also shown in this figure are the discrete N_{60} values that would be "measured" beneath a hypothetical toe, lower bench, upper bench, and crest with effective overburden stresses of 1, 4, 6, and 8 atm, respectively. The C_N relationship corresponding to the assumed $m = 0.34$ is shown in Figure 13b. Now suppose that the "measured" N_{60} values from beneath the toe, lower bench, upper bench, and crest are used to back-calculate a C_N relationship. If the effects of densification are neglected (i.e., assumed to be negligible), the "measured" N_{60} values in Figure 7.13a produce the discrete C_N values shown in Figure 7.13b. The best fit to these discrete C_N values produces an exponent $m = 0.427$, which is about 25% greater than the correct value of 0.34. This result illustrates how neglecting the densification of soils under the weight of the dam would lead to the back-calculation of an m exponent that is greater than the true value.

The numerical example for evaluating the potential effects of changes in OCR on the interpretation of SPT data from beneath a dam, with the same conditions as used for the previous example, was developed based on the following assumptions.

- The dam is founded on a uniform layer of clean sand with $D_R = 69\%$ and $OCR = 2$ before construction of the dam; this value of OCR is consistent with results of tests on soils near the downstream toe of Perris Dam.
- The sand's compressibility is sufficiently small that the D_R does not change under the weight of the dam.
- The coefficient of lateral earth pressure at rest, K_o , varies with OCR as,

$$K_o = (K_o)_{NC} \sqrt{OCR} = 0.45\sqrt{OCR} \quad (7.6)$$

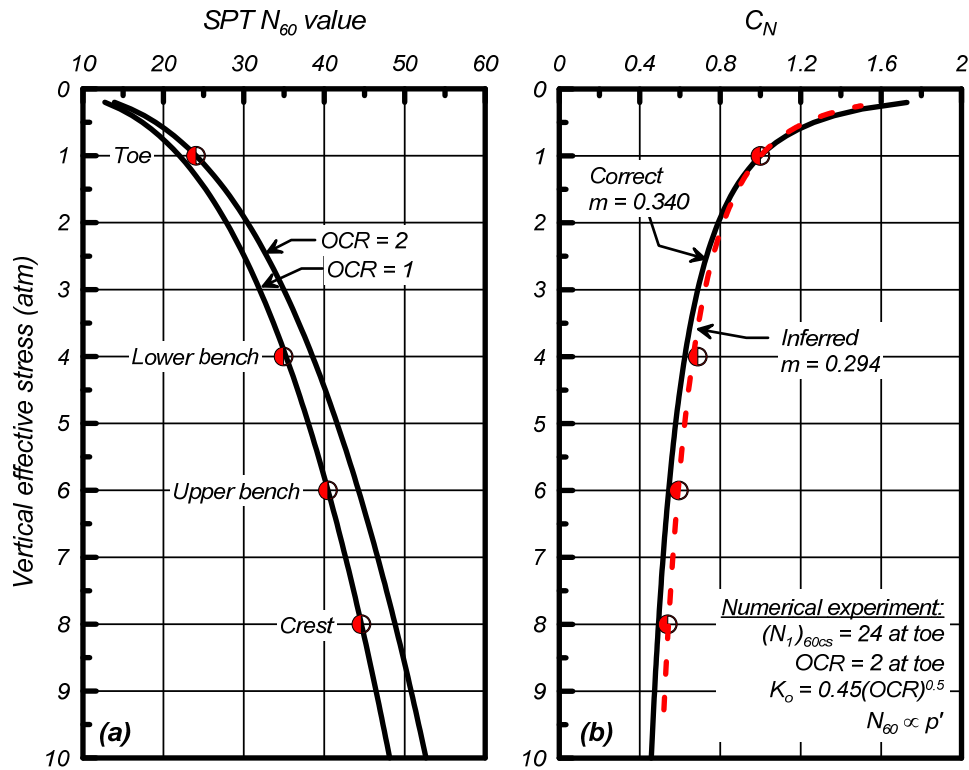


Figure 7.14. Numerical experiment to illustrate how changes in OCR caused by placement of the dam may have affected the back-calculated C_N relationship

- The variation of N_{60} with D_R , σ'_v and K_o in the sand is expressed by modifying equation 7.5 to include an effect of changing the mean effective stress, as:

$$N_{60} = \left[46(D_R)^2 \right] \left(\frac{\sigma'_v}{P_a} \right)^m \sqrt{\frac{1+2K_0}{1+2(K_0)_{NC}}} \quad (7.7)$$

This expression produces $(N_1)_{60} = 22$ for the sand if it is normally consolidated (OCR = 1).

- The stress exponent m in equation 7.7 is equal to 0.34 and is independent of D_R , as assumed for the previous example.

These assumptions provide a complete description of how the OCR and N_{60} values would theoretically vary with location beneath the dam. The computed variations in N_{60} versus effective overburden stress for OCR = 2 (applicable at the toe) and OCR = 1 (applicable beneath the crest of the dam) are shown in Figure 7.14a. Also shown on this figure are the discrete N_{60} values that would be "measured" beneath the hypothetical toe, lower bench, upper bench, and crest with effective overburden stresses of 1, 4, 6, and 8 atm, respectively. The C_N relationship corresponding to the assumed $m = 0.34$ is shown in Figure 14b. Now suppose that the "measured" N_{60} values from beneath the toe, lower bench, upper bench, and crest are used to back-calculate a C_N relationship. If the effects of changes in OCR are neglected (i.e., assumed to be negligible), the "measured" N_{60} values from Figure 7.14a produce the discrete C_N values shown in Figure 7.14b. The best fit to these discrete C_N values produces an exponent $m = 0.294$, which is about 14% smaller than the correct value of 0.34. This result illustrates how neglecting the changes in OCR caused by the weight of the dam would lead to the back-calculation of an m exponent that is smaller than the true value.

The preceding numerical examples illustrate the order of the errors that might be anticipated due to neglecting the effects of densification and OCR changes and that these errors appear to be partially compensating. The effects of any breakdown in cementation or ageing effects would be similar to the effect of OCR changes, in that neglecting this effect would result in the back-calculated m value being smaller than the true value. While the available information is not sufficient to quantify the effects of densification, OCR changes, and damage to cementation on the field testing data, it seems reasonable to consider that these effects have been at least partially compensating and that the values and trends derived by Wehling and Rennie (2008) are unlikely to be in significant error.

7.3.2. Role of K_σ relationship

The K_σ relationship results from fundamental characteristics of cohesionless soil behavior and, as such, it should be consistent across all empirical liquefaction triggering correlations (e.g., SPT- or CPT-based). The differences in the K_σ relationships derived by statistical analyses of the liquefaction case histories for SPT data (Cetin et al. 2004) and CPT data (Moss et al. 2006) illustrate the limitations in using statistical methods, without theoretical or experimental constraints, to define individual components of the liquefaction analysis framework.

Cetin et al. (2004) and Moss et al. (2006) incorporated the effects of K_σ using a Bayesian regression method as part of their interpretations of the case history databases for SPT and CPT data, respectively. Since similar approaches were used for the SPT and for the CPT databases, it is instructive to compare the K_σ expressions they obtained. Expressions for K_σ can be algebraically extracted from their equations for CRR, given the definition of K_σ , i.e.:

$$K_\sigma = \frac{CRR_\sigma}{CRR_{\sigma'_v=1atm}} \quad (7.8)$$

For Cetin et al. (2004), the equation for computing the CRR for a given probability of liquefaction is:

$$CRR = \exp \left[\frac{(N_1)_{60} \cdot (1 + 0.004 \cdot FC) + 0.05 \cdot FC - 29.53 \cdot \ln(M_w) - 3.70 \cdot \ln \left(\frac{\sigma'_v}{P_a} \right) + 16.85 + 2.70 \cdot \Phi^{-1}(P_L)}{13.32} \right] \quad (7.9)$$

Substituting the expression for CRR in the previous equation defining K_σ , and canceling common terms, leads to:

$$K_\sigma = \frac{\exp \left[-\frac{3.70}{13.32} \cdot \ln \left(\frac{\sigma'_v}{P_a} \right) \right]}{\exp \left[-\frac{3.70}{13.32} \cdot \ln(1) \right]} \quad (7.10)$$

$$K_{\sigma} = \left(\frac{\sigma'_v}{P_a} \right)^{-0.278} \quad (7.11)$$

This is the same functional form used by Hynes and Olson (1998), as published in Youd et al. (2001). The exponent of 0.278 would correspond to the value recommended by Youd et al. for a $D_R \approx 56\%$. Cetin et al. (2004) also recommended that their K_{σ} be limited to a maximum value of 1.5.

The K_{σ} effect in Moss et al. (2006) can similarly be extracted from their equation for CRR, i.e.:

$$CRR = \exp \left[\frac{q_{c,1}^{1.045} + q_{c,1} \cdot (0.110 \cdot R_f) + (0.001 \cdot R_f) + c(1 + 0.850 \cdot R_f) - 0.848 \cdot \ln(M_w) - 0.002 \cdot \ln(\sigma'_v) - 20.923 + 1.632 \cdot \Phi^{-1}(P_L)}{7.177} \right] \quad (7.12)$$

The corresponding K_{σ} relationship is:

$$K_{\sigma} = \frac{\exp \left[-\frac{0.002}{7.177} \cdot \ln(\sigma'_v) \right]}{\exp \left[-\frac{0.002}{7.177} \cdot \ln(P_a) \right]} = \left(\frac{\sigma'_{vc}}{P_a} \right)^{-0.00028} \quad (7.13)$$

The very small exponent in this K_{σ} expression results in K_{σ} values that are essentially equal to unity across the full range of stresses encountered in practice.

The very different K_{σ} relationships embedded in the regression models of Cetin et al. (2004) and Moss et al. (2006) are compared to those used by Idriss and Boulanger (2008) in Figure 7.15. Both the Cetin et al. and Moss et al. relationships neglect the experimentally-observed dependence of K_{σ} on relative density, D_R . The steepness of the Cetin et al. relationship is partly attributed to how they interpreted key case histories, as discussed in the previous section and in Appendix A. The essentially flat relationship by Moss et al. represents the best statistical fit to the CPT case history data conditional on the assumed forms for the other functional relationships in their liquefaction analysis framework; i.e., the regressed K_{σ} depends on the assumed relationships for C_N and r_d , the shape of the triggering curve, and the degree to which the case histories constrain the triggering relationship over the full range of stresses represented in the database.

The fact that the K_{σ} relationships regressed by Moss et al. and Cetin et al using CPT- and SPT-based case histories, respectively, are inconsistent with each other and inconsistent with available experimental data on the cyclic loading behavior of sands illustrate the limitations with using the case histories to infer this aspect of soil behavior. These observations also raise significant concerns about the use of these relationships outside the range of the case history data for which they were regressed (i.e., for depths greater than about 12 m).

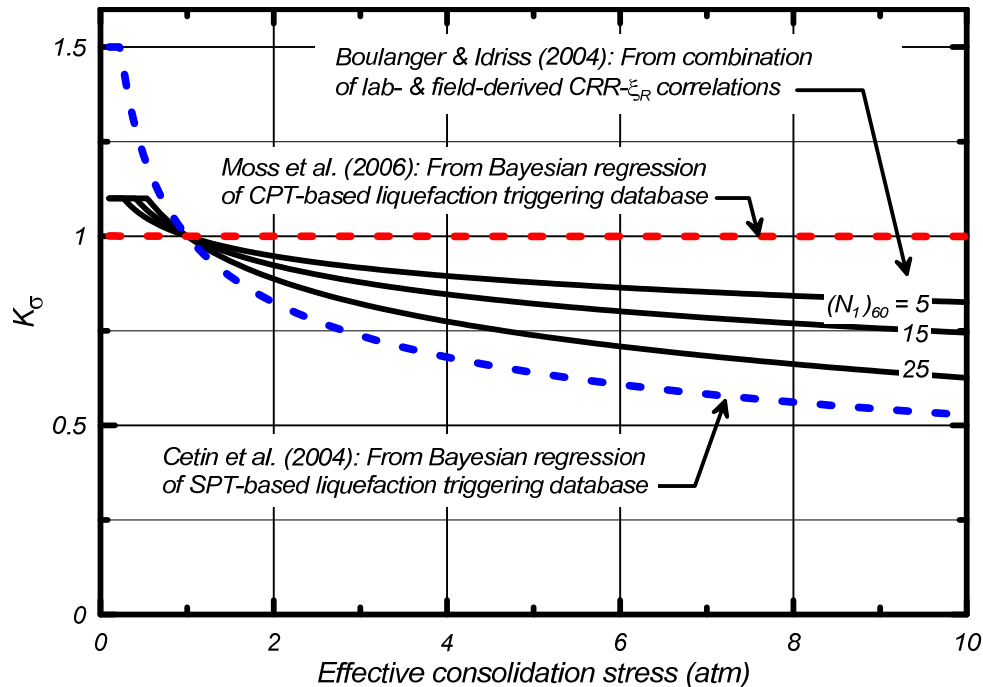


Figure 7.15. Comparison of K_σ relationships from the Idriss and Boulanger (2004, 2008), Cetin et al. (2004), and Moss et al. (2006) liquefaction triggering correlations.

7.3.3. Role of r_d relationship

The effects of different r_d relationships on the interpretation of the liquefaction case histories, which are limited to depths less than about 12 m, was discussed in Section 4.2.4. The effect of using the Kishida et al. (2009b) relationship instead of the Idriss (1999) relationship was illustrated in Figure 4.18, and shown to be relatively minor. Use of the Cetin et al. (2004) relationship did move several more case history points below the triggering curve (Figure 4.19), but the effect was relatively small compared to the effects of the issues identified with the Cetin et al. database in Appendix A.

For extrapolation to depths larger than about 12 m (i.e., beyond the range covered by the case histories), the r_d relationship should play a relatively minor role because dynamic site response analyses are often warranted when liquefaction at large depths is of concern (e.g., for dams or under deep fills). Dynamic site response analyses may use total stress-based models for computing the CSR values that are then used to evaluate the potential for liquefaction triggering, or effective stress-based models to directly simulate the liquefaction triggering process. Dynamic site response analyses by either approach do, however, require a good site characterization (e.g., V_s profile and soil characteristics), use of an adequate number of ground motion time series (e.g., typically, a minimum of seven), and an understanding of the limitations in predictions of site response using various types of numerical models.

7.3.4. Role of MSF relationship

The MSF represents a combination of earthquake ground motion characteristics and cohesionless soil behavior, and thus it should be consistent across all empirical liquefaction triggering correlations (e.g., SPT- or CPT-based). The differences in the MSF relationships derived by statistical analyses of the liquefaction case histories for SPT data (Cetin et al. 2004) and CPT data (Moss et al. 2006) provide a further illustration of the limitations in using empirical methods to define individual components of the liquefaction analysis framework.

Cetin et al. (2004) and Moss et al. (2006) included MSF effects (referred to as duration weight factors, DWF, in their work) in their Bayesian regression analyses of the SPT and CPT data, respectively. Expressions for MSF can be algebraically extracted from their expressions for CRR, given the definition of MSF, i.e.:

$$MSF = \frac{CRR_M}{CRR_{M=7.5}} \quad (7.14)$$

Using equation (7.9), the resulting MSF expression from Cetin et al. (2004) is:

$$MSF = \frac{\exp\left[-\frac{29.53}{13.32} \cdot \ln(M_w)\right]}{\exp\left[-\frac{29.53}{13.32} \cdot \ln(7.5)\right]} = \left(\frac{M_w}{7.5}\right)^{-2.217} \quad (7.15)$$

This expression results in $MSF = 1.99$ at $M = 5.5$ and $MSF = 0.76$ at $M = 8.5$, as shown in Figure 7.16.

Using equation (7.12), the expression for MSF derived from the Moss et al. (2006) liquefaction triggering equation is:

$$MSF = \frac{\exp\left[-\frac{0.848}{7.177} \cdot \ln(M_w)\right]}{\exp\left[-\frac{0.848}{7.177} \cdot \ln(7.5)\right]} = \left(\frac{M_w}{7.5}\right)^{-0.118} \quad (7.16)$$

The small exponent for this MSF expression results in $MSF = 1.04$ at $M = 5.5$ and $MSF = 0.99$ at $M = 8.5$, which represents an almost flat MSF relationship as shown in Figure 7.16. However, Moss et al. (2006) state that $CSR_{M=7.5}$ can be computed using the following equation:

$$MSF = 17.84(M_w)^{-1.43} = \left(\frac{M_w}{7.5}\right)^{-1.43} \quad (7.17)$$

This expression results in $MSF = 1.56$ at $M = 5.5$ and $MSF = 0.84$ at $M = 8.5$, which reflects an MSF relationship which is flatter than the Cetin et al. (2004) relationship although Moss et al. (2006) indicated it was intended as an approximation of the Cetin et al. relationship. The treatment of MSF effects in the Moss et al. procedure would appear to result in different options for computing a factor of safety against liquefaction. One option is to compute the CSR and CRR for the M and σ'_v of interest, i.e.:

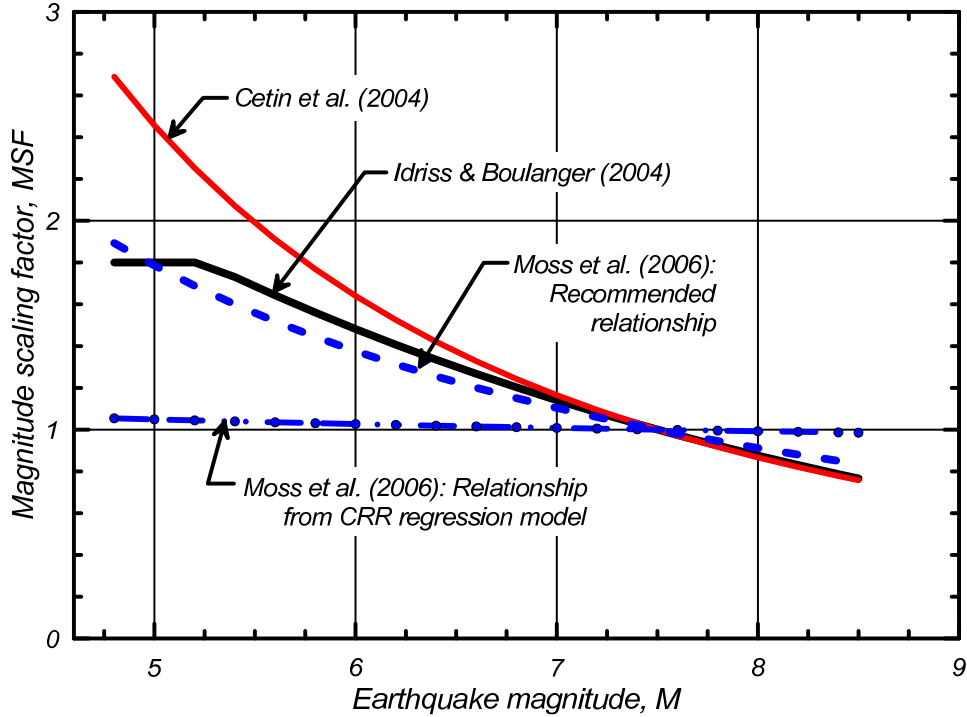


Figure 7.16. Comparison of MSF relationships from the liquefaction triggering procedures of Idriss and Boulanger (2004, 2008), Cetin et al. (2004), and Moss et al. (2006)

$$FS = \frac{CRR_{M,\sigma'_v}}{CSR_{M,\sigma'_v}} \quad (7.18)$$

in which case the relationships give an unacceptably flat MSF relationship. A second option is to compute the $CRR_{M=7.5}$ using the CRR expression with $M = 7.5$ and then use the steeper MSF relationship to convert the CSR to the desired $CSR_{M=7.5}$ as, i.e.:

$$FS = \frac{CRR_{M=7.5,\sigma'_v}}{(CSR_{M,\sigma'_v} / MSF)} \quad (7.19)$$

The latter option would include a more realistic representation of the MSF effect. It is not clear how this inconsistent treatment of the MSF effect may have influenced the regression model, or how it is intended that engineers in practice should implement these relationships.

The differences in the MSF relationships regressed by Moss et al. and Cetin et al. using CPT- and SPT-based case histories, respectively, illustrate the limitations in using the case history databases to regress this aspect of the liquefaction analysis framework.

It should be noted that the MSF relationships from Cetin et al. (2004), as shown in Figure 7.16, have been plotted differently in several publications. The paper by Seed et al. (2003) presented the liquefaction triggering correlations that were later published in Cetin et al. (2004), but plotted the MSF differently

from how it was later (correctly) shown in the Cetin et al. (2004) paper. Idriss and Boulanger (2004) included the MSF plot from Seed et al. (2003) in their figures, and then in Idriss and Boulanger (2008) incorrectly attributed the Seed et al. (2003) plot to Cetin et al. (2004). Despite these regrettable mistakes in presentation, the differences between the MSF relationships by Cetin et al. (2004) and Idriss and Boulanger (2004, 2008) are small over the range of M covered by the case history database and thus are a very minor source of differences in the respective SPT-based liquefaction correlations.

8. SUMMARY AND CONCLUSIONS

An updated examination of SPT-based liquefaction triggering procedures and the key technical issues affecting their development is presented in this report. This examination includes an update of the case history database, a reassessment of the SPT-based liquefaction triggering correlation recommended by Idriss and Boulanger (2004, 2008), and an evaluation of the reasons for the differences between some current liquefaction triggering correlations.

Updated case history database and its distribution

The updated case history database is summarized in Table 3.1 with supporting information provided in Appendix C. A number of case histories were reviewed in detail to illustrate several issues important to the interpretation of case histories, including the importance of a geologic understanding of the site and the methodology used for selecting representative SPT $(N_1)_{60cs}$ values from critical strata.

The distributions of the case history data with respect to the major parameters and the liquefaction triggering correlation of Idriss and Boulanger (2004, 2008) are described in Sections 3 and 4.1. The case history data do not adequately cover certain ranges of parameters and thus provide little or no empirical constraint on liquefaction triggering correlations for some ranges of conditions that are of interest to practice. In particular, the case history data are lacking for depths greater than about 10-12 m, for combinations of high FC and high $(N_1)_{60}$ values, and for small and large magnitude earthquakes.

Reexamination of liquefaction triggering procedures

The liquefaction triggering correlation recommended by Idriss and Boulanger (2004, 2008) is based on a synthesis of theoretical, experimental, and empirical information, and thus aspects of each of these sources of information have been reexamined in this report. A combination of theoretical, experimental, and empirical observations is considered essential for arriving at: (1) reasonable relationships that are consistent with the cumulative available information while overcoming the unavoidable limitations in each individual source of information, and (2) relationships that provide a rational basis for extrapolating outside the range of conditions covered by the case history database.

The distributions of the updated case history data with respect to the case history conditions (e.g., fines content, effective overburden stress, earthquake magnitude) and data sources (e.g., data from the U.S., Japan, pre- and post-1985 studies, and sites with strong ground motion recordings) are found to exhibit no evidence of significant trends or biases relative to the liquefaction triggering correlation by Idriss and Boulanger (2004, 2008).

Sensitivity analyses are used to examine how the positions of the case history data points relative to the liquefaction triggering correlation by Idriss and Boulanger (2004, 2008) are affected by select components and aspects of the liquefaction triggering analysis framework. The interpreted data points and their support for the current position of the liquefaction triggering correlation were not significantly affected by switching to the Liao and Whitman (1986) C_N relationship, eliminating the upper limit on the K_σ relationship, using greater rod extension lengths for determining the short-rod correction factors, switching to the r_d relationship by Kishida et al. (2009b), or switching to the equivalent clean sand adjustment $\Delta(N_1)_{60}$ relationship used in Youd et al. (2001). Switching to the r_d relationship by Cetin et al. (2004) moved a number of data points downward such that they would be consistent with a triggering curve that is about 10% lower than the Idriss-Boulanger triggering curve. The results of these sensitivity

studies indicate that the interpretations of the case history data and the position of the liquefaction triggering correlation are not sensitive to these aspects of the liquefaction analysis framework.

For $(N_1)_{60cs}$ values less than about 15, the cyclic resistances obtained from laboratory tests on frozen sand samples and from analyses of the field case history data are in good agreement. Specifically, the liquefaction triggering curve by Idriss and Boulanger (2004, 2008) is in good agreement with the results of the cyclic laboratory test on frozen sand samples and the associated correlations by Tokimatsu and Yoshimi (1983) and Yoshimi et al. (1994) for this range of $(N_1)_{60cs}$ values.

For $(N_1)_{60cs}$ values greater than about 15, the cyclic resistances obtained from laboratory tests on frozen sand samples are smaller than obtained from analyses of the field case history data. Specifically, the liquefaction triggering curve by Idriss and Boulanger (2004, 2008) and the similar Seed et al. (1984)/Youd et al. (2001) curve turn sharply upward near $(N_1)_{60cs}$ values of about 30, whereas the curves based on cyclic tests of frozen sand samples (Tokimatsu and Yoshimi 1983; Yoshimi et al. 1994) turn sharply upward near $(N_1)_{60cs}$ values of about 40.

The position of the Idriss-Boulanger (2004, 2008) liquefaction triggering curve at high $(N_1)_{60cs}$ values has been guided more closely toward the field case history data than to the results of the cyclic tests on frozen sand samples. The cyclic tests on frozen sand samples show that it may be possible to generate peak excess pore pressure ratios of 100% in very dense sands under very strong cyclic triaxial loads, but that the associated shear strains will generally be small. The field case history data suggest that no significant damage may be expected in sands with $(N_1)_{60cs}$ values greater than about 25 to 30, which may be because the in-situ permanent shear and volumetric strains are small enough that they do not result in any visible consequences at the ground surface in most situations. For practice, the current position of the Idriss and Boulanger (2004, 2008) liquefaction triggering curve at high $(N_1)_{60cs}$ values is considered appropriate for predicting the conditions required to trigger the onset of visible consequences of liquefaction.

A probabilistic version of the Idriss and Boulanger (2004, 2008) liquefaction triggering correlation was developed using the updated case history database and a maximum likelihood approach. Measurement and estimation uncertainties in CSR and $(N_1)_{60cs}$ and the effects of the choice-based sampling bias in the case history database were accounted for. The results of sensitivity analyses showed that the position of the most likely triggering curve was well constrained by the data and that the magnitude of the total error term was also reasonably constrained. The most likely value for the standard deviation of the error term in the triggering correlation was, however, found to be dependent on the uncertainties assigned to CSR and $(N_1)_{60cs}$. Despite this and other limitations, the results of the sensitivity study appear to provide reasonable bounds on the effects of different interpretations on the positions of the triggering curves for various probabilities of liquefaction. The probabilistic relationship for liquefaction triggering proposed herein is considered a reasonable approximation in view of these various findings.

The deterministic liquefaction triggering correlation by Idriss and Boulanger (2004, 2008) is found to correspond to a probability of liquefaction of 16% based on the probabilistic liquefaction triggering relationship developed herein and considering model uncertainty alone.

Probabilistic liquefaction hazard analyses need to consider the uncertainties in the seismic hazard, the site characterization, and the liquefaction triggering model. The uncertainty in the liquefaction triggering model is much smaller than the uncertainty in the seismic hazard, and will often be smaller than the uncertainty in the site characterization. For this reason, the seismic hazard analysis and the site characterization efforts are often the more important components of any probabilistic assessment of liquefaction hazards.

The two functional relationships that largely control the extrapolation of liquefaction triggering correlations to large depths (i.e., C_N and K_σ) are evaluated using the recent field studies for Perris Dam (Wehling and Rennie 2008) and the field and laboratory frozen sand sample test data for Duncan Dam (e.g., Pillai and Byrne 1994). The field studies for Perris Dam provided data at overburden stresses ranging from less than 1 atm to as high as 8 atm (Section 7.3.1). The results provided additional support for the C_N relationship by Idriss and Boulanger (2004, 2008) and illustrated how the Liao-Whitman (1986) C_N relationship used with the NCEER/NSF (Youd et al. 2001) and Cetin et al. (2004) procedures can result in a significant underestimation of in-situ $(N_1)_{60}$ values for dense sands at high overburden stresses. The field and laboratory frozen sand sample test data for Duncan Dam provided a test of liquefaction triggering procedures for overburden stresses ranging from 2 atm to 12 atm (Section 5.2). The results demonstrate that the Idriss and Boulanger relationships were consistent with these field/laboratory studies, whereas the relationships used in the NCEER/NSF (Youd et al. 2001) and Cetin et al. (2004) procedures would have contributed to a significant underestimation of the in-situ cyclic resistance ratios at these high overburden stresses.

Reasons for differences between some liquefaction triggering procedures

The primary reasons for the differences between the liquefaction triggering relationships published by the late Professor H. Bolton Seed and colleagues (Seed et al. 1984), which were adopted with slight modifications in the NCEER/NSF workshops (Youd et al. 2001), and those published more recently by Cetin et al. (2004) and those recommended by Idriss and Boulanger (2004, 2008) are identified by examining the respective databases and correlations in detail. The differences in the r_d , K_σ , and C_N relationships are found to have been secondary contributors to the differences in the resulting liquefaction triggering correlations. The primary causes of the differences in the liquefaction triggering correlations are found to be the interpretations and treatment of 8 key case histories with vertical effective stresses between 0.65 atm and 1.5 atm in the Cetin et al. (2000, 2004) database. This included having classified four key case histories as liquefaction cases in conflict with the original sources' classification as being no-liquefaction cases and having significant numerical errors between the r_d values used to develop their correlation and the r_d values computed using their applicable equation. The consequence of these misclassifications and errors was the regression of an overly steep K_σ relationship and an overly low liquefaction triggering curve. These findings were communicated to Professor Onder Cetin in the summer of 2010, but there has been no indication from him or his co-authors that these issues will be addressed and their procedure corrected as may be appropriate. Our examination of the Cetin et al. (2000, 2004) case history database and these 8 key cases are presented in detail in Appendix A for the purpose of facilitating discussions and independent examinations by the profession.

Concluding remarks

It is concluded that the NCEER/NSF (Youd et al. 2001) and Idriss-Boulanger (2004, 2008) liquefaction triggering procedures are reasonable for depths covered by the case history database (i.e., less than 12 m), and that the Idriss-Boulanger procedures are better-supported by existing field and laboratory data for extrapolations to greater depths.

It is hoped that the findings presented in this report will enable the geotechnical earthquake engineering profession to more accurately evaluate liquefaction hazards and to do so with greater confidence. It is also hoped that this report will serve as a helpful resource for practicing engineers and researchers working in the field of soil liquefaction and that it will be a useful technical supplement to the 2008 EERI Monograph on *Soil Liquefaction During Earthquakes* by Idriss and Boulanger (2008).

ACKNOWLEDGMENTS

The authors are grateful for information and insights provided by numerous colleagues regarding liquefaction case histories and analysis procedures over the years. For this current report, specific information on certain case histories was provided by Professor Kohji Tokimatsu and by Drs. Michael Bennett, Tom Holzer, and Rob Kayen. Dr. Dan Wilson provided significant assistance with the compilation and checking of the case history databases. Professor Russell Green and Ms. Kathryn Gunberg provided valuable review comments on portions of the database. Dr. Mike Beaty made a thorough review of a draft of this report and offered useful detailed and comprehensive suggestions. Professor Steve Kramer provided comprehensive comments and suggestions regarding the development of probabilistic relationships, as well as comments on other portions of the draft report. Additional comments and suggestions regarding different components of the report were provided by Drs. Richard Armstrong, David Gillette, Thomas Holzer, Erik Malvick, Yoshi Moriwaki, and Lelio Mejia, Professors Jon Bray, Steve Kramer, Bruce Kutter, James Mitchell, and Jon Stewart, and Messrs. Jack Montgomery and Steve Verigin. The comments and suggestions received from these valued colleagues helped improve the report significantly.

The authors are, however, solely responsible for the data, interpretations, and recommendations presented in this report.

REFERENCES

- Abrahamson, N., Atkinson, G., Boore, D., Bozorgnia, Y., Campbell, K., Chiou, B., Idriss, I. M., Silva, W., and Youngs, R. (2008). "Comparisons of the NGA ground-motion relations." *Earthquake Spectra*, 24(1), 45-66.
- Abrahamson, N., and Silva, W. (2008). "Summary of the Abrahamson & Silva NGA ground-motion relations." *Earthquake Spectra*, 24(1), 67-97.
- Bennett, M. J., McLaughlin, P. V., Sarmiento, J. S., and Youd, T. L. (1984). Geotechnical investigation of liquefaction sites, Imperial Valley, California. U.S. Geological Survey, Open-File Report 84-252, 103 pp.
- Bennett, M. J., Ponti, D. J., Tinsley, J. C., III, Holzer, T. L., and Conaway, C. H. (1998). Subsurface geotechnical investigations near sites of ground deformations caused by the January 17, 1994, Northridge, California, earthquake. U.S. Geological Survey, Open-file report 98-373, 148 pp.
- Bennett, M. J., and Tinsley, J. C, III (1995). Geotechnical data from surface and subsurface samples outside of and within liquefaction-related ground failures caused by the October 17, 1989, Loma Prieta earthquake, Santa Cruz and Monterey Counties, California. U.S. Geological Survey, Open-File Report 95-663, 360 pp.
- Bennett, M. J., Youd, T. L., Harp, E. L., and Wieczorek, G. F. (1981). Subsurface investigation of liquefaction, Imperial Valley earthquake, California, October 15, 1979. U.S. Geological Survey, Open-File Report 81-502, 83 pp.
- Bertero, V. V., et al. (1985). "Damage survey of the Nihon-Kai-Chubu, Japan earthquake of May 26, 1983. *Earthquake Spectra*, 1(2), 319-352.
- Boore, D. M., and Atkinson, G. M. (2008). "Ground-motion prediction equations for the Average Horizontal Component of PGA, PGV, and 5%-damped PSA at spectral periods between 0.01 s and 10.0 s." *Earthquake Spectra*, 24(1), 99-138.
- Boulanger, R. W. (2003). High overburden stress effects in liquefaction analyses, *J. Geotechnical and Geoenvironmental Eng.*, ASCE **129**(12), 1071–082.
- Boulanger, R. W. and Idriss, I. M. (2004). State normalization of penetration resistances and the effect of overburden stress on liquefaction resistance, in *Proceedings, 11th International Conference on Soil Dynamics and Earthquake Engineering, and 3rd International Conference on Earthquake Geotechnical Engineering*, D. Doolin et al., eds., Stallion Press, Vol. 2, pp. 484–91.
- Boulanger, R. W., Mejia, L. H., and Idriss, I. M. (1997). Liquefaction at Moss Landing during Loma Prieta earthquake, *J. Geotechnical and Geoenvironmental Eng.*, ASCE **123**(5), 453–67.
- California Department of Water Resources (CDWR) (2005). *Perris Dam Foundation Study – Final Report*. State of California, The Resources Agency, Department of Water Resources, Division of Engineering, December.
- Campbell, K. W., and Bozorgnia, Y. (2008). "NGA ground motion model for the geometric mean horizontal component of PGA, PGV, PGD and 5% damped linear elastic response spectra for periods ranging from 0.01 to 10 s." *Earthquake Spectra*, 24(1), 139-171.

- Casagrande, A. (1976). "Liquefaction and cyclic deformation of sands – A critical review." Harvard Soil Mechanics Series No. 88, Harvard University, Cambridge, Mass.
- Casagrande, A. (1980). Discussion of "Liquefaction potential: Science versus practice" by R. B. Peck, *Journal of Geotechnical Engineering Div., ASCE*, 106(GT6), 725-727.
- Castro, G. (1975). "Liquefaction and cyclic mobility of saturated sands." *Journal of the Geotechnical Engineering Division, ASCE*, 101(GT6), 551-569.
- Cetin, K. O., Der Kiureghian, A., Seed, R. B. (2002). "Probabilistic models for the initiation of seismic soil liquefaction." *Structural Safety*, 24: 67-82.
- Cetin, K. O., Seed, R. B., Moss, R. E. S., Der Kiureghian, A. K., Tokimatsu, K., Harder, L. F., and Kayen, R. E. (2000). *Field Performance Case Histories for SPT-Based Evaluation of Soil Liquefaction Triggering Hazard*, Geotechnical Engineering Research Report No. UCB/GT-2000/09, Geotechnical Engineering, Department of Civil Engineering, University of California at Berkeley.
- Cetin, K. O., and Seed, R. B. (2004). "Nonlinear shear mass participation factor (r_d) for cyclic shear stress ratio evaluation." *Soil Dynamics and Earthquake Engineering, Elsevier*, 24: 103-113.
- Cetin, K. O., Seed, R. B., Der Kiureghian, A., Tokimatsu, K., Harder, L. F., Kayen, R. E., and Moss, R. E. S. (2004). Standard penetration test-based probabilistic and deterministic assessment of seismic soil liquefaction potential, *J. Geotechnical and Geoenvironmental Eng., ASCE* **130**(12), 1314–340.
- Chiou, B., Darragh, R., Gregor, N., and Silva, W. (2008). "NGA project strong-motion database." *Earthquake Spectra, EERI*, 24(1), 23-44.
- Chiou, B. S. J., and Youngs, R. R. (2008). "An NGA model for the average horizontal component of peak ground motion and response spectra." *Earthquake Spectra*, 24(1), 173-215.
- Christian, J. T., and Swiger, W. F. (1975). "Statistics of liquefaction and SPT results." *Journal of Geotechnical Engineering Div., ASCE*, 101(GT11), 1135-1150.
- Chu, D. B., Stewart, J. P., Youd, T. L., and Chu, B. L. (2006). "Liquefaction-induced lateral spreading in near-fault regions during the 1999 Chi-Chi, Taiwan earthquake." *J. Geotechnical and Geoenvironmental Eng., ASCE*, 132(12), 1549-1565.
- Chu, D. B., Stewart, J. P., Boulanger, R. W., and Lin, P. S. (2008). "Cyclic softening of low-plasticity clay and its effect on seismic foundation performance." *J. Geotechnical and Geoenvironmental Eng., ASCE*, 134(11), 1595-1608.
- Daniel, C. R., Howie, J. A., Jackson, R. W., and Walker, B. (2005). "Review of standard penetration test short rod corrections." *J. Geotechnical and Geoenvironmental Eng., ASCE*, 131(4), 489-497.
- Engdahl, E. R., and Villasenor, A. (2002). "Global seismicity: 1900-1999." *International Handbook of Earthquake and Engineering Seismology, Intl. Assoc. Seismol. And Phys. Earth's Interior, Committee on Education, Vol. 81A*, 665-690.
- Fear, C. E., and McRoberts, E. C. (1995). Report on liquefaction potential and catalogue of case histories. Internal Research Report, Geotechnical Engineering Library, Dept. of Civil Engineering, University of Alberta, Edmonton, Alberta, Canada, March (revision of September 1993 report).

- Finn, W. D. (1988). "Liquefaction potential of level ground: Deterministic and probabilistic assessment." *Computers and Geotechnics*, 5, 3-37.
- Golesorkhi, R. (1989). *Factors Influencing the Computational Determination of Earthquake-Induced Shear Stresses in Sandy Soils*, Ph.D. thesis, University of California at Berkeley, 395 pp.
- Goto, S., and Nishio, S. (1988). Influence of freeze thaw history on undrained cyclic strength of sandy soils (in Japanese), in *Proceedings, Symposium on Undrained Cyclic Tests on Soils, Japanese Society for Soil Mechanics and Foundation Engineering*, pp. 149–54.
- Holzer, T. L. (1998). The Loma Prieta, California, Earthquake of October 17, 1989 – Liquefaction. Thomas L. Holzer, editor, U.S. Geological Survey Professional Paper 1551-B, 314 pp.
- Holzer, T. L., Bennett, M. J., Ponti, D. J., and Tinsley, J. C., III (1999). "Liquefaction and soil failure during 1994 Northridge earthquake." *J. Geotechnical and Geoenvironmental Engineering, ASCE*, 125(6), 438-452.
- Holzer, T. L., and Bennett, M. J. (2007). Geologic and hydrogeologic controls of boundaries of lateral spreads: Lessons from USGS liquefaction case histories, *Proceedings, First North American Landslide Conference*, Schaefer, V. R., Schuster, R. L., and Turner, A. K., eds., Association of Engineering Geologists Special Publication 23, 502-522.
- Holzer, T. L., Tinsley, J. C., III, Bennett, M. J., and Mueller, C. S. (1994). "Observed and predicted ground deformation – Miller Farm Lateral Spread, Watsonville, California." *Proceedings, 5th U.S.-Japan Workshop on Earthquake Resistant Design of Lifeline Facilities and Countermeasures Against Soil Liquefaction*. National Center for Earthquake Engineering Research, Report NCEER-94-0026, 79-99.
- Holzer, T. L., and Youd, T. L. (2007). "Liquefaction, Ground Oscillation, and Soil Deformation at the Wildlife Array, California." *Bulletin of the Seismological Society of America*, 97(3), 961-976.
- Hynes, M. E., and Olsen, R. (1998). Influence of confining stress on liquefaction resistance, in *Proceedings, International Symposium on the Physics and Mechanics of Liquefaction*, Balkema, Rotterdam, pp. 145–52.
- Iai, S., and Kurato, E. (1991). "Pore water pressures and ground motions measured during the 1987 Chiba-Toho-Oki earthquake (In Japanese). Technical Note 718, pp 1-18. Yokosuka: Port and Harbour Research Institute, Ministry of Transport, Japan.
- Iai, S., Matsunaga, Y., Morita, T., Miyata, M., Sakurai, H., Oishi, H., Ogura, H., Ando, Y., Tanaka, Y., and Kato, M. (1994). "Effects of remedial measures against liquefaction at 1993 Kushiro-Oki earthquake." *Proc., Fifth U.S.-Japan Workshop on Earthquake Resistant Design of Lifeline Facilities and Countermeasures Against Soil Liquefaction*, NCEER-94-0026, November, 135-152.
- Iai, S., Morita, T., Kameoka, T., Matsunaga, Y., and Abiko, K. (1995). "Response of a dense sand deposit during 1993 Kushiro-Oki earthquake." *Soils and Foundations*, 35(1), 115-131.
- Iai, S., Tsuchida, H., and Koizumi, K. (1989). "A liquefaction criterion based on field performances around seismograph stations." *Soils and Foundations*, 29(2), 52-68.

- Idriss, I. M. (1999). An update to the Seed-Idriss simplified procedure for evaluating liquefaction potential, in *Proceedings, TRB Workshop on New Approaches to Liquefaction*, Publication No. FHWA-RD-99-165, Federal Highway Administration, January.
- Idriss, I. M., and Boulanger, R. W. (2003). Relating K_α and K_σ to SPT blow count and to CPT tip resistance for use in evaluating liquefaction potential, in *Proceedings of the 2003 Dam Safety Conference*, ASDSO, September 7–10, Minneapolis, MN.
- Idriss, I. M., and Boulanger, R. W. (2004). Semi-empirical procedures for evaluating liquefaction potential during earthquakes, in *Proceedings, 11th International Conference on Soil Dynamics and Earthquake Engineering, and 3rd International Conference on Earthquake Geotechnical Engineering*, D. Doolin et al., eds., Stallion Press, Vol. 1, pp. 32–56.
- Idriss, I. M., and Boulanger, R. W. (2006). Semi-empirical procedures for evaluating liquefaction potential during earthquakes, *J. Soil Dynamics and Earthquake Eng.* **26**, 115–30.
- Idriss, I. M., and Boulanger, R. W. (2008). *Soil liquefaction during earthquakes*. Monograph MNO-12, Earthquake Engineering Research Institute, Oakland, CA, 261 pp.
- Ishihara, K. (1977). "Simple method of analysis for liquefaction of sand deposits during earthquakes." *Soils and Foundations*, 17(3), 1-17.
- Ishihara, K., Kawase, Y., and Nakajima, M. (1980). "Liquefaction characteristics of sand deposits at an oil tank site during the 1978 Miyagiken-Oki earthquake." *Soils and Foundations*, 20(2), 97-111.
- Ishihara, K., and Koga, Y. (1981). "Case studies of liquefaction in the 1964 Niigata earthquake." *Soils and Foundations*, 21(3), 35-52.
- Ishihara, K., Shimizu, K., and Yamada, Y. (1981). "Pore water pressures measured in sand deposits during an earthquake." 21(4), 85-100.
- Iwasaki, T. (1986). "Soil liquefaction studies in Japan: state-of-the-art." *Soil Dynamics and Earthquake Engineering*, 5(1), 2-68.
- Iwasaki, T., Arakawa, T., and Tokida, K. (1984). "Simplified procedures for assessing soil liquefaction during earthquakes." *Soil Dynamics and Earthquake Engineering*, 3(1), 49-59.
- Iwasaki, T., and Tokida, K. (1980). "Studies on soil liquefaction observed during the Miyagi-ken Oki earthquake of June 12, 1978." *Seventh World Conference on Earthquake Engineering*, Istanbul, Turkey, Sept 8-13, 1-8.
- Iwasaki, T., Tatsuoka, F., Tokida, K., and Yasuda, S. (1978). "A practical method for assessing soil liquefaction potential based on case studies at various sites in Japan." *Proc., Second International Conference on Microzonation for Safer Construction – Research and Application*. San Francisco, California, Nov 26 – Dec 1, 885-896.
- Juang, C. H., Jiang, T., and Andrus, R. D. (2002). "Assessing probability-based methods for liquefaction potential evaluation." *J. Geotechnical and Geoenvironmental Engineering*, ASCE, 128(7), 580-589.
- Kayen, R. E., Mitchell, J. K., Seed, R. B., Lodge, A., Nishio, S., and Coutinho, R. (1992). "Evaluation of SPT-, CPT-, and shear wave-based methods for liquefaction potential assessment using Loma Prieta

data." Proc., 4th Japan-U.S. Workshop on Earthquake-Resistant Des. of Lifeline Fac. and Countermeasures for Soil Liquefaction, Vol. 1, 177–204.

Kayen, R. E., Mitchell, J. K., Seed, R. B., and Nishio, S. (1998). "Soil liquefaction in the east bay during the earthquake." *The Loma Prieta, California, Earthquake of October 17, 1989 – Liquefaction*. Thomas L. Holzer, editor, U.S. Geological Survey Professional Paper 1551-B, B61-B86.

Kayen, R.E. and Mitchell, J. K. (1998). "Arias Intensity Assessment of Liquefaction Test Sites on the East Side of San Francisco Bay Affected by the Loma Prieta, California, Earthquake of 17 October 1989," in M.I. El-Sabh, S. Venkatesh, C. Lomnitz and T.S. Murty, eds., *Earthquake and Atmospheric Hazards: Preparedness Studies*. Kluwer Academic Publishers, The Netherlands, p 243-265.

Kishida, H. (1969). "Characteristics of liquefied sands during Mino-Owari, Tohnankai, and Fukui earthquakes." *Soils and Foundations*, IX(1), 75-92.

Kishida, H. (1970). "Characteristics of liquefaction of level sandy ground during the Tokachioki earthquake." *Soils and Foundations*, X(2), 103-111.

Kishida, T., Boulanger, R. W., Abrahamson, N. A., Driller, M. W., and Wehling, T. M. (2009a). "Site effects for the Sacramento-San Joaquin Delta." *Earthquake Spectra*, EERI, 25(2), 301-322.

Kishida, T., Boulanger, R. W., Abrahamson, N. A., Driller, M. W., and Wehling, T. M. (2009b). "Seismic response of levees in Sacramento-San Joaquin Delta." *Earthquake Spectra*, EERI, 25(3), 557-582.

Koizumi, Y. (1966). "Changes in density of sand subsoil caused by the Niigata earthquake." *Soils and Foundations*, VI(2), 38-44.

Liao, S. S. C., and Lum, K. Y. (1998). "Statistical analysis and application of the magnitude scaling factor in liquefaction analysis." *Geotechnical Earthquake Engineering and Soil Dynamics III*, ASCE, 1:410–21.

Liao, S. S. C., Veneziano, D., and Whitman, R. V. (1988). "Regression models for evaluating liquefaction probability." *J. Geotech. Eng. Div.*, ASCE, 114(4), 389–411.

Liao, S. C., and Whitman, R. V. (1986). Overburden correction factors for SPT in sand, *J. Geotechnical Eng.*, ASCE **112**(3), 373–77.

Manski, C. F., and Lerman, S. R. (1977). "The estimation of choice probabilities from choice-based samples." *Econometrica*, 45(8): 1977-1998.

Marcuson, W. F., and Bieganousky, W. A. (1977a). Laboratory standard penetration tests on fine sands, *J. Geotechnical Eng. Div.*, ASCE **103**(GT6), 565–88.

Marcuson, W. F., and Bieganousky, W. A. (1977b). SPT and relative density in coarse sands, *J. Geotechnical Eng. Div.*, ASCE **103**(GT11), 1295–309.

Mitchell, J. K., Lodge, A. L., Coutinho, R. Q., Kayen, R. E., Seed, R. B., Nishio, S., and Stokoe, K. H., II (1994). In situ test results from four Loma Prieta earthquake liquefaction sites: SPT, CPT, DMT and shear wave velocity. Earthquake Engineering Research Center, University of California at Berkeley, Report No. UCB/EERC-94/04, 186 pp.

- Moss, R. E. S., Seed, R. B., Kayen, R. E., Stewart, J. P., Der Kiureghian, A., and Cetin, K. O. (2006). CPT-based probabilistic and deterministic assessment of in situ seismic soil liquefaction potential, *J. Geotechnical and Geoenvironmental Eng.*, ASCE **132**(8), 1032–051.
- National Center for Earthquake Engineering Research (NCEER) (1997). *Proceedings of the NCEER Workshop on Evaluation of Liquefaction Resistance of Soils*, T. L. Youd and I. M. Idriss, editors, Technical Report NCEER-97-022, NCEER, NY.
- National Research Council (NRC) (1985). *Liquefaction of Soils During Earthquakes*, National Academy Press, Washington, DC, 240 pp.
- Ohsaki, Y. (1970). "Effects of sand compaction on liquefaction during the Tokachioki earthquake." *Soils and Foundations*, X(2), 112-128.
- Orchant, C. J., Kulhawy, F. H., and Trautman, C. H. (1988). "Reliability-based foundation design for transmission line structures: Critical evaluation of in-situ test methods." Report EL-5507, Vol. 2, Electric Power Research Institute, Palo Alto, 214 pp.
- O'Rourke, T. D. (1998). "An overview of geotechnical and lifeline earthquake engineering." Proc., Geotechnical Earthquake Engineering and Soil Dynamics – III, ASCE, 1392-1426.
- Pass, D. G. (1994). *Soil characterization of the deep accelerometer site at Treasure Island, San Francisco, California*. MS thesis in Civil Engineering, University of New Hampshire, May.
- Peck, R. B. (1979). "Liquefaction potential: Science versus practice." *J. Geotechnical Engineering Div.*, ASCE, 105(GT3), 393-398.
- Pillai, V. S., and Byrne, P. M. (1994). "Effect of overburden pressure on liquefaction resistance of sand." *Canadian Geotechnical Journal*, 31, 53-60.
- Pillai, V. S., and Stewart, R. A. (1994). "Evaluation of liquefaction potential of foundation soils at Duncan Dam." *Canadian Geotechnical Journal*, 31, 951-966.
- Plewes, H. D., Pillai, V. S., Morgan, M. R., and Kilpatrick, B. L. (1994). "In situ sampling, density measurements, and testing of foundation soils at Duncan Dam." *Canadian Geotechnical Journal*, 31, 927-938.
- Rathje, E. M., Abrahamson, N. A., and Bray, J. D. (1998). "Simplified frequency content estimates of earthquake ground motions." *J. Geotechnical and Geoenvironmental Eng.*, ASCE, 124(2), 150-159.
- Salgado, R., Boulanger, R. W., and Mitchell, J. K. (1997a). Lateral stress effects on CPT liquefaction resistance correlations, *J. Geotechnical and Geoenvironmental Eng.*, ASCE **123**(8), 726–35.
- Salgado, R., Mitchell, J. K., and Jamiolkowski, M. (1997b). Cavity expansion and penetration resistance in sands, *J. Geotechnical and Geoenvironmental Eng.*, ASCE **123**(4), 344–54.
- Schmertmann, J. S., and Palacios, A. (1979). Energy dynamics of SPT, *J. Soil Mechanics and Foundations Div.*, ASCE **105**(GT8), 909–26.
- Seed, H. B. (1979). "Soil liquefaction and cyclic mobility evaluation for level ground during earthquakes." *J. Geotechnical Eng. Div.*, ASCE **105**(GT2), 201–55.

Seed, H. B., Arango, I., Chan, C. K., Gomez-Masso, A., and Ascoli, R. G. (1979). Earthquake-induced liquefaction near Lake Amatitlan, Guatemala. Earthquake Engineering Research Center, University of California, Berkeley, Report No. UCB/EERC-79/27, 34 pp.

Seed, H. B., and Idriss, I. M. (1967). "Analysis of liquefaction: Niigata earthquake." Proc., ASCE, 93(SM3), 83-108.

Seed, H. B., and Idriss, I. M. (1971). "Simplified procedure for evaluating soil liquefaction potential." *J. Soil Mechanics and Foundations Div.*, ASCE **97**(SM9), 1249–273. Seed, H. B., and Idriss, I. M. (1982). *Ground Motions and Soil Liquefaction During Earthquakes*, Earthquake Engineering Research Institute, Oakland, CA, 134 pp.

Seed, H. B., Idriss, I. M., and Kiefer, F. W. (1969). "Characteristics of rock motions during earthquakes." *J. Soil Mech. and Found. Div.*, ASCE, **95**(5), 1199-1218.

Seed, H. B., Tokimatsu, K., Harder, L. F. Jr., and Chung, R. (1984). The influence of SPT procedures in soil liquefaction resistance evaluations. Earthquake Engineering Research Center, University of California, Berkeley, Report No. UCB/EERC-84/15, 50 pp.

Seed, H. B., Tokimatsu, K., Harder, L. F. Jr., and Chung, R. (1985). Influence of SPT procedures in soil liquefaction resistance evaluations, *J. Geotechnical Eng.*, ASCE **111**(12), 1425–445.

Seed, R. B., Cetin, K. O., Moss, R. E. S., Kammerer, A., Wu, J., Pestana, J., Riemer, M., Sancio, R. B., Bray, J. D., Kayen, R. E., and Faris, A. (2003). *Recent Advances in Soil Liquefaction Engineering: a Unified and Consistent Framework*, Keynote presentation, 26th Annual ASCE Los Angeles Geotechnical Spring Seminar, Long Beach, CA.

Shengcong, F., and Tatsuoka, F. (1984). "Soil liquefaction during Haicheng and Tangshan earthquake in China; A review." *Soils and Foundations*, **24**(4), 11-29.

Shibata, T. (1981). "Relations between N-value and liquefaction potential of sand deposits." Proc. 16th Annual Convention of Japanese Society of Soil Mechanics and Foundation Engineering, pp. 621-4 (in Japanese)

Singh, S., Seed, H. B., and Chan, C. K. (1982). Undisturbed sampling of saturated sands by freezing, *J. Geotechnical Engineering Division*, ASCE **108**(GT2), 247–64.

Tohno, I., and Yasuda, S. (1981). "Liquefaction of the ground during the 1978 Miyagiken-Oki earthquake." *Soils and Foundations*, **21**(3), 18-34.

Tokimatsu, K. (2010, personal communication). Boring logs for the 44 sites affected by the 1995 Kobe earthquake and listed in the Cetin et al. (2000) report.

Tokimatsu, K., and Yoshimi, Y. (1983). "Empirical correlation of soil liquefaction based on SPT N-value and fines content." *Soils and Foundations*, **23**(4), 56-74.

Tokimatsu, K., Yoshimi, Y., and Ariizumi, K. (1990). "Evaluation of liquefaction resistance of sand improved by deep vibratory compaction." *Soils and Foundations*, **30**(3), 153-158.

- Toprak, S., Holzer, T. L., Bennett, M. J., Tinsley, J. C. (1999). "CPT- and SPT-based probabilistic assessment of liquefaction potential." Proceedings of Seventh US Japan Workshop on Earthquake Resistant Design of Lifeline Facilities and Counter-measures Against Liquefaction, T. D. O'Rourke, J. P. Bardet, and M. Hamada, eds., Report MCEER-99-0019, MCEER, NY.
- Toprak, S., and Holzer, T. L. (2003). "Liquefaction potential index: Field assessment." Journal of Geotechnical and Geoenvironmental Engineering, ASCE, 129(4), 315-322.
- Tsuchida, H., Iai, S., and Hayashi, S. (1980). "Analysis of liquefactions during the 1978 OFF Miyagi Prefecture earthquake." Seventh World Conference on Earthquake Engineering, Istanbul, Turkey, Sept 8-13, 211-218.
- Wakamatsu, K., Yoshida, N., Suzuki, N., and Tazoh, T. (1993). "Liquefaction-induced ground failures and their effects on structures in the 1990 Luzon Philippines earthquake." 13th International Conference on Soil Mechanics and Foundation Engineering, JSSMFE, 17-26.
- Wehling, T. M., and Rennie, D. C. (2008). "Seismic evaluation of liquefaction potential at Perris Dam." Proceedings, Dam Safety 2008, Association of State Dam Safety Officials, Lexington, KY.
- Worden, C. B., Wald, D. J., Allen, T. I., Lin, K., and Cua, G. (2010). "Integration of macroseismic and strong-motion earthquake data in ShakeMap for real-time and historic earthquake analysis." USGS web site, <http://earthquake.usgs.gov/earthquakes/shakemap/>.
- Yasuda, S., and Tohno, I. (1988). "Sites of reliquefaction caused by the 1983 Nihonkai-Chubu earthquake." Soils and Foundations, 28(2), 61-72.
- Yoshimi, Y. (1970). "An outline of damage during the Tokachioki earthquake." Soils and Foundations, X(2),1-14.
- Yoshimi, Y., Hatanaka, M., and Oh-oka, H. (1978). "Undisturbed sampling of saturated sands by freezing." Soils and Foundations, 18(3), 59-73.
- Yoshimi, Y., Tokimatsu, K., Kaneko, O., and Makihara, Y. (1984). Undrained cyclic shear strength of a dense Niigata sand, *Soils and Foundations*, Japanese Society of Soil Mechanics and Foundation Engineering 24(4), 131-45.
- Yoshimi, Y., Tokimatsu, K., and Hosaka, Y. (1989). "Evaluation of liquefaction resistance of clean sands based on high-quality undisturbed samples." Soils and Foundations, 29(1), 93-104.
- Yoshimi, Y., Tokimatsu, K., and Ohara, J. (1994). In situ liquefaction resistance of clean sands over a wide density range, *Geotechnique*, 44(3), 479-94.
- Youd, T. L., and Bennett, M. J. (1983). "Liquefaction sites, Imperial Valley, California." Journal of the Geotechnical Engineering Division, ASCE, 109(3), 440-457.
- Youd, T. L., and Carter, B. L. (2005). "Influence of soil softening and liquefaction on spectral acceleration." Journal of Geotechnical and Geoenvironmental Engineering, ASCE, 131(7), 811-825.

Youd, T. L., DeDen, D. W., Bray, J. D., Sancio, R., Cetin, K. O., and Gerber, T. M. (2009). "Zero-displacement lateral spreads, 1999 Kocaeli, Turkey, earthquake." *J. Geotechnical and Geoenvironmental Eng.*, ASCE, 135(1), 46-61.

Youd, T. L., Idriss, I. M., Andrus, R. D., Arango, I., Castro, G., Christian, J. T., Dobry, R., Finn, W. D. L., Harder, L. F., Hynes, M. E., Ishihara, K., Koester, J. P., Liao, S. S. C., Marcuson, W. F., Martin, G. R., Mitchell, J. K., Moriwaki, Y., Power, M. S., Robertson, P. K., Seed, R. B., and Stokoe, K. H. (2001). Liquefaction resistance of soils: summary report from the 1996 NCEER and 1998 NCEER/NSF workshops on evaluation of liquefaction resistance of soils, *J. Geotechnical and Geoenvironmental Eng.*, ASCE **127**(10), 817–33.

Youd, T. L., and Noble, S. K. (1997). "Liquefaction criteria based on statistical and probabilistic analyses." Proceedings of the NCEER workshop on evaluation of liquefaction resistance of soils, Technical Report NCEER-97-022, 201–205.

APPENDIX A:

**EXAMINATION OF THE CETIN ET AL (2004)
LIQUEFACTION TRIGGERING CORRELATION**

APPENDIX A

EXAMINATION OF THE CETIN ET AL (2004) LIQUEFACTION TRIGGERING CORRELATION

A-1. INTRODUCTION

An examination of the Cetin et al. (2004) liquefaction triggering correlation is summarized in this Appendix. This examination was carried out as part of determining why the correlation of CRR adjusted for $M = 7.5$ and $\sigma'_v = 1$ atm versus $(N_1)_{60cs}$ proposed by Cetin et al. (2004) is significantly lower than: (1) the correlation developed by the late Professor H. Bolton Seed and his colleagues (Seed et al. 1984), which was subsequently adopted with slight modification during the NCEER/NSF workshops in 1996/1997 (Youd et al. 2001); and (2) the correlation developed by Idriss and Boulanger (2004, 2008). These three liquefaction triggering correlations are compared in Figure A-1, illustrating the significantly lower position of the Cetin et al. (2004) correlation and the relatively good agreement between the Seed et al. (1984) and Idriss and Boulanger (2004, 2008) correlations. Accordingly, the purpose of this assessment is to address the following question:

"Why are these published curves of CRR versus $(N_1)_{60}$ or $(N_1)_{60cs}$ so different although they are based on essentially the same case history data?"

The remaining pages of this Appendix examine the data, plots and various relationships included in Cetin et al. (2000, 2004) to provide the means for assessing whether this information supports their recommendation of a significantly lower correlation for $CRR_{M=7.5, \sigma'_v=1 \text{ atm}}$ versus $(N_1)_{60cs}$. Emphasis is placed on examining the details for those case histories that *control the position* of the Cetin et al. correlation of CRR adjusted for $M = 7.5$ and $\sigma'_v = 1$ atm versus $(N_1)_{60cs}$. The results of this examination provide clarification on the primary reasons why the Cetin et al. correlation is significantly lower than the other correlations.

A-2. DATABASE OF CETIN ET AL (2004)

The liquefaction triggering correlation published by Cetin et al. (2004) is based on the doctoral dissertation of Professor O. Cetin, which was completed in 2000 at UC Berkeley under the direction of Professor R. Seed. The liquefaction and no-liquefaction case histories used in deriving this correlation are included in Cetin et al. (2000) and summarized in Cetin et al. (2004). These case histories were organized in three groups: "the 1984" or "old" cases, which are those published by Seed et al. (1984) less a few that Cetin et al. considered not adequately documented; "the 2000" or "new" cases gathered by Cetin et al. (2000); and "the Kobe" or "Kobe proprietary" cases acquired from Professor K. Tokimatsu at the Tokyo Institute of Technology. The key parameters for these cases are summarized in Tables 5, 7 and 8, respectively, in Cetin et al. (2004).

The 1984 cases include 47 cases designated as having surface evidence of liquefaction, or simply "liquefaction" cases, 40 cases with no surface evidence of liquefaction, or simply "no liquefaction" cases, and 2 cases of marginal liquefaction. The 2000 cases include 42 cases of "liquefaction" and 25 cases of "no liquefaction". The Kobe proprietary cases, as listed in Cetin et al. (2004), include 20 liquefaction cases, 23 cases of no liquefaction and 1 case of marginal liquefaction.

Descriptions regarding liquefaction/no liquefaction and key measured, calculated or assigned parameters (e.g., critical depth, depth to the water table, σ_v , σ'_v , a_{max} , CSR, N, $(N_1)_{60}$, FC ... etc.) were provided in Cetin et al. (2000) in a 2-page summary for each case history. The upper part of the first page gives the name of the case history, the relevant references, the nature of the surface observations (i.e., liquefaction or no liquefaction), and other details regarding the site and any calculations (e.g., site response) carried out by Cetin et al. The bottom part of the first page indicates whether there was surface evidence of liquefaction (designated as "Yes" in this part) or no liquefaction (designated as "No" in this part), and provides values of the key parameters for that case. This part of the first page also lists the values given by Seed et al. (1984) and/or Fear and McRoberts (1995), as applicable. The second page shows available boring logs, measured SPT N values and the calculated values of $(N_1)_{60}$. An example of such information is illustrated in Figure A-2 for the Heber Road A2 case history. Except for one of the 1984 case histories (which will be discussed later), the top and the bottom parts of the first page were consistent in the description of the nature of the surface observations for the 1984 and for the 2000 case histories.

The 2-page summaries for the 44 Kobe proprietary cases, however, are not as consistent. The Cetin et al. (2000) report contained 21 apparently inconsistent classifications (liquefaction/no-liquefaction) between the top and bottom parts of the first summary page for these 21 cases. Figure A-3 shows four such first pages; (1) a consistent description of no liquefaction at the top and bottom of the page (Figure A-3a); (2) a consistent description of liquefaction at the top and bottom of the page (Figure A-3b); (3) an inconsistent description of liquefaction at the top of the page versus no liquefaction at the bottom of the page (Figure A-3c); and (4) an inconsistent description of no liquefaction at the top of the page versus liquefaction at the bottom of the page (Figure A-3d).

Clarification of the appropriate classifications for the Kobe propriety cases was obtained from Professor K. Tokimatsu (2010, personal communication). Professor Tokimatsu confirmed that the listings at the bottom of the Cetin et al. (2000) summary pages were consistent with his records, except that sites 6 and 16 were no-liquefaction cases in his opinion (Cetin et al. listed site 6 as a liquefaction case and site 16 as a no/yes or marginal case).

A-3. REPRODUCING KEY PLOTS FROM CETIN ET AL (2004)

The Cetin et al. (2000, 2004) database was entered into a spreadsheet and used to recreate key plots from the Cetin et al. (2004) paper. The ability to recreate key plots was an essential first step in examining the database and procedures included in these references.

Cyclic stress ratios versus SPT blow counts for the case histories

The four plots from Cetin et al. (2004) showing $CSR_{M=7.5, \sigma'_v = 0.65 \text{ atm}}$ or $CSR_{M=7.5, \sigma'_v = 1.0 \text{ atm}}$ versus $(N_1)_{60}$ or $(N_1)_{60cs}$ values were examined first because it was necessary to resolve the apparent inconsistency in how the case histories are plotted in these figures. For ease of reference, Figures A-4 and A-5 in this Appendix show Figures 9 and 14 from Cetin et al. (2004), respectively. The y-axis for parts (a) and (b) of Figure A-4 are indicated to be the cyclic stress ratio, adjusted for duration to $M = 7.5$ [using a magnitude-scaling factor (MSF), designated in the paper as a magnitude-correlated duration weighting factor, DWF_M] and for overburden pressure to $\sigma'_v = 0.65 \text{ atm}$. Part (a) shows this $CSR_{M=7.5, \sigma'_v = 0.65 \text{ atm}}$ plotted versus $(N_1)_{60cs}$ whereas part (b) shows it plotted against $(N_1)_{60}$. Figure A-5 shows a similar pair of plots, but with the cyclic stress ratio now normalized to $\sigma'_v = 1.0 \text{ atm}$ (as shown in the legend of that figure); i.e., plots of $CSR_{M=7.5, \sigma'_v = 1.0 \text{ atm}}$ versus $(N_1)_{60cs}$ or $(N_1)_{60}$. Examination of the four plots in Figures 9 and 14

in Cetin et al. (2004), however, shows that the case history data points are plotted identically in all four plots, with no explanation in the paper.

CSR and $(N_1)_{60}$ values for each case history were listed in Tables 5, 7 and 8 of Cetin et al. (2004), but the MSF, K_σ , and $(N_1)_{60cs}$ values needed to generate their Figure 9 (Figure A-4 in this Appendix) or Figure 14 (Figure A-5 in this Appendix) were not listed. The relevant expressions to calculate MSF, K_σ , and $(N_1)_{60cs}$ values can be derived directly from equation (20) in Cetin et al. (2004), which is reproduced below:

$$CRR = \exp \left[\frac{(N_1)_{60} \cdot (1 + 0.004 \cdot FC) + 0.05 \cdot FC - 29.53 \cdot \ln(M_w) - 3.70 \cdot \ln\left(\frac{\sigma'_v}{P_a}\right) + 16.85 + 2.70 \cdot \Phi^{-1}(P_L)}{13.32} \right] \quad (\text{A.1})$$

Thus,

$$MSF = \frac{CRR_M}{CRR_{M=7.5}} = \frac{\exp\left[-\frac{29.53}{13.32} \cdot \ln(M)\right]}{\exp\left[-\frac{29.53}{13.32} \cdot \ln(7.5)\right]} = \left(\frac{M}{7.5}\right)^{-2.217} \quad (\text{A.2})$$

$$K_\sigma = \frac{CRR_{\sigma'_v}}{CRR_{\sigma'_v=1atm}} = \frac{\exp\left[-\frac{3.70}{13.32} \cdot \ln\left(\frac{\sigma'_v}{P_a}\right)\right]}{\exp\left[-\frac{3.70}{13.32} \cdot \ln(1)\right]} = \left(\frac{\sigma'_v}{P_a}\right)^{-0.278} \quad (\text{A.3})$$

and

$$C_{FINES} = (1 + 0.004 \cdot FC) + 0.05 \frac{FC}{(N_1)_{60}}$$

$$(N_1)_{60cs} = (N_1)_{60} \cdot C_{FINES} \quad (\text{A.4})$$

Cetin et al. (2004) specify that the above fines correction equation is applicable for $5\% \leq FC \leq 35\%$, and that for $FC < 5\%$, the value of FC should be set equal to zero in the above expressions.

These equations were applied to the individual listings in Tables 5, 7 and 8 in Cetin et al. (2004) to generate the parameters needed to recreate the plots in Figures A-4 and A-5. The value of $CSR_{M=7.5, \sigma'_v=1atm}$ for each case history was computed as,

$$CSR_{M=7.5, \sigma'_v=1atm} = \left(\frac{0.65\sigma_v a_{\max} r_d}{\sigma'_v}\right) \left(\frac{1}{MSF}\right) \left(\frac{1}{K_\sigma}\right)$$

$$= CSR_{M, \sigma'_v} \left(\frac{1}{MSF}\right) \left(\frac{1}{K_\sigma}\right) \quad (\text{A.5})$$

using the values of $CSR_{M,\sigma'}$ listed by Cetin et al. and the values of MSF and K_σ calculated using equations (A.2) and (A.3) with the values of M and σ'_v listed for that case in Cetin et al. The corresponding values of $CSR_{M=7.5, \sigma'_v=0.65 \text{ atm}}$ for each case history were then obtained by multiplying the value of $CSR_{M=7.5, \sigma'_v=1 \text{ atm}}$ by the K_σ calculated for $\sigma'_v = 0.65 \text{ atm}$. The value of $(N_1)_{60cs}$ for each case history was also calculated using equation (A.4) with the listed values of $(N_1)_{60}$ and FC for that case.

The values of $CSR_{M=7.5, \sigma'_v=0.65 \text{ atm}}$ and $(N_1)_{60cs}$ computed for the case histories were subsequently found to be the values that were plotted in Figure 9a of Cetin et al. (2004) and plotted identically in their Figures 9a, 9b, 14a, and 14b. This is illustrated in Figures A-6a and A-6b where the values computed herein are plotted on top of Figure 9a from Cetin et al. (2004); the values presented in Figure A-6a were computed assuming $1 \text{ atm} = 2000 \text{ psf}$, whereas the values presented in Figure A-6b were computed using $1 \text{ atm} = 2116 \text{ psf}$. The data points in both of these figures basically match Cetin et al.'s points (except for 3 or 4 points which are well away from the liquefaction boundary line), with the results for $1 \text{ atm} = 2000 \text{ psf}$ perhaps providing slightly better agreement. The minor differences in position for some data points is attributable to round-off errors in the table listings.

A similar exercise was performed to determine if the CRR curves plotted by Cetin et al. (2004) in their Figures 9 and 14 (Figures A-4 and A-5 herein) could be recreated. It was found that their curves did match the axis labels and legends in each of these four plots. Thus, their Figure 14a (recreated in A-5a), for example, presents a comparison of: (1) a triggering curve for $M = 7.5$ and $\sigma'_v = 1 \text{ atm}$, as the legend in the figure shows, versus $(N_1)_{60}$, and (2) case history data points for $M = 7.5$ and $\sigma'_v = 0.65 \text{ atm}$ versus $(N_1)_{60cs}$.

These comparisons and evaluations indicate that the calculation scheme followed in this Appendix does reproduce the values and the curves plotted by Cetin et al.

Calculated CSR versus listed CSR

The tables in Cetin et al. (2004) list a CSR value, along with the values of a_{max} , r_d , σ_v , and σ'_v , for each case history. The consistency of these listings was checked by computing CSR values using the listed values for a_{max} , r_d , σ_v , and σ'_v . The computed CSR values are plotted versus the listed CSR values in Figure A-7. The very small differences between the computed and listed CSR values can be attributed to round off errors, with the one exception being that the computed CSR was about 12% greater than the listed CSR value for the Miller Farm CMF-10 site. This site is discussed later for other reasons. Note that the values of CSR listed in Tables 5, 7 and 8 in Cetin et al. (2004) were used in the subsequent evaluations in this Appendix.

Critical depths, vertical stresses, and unit weights

The tables in Cetin et al. (2004) list a critical depth range, the depth to the water table, and values of σ_v and σ'_v . It appears that the critical depth corresponds to the middle of the critical depth "range", and that this critical depth is the depth at which the listed CSR was computed and the $(N_1)_{60}$ values are considered applicable. This assumption was checked using the detailed case history descriptions in Cetin et al. (2000).

For example, consider the pages for Heber Road A2 as reproduced in Figure A-2. Cetin et al. indicate on the soil profile that they used total unit weights of 90 pcf and 95 pcf above and below the water table, respectively. The critical depth range is listed as 6.0-15.1 ft, from which the average critical depth would appear to be at $(6.0+15.1)/2 = 10.55 \text{ ft}$. The water table is at a depth of 5.9 ft. The total vertical stress

(σ_v) at the critical depth would then be = 5.9 ft (90 pcf) + (10.55 - 5.9 ft)(95 pcf) = 972 psf. The listed value for σ_v is 974 psf, which agrees with the value calculated at the middle of the critical depth range. The pages in Figure A-2 further show that the representative $(N_1)_{60}$ value is taken as the average of the computed $(N_1)_{60}$ values; this approach generates representative $(N_1)_{60}$ values that approximately correspond to the stresses at the average depth.

The total unit weights used by Cetin et al. (2000, 2004), such as those listed for Heber Road A2 in Figure A-2, appear significantly smaller than used by Seed et al. (1984). The total unit weights used by Cetin et al. (2000, 2004) also seem to be lower than would be expected for the soils encountered at the sites of the case histories. To compare unit weights across the databases, an average total unit weight was computed for each case history as the value of σ_v divided by the critical depth. The average total unit weights from the Cetin et al. database are plotted versus critical depth in Figure A-8, along with the values from the Seed et al. (1984) database, the Kobe proprietary cases (Tokimatsu 2010, personal communication), and the updated database described in this report. The overall average total unit weight was 16.3 kN/m³ (104 pcf) for the Cetin et al. database compared to values of about 18.3 kN/m³ (116 pcf) for the other databases. The effect of this difference in unit weights on the liquefaction triggering correlation is examined in the next section.

Calculated r_d versus listed r_d

The tables in Cetin et al. (2004) list values of the shear stress reduction factor, r_d , that were obtained by one of two methods; some were computed using the Cetin et al. regression model for r_d , and the others were obtained from the results of seismic site response analyses. The regression model for r_d requires the use of the average shear wave velocity in the upper 12 m (≈ 40 ft), V_{s12} , as an input parameter, and the tables include a listed value of V_{s12} for those cases where the regression model was used to compute r_d . A few of the V_{s12} values listed in Cetin et al. (2004) were inadvertently shifted to different case histories, likely during typesetting (Cetin 2010, personal communication). The V_{s12} values were thus checked against the listings in Cetin (2000), and the Cetin (2000) listings taken as correct for the few cases of disagreement.

Values of r_d were computed using the Cetin et al. (2004) equation for those case histories where the listed r_d value was reportedly obtained using the regression model. The values of r_d were computed at the critical depth (i.e., middle of the critical depth range) using the listed values for M , V_{s12} , and a_{max} . The computed r_d values are plotted versus the listed r_d values in Figure A-9, from which it is clear that the r_d values listed in their database are systematically smaller than the values computed using their own r_d equation. Since the listed r_d values can be used to reproduce the data points shown in Figure A-6, it appears that the listed r_d values are consistent with the values used to develop their CRR relationship. The difference between computed and listed r_d values increases from a few percent at shallow depths to over 30% at the greater depths covered by the database. This discrepancy was communicated to Professor Cetin and his coauthors in May 2010; they acknowledged the discrepancy, indicated that they found the difference to be only 5.5% on average across the applicable cases in the database, and indicated that the published r_d equation was correct. The effect of this discrepancy on the liquefaction triggering correlation is examined in the next section.

A-4. LIQUEFACTION TRIGGERING CORRELATION FOR $M = 7.5$ & $\sigma'_v = 1$ atm

Cetin et al. (2004) argue that Seed et al. (1984) did not incorporate a K_σ in evaluating the case histories and, therefore, the Seed et al. (1984) liquefaction triggering correlation should not be considered to represent the liquefaction/no liquefaction boundary curve for $\sigma'_v = 1$ atm. Instead, Cetin et al. (2004)

suggest that the boundary curve published by Seed et al. (1984) is representative of $\sigma'_v = 1300$ psf (≈ 0.65 atm), mainly because the average σ'_v for the case histories in Cetin et al's database is about 1300 psf; the average σ'_v for the cases listed by Seed et al. (1984) is about 1400 psf.

Laboratory cyclic test results on undisturbed, as well as on reconstituted samples, show that cyclic resistance of cohesionless soils is nonlinear as a function of effective confining stress. The degree of nonlinearity depends on the denseness of the soil; the denser the soil, the more nonlinear is the relationship between cyclic resistance and effective confining stress, as illustrated by results by Vaid and Sivathayalan (1996) for Fraser Delta sand in Figure A-10. The left part of the figure shows the cyclic shear stress required to reach 3% shear strain in 10 cycles versus the effective consolidation stress for specimens prepared at relative densities, D_R , of 31, 40, 59, and 72%. This plot shows that cyclic strength increases with increasing consolidation stress for all values of D_R , but that the shape of these relationships ranged from being nearly linear for the specimens prepared at the lowest D_R to being most strongly concave at the highest D_R . The right side of the figure shows the CRR at 3% axial strain in 10 cycles versus D_R for different consolidation stresses. This plot shows that CRR increases with increasing D_R , but that it also decreases as the effective consolidation stress is increased from 50 kPa to 400 kPa for D_R greater than 30%. As noted earlier, the overburden correction factor K_σ is defined as the ratio of CRR at a given σ'_v divided by CRR at $\sigma'_v = 1$ atm. The data presented in the right part of Figure A-10 result in obtaining K_σ values that vary not only with σ'_v but also with relative density.

Therefore, a single K_σ relationship that is independent of soil denseness, such as that proposed by Cetin et al. (2004), incorporates a significant simplification and may not provide appropriate guidance for soils across the entire case history database, with $(N_1)_{60cs}$ varying from about 5 up to over 40 (i.e., relative density, D_R , ranging from about 30 to 100%). In addition, an average σ'_v cannot be expected to be representative of the entire case history database or used in comparing databases, given the wide range of D_R and σ'_v covered by the databases.

In as much as the intent is to develop a liquefaction triggering curve applicable to $M = 7.5$ and $\sigma'_v = 1$ atm, it is essential that the derived liquefaction triggering correlation for $M = 7.5$ and $\sigma'_v = 1$ atm be supported by the case histories with σ'_v close to 1 atm. In this regard, it is important to note that Cetin et al. treated the K_σ relationship as a fitting variable in their regression analysis of the case history data, and thus the position of their triggering curve for $M = 7.5$ and $\sigma'_v = 1$ atm should be primarily controlled by the case histories with σ'_v close to 1 atm. The K_σ relationships in the Seed et al. (1984)/Youd et al. (2001) and Idriss-Boulanger (2004, 2008) procedures were fixed independently of the case histories, and thus the position of the triggering curve adjusted to $M = 7.5$ and $\sigma'_v = 1$ atm is guided by all the case histories. Examining the case histories with σ'_v close to 1 atm was found to be the key for identifying and understanding the primary reasons for the differences between the liquefaction triggering curves in Figure A-1.

The following discussion therefore focuses on further examining the differences in the liquefaction analysis procedures and the details of the case histories for σ'_v close to 1 atm.

Each of the three liquefaction triggering correlations shown in Figure A-1 is based on using different expressions for MSF and K_σ for adjusting the case histories to $M = 7.5$ and $\sigma'_v = 1$ atm. The variations of MSF with magnitude used in developing these correlations are shown in Figure A-11, which indicate that the differences are minimal among these relations for the range of magnitudes covering the case histories that mostly control the liquefaction triggering curve for $M = 7.5$ and $\sigma'_v = 1$ atm (see Sections 3 and 4.1 of the main report). Therefore, the influence of MSF on the case histories evaluated in this Appendix is also minimal.

The Seed et al. (1984) correlation did not incorporate K_σ (i.e., essentially assumed that $K_\sigma = 1$ for all case histories, which implies a linear variations of the shear stress required to cause liquefaction with effective vertical stress for all SPT blow counts or relative densities). The NCEER/NSF Workshop (Youd et al. 2001) retained the original Seed et al. (1984) liquefaction triggering correlation for $(N_1)_{60cs}$ greater than about 3 and proposed, for forward calculations, using a K_σ relationship that varied with relative density as shown in Figure A-12. Cetin et al. (2004) obtained a relationship for K_σ based on "regressing" the case history information; their relationship for K_σ can be obtained directly from the equation they published for CRR, as noted above. The resulting Cetin et al. K_σ relationship is also plotted versus σ'_v in Figure A-12 indicating that the relationship by Cetin et al. is almost equal to that recommended by Youd et al. (2001) for a $D_R = 60\%$ and for $\sigma'_v > 1$ atm, but is significantly greater for $\sigma'_v < 1$ atm since the Youd et al. relationship was capped at $K_\sigma = 1.0$. The variations of K_σ with σ'_v for $D_R = 40\%$, 60% and 80% using the relationships derived by Boulanger and Idriss (2004) are presented in Figure A-13.

Examination of the information in Figures A-12 and A-13 indicate that the values of K_σ do not vary greatly for reasonable variations in σ'_v near 1 atm. The latter point is illustrated in Figure A-14, which shows the variations of K_σ with σ'_v based on the relationship recommended by Cetin et al. (2004) for all relative densities, and the relationships recommended by Youd et al. (2001) and Boulanger and Idriss (2004) for the case of $D_R = 60\%$. A close-up of the variations of K_σ over the range of σ'_v from 0.6 to 1.6 atm is presented in Figure A-15, which indicates that the difference in K_σ over $\sigma'_v \approx 0.65$ to 1.5 atm is no more than about 7% over this range of effective vertical stress. Therefore, the influence of different K_σ relationships on the interpretations of the case histories with σ'_v ranging from about 0.65 to 1.5 atm is minimal.

The values of C_N used in these three different procedures also do not differ significantly over the range of $\sigma'_v \approx 0.65$ to 1.5 atm. Both Youd et al. (2001) and Cetin et al. (2004) used the C_N relationship by Liao and Whitman (1986). The C_N relationship used by Idriss and Boulanger (2004, 2008) depends on the soil's relative density, but the differences relative to the Liao-Whitman relationship are small for $\sigma'_v \approx 0.65$ to 1.5 atm as previously illustrated in Figure 2.2b of the main report.

The number of case histories listed in Cetin et al. (2004) with σ'_v ranging from about 0.65 to 1.5 atm is 61; this includes 33 cases of liquefaction, one marginal case, and 27 cases of no liquefaction. These case histories are listed in Table A-1 for the 1984 cases, the 2000 cases and the Kobe proprietary cases. The columns for earthquake name, site, liquefaction/no liquefaction, magnitude, depth to the mid-point of the liquefaction layer, depth of the water table, effective vertical stress, $(N_1)_{60}$, FC, a_{max} , r_d , and site CSR in this table contain information exactly as it appears in Table 5, 7 or 8 in Cetin et al. (2004). The other columns contain values of K_σ and MSF calculated using the two expressions obtained from the CRR expression in Cetin et al., as noted above. The last two columns in Table A-1 list the value of $(N_1)_{60cs}$ obtained by multiplying the listed value of $(N_1)_{60}$ by the coefficient C_{FINES} calculated using the expressions given in Cetin et al., and the value of CSR adjusted for $M = 7.5$ and $\sigma'_v = 1$ atm by dividing the site CSR by MSF and by K_σ .

The values of CSR adjusted for $M = 7.5$ and $\sigma'_v = 1$ atm and listed in Table A-1 are plotted versus the corresponding $(N_1)_{60cs}$ in Figure A-16, which, at a first glance, suggests that the case histories interpreted using the parameters selected or derived by Cetin et al. (2004) fully support their liquefaction triggering curve for $M = 7.5$ and $\sigma'_v = 1$ atm. However, upon more careful examination, eleven points, which control the position of the liquefaction triggering curve, are found to raise significant questions. These points are numbered 1 through 11 in Figure A-16.

The questions regarding these eleven points emanate from the following four issues.

1. Four of these eleven key case histories were identified by the original investigators as "no liquefaction" sites, but were listed and used as "liquefaction" sites by Cetin et al. (2004). These sites are identified as Points 1, 2, 3 and 10 in Figure A-16 and are:

Identifying number in Figure A-16	Site	Earthquake
1	Miller Farm CMF-10	1989 Loma Prieta earthquake; M = 6.9
2	Malden Street, Unit D	1994 Northridge earthquake; M = 6.7
3	Kobe #6	1995 Kobe earthquake; M = 6.9
10	Shuang Tai Zi River	1975 Haicheng earthquake; M = 7.0

Observations available from the original investigators regarding each of these sites are summarized as follows:

- ***Point 1 (Miller Farm CMF-10 site in the 1989 Loma Prieta earthquake):*** The Miller Farm site was investigated by Holzer et al. (1994) and reported upon again by Holzer and Bennett (2007). Holzer et al. (1994) drilled a number of borings in the zone of deformations. They noted that the CMF-10 boring was intentionally located outside the zone of ground deformation, and was later shown to be located in geologic facies that were distinctly different from the channel sands that coincided with the zone of ground deformation along the river, as illustrated in Figure A-17. This interpretation was confirmed by Holzer (2010, personal communication).
- ***Point 2 (Malden Street site in the 1994 Northridge earthquake):*** This site was investigated by Holzer et al. (1998), who drilled several borings and advanced a number of CPT soundings. They attributed the ground deformations to cyclic failure in a localized zone of soft lean clays (Figure A-18) under the strong shaking experienced at the site (about 0.5 g). Liquefaction of the underlying dense Pleistocene silty and clayey sands would not explain the observed pattern of ground deformations and was ruled out by Holzer et al. (1998) and O'Rourke (1998) as the cause of ground failure at this site. This interpretation was confirmed by Holzer (2010, personal communication).
- ***Point 3 (Kobe No. 6 site in the 1995 Kobe earthquake):*** The data for this site are part of the proprietary data set from Tokimatsu, as reported in Cetin et al. (2004). Cetin et al. listed this site as a "liquefaction" case although the site was documented as a "no liquefaction site" with no evidence of ground deformations or boils (Tokimatsu 2010, personal communication), as shown in Figure A-19.
- ***Point 10 (Shuang Tai Zi River site in the 1975 Haicheng earthquake):*** This site was presented as an example of a no liquefaction site in the paper by Shengcong and Tatsuoka (1984; Figure A-20) and used as a "no liquefaction" case by Seed et al. in 1984, as shown in Figure A-21. Cetin et al. list this site and plot it in all their figures as a "liquefaction" case.

Cetin et al. (2000, 2004) do not provide explanations for changing the interpretations of these four case histories. Such explanations are needed, given the importance of these data points.

Accordingly, these 4 points were replotted as "no liquefaction" cases in Figure A-22, which demonstrates the significant effect of using the original and accepted interpretations for these critical data points.

2. Six of these eleven key cases were among those case histories for which the values of r_d obtained using equation 8 in Cetin et al. (2004) are greater than the values of r_d listed in Tables 5 and 8 in Cetin et al. (2004), as illustrated in Figure A-9. These 6 sites are identified as Points 3, 4, 6, 9, 10 and 11 in Figure A-16 and are:

Identifying number in Figure A-16	Site	Critical Depth (m)	Earthquake
3	Kobe #6	5.8	1995 Kobe earthquake; M = 6.9
4	Kobe #7	6.3	1995 Kobe earthquake; M = 6.9
6	Rail Road #2	10	1964 Niigata earthquake; M = 7.6
9	Panjin Chem Fertilizer Plant	8	1975 Haicheng earthquake; M = 7.0
10	Shuang Tai Zi River	8.5	1975 Haicheng earthquake; M = 7.0
11	San Juan B-3	11.7	1974 Argentina earthquake; M = 7.4

The computed r_d values for these 6 sites using equation 8 in Cetin et al. increased the CSR by 5% to 25%, which resulted in these case histories plotting farther above the liquefaction triggering curve, as shown in Figure A-23. For example, consider the Rail Road #2 site in the 1964 Niigata earthquake (Point 6). The value of r_d computed at the critical depth using the Cetin et al. equation for this site is 0.76, whereas a value of 0.65 is listed in Table 5 in Cetin et al. (2004). The computed r_d value increases the CSR by about 17%, moving the data point upward on the liquefaction triggering plot. These results demonstrate how the discrepancy in Cetin et al.'s r_d values (Figure A-9) significantly affected their interpretation of case histories with σ'_v near 1 atm.

3. The boring data obtained at Kobe site No. 7 (Point 4 in Figure A-16) were not fully utilized by Cetin et al. (2004) in assigning a representative $(N_1)_{60}$ value for this site. The boring data provided by Professor Tokimatsu (2010, personal communication) showed the depth to water to be at 3.2 m (which is the depth that had been used by Cetin et al. in 2000) and included the following measurements of SPT blow counts:

Depth (m)	N_m
3.3	8
4.3	21
6.3	32
7.3	23
8.3	21

This site had no observed ground deformations despite having experienced a PGA of about 0.4 g, but is classified as a liquefaction case because there were sand boils in the area. As shown above, the SPT blow counts in the sand below the water table were 8, 21, 32, 23, and 21. Cetin et al. (2004) used only the N values of 21, 23, and 21 to arrive at an $(N_1)_{60}$ of 27.3; these selections imply that the total thickness of liquefied soil was about 4 m, which would seem to be thick enough that some amount of ground deformation would be observed. It seems more likely that the presence of boils without any observable ground deformations could be explained by liquefaction of the shallower $N = 8$ zone, which would correspond to an $(N_1)_{60}$ of 11.0 by the Cetin et al. procedures (A value of 10.4 is obtained using the Idriss-Boulanger procedures and is

adopted in the updated case history database in the main report). If the $N = 8$ value is at least included with the N values of 21, 23, and 21, then the resulting average $(N_1)_{60}$ is 23.2 using the Cetin et al. procedures, as shown in the table below.

Avg depth (m)	σ_v (kPa)	σ'_v (kPa)	(N_m)	$(N_1)_{60}$	C_B	C_E	C_N	C_R	C_S	FC (%)	$(N_1)_{60cs}$
3.3	57	56	8	11.0	1	1.22	1.31	0.86	1	0	11.0
4.3	75	64	21	28.0	1	1.22	1.22	0.90	1	0	28.0
6.3	111	81	32	40.7	1	1.22	1.09	0.96	1	12	43.3
7.3	129	89	23	28.6	1	1.22	1.04	0.98	1	0	28.6
8.3	148	97	21	25.4	1	1.22	0.99	1.00	1	0	25.4
Averages:											
5.8	102.4	76.5	18.3	23.2						0.0	23.2

The effect of at least including the $N = 8$ blow count in the computation of an average $(N_1)_{60} = 23.2$ for the Kobe No. 7 site (Point 4) is illustrated in Figure A-24. The revised point is now located considerably above the Cetin et al. (2004) liquefaction triggering curve for $M = 7.5$ and $\sigma'_v = 1$ atm. If the shallower $N = 8$ zone had been considered the critical zone by itself, then the resulting $(N_1)_{60} = 11.0$ would be even farther above the Cetin et al.'s triggering curve.

- The case history associated with Point 6 (Rail Road #2 – 1964 Niigata earthquake) is one of those cases where Cetin et al.'s selection of relatively low total unit weights (Figure A-8) affected the resulting data point. This case history was originally used by Seed et al. (1984) and identified as a case of "marginal liquefaction" by both Seed et al. and Cetin et al. Cetin et al. used total unit weights of 100 pcf (≈ 15.7 kN/m³) and 110 pcf (≈ 15.7 kN/m³) above and below the water table (0.9 m depth), respectively, resulting in an effective vertical stress at the critical depth (10.1 m) of 1719 psf (≈ 82 kPa). Seed et al. had computed an effective vertical stress of 2090 psf (≈ 100 kPa), which is about 22% greater than the Cetin et al.'s value and which is consistent with the use of total unit weights equal to 111 pcf (≈ 17.5 kN/m³) and 121 pcf (≈ 19.0 kN/m³) above and below the water table, respectively. The unit weights used by Seed et al. appear to be more reasonable for the saturated sands encountered at this site. Using the stress estimates by Seed et al. (1984), the C_N and hence $(N_1)_{60cs}$ values are about 10% smaller, and the $CSR_{M=7.5, \sigma'_v=1}$ is also about 8% smaller for this case history, which causes the data point to move left and downward on the liquefaction triggering plots, as shown in Figure A-25.

The cumulative effect of the above reasonable adjustments and corrections to 8 of the 11 key case history data points for σ'_v ranging from 0.65 to 1.5 atm in Cetin et al.'s database (Figure A-16) are summarized in Figure A-25. The revised data points are located significantly above the Cetin et al. liquefaction triggering curve for $M = 7.5$ and $\sigma'_v = 1$ atm.

The effect of the above adjustments and corrections are further illustrated in Figure A-26, which shows the liquefaction triggering curves proposed by Cetin et al. (2004), Idriss and Boulanger (2004, 2008), and NCEER/Youd et al. (2001) along with Cetin et al.'s case history data for σ'_v ranging from 0.65 to 1.5 atm with the above adjustments and corrections. The adjusted/corrected database from Cetin et al. is now reasonably consistent with the liquefaction triggering curves proposed by Idriss and Boulanger (2004, 2008) and NCEER/Youd et al. (2001).

The locations of Points 5 (CMF-5), 7 (POO7-2), and 8 (POO7-3) were not adjusted in these figures, but the classification of Point 8 does warrant a comment. Point 8 corresponds to boring POO7-3 located in an

area of no surface manifestations at the Port of Oakland during the 1989 Loma Prieta earthquake. This case was initially classified as a "no liquefaction" case by Kayen et al. (1998), classified as a "liquefaction" case by Cetin et al. (2004), and classified as a "marginal" case in the updated database presented in the main report. The conclusions from this examination of the Cetin et al. database do not depend on the classification of Point 8, and therefore it is shown with Cetin et al.'s classification in these figures. Additional details regarding this case are discussed in Section 3.4 of the main report.

The Cetin et al. triggering correlation, if it were updated after incorporating the above adjustments and corrections, would thus be expected to move closer to the Idriss-Boulanger and NCEER/Youd et al. correlations at effective vertical stresses ranging from about 0.65 to 1.5 atm. This would also cause the Cetin et al. K_σ relationship to become flatter because it is regressed as part of their analyses, and higher CRR values at higher confining stresses would dictate a flatter K_σ relationship. The combination of these changes would be expected to reduce the degree to which the Cetin et al. procedure predicts significantly smaller CRR values than the other liquefaction triggering correlations.

Lastly, the case histories for σ'_v ranging from 0.65 to 1.5 atm from the updated case history database in the main report, as processed using the Idriss and Boulanger (2004, 2008) liquefaction triggering procedures, are shown in Figure A-27. The differences in the locations of the case history data points between Figure A-26 and A-27 represent the effects of the different liquefaction analysis components (e.g., C_N , K_σ , r_d , FC adjustment) and other differences in the interpretation of specific case histories (e.g., a_{max} , critical layers, stresses). Despite the differences in individual data points, the databases shown in Figures A-26 and A-27, respectively, would support relatively similar liquefaction triggering boundary curves for this range of stresses. This comparison further suggests that the differences between the Cetin et al. (2004), NCEER/Youd et al. (2001), and Idriss and Boulanger (2004, 2008) liquefaction triggering correlations for $M = 7.5$ and $\sigma'_v = 1$ atm, as shown in Figure A-1, are largely explained by the above-described issues with the Cetin et al. (2004) database.

A-5. SUMMARY AND CONCLUSIONS

The Cetin et al. (2004) liquefaction triggering correlation and case history database were examined for the purpose of assessing whether their data and procedures support their recommendation of a liquefaction triggering correlation that is significantly lower than: (1) the correlation developed by the late Professor H. Bolton Seed and his colleagues (Seed et al. 1984), which was subsequently adopted with slight modification during the NCEER/NSF workshops (Youd et al. 2001); and (2) the correlation developed Idriss and Boulanger (2004, 2008).

The lower position of the Cetin et al. (2004) liquefaction triggering correlation for $M = 7.5$ and $\sigma'_v = 1$ atm was shown to be primarily caused by their interpretations for 8 of 11 key case histories at effective vertical stresses ranging from about 0.65 to 1.5 atm. Four significant issues affecting the Cetin et al. interpretations for these key case histories were identified: (1) four of the most important case histories were listed and utilized as "liquefaction" cases in Cetin et al. despite the original investigators describing these as "no liquefaction" cases based on the original investigators' field observations and geologic interpretations; (2) the r_d values listed in Cetin et al.'s tables are significantly smaller than those computed using the applicable r_d regression equation for six of these key cases; (3) the lowest SPT N value was not considered in the selection of a representative $(N_1)_{60cs}$ value for a site that experienced sand boils but no observable ground deformations; and (4) the total unit weights that were used were often small, which had a notable effect on one of the key case histories. Items 1 and 2 represent significant inconsistencies in the case history database by Cetin et al. (2004). Items 3 and 4 are interpretation issues that are not as serious.

These observations raise significant questions regarding the basis for the relationships recommended by Cetin et al. (2004). In particular, the results presented herein demonstrated that reasonable adjustments and corrections to only 8 of the case histories in the Cetin et al. database would be expected to raise their liquefaction triggering correlation for $M = 7.5$ and $\sigma'_v = 1$ atm and flatten their K_σ relationship. Given the potential significance of these observations, it would appear prudent that the Cetin et al. (2004) procedure not be used until these issues have been addressed and corrected.

TABLE A-1
Case histories of liquefaction/no liquefaction published by Cetin et al. (2004) with $\sigma'_v = 0.65$ to 1.5 atm

Earthquake	Site	Liquefaction?	M	Depth (ft)	Water (ft)	σ'_v (psf)	$(N_1)_{60}$	FC (%)	a_{max} (g)	r_d	Site CSR	K_σ	MSF	$(N_1)_{60cs}$	CSR (adj. for $M=7.5$ & $\sigma'_v=1$ atm)
1984 Cases [Table 5 in Cetin et al. (2004)]															
1977 Argentina	San Juan B-3	Yes	7.4	38.3	22	2,782	7.3	20	0.2	0.56	0.10	0.93	1.03	8.9	0.105
1977 Argentina	San Juan B-1	Yes	7.4	27.0	15	1,996	6.7	20	0.2	0.78	0.14	1.02	1.03	8.2	0.134
1948 Fukui	Takaya 45	Yes	7.3	26.2	12.3	1,897	21.5	4	0.35	0.79	0.26	1.03	1.06	21.5	0.238
1971 San Fernando	Van Norman	Yes	6.6	20.5	17	1,764	8.2	50	0.45	0.86	0.28	1.05	1.33	11.1	0.201
1978 Miyagiken-Oki	Oiiri-1	Yes	7.4	19.5	14	1,564	9.8	5	0.24	0.74	0.14	1.09	1.03	10.2	0.125
1971 San Fernando	Juvenile Hall	Yes	6.6	17.6	14	1,481	4.1	55	0.45	0.81	0.27	1.10	1.33	6.4	0.184
1975 Haicheng	Shuang Tai Zi R.	Yes	7.3	27.9	5	1,449	11.1	5	0.1	0.77	0.10	1.11	1.06	11.6	0.085
1975 Haicheng	Panjin Ch. F.	Yes	7.3	26.3	5	1,379	8.2	67	0.13	0.79	0.13	1.13	1.06	11.1	0.109
1964 Niigata	Rail Road-2	No/Yes	7.5	32.8	3	1,719	18.8	2	0.16	0.65	0.14	1.06	1	18.8	0.132
1964 Niigata	Old Town -2	No	7.5	37.8	6	2,428	27.1	8	0.18	0.55	0.12	0.96	1	28.4	0.125
1978 Miyagiken-Oki	Ishinomaki-4	No	7.4	13.8	4.6	2,213	25.2	10	0.2	0.95	0.16	0.99	1.03	26.7	0.157
1980 Mid-Chiba	Owi-2	No	6.1	47.6	3	2,199	3.7	27	0.1	0.33	0.05	0.99	1.58	5.4	0.032
1964 Niigata	Old Town -1	No	7.5	24.6	6	1,672	22.7	8	0.18	0.75	0.15	1.07	1	23.8	0.140
1978 Miyagiken-Oki	Oiiri-1	No	6.7	19.5	14	1,564	9.8	5	0.14	0.73	0.08	1.09	1.28	10.2	0.057
1968 Tokachi-Oki	Hachinohe -2	No	7.9	18.0	7	1,494	37.4	5	0.23	0.93	0.20	1.10	0.89	38.4	0.204
1978 Miyagiken-Oki	Yuriage Br-5	No	7.4	24.6	4.3	1,475	26.3	17	0.24	0.86	0.25	1.11	1.03	28.9	0.220
1964 Niigata	Road Site	No	7.5	21.3	8.2	1,404	15.1	0	0.18	0.78	0.14	1.12	1	15.1	0.125

TABLE A-1 (Cont'd)
Case histories of liquefaction/no liquefaction published by Cetin et al. (2004) with $\sigma'_v = 0.65$ to 1.5 atm

Earthquake	Site	Liquefaction?	M	Depth (ft)	Water (ft)	σ'_v (psf)	$(N_1)_{60}$	FC (%)	a_{max} (g)	r_d	Site CSR	K_σ	MSF	$(N_1)_{60cs}$	CSR (adj. for $M=7.5$ & $\sigma'_v=1$ atm)
2000 Cases [Table 7 in Cetin et al. (2004)]															
1993 Kushiro-Oki	Kushiro Port Seismo St.	Yes	8	67.3	5.2	4,149	7.2	10	0.4	0.47	0.23	0.83	0.87	8.0	0.320
1994 Northridge	Balboa B1v. Unit C	Yes	6.7	29.6	23.6	2,968	18.5	43	0.69	0.71	0.36	0.91	1.28	22.8	0.308
1995 Hyogoken-Nambu	Ashiyama C-D-E (Mountain Sand 2)	Yes	6.9	44.6	11.5	2,949	5.8	18	0.4	0.41	0.18	0.91	1.20	7.1	0.164
1995 Hyogoken-Nambu	Rokko Island Site G	Yes	6.9	37.7	13.1	2,861	12.2	20	0.34	0.59	0.20	0.92	1.20	14.2	0.181
1994 Northridge	Malden Street Unit D	Yes	6.7	30.4	12.8	2,506	24.4	25	0.51	0.7	0.34	0.95	1.28	28.1	0.278
1995 Hyogoken-Nambu	Port Island Site I	Yes	6.9	32.8	9.8	2,406	10.8	20	0.34	0.67	0.24	0.96	1.20	12.7	0.207
1995 Hyogoken-Nambu	Rokko Island Building D	Yes	6.9	24.6	13.1	2,162	17.1	25	0.4	0.89	0.31	0.99	1.20	20.1	0.259
1995 Hyogoken-Nambu	Ashiyama C-D-E (Marine Sand)	Yes	6.9	28.7	11.5	2,112	12.9	2	0.4	0.64	0.25	1.00	1.20	12.9	0.208
1995 Hyogoken-Nambu	Port Island Borehole Array Station	Yes	6.9	25.5	7.9	1,965	6.9	20	0.34	0.71	0.24	1.02	1.20	8.5	0.195
1994 Northridge	Wynne Ave. Unit C1	Yes	6.7	20.5	14.1	1,952	11.0	38	0.54	0.86	0.35	1.02	1.28	14.3	0.267
1989 Loma Prieta	Miller Farm CMF 5	Yes	7	23.0	15.4	1,939	21.9	13	0.41	0.9	0.29	1.02	1.17	23.7	0.243
1994 Northridge	Potrero Canyon C1	Yes	6.7	21.4	10.8	1,848	10.5	37	0.4	0.72	0.25	1.04	1.28	13.7	0.187
1989 Loma Prieta	Miller Farm CMF 3	Yes	7	21.8	18.7	1,828	11.6	27	0.46	0.83	0.26	1.04	1.17	14.2	0.214
1989 Loma Prieta	SFOBB-1&2	Yes	7	20.5	9.8	1,795	8.1	8	0.27	0.77	0.19	1.05	1.17	8.8	0.156
1989 Loma Prieta	POO7-3	Yes	7	21.4	9.8	1,736	13.2	5	0.22	0.83	0.16	1.06	1.17	13.7	0.130
1989 Loma Prieta	Miller Farm CMF 8	Yes	7	21.3	16.1	1,725	10.3	15	0.46	0.73	0.25	1.06	1.17	11.7	0.203
1989 Loma Prieta	POO7-2	Yes	7	20.2	9.8	1,676	13.0	3	0.22	0.95	0.17	1.07	1.17	13.0	0.137
1990 Mw=7.6 Luzon	Perez Blvd. B-11	Yes	7.6	23.8	7.5	1,647	14.0	19	0.25	0.82	0.22	1.07	0.97	16.0	0.211
1989 Loma Prieta	Farris Farm	Yes	7	19.7	14.8	1,489	10.9	8	0.37	0.9	0.28	1.10	1.17	11.6	0.218
1989 Loma Prieta	Miller Farm CMF10	Yes	7	27.9	9.8	1,474	24.0	20	0.41	0.88	0.37	1.11	1.17	26.9	0.287
1989 Loma Prieta	Miller Farm	Yes	7	19.7	13.1	1,395	10.0	22	0.42	0.84	0.32	1.12	1.17	12.0	0.245
1995 Hyogoken-Nambu	Port Island Improved Site (Tanahashi)	No	6.9	32.8	16.4	2,831	18.6	20	0.4	0.73	0.26	0.92	1.20	21.1	0.234

TABLE A-1 (Cont'd)
Case histories of liquefaction/no liquefaction published by Cetin et al. (2004) with $\sigma'_v = 0.65$ to 1.5 atm

Earthquake	Site	Liquefaction?	M	Depth (ft)	Water (ft)	σ'_v (psf)	$(N_1)_{60}$	FC (%)	a_{max} (g)	r_d	Site CSR	K_σ	MSF	$(N_1)_{60cs}$	CSR (adj. for $M=7.5$ & $\sigma'_v=1$ atm)
1995 Hyogoken-Nambu	Port Island Improved Site (Watanabe)	No	6.9	31.2	16.4	2,729	32.2	20	0.4	0.84	0.29	0.93	1.20	35.8	0.259
1995 Hyogoken-Nambu	Port Island Improved Site (Ikegaya)	No	6.9	27.9	16.4	2,523	21.9	20	0.4	0.8	0.27	0.95	1.20	24.7	0.236
1993 Kushiro-Oki	Kushiro Port Site D	No	8	35.3	5.2	2,307	30.3	0	0.4	0.79	0.37	0.98	0.87	30.3	0.437
1995 Hyogoken-Nambu	Ashiyama A (Marine Sand)	No	6.9	26.1	11.5	2,047	31.3	2	0.4	0.82	0.31	1.01	1.20	31.3	0.255
1989 Loma Prieta	Alameda BF Dike	No	7	21.4	9.8	1,900	42.6	7	0.24	0.95	0.20	1.03	1.17	44.1	0.167
1983 Nihonkai-Chubu	Arayamotomachi Coarse Sand	No	7.1	30.3	3.3	1,617	17.7	0	0.15	0.63	0.13	1.08	1.13	17.7	0.107
1995 Hyogoken-Nambu	Ashiyama A (Mountain Sand 1)	No	6.9	17.1	11.5	1,499	21.6	18	0.4	0.89	0.29	1.10	1.20	24.1	0.219
Kobe Proprietary Cases [Table 8 in Cetin et al. (2004)]															
1995 Hyogoken-Nambu	5	Yes	6.9	28.7	9.9	2,079	6.9	2	0.35	0.71	0.25	1.00	1.20	6.9	0.207
	38	Yes	6.9	26.3	9.8	1,683	20.1	5	0.5	0.73	0.38	1.07	1.20	20.8	0.296
	7	Yes	6.9	20.7	10.4	1,682	27.3	0	0.4	0.81	0.29	1.07	1.20	27.3	0.226
	15	Yes	6.9	19.0	12	1,495	19.9	5	0.5	0.76	0.32	1.10	1.20	20.5	0.241
	6	Yes	6.9	19.1	7.5	1,434	22.7	25	0.4	0.84	0.33	1.11	1.20	26.2	0.246
1995 Hyogoken-Nambu	18	No	6.9	34.5	25.1	3,253	38.6	0	0.7	0.62	0.33	0.89	1.20	38.6	0.309
	19	No	6.9	24.6	20	2,343	21.7	10	0.6	0.86	0.38	0.97	1.20	23.1	0.325
	10	No	6.9	24.6	14.6	2,011	27.7	9	0.6	0.75	0.38	1.01	1.20	29.1	0.311
	2	No	6.9	27.9	9.5	1,964	42.7	15	0.4	0.83	0.34	1.02	1.20	46.0	0.277
	33	No	6.9	26.3	6.6	1,495	30.3	50	0.5	0.74	0.44	1.10	1.20	36.3	0.332
	30	No	6.9	27.9	4.9	1,471	43.4	10	0.6	0.73	0.57	1.11	1.20	45.6	0.428
	22	No	6.9	19.7	7.9	1,448	40.8	6	0.6	0.86	0.51	1.11	1.20	42.1	0.381
	1	No	6.9	19.7	7.7	1,439	57.7	4	0.4	0.93	0.37	1.11	1.20	57.7	0.276
	20	No	6.9	19.7	6.6	1,379	64.3	0	0.55	0.93	0.53	1.13	1.20	64.3	0.391

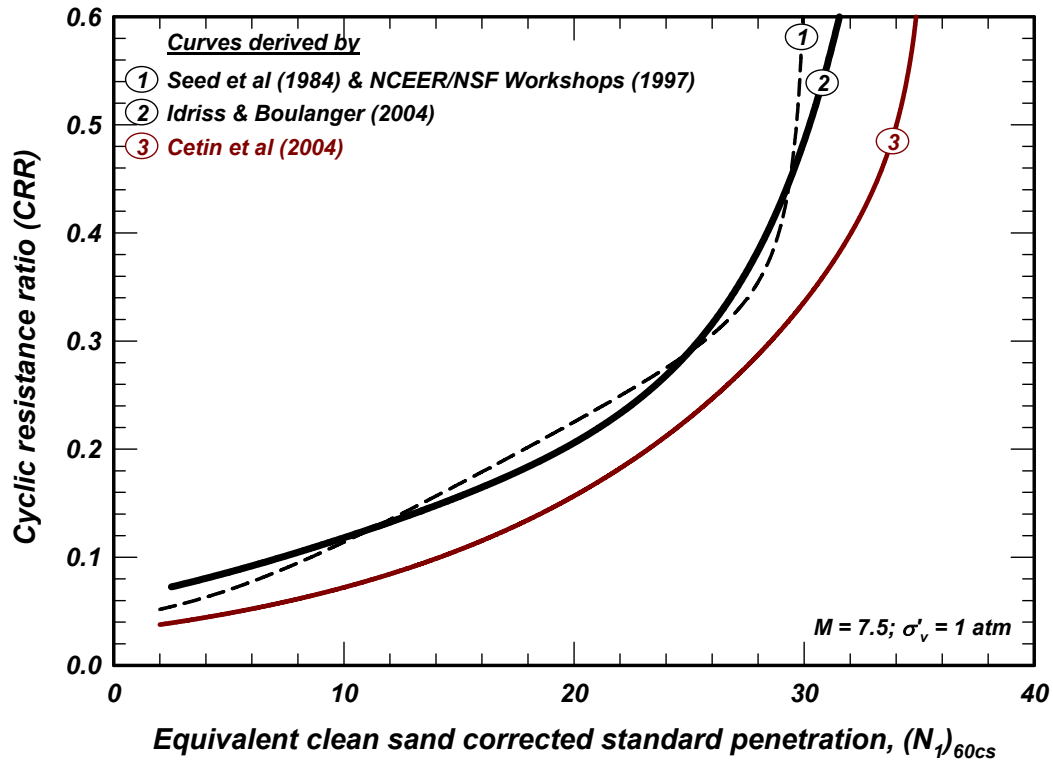
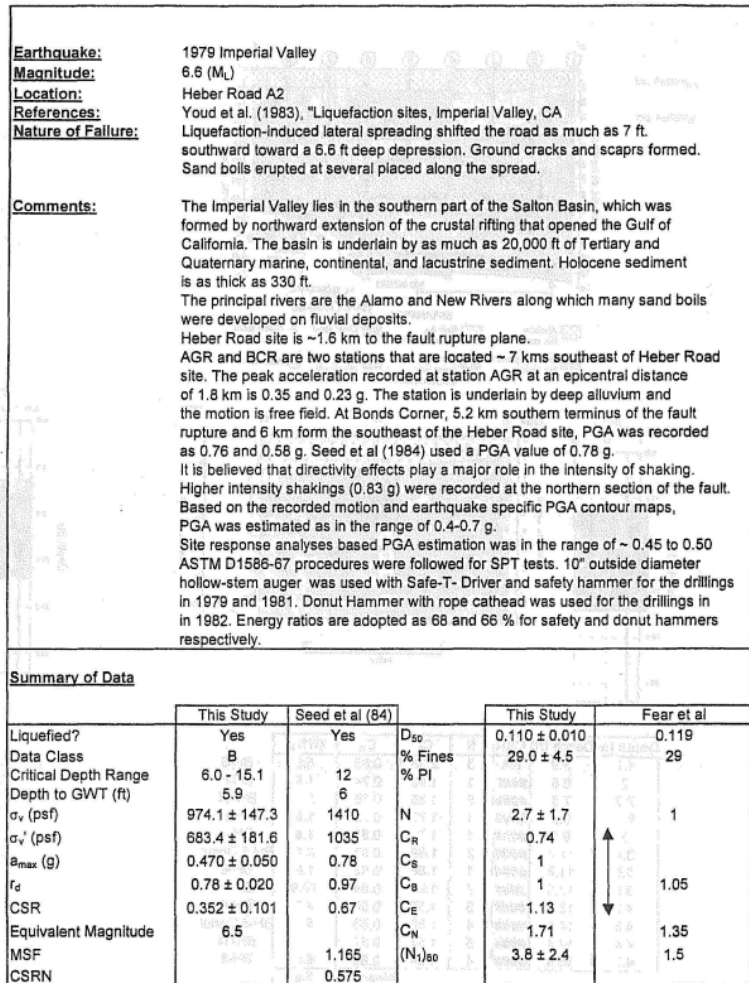
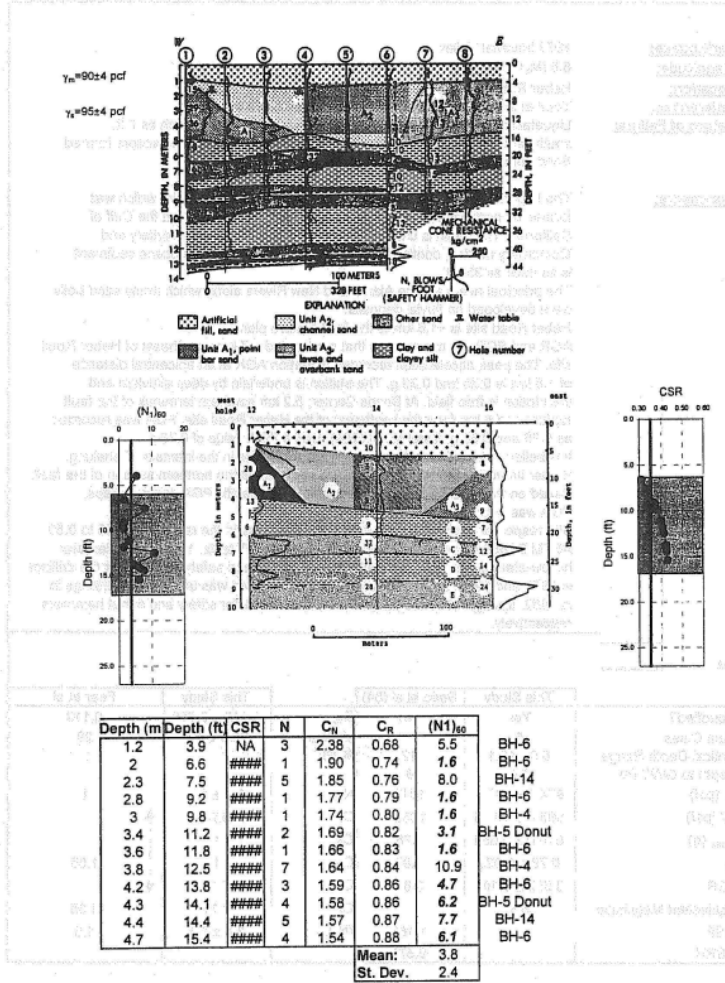


Figure A-1. Liquefaction triggering correlations for $M = 7.5$ and $\sigma'_v = 1 \text{ atm}$ developed by: (1) Seed et al. (1984), as modified by the NCEER/NSF Workshops (1997) and published in Youd et al. (2001); (2) Idriss and Boulanger (2004, 2008); and (3) Cetin et al. (2004)



(a) First page for the Heber Road A2 case history [page 75 in Cetin et al. (2000)]



(b) First page for the Heber Road A2 case history [page 76 in Cetin et al. (2000)]

Figure A-2. Illustration of the information provided in Cetin et al. (2000) for each of the 1984 and 2000 case histories

Earthquake:	1995 Hyogoken-Nambu		
Magnitude:	7.2 (M _s)		
Location:	Kobe No : 1		
References:	Kobe City Office, 1999 (In Japanese), Confidential		
Nature of Failure:	Non-liquefied		
Comments:			
Summary of Data			
Liquefied?	No	D ₅₀	0.000 ± 0.000
Data Class	B	% Fines	4.0 ± 1.5
Critical Depth Range	16.4 - 23.0	% PI	
Depth to GWT (ft)	7.7 ± 1.0	N	42.3 ± 2.3
σ _v (psf)	2186.7 ± 138.4	C _R	0.95
σ _{v'} (psf)	1439.4 ± 96.4	C _S	1
a _{max} (g)	0.400 ± 0.060	C _B	1
f _d	0.93 ± 0.082	C _E	1.22
CSR	0.368 ± 0.066	C _N	1.18
Equivalent Magnitude	6.9	(N ₁) ₆₀	57.7 ± 3.2
MSF			
CSR _N			

(c) Kobe No. 1 [page 154 in Cetin et al. (2000)]

Earthquake:	1995 Hyogoken-Nambu		
Magnitude:	7.2 (M _s)		
Location:	Kobe No : 11		
References:	Kobe City Office, 1999 (In Japanese), Confidential		
Nature of Failure:	Liquefied		
Comments:			
Summary of Data			
Liquefied?	Yes	D ₅₀	0.000 ± 0.000
Data Class	B	% Fines	5.0 ± 1.0
Critical Depth Range	12.3 - 32.0	% PI	
Depth to GWT (ft)	4.8 ± 1.0	N	5.5 ± 1.5
σ _v (psf)	2301.5 ± 352.0	C _R	0.97
σ _{v'} (psf)	1216.5 ± 167.4	C _S	1
a _{max} (g)	0.500 ± 0.075	C _B	1
f _d	0.70 ± 0.090	C _E	1.22
CSR	0.429 ± 0.090	C _N	1.28
Equivalent Magnitude	6.9	(N ₁) ₆₀	8.3 ± 2.3
MSF			
CSR _N			

(d) Kobe No. 11 [page 404 in Cetin et al. (2000)]

Earthquake:	1995 Hyogoken-Nambu		
Magnitude:	7.2 (M _s)		
Location:	Kobe No : 12		
References:	Kobe City Office, 1999 (In Japanese), Confidential		
Nature of Failure:	Liquefied		
Comments:			
Summary of Data			
Liquefied?	No	D ₅₀	0.000 ± 0.000
Data Class	A	% Fines	13.0 ± 3.0
Critical Depth Range	14.1 - 20.7	% PI	
Depth to GWT (ft)	10.5 ± 1.0	N	19.6 ± 1.0
σ _v (psf)	1773.3 ± 125.4	C _R	0.92
σ _{v'} (psf)	1343.4 ± 89.4	C _S	1
a _{max} (g)	0.500 ± 0.075	C _B	1
f _d	0.83 ± 0.073	C _E	1.22
CSR	0.365 ± 0.065	C _N	1.22
Equivalent Magnitude	6.9	(N ₁) ₆₀	26.7 ± 1.3
MSF			
CSR _N			

(e) Kobe No. 12 [page 406 in Cetin et al. (2000)]

Earthquake:	1995 Hyogoken-Nambu		
Magnitude:	7.2 (M _s)		
Location:	Kobe No : 24		
References:	Kobe City Office, 1999 (In Japanese), Confidential		
Nature of Failure:	Nonliquefied		
Comments:			
Summary of Data			
Liquefied?	Yes	D ₅₀	0.000 ± 0.000
Data Class	B	% Fines	0.0 ± 0.0
Critical Depth Range	9.8 - 13.1	% PI	
Depth to GWT (ft)	7.7 ± 1.0	N	17.0 ± 0.9
σ _v (psf)	1243.4 ± 72.3	C _R	0.87
σ _{v'} (psf)	1008.0 ± 68.9	C _S	1
a _{max} (g)	0.500 ± 0.075	C _B	1
f _d	0.96 ± 0.052	C _E	1.22
CSR	0.383 ± 0.066	C _N	1.41
Equivalent Magnitude	6.9	(N ₁) ₆₀	25.3 ± 1.4
MSF			
CSR _N			

(f) Kobe No. 24 [page 430 in Cetin et al. (2000)]

Figure A-3. Illustration of information provided in Cetin et al. (2000) for the Kobe proprietary cases: (a) Kobe No. 1 is consistently identified as a no liquefaction case at top and bottom of page 154; (b) Kobe No. 11 is consistently identified as a liquefaction case at top and bottom of page 404; (c) Kobe No. 12 is inconsistently identified as a liquefaction case at top and as a no liquefaction case at bottom of page 406; and (d) Kobe No. 24 is inconsistently identified as a no liquefaction case at top and as a liquefaction case at bottom of page 430.

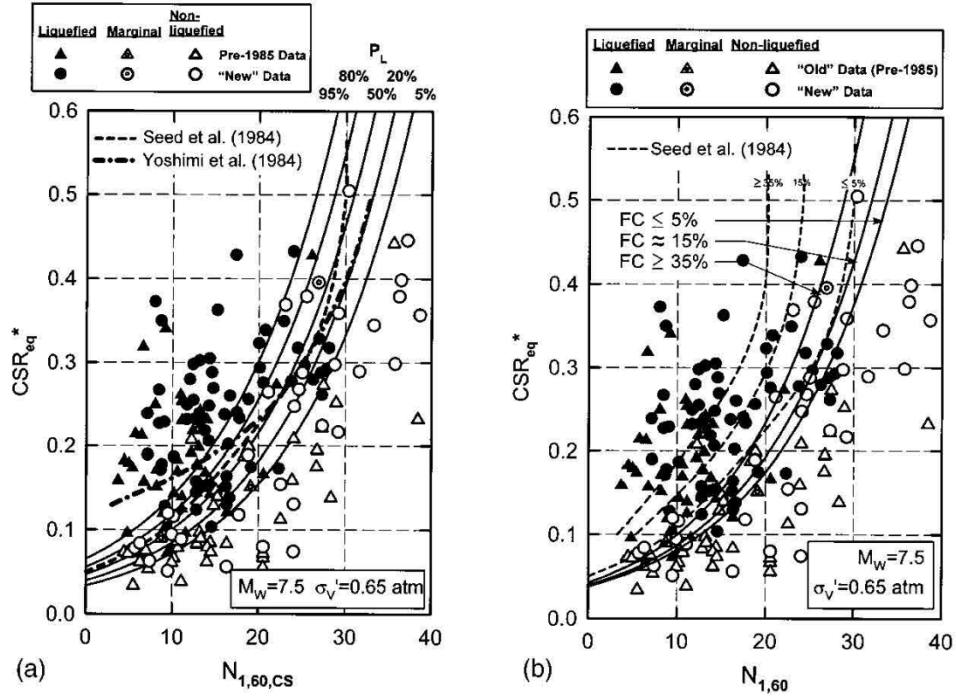


Figure A-4. Parts (a) and (b) of Figure 9 in Cetin et al. (2004); note that the points representing case histories are identical in both plots, although the x-axes are labeled differently.

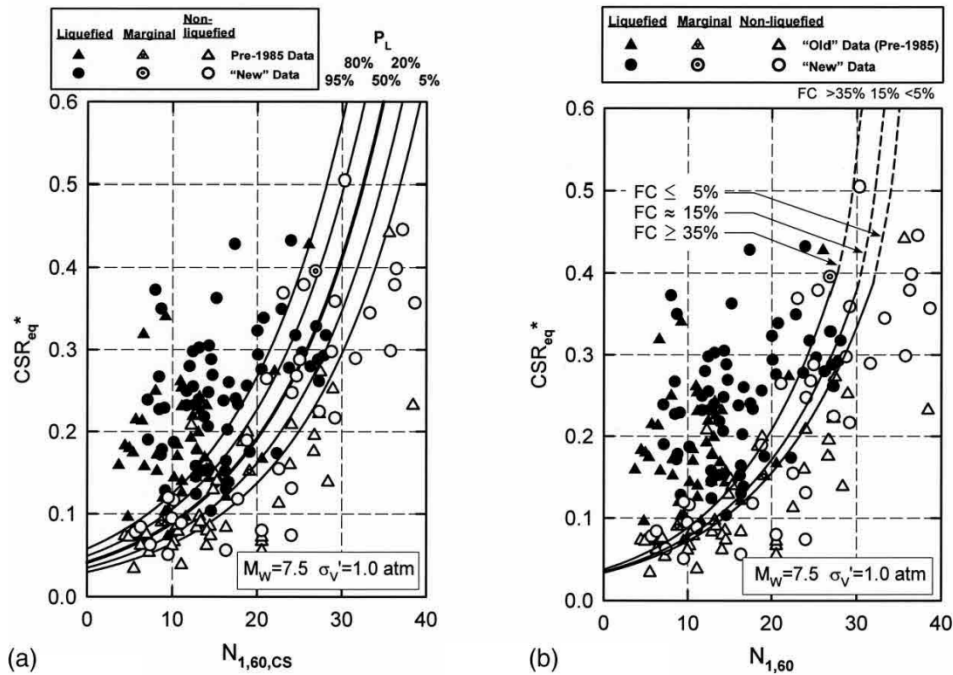


Figure A-5. Parts (a) and (b) of Figure 14 in Cetin et al. (2004); note that the points representing case histories are identical in parts (a) and (b) of this figure and also identical to those presented in Figure 9 in Cetin et al. (2004) (see above) although Figure 9 is referenced by Cetin et al. (2004) as representing conditions with $\sigma'_v = 0.65$ atm and Figure 14 as representing conditions with $\sigma'_v = 1$ atm.

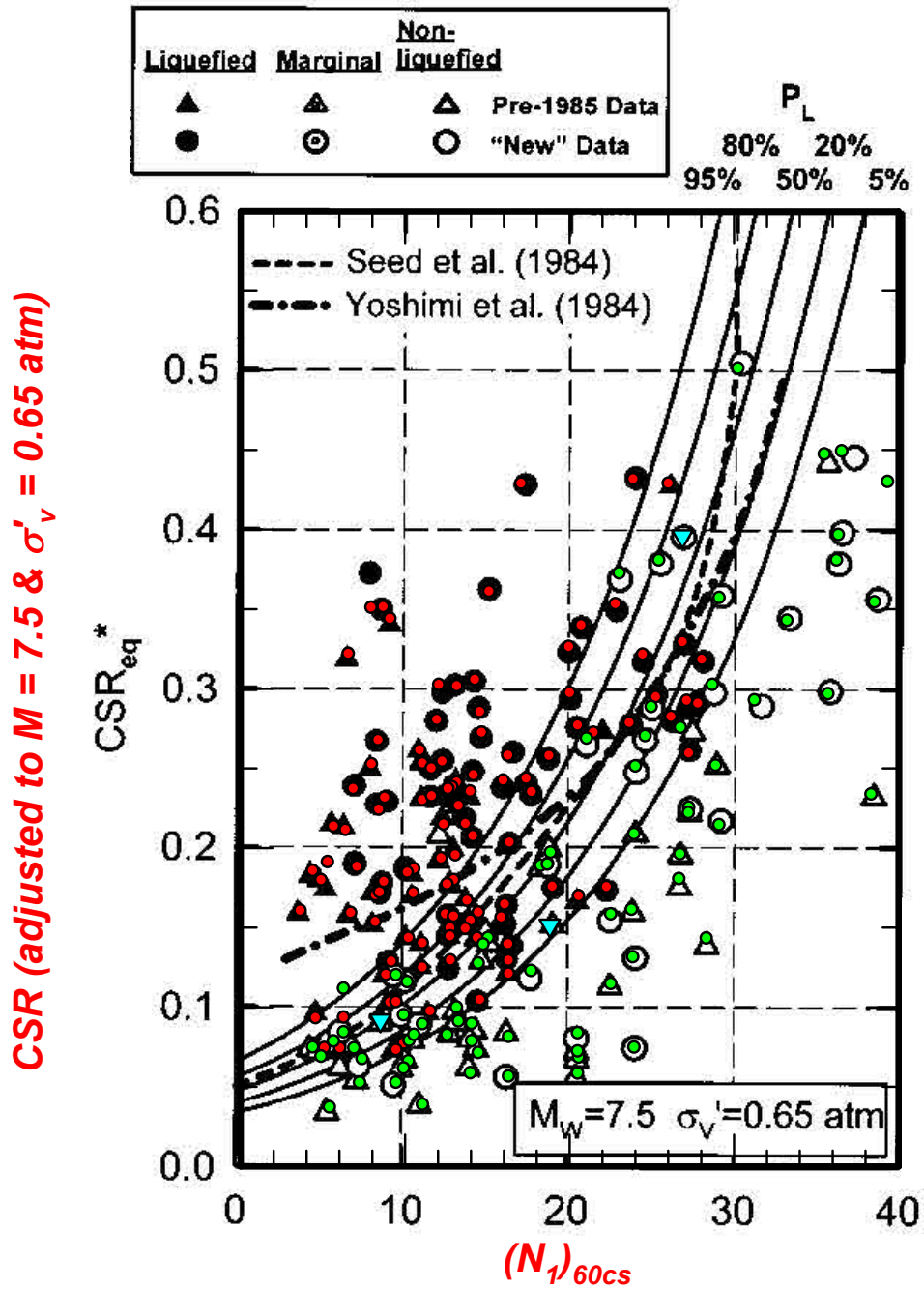


Figure A-6a. Values of CSR (adjusted to $M = 7.5$ & $\sigma'_v = 0.65 \text{ atm}$), calculated using values listed in Tables 5, 7 and 8 and relationships for MSF and K_σ provided in Cetin et al. (2004), plotted versus $(N_1)_{60cs}$ and compared to points representing case histories presented in Figures 9 and 14 in Cetin et al. (2004); note the values shown in this figure are calculated using $1 \text{ atm} = 2000 \text{ psf}$, which appears to be the value used by Cetin et al. (2004).

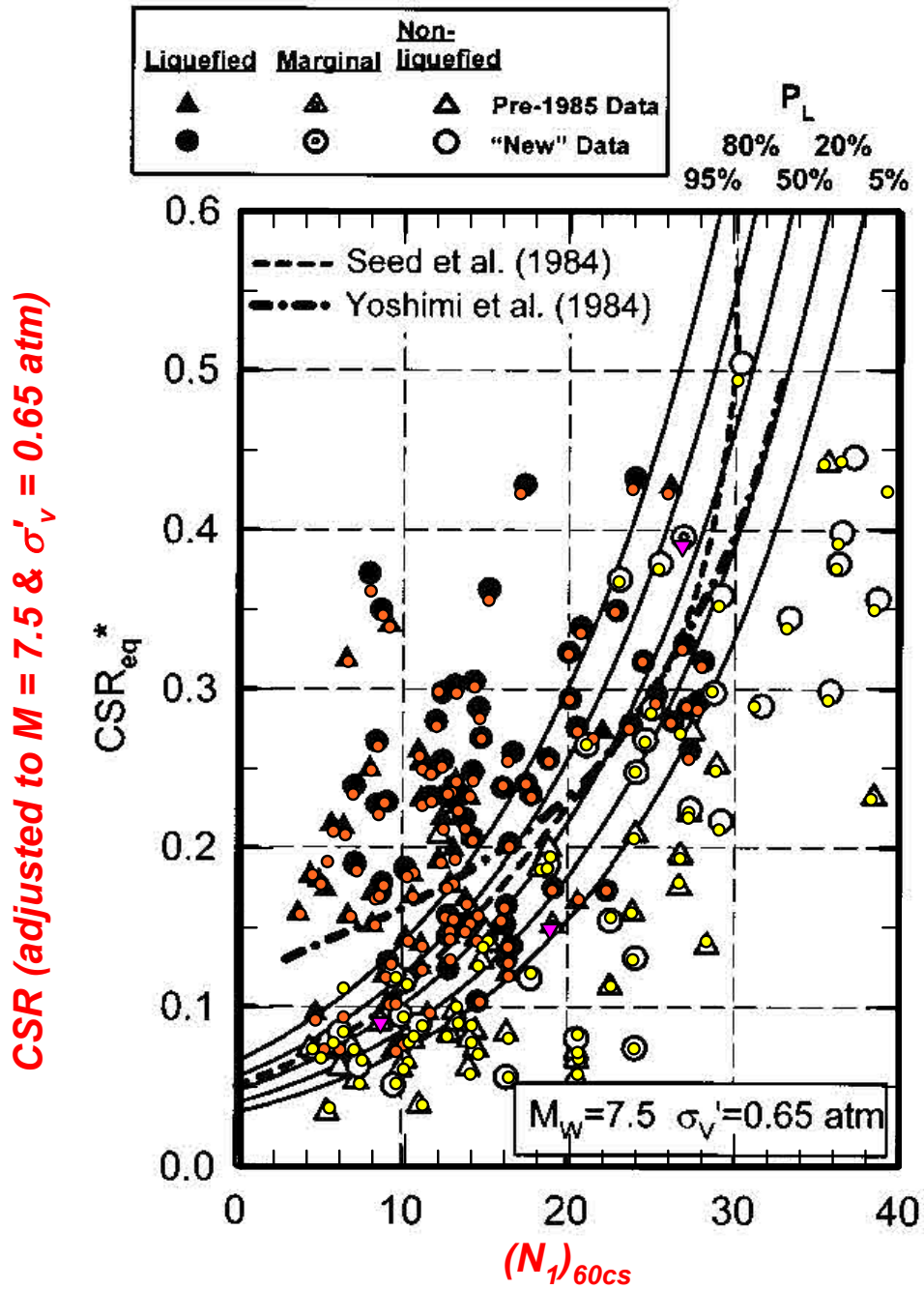


Figure A-6b. Values of CRR (adjusted to $M = 7.5$ & $\sigma'_v = 0.65 \text{ atm}$), calculated using values listed in Tables 5, 7 and 8 and relationships for MSF and K_σ provided in Cetin et al. (2004), plotted versus $(N_1)_{60cs}$ and compared to points representing case histories presented in Figures 9 and 14 in Cetin et al. (2004); note the values shown in this figure are calculated using $1 \text{ atm} = 2116 \text{ psf}$.

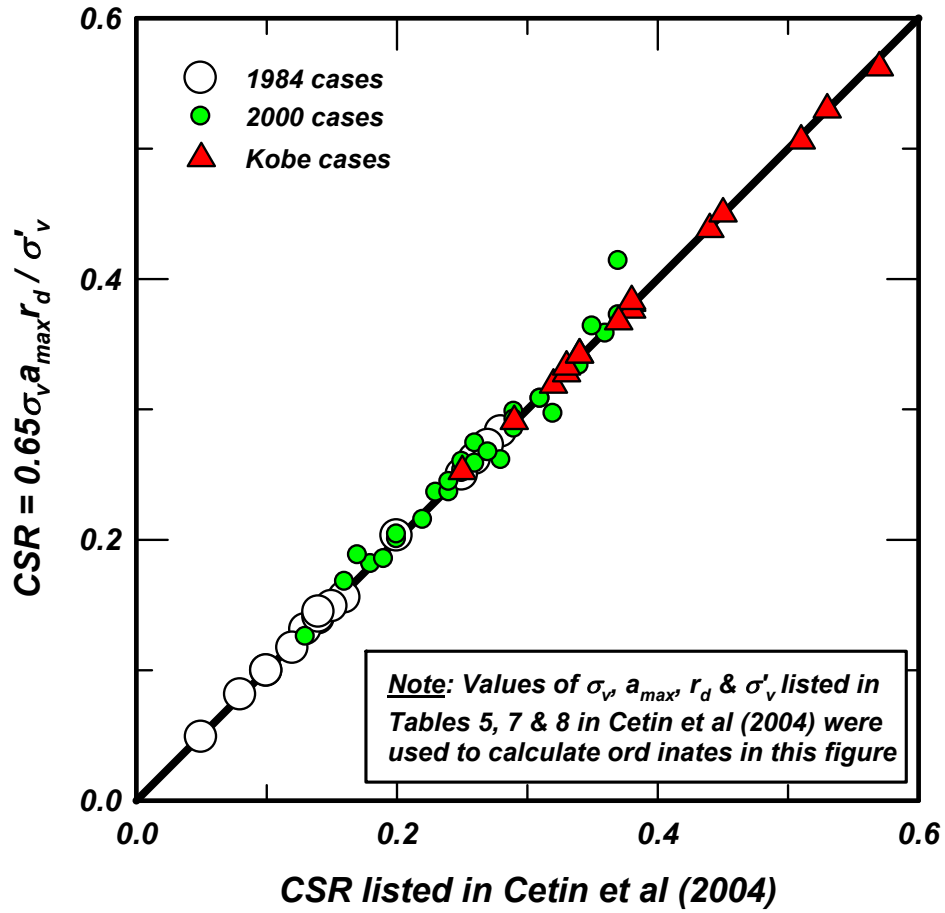


Figure A-7. Comparison of values of CSR listed in Tables 5, 7 and 8 in Cetin et al. (2004) with the values of CSR calculated using σ_v , a_{max} , r_d and σ'_v , whose values are also listed in the same tables.

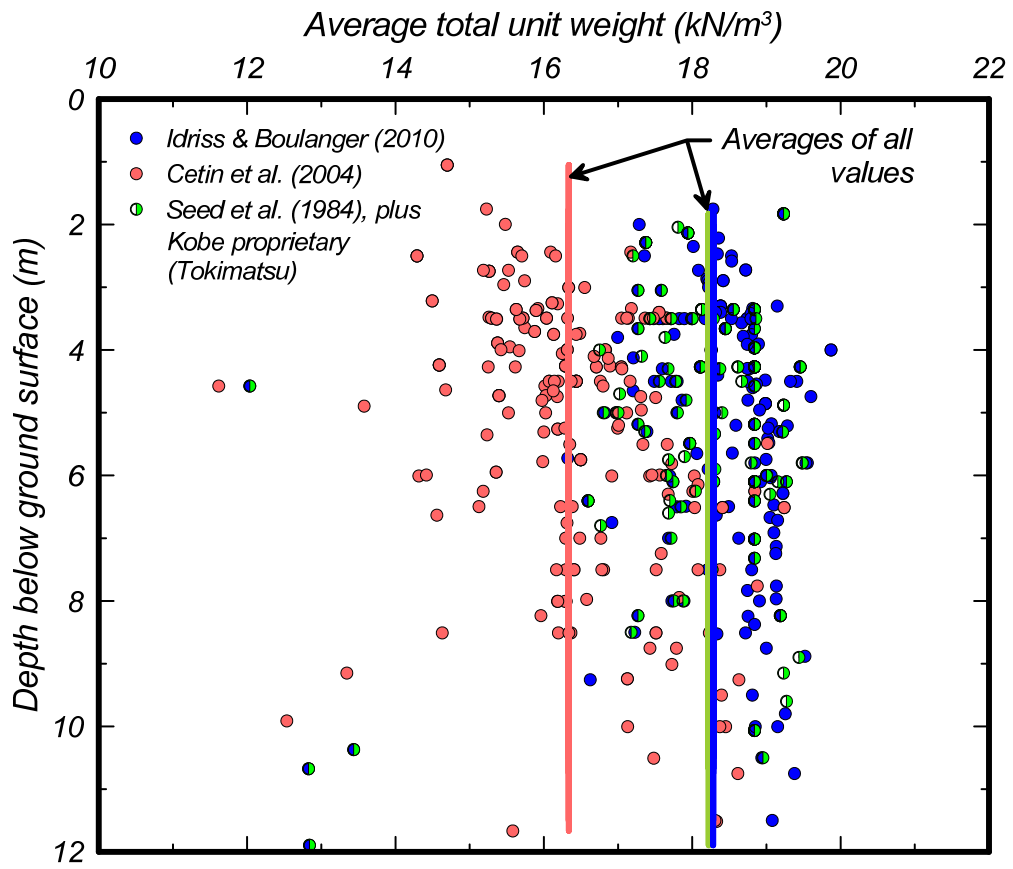


Figure A-8. Average total unit weights used in the different liquefaction triggering databases

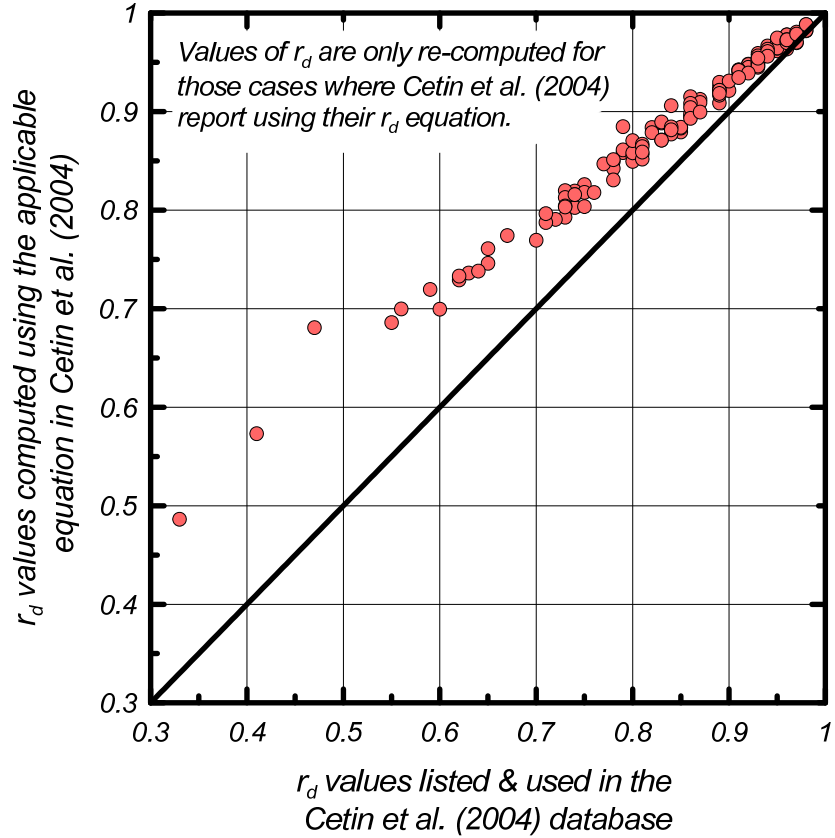


Figure A-9. Discrepancy between r_d values used in the Cetin et al. (2004) database and the r_d values computed using their referenced r_d equation

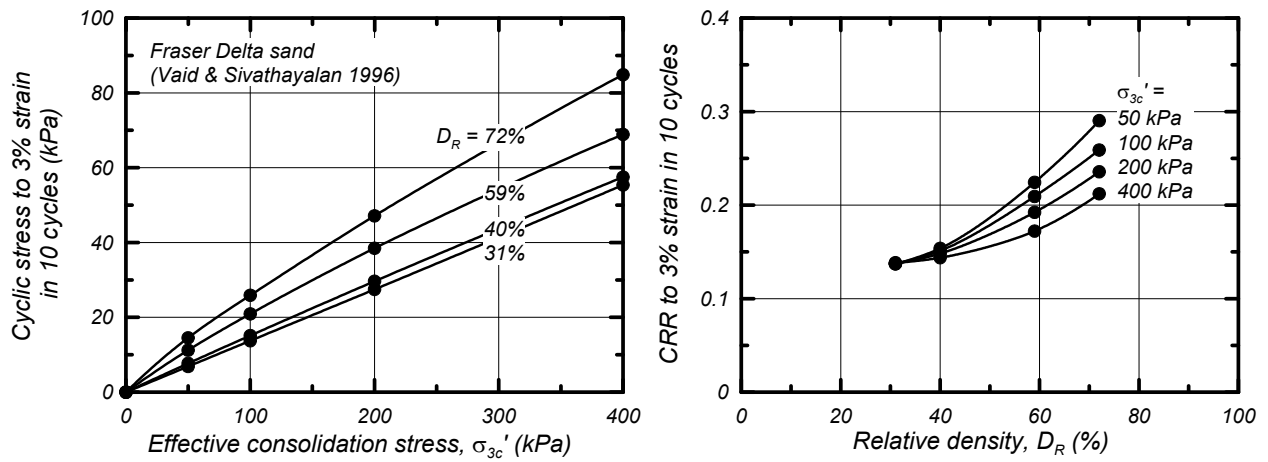


Figure A-10. Cyclic triaxial test results for clean Fraser Delta sand showing cyclic stress and CRR to cause 3% shear strain in 10 uniform cycles at D_R of 31 to 72% and effective consolidation stresses of 50 to 400 kPa (original data from Vaid & Sivathayalan 1996)

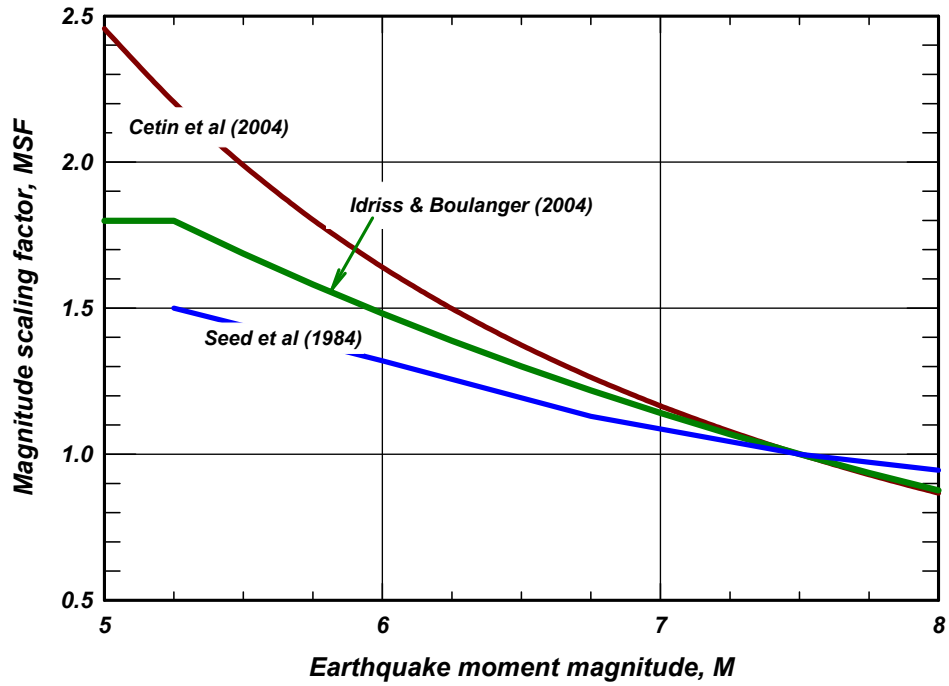


Figure A-11. Magnitude scaling factors used by Seed et al. (1984), by Cetin et al. (2004) and by Idriss and Boulanger (2004)

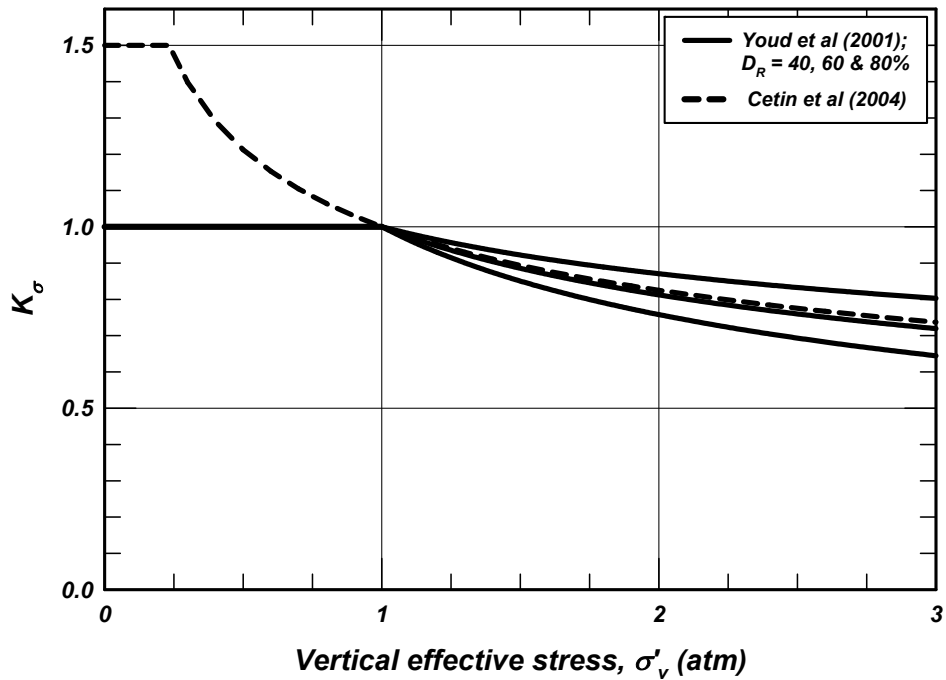


Figure A-12. K_σ values recommended by Youd et al. (2001) for $D_R = 40, 60$ and 80% , and values used by Cetin et al. (2004)

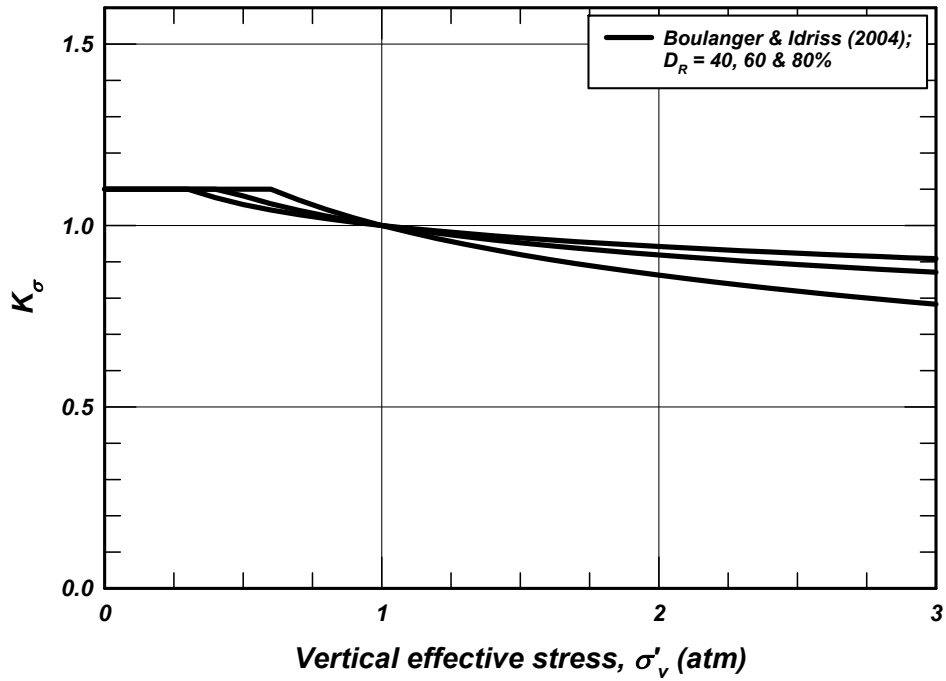


Figure A-13. K_{σ} values recommended by Boulanger and Idriss (2004) for $D_R = 40, 60$ and 80% .

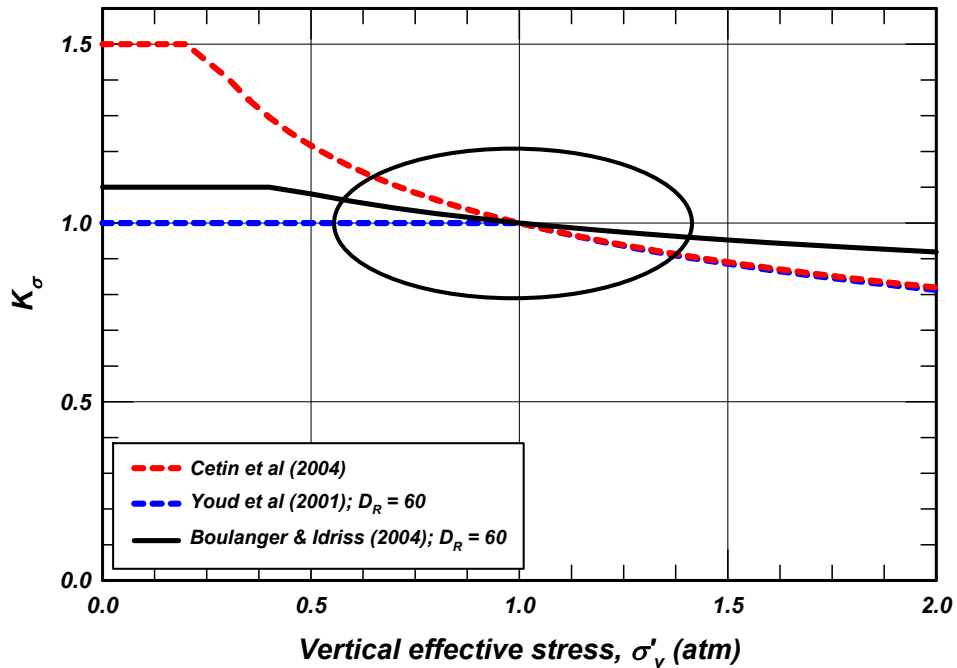


Figure A-14. Comparison of the K_{σ} relationship by Cetin et al. (2004) with those computed for $D_r = 60\%$ using the relationships in Youd et al. (2001) and Boulanger and Idriss (2004).

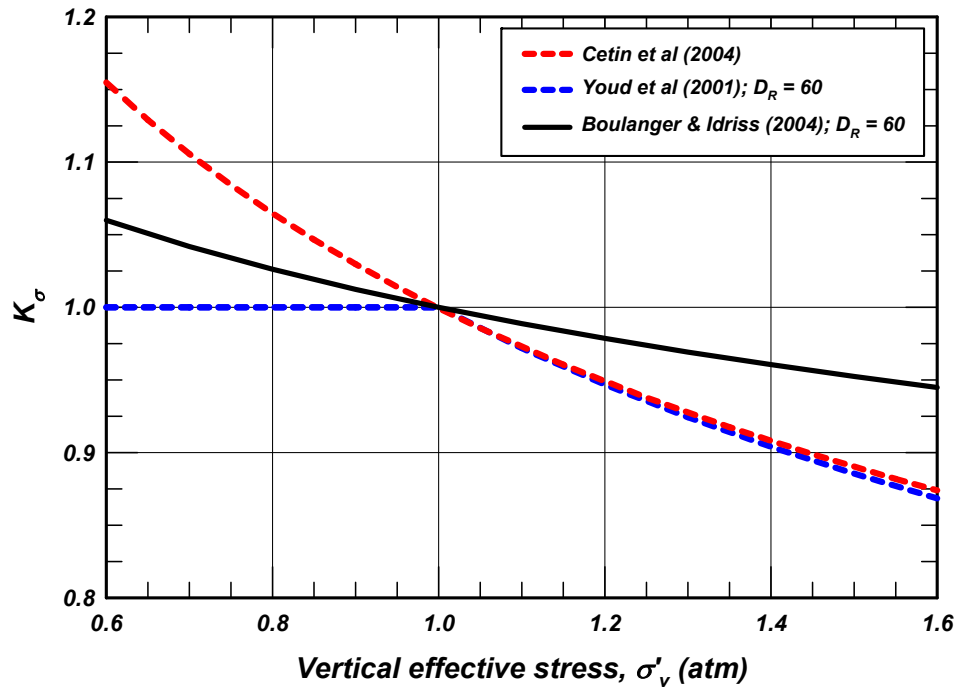


Figure A-15. Comparison of the three K_σ relationships in Figure A-14 for the narrower range of vertical effective stresses from 0.6 to 1.6 atm.

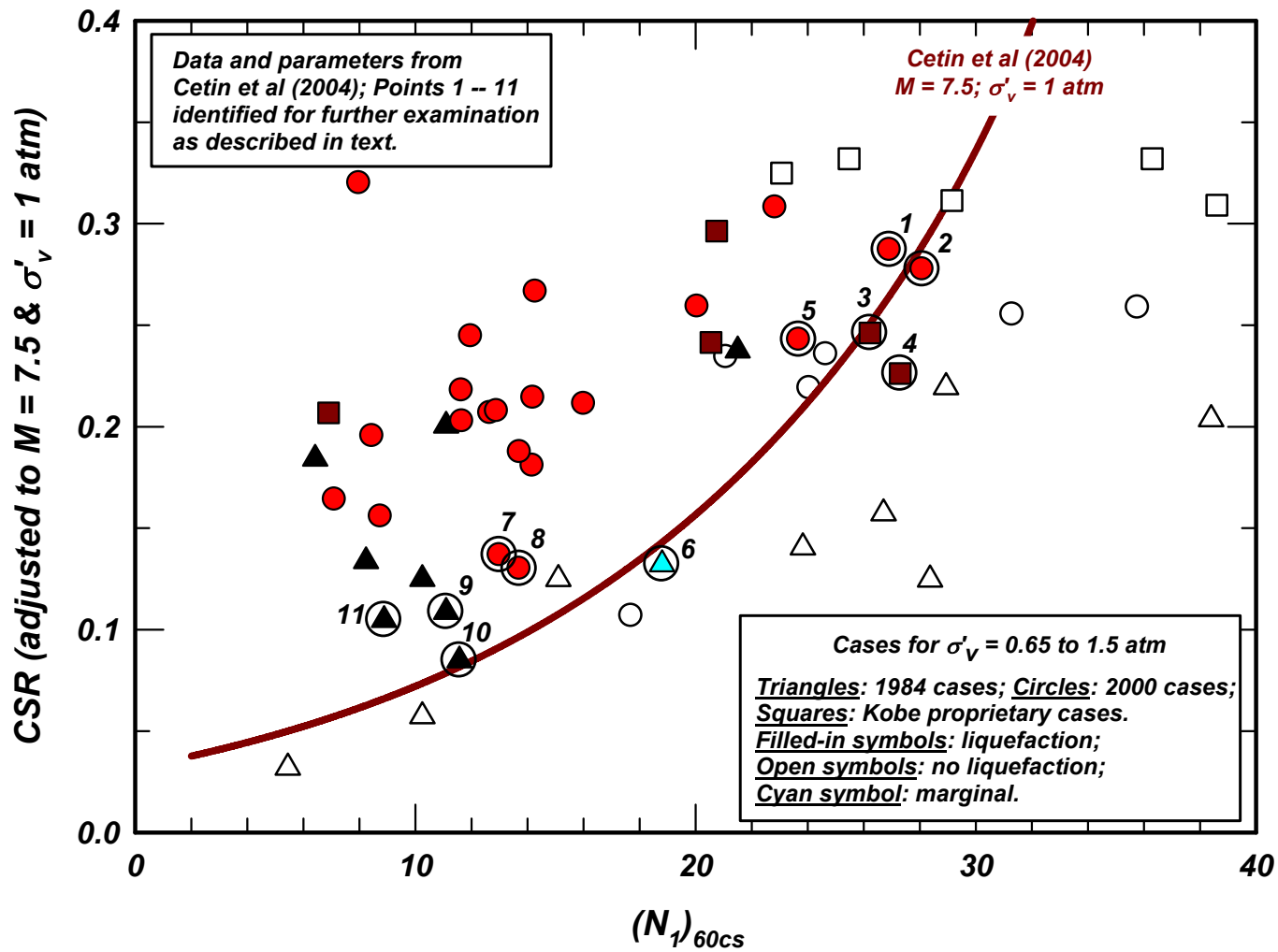


Figure A-16. Case histories for $\sigma'_v = 0.65$ to 1.5 atm published by Cetin et al. (2004) using values listed in Table A-1, with eleven points (cases) identified for further examination.

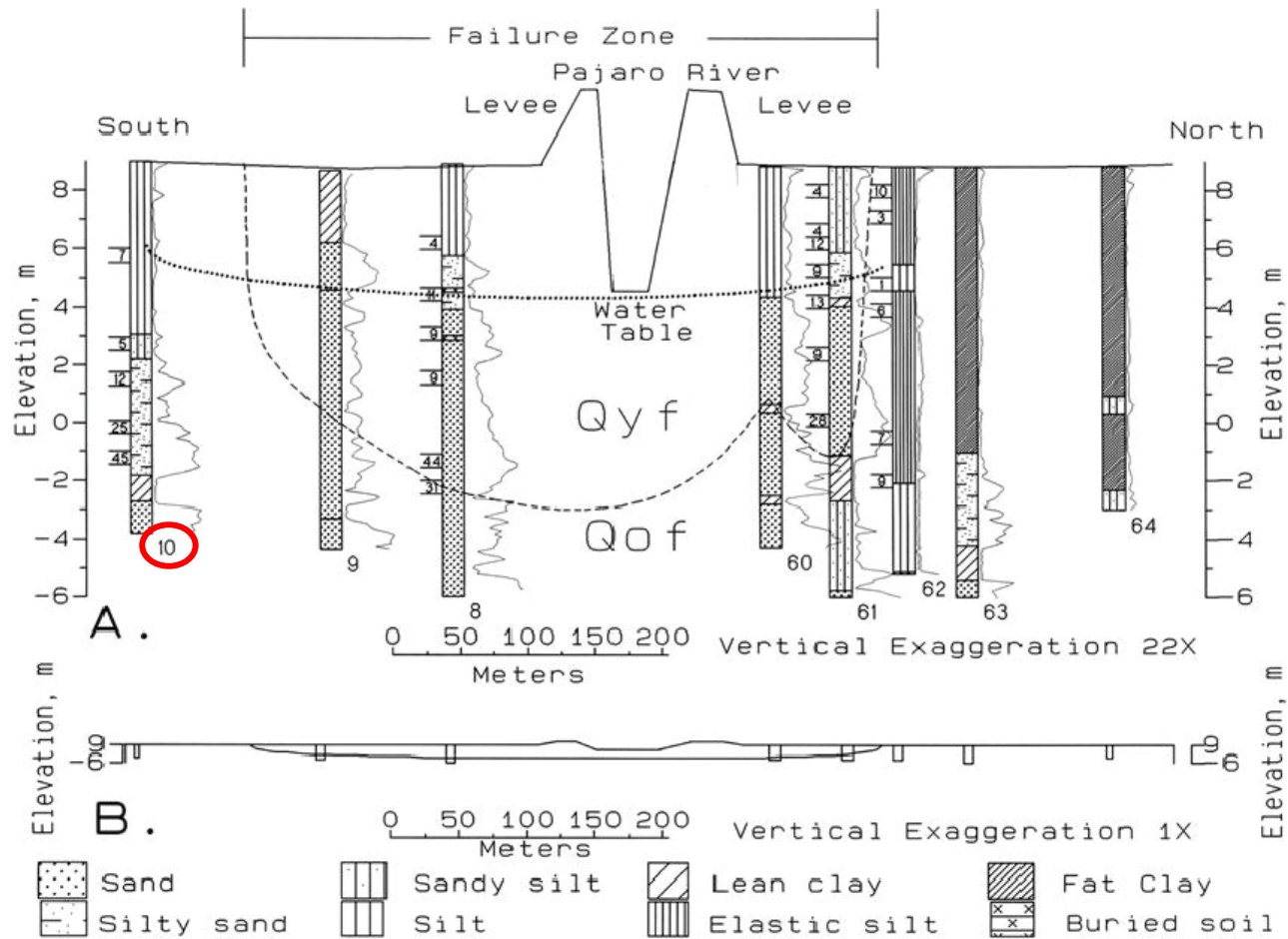


Figure A-17. Profile across the failure zone at the Miller (south side of Pajaro River) and Farris Farms (north side of Pajaro River) during the 1989 Loma Prieta Earthquake (Holzer et al. 1994) and location of CMF-10 boring, some 50 meters away from the failure zone.

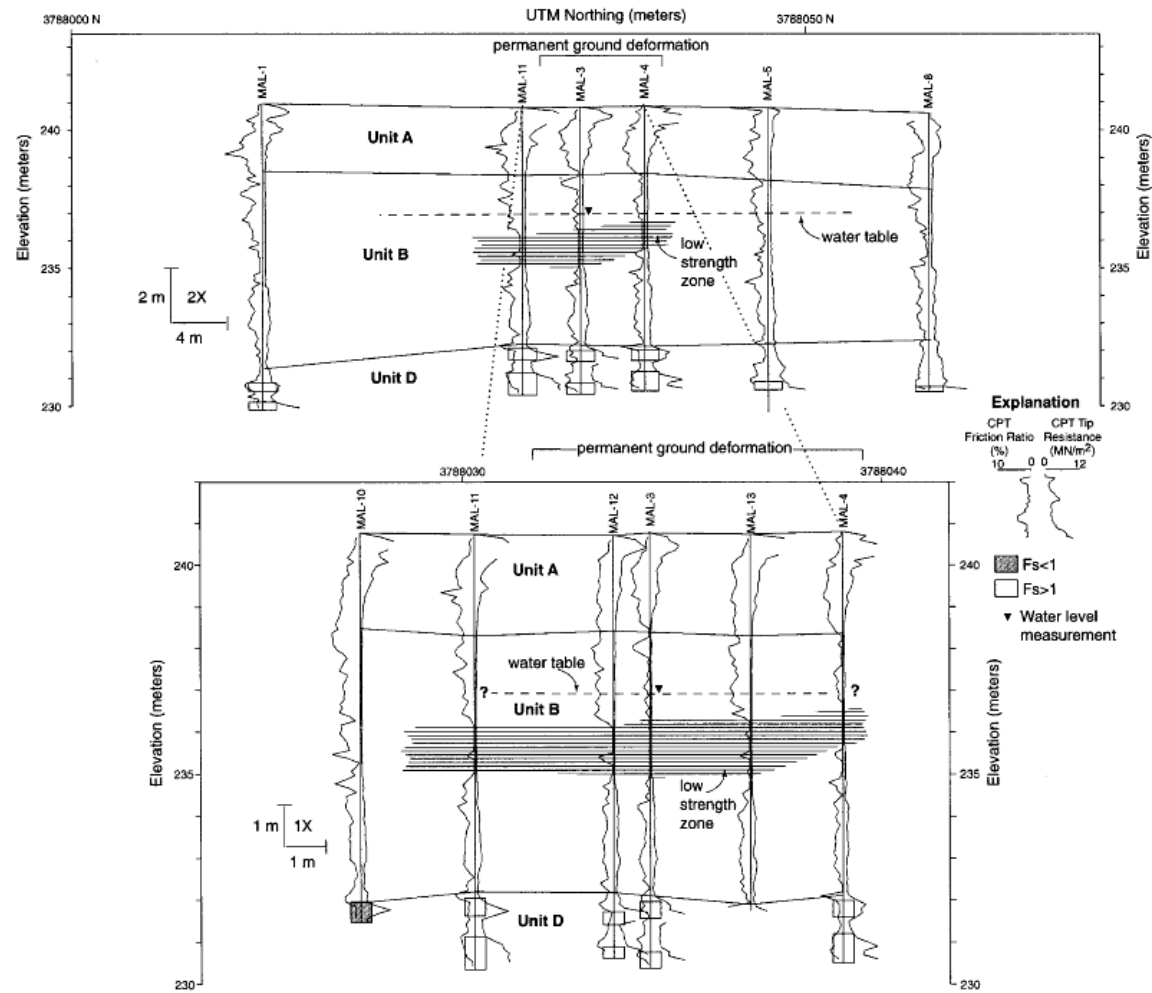


Figure A-18. Profile across the failure zone at the Malden Street site during the 1994 Northridge Earthquake (Holzer et al. 1998) showing the Unit B soils consisting of low strength clay, identified by Holzer et al. (1998) and O'Rourke (1998) as the cause of "lurching" leading to the observed ground deformations.

Site No.	Liquefied	Reference	Original Site ID
1	No		2 kt00989
2	No		2 kt00996
3	No		2 kt03034
4	No		2 kx20034
5	Yes		2 kt00990
6	No		2 kt00998
7	Yes		2 kt00991
8	Yes		1 5513
9	Yes		2 kt00999
10	No		1 hy104951
11	Yes		1 ch109423
12	No		2 kg00464
13	Yes		1 4499
14	No		2 kt03012
15	Yes		2 kp8051
16	No		1 ch104521
17	Yes		1 7524
18	No		1 ch084841

(a) Listing in the original files from Tokimatsu

Earthquake:	1995 Hyogoken-Nambu			
Magnitude:	7.2 (M _L)			
Location:	Kobe No : 6			
References:	Kobe City Office, 1999 (In Japanese), Confidential			
Nature of Failure:	Liquefied			
Comments:				
Summary of Data				
Liquefied?	Yes		D ₅₀	0.000 ± 0.000
Data Class	A		% Fines	25.0 ± 3.0
Critical Depth Range	14.1 - 24.0		% PI	
Depth to GWT (ft)	7.5 ± 1.0		N	16.8 ± 2.9
σ _v (psf)	2150.6 ± 196.6		C _R	0.95
σ' _v (psf)	1434.1 ± 117.3		C _S	1
a _{max} (g)	0.400 ± 0.060		C _B	1
r _s	0.84 ± 0.079		C _E	1.22
CSR	0.328 ± 0.061		C _N	1.18
Equivalent Magnitude	6.9		(N ₁) ₅₀	22.7 ± 3.9
MSF				
CSR _N				

(b) Listing in Cetin et al. (2000)

Figure A-19. Listing of the Kobe No. 6 site in the original files provided by Tokimatsu and in the Cetin et al. (2000) report

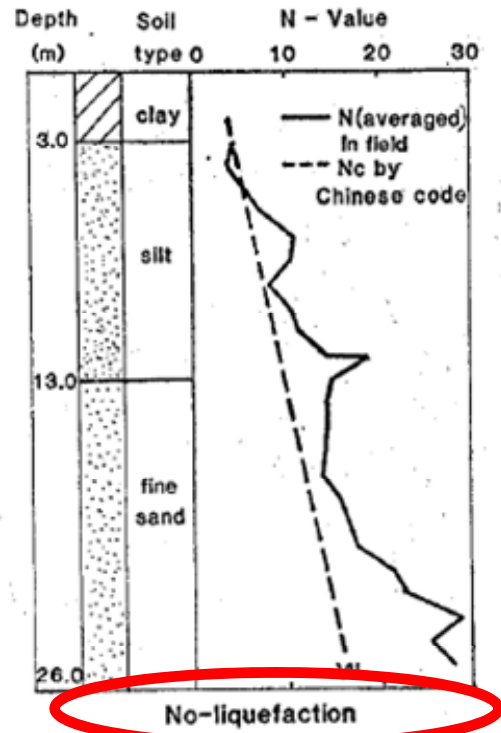


Fig. 9. Soil profile at Shuang Tai Zi river sluice gate site (non-liquefied, reproduced from Ref. 7)

Figure A-20. Original figure from Shengcong and Tatsuoka (1984) listing the Shuang Tai Zi River site as a "no liquefaction" case.

TABLE 8: CHINESE DATA FOR SPT-LIQUEFACTION CORRELATION

Site	Liquefied?	Critical Depth(ft)	Water Depth(ft)	σ_o (psf)	σ_o' (psf)	r_d	D_{60} (mm)	FC (%)	N	C_N	N_1	SPT Correction	$(N_1)_{60}$	σ_{max}^a (g)	(τ/σ_o') M	(τ/σ_o') M=7.5	References
1975 HAICHENG EARTHQUAKE (M=7.3)																	
Shuangtaihe E. B.	No	19.7	6.6	2325	1505	0.96	Fine Sand		9.5	1.14	11.	1.00	11.	0.10	0.095	0.095	Xie (1979)
Shenglitang	No	42.7	6.6	5290	3038	0.83	Sand		14.5	0.81	11.5	1.00	11.5	0.10	0.095	0.09	"
Ligohe Ch. F. P.	Yes	20.3	5	2505	1550	0.96	Sand		6	1.12	6.5	1.00	6.5	0.10	0.10	0.10	"
Nanheyuan Irr. S.	Yes	9.8*	6.6	1180	980	0.98	Sand		6	1.40	8.5	0.75	6.5	0.13	0.10	0.095	"
Shuiyuan Comm.	Yes	32.8	6.6	4055	2420	0.91	Sand		9	0.91	8.	1.00	8.	0.20	0.20	0.195	"
Yingkou Gate	Yes	33.8	6.6	4180	2480	0.90	Sand		9	0.89	8.	1.00	8.	0.20	0.195	0.19	"
Panjin Ch. F. P.	Yes	30	5	3675	2115	0.92	0.064	67	8	0.98	8.	0.83	6.5	0.13	0.135	0.13	Shengcong et al (1983)
Yingkou P. P.	Yes	27	5	3300	1930	0.93	Silt&Sand		11	1.02	11.	1.00	11.	0.20	0.21	0.20	"
Yingkou C. F. P.	Yes	27	5	3300	1930	0.93	0.078	48	13	1.02	13.5	1.00	13.5	0.20	0.21	0.20	"
Shuang Tai Zi R.	No	27	5	3300	1930	0.93	Silt		9	1.02	9.	1.00	9.	0.10	0.105	0.10	"
1976 TANGSHAN EARTHQUAKE (M=7.6)																	
Weigezhuang	Yes	7.5*	4.5	875	685	0.98	Fine Sand		11	1.62	18.0	0.75	13.5	0.20	0.16	0.17	Xie (1979)
Lujiatuo Mine	Yes	23.	3.3	2740	1510	0.94	Fine Sand		4	1.14	4.5	1.00	4.5	0.35	0.39	0.405	"
Tangshan City	No	17.5	10	2040	1570	0.96	0.196	10	30	1.12	33.5	1.00	33.5	0.50	0.405	0.42	Shengcong et al (1983)
Qing Yin	Yes	17.4	3	2130	1230	0.96	0.137	20	17	1.25	21.5	1.00	21.5	0.35	0.38	0.395	"
Luan Nan	Yes	17.6	12	2020	1670	0.96	0.17	20	20	1.09	22.	1.00	22.	0.22	0.165	0.175	"
Le Ting	Yes	6.7*	5	760	655	0.99	0.22	12	10	1.65	16.5	0.75	12.5	0.20	0.155	0.16	"
Coastal Region	Yes	20	4	2440	1440	0.96	0.14	12	10	1.16	11.5	1.00	11.5	0.13	0.14	0.145	"
Yao Yuan Village	Yes	20	3	2455	1395	0.96	Silt & Sand		9	1.19	11.	1.00	11.	0.20	0.22	0.23	"
Ma Feng	No	30	13	3555	2495	0.92	0.30	1	13	0.90	11.5	1.00	11.5	0.07	0.06	0.06	"
Wang Zhuang	Yes	23	5	2800	1675	0.94	0.32	2	11	1.06	12.5	1.00	12.5	0.20	0.205	0.21	"

Notes: (1) Critical Depth is the depth at which liquefaction would most likely occur
 (2) FC denotes fines content, defined as the fraction finer than the No. 200 sieve size
 (3) * denotes that a correction factor for short rod length (0.75) is incorporated in the correction to $(N_1)_{60}$
 (4) ** denotes that the gravel content exceeds 20 percent by weight

Figure A-21. Listing of the Shuang Tai Zi River in Seed et al. (1984) identifying this site as a "no liquefaction" case.

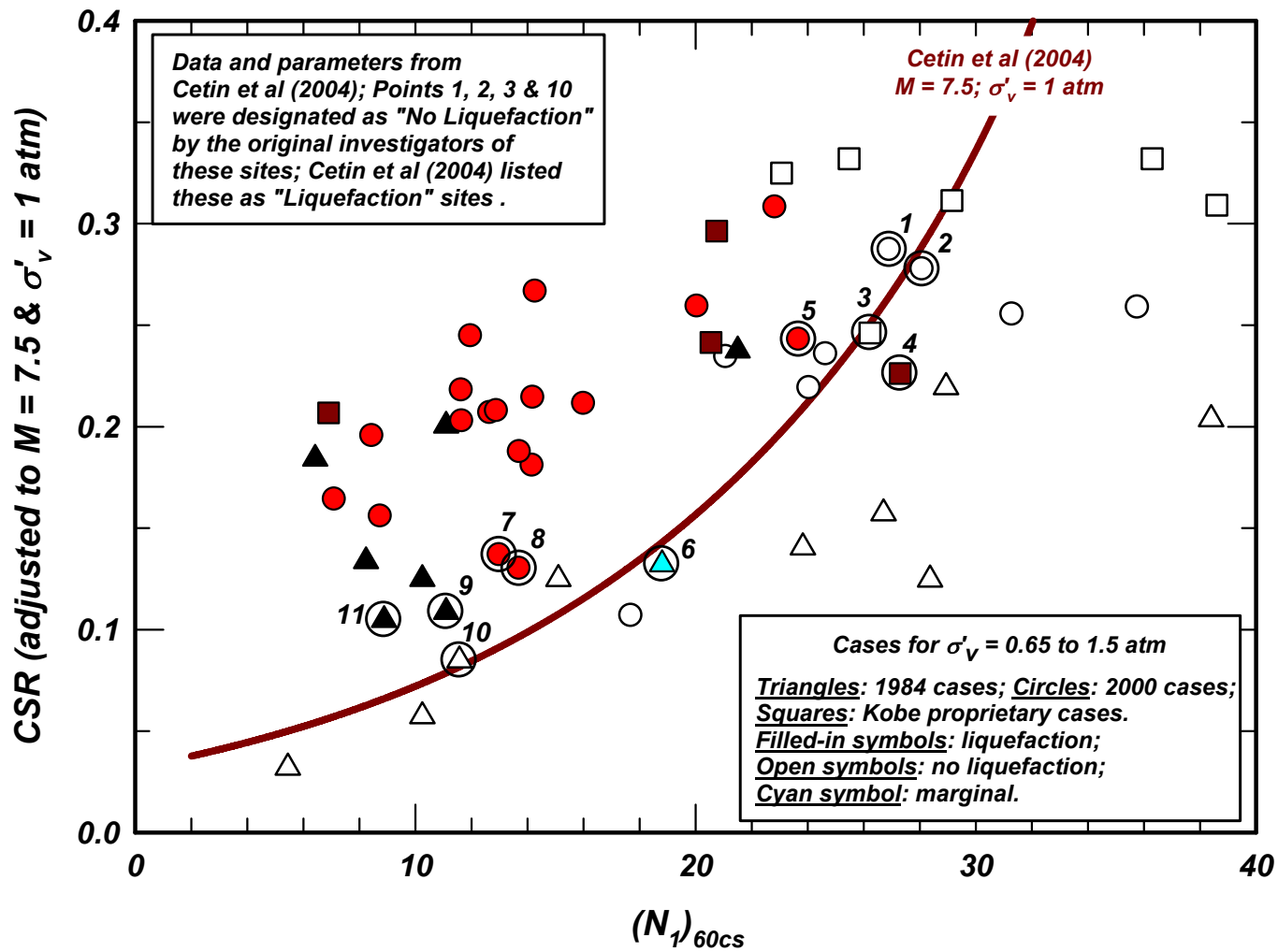


Figure A-22. Case histories for $\sigma'_v = 0.65$ to 1.5 atm published by Cetin et al. (2004), but with Points 1, 2, 3, & 10 corrected to "no liquefaction" based on the original investigators' observations and interpretations.

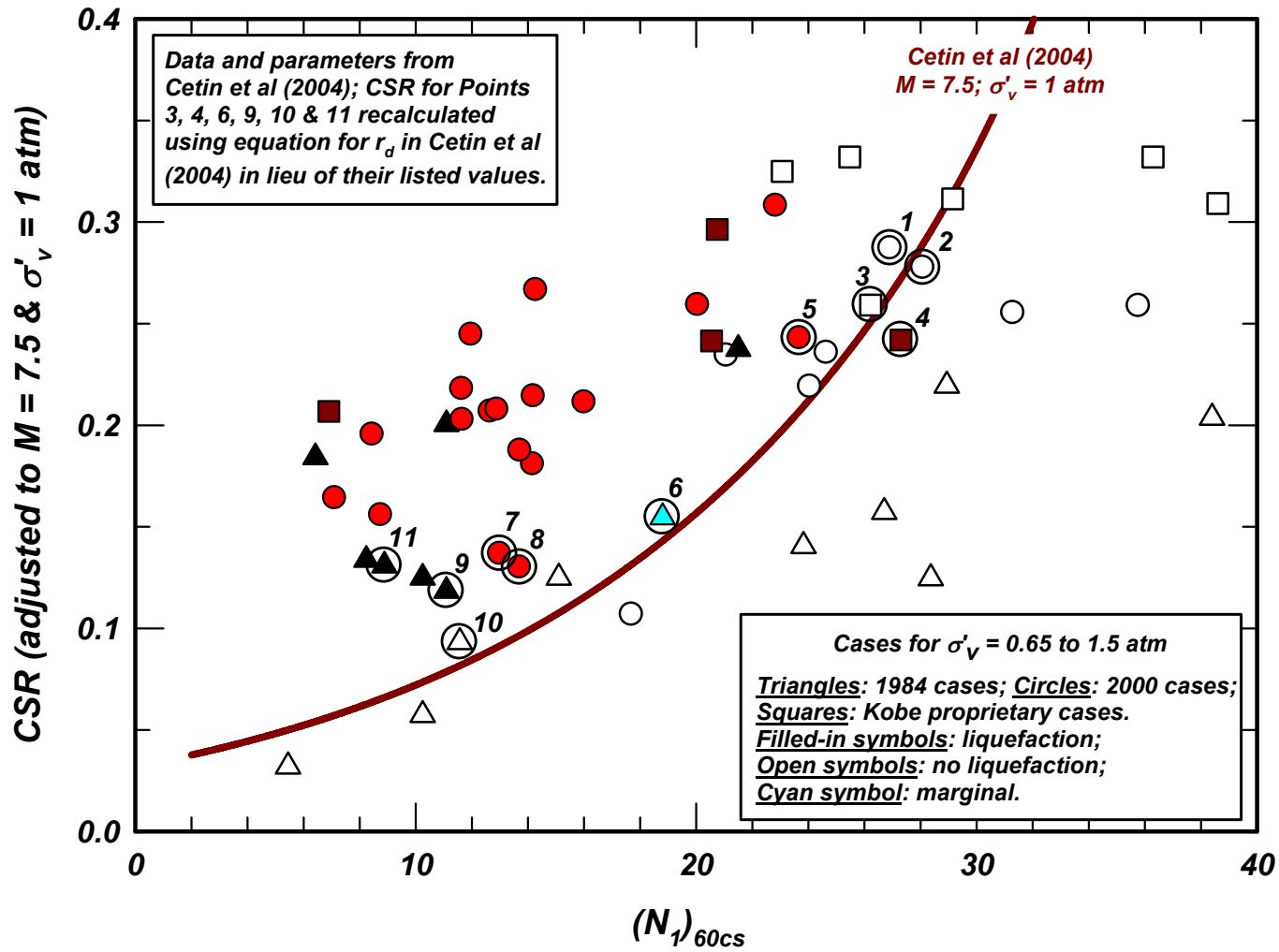


Figure A-23. Case histories for $\sigma'_v = 0.65$ to 1.5 atm published by Cetin et al. (2004) with the corrections in Figure A-22 and with the r_d values for Points 3, 4, 6, 9, 10 & 11 re-computed using the equation for r_d in Cetin et al. in lieu of their listed r_d values.

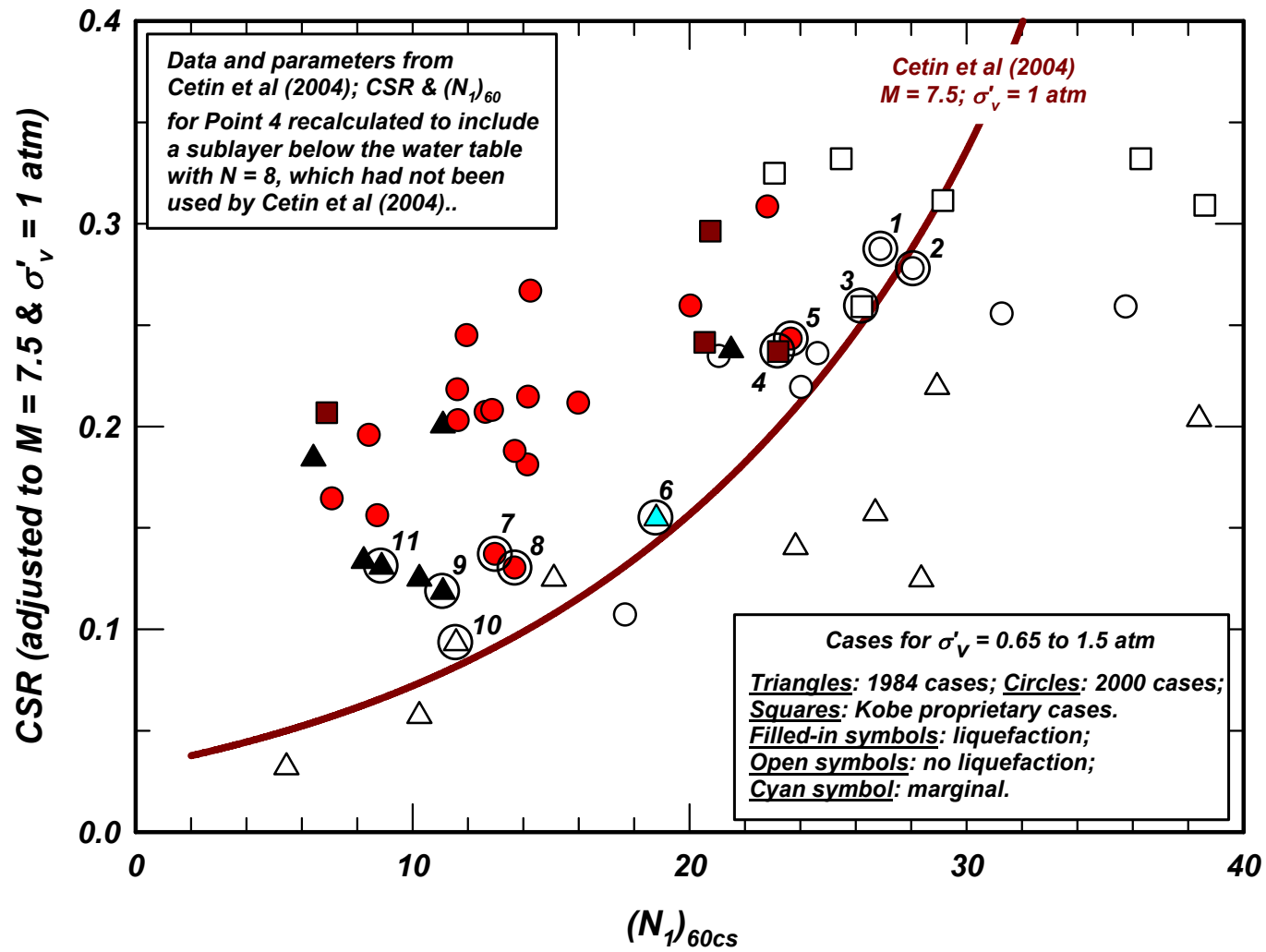


Figure A-24. Case histories for $\sigma'_v = 0.65$ to 1.5 atm published by Cetin et al. (2004) with the corrections in Figure A-23 and with the CSR and $(N_1)_{60}$ values for Point 4 recalculated to include a sublayer below the water table with $N = 8$ which had not been used by Cetin et al. (2004).

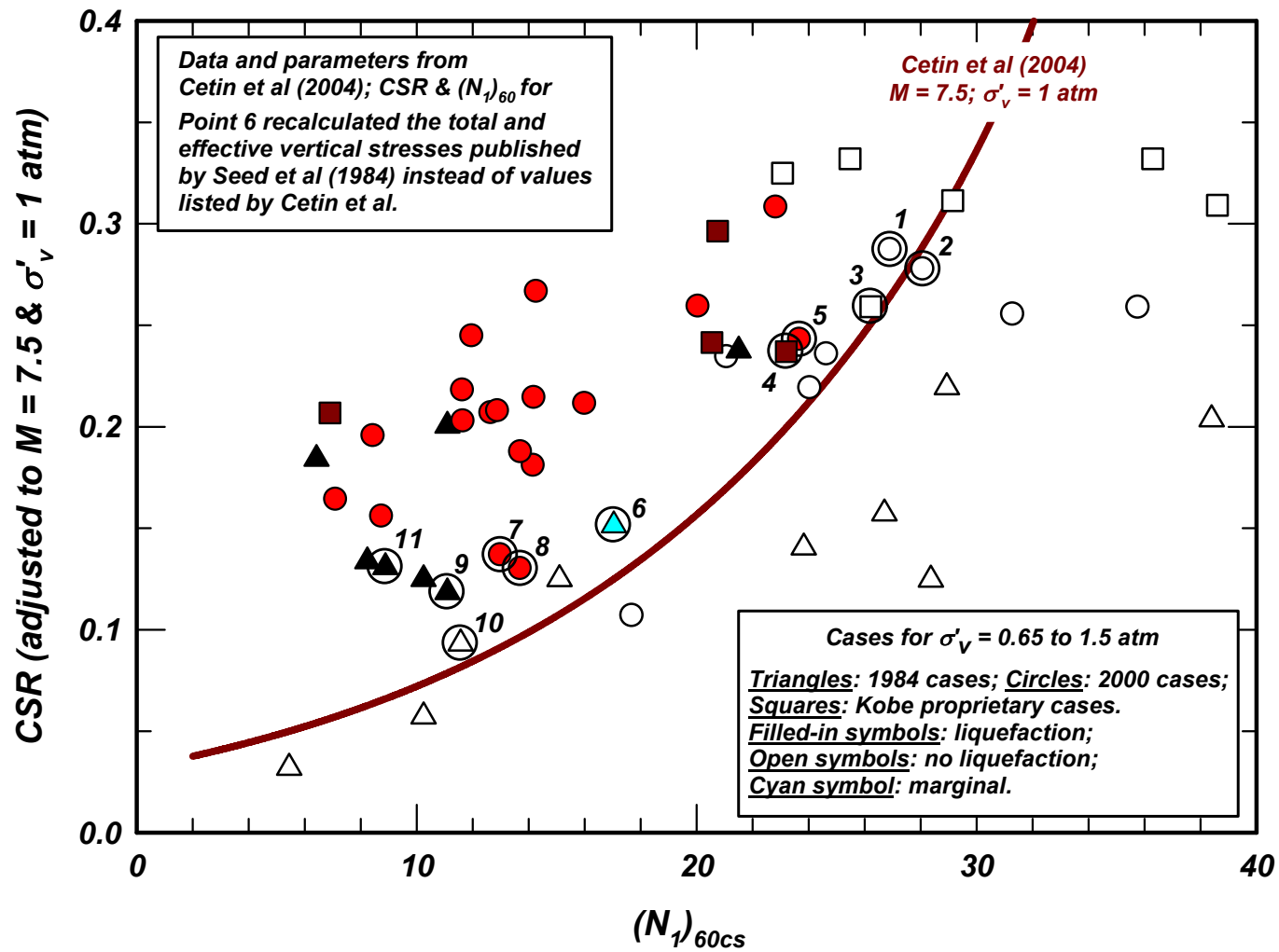


Figure A-25. Case histories for $\sigma'_v = 0.65$ to 1.5 atm published by Cetin et al. (2004) with the corrections shown in Figure A-24 and using the total and effective vertical stresses published by Seed et al. (1984) for Point 6 instead of the values listed by Cetin et al. (2004).

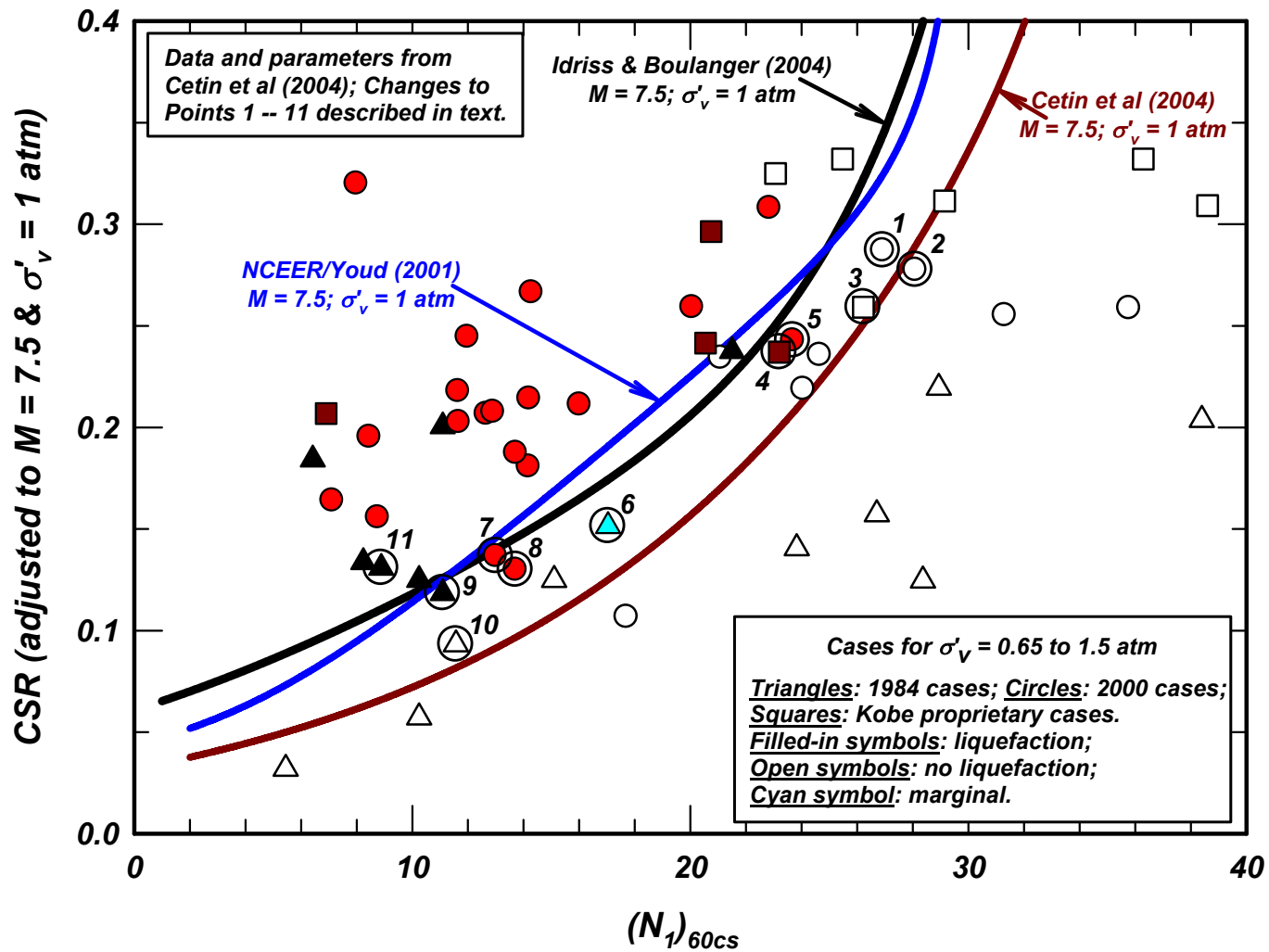


Figure A-26. Case histories for $\sigma'_v = 0.65$ to 1.5 atm published by Cetin et al. (2004) with the corrections shown in Figure A-25, compared with the liquefaction triggering curve by Idriss and Boulanger (2004), the modified version of the Seed et al. (1984) curve adopted by the NCEER/NSF Workshops (Youd et al. 2001), and correlation by Cetin et al. (2004).

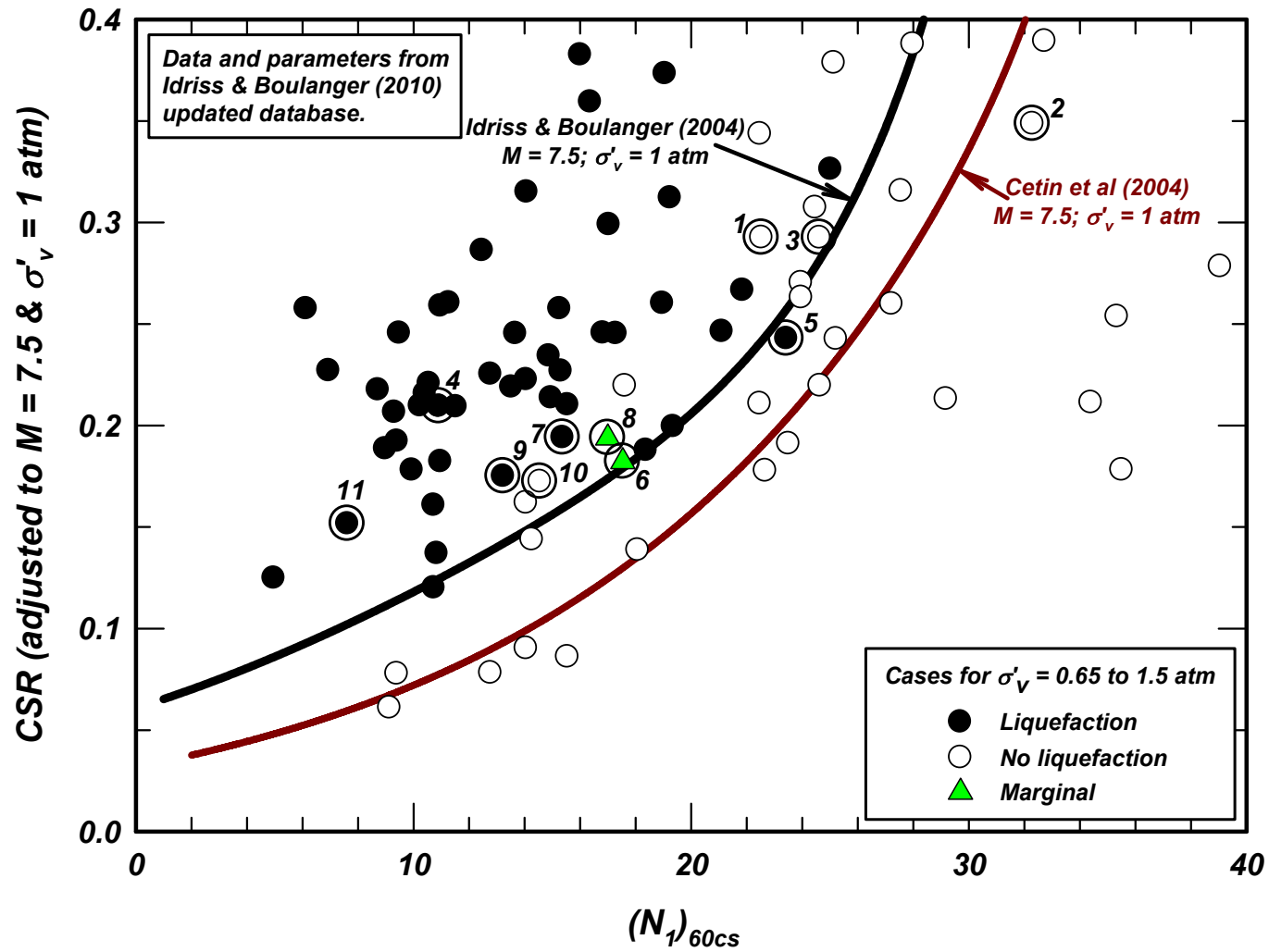


Figure A-27. Case histories for $\sigma'_v = 0.65$ to 1.5 atm from the updated case history database in the main report, as processed using the Idriss and Boulanger (2004, 2008) liquefaction triggering procedures.

APPENDIX B:
SHEAR STRESS REDUCTION COEFFICIENT

APPENDIX B

SHEAR STRESS REDUCTION COEFFICIENT

B-1. INTRODUCTION

The shear stresses induced at any point in a level deposit of soil during an earthquake are primarily due to the vertical propagation of shear waves in the deposit. Analytical procedures are available to calculate these stresses if the characteristics of the soils comprising this deposit and the input motion are known. Such information is not available for most of the "liquefaction/no liquefaction" case histories that have been used to develop correlations based on field observations. In addition, borings drilled for most projects seldom extend to the depths needed to define the soil profile in sufficient detail for site response studies.

For these reasons, the following equation developed as part of the Seed-Idriss (1971) simplified liquefaction evaluation procedure for calculating the induced shear stresses and hence the cyclic stress ratio, continues to be used:

$$CSR = 0.65 \left(\frac{\sigma_v a_{\max}}{\sigma'_v g} \right) r_d \quad (B-1)$$

where a_{\max} is the maximum horizontal acceleration at the ground surface, σ_v is the total vertical stress and σ'_v is the effective vertical stress at depth z below the ground surface. The parameter r_d is a stress reduction coefficient, which is shown schematically in Figure B-1. The values of r_d for use in the simplified liquefaction evaluation procedure were originally defined by Seed and Idriss (1971) as a function of depth, and an average curve, extending to a depth of about 12 m (40 ft), was proposed for use for all earthquake magnitudes and for all soil profiles. The average r_d curve by Seed and Idriss (1971) was used by Seed et al. (1984) to interpret the case histories of liquefaction/no liquefaction and develop their liquefaction triggering correlation. The average r_d curve by Seed and Idriss (1971) was adopted, along with a slightly modified version of the triggering correlation by Seed et al. (1984), by the NCEER/NSF workshop (Youd et al. 2001).

In 1999, Idriss proposed a new r_d relationship that included dependency of r_d on both depth and earthquake magnitude. This relationship was included in the Proceedings of a Transportation Research Board Workshop (Idriss 1999), but that publication was not widely distributed and did not include all the details of the approach and analysis results. This Appendix, therefore, summarizes the approach and results of analyses completed from 1996 – 1999 that were used to derive the expressions presented in Idriss (1999) for calculating values of the stress reduction coefficient, r_d , as a function of magnitude as well as depth.

B-2. CALCULATION OF THE STRESS REDUCTION COEFFICIENT, r_d , USING UNIFORM SINUSOIDAL INPUT MOTIONS

Theoretical considerations (e.g., Ishihara 1977, Golesorkhi 1989) indicate that the value of r_d can be influenced by the frequency of the input motion and by the stiffness of the soil profile. Therefore, a series of analyses using uniform soil profiles and sinusoidal input motions were performed to examine potential functional forms for the dependency of r_d on input motion frequency.

Possible variations of the coefficient r_d with depth and with the frequency of the input motion were tested by analyzing six 30-m deep soil layers, each having a uniform shear wave velocity. The shear wave velocities of these six soil layers were 120, 240, 360, 480, 600, and 720 m/sec. The corresponding fundamental frequencies for the soil layers were 1, 2, 3, 4, 5, and 6 Hz. The total unit weight of the soil was assumed to be 19.65 kN/m³ and a damping ratio of 0.05 was used for all cases.

Each layer was subjected to five sinusoidal input motions, each motion having uniform amplitude and a single frequency. The frequencies used were 1, 1½, 2, 5 and 8 Hz resulting in a total of 30 cases for the 30-m deep layer.

To check the effects of total thickness of the soil layer, six 60-m deep soil layers were also analyzed. The shear wave velocities of these six soil layers were also 120, 240, 360, 480, 600, and 720 m/sec. The corresponding fundamental frequencies were ½, 1, 1½, 2, 2½, and 3 Hz. Each layer was subjected to two sinusoidal input motions, each motion having a uniform amplitude and a single frequency. The frequencies used were 2 and 8 Hz resulting in a total of 12 cases for the 60-m deep layer.

The average values of r_d obtained for each set of cases using the input motion having a frequency of 1 Hz, 1½ Hz, 2 Hz, 5 Hz and 8 Hz are presented in Figure B-2 in terms of r_d versus depth for the 30-m layers. The results in Figure B-2 indicate that the value of r_d decreases with increasing frequency of the input motion at all depths.

The results for the 60-m layers are compared to the corresponding results for the 30-m layers in Figure B-3. The plots in Figure B-3 indicate that the total depth of the layer had little or no effect on the value of r_d , especially in the upper 15 m of the soil profile.

The results for the 30-m deep soil layers are re-plotted in Figure B-4 in terms of r_d versus frequency of the input motion at depths of 3.8, 6.8, 9.9, 14.5, and 25.9 m. Examination of the information in this figure indicates that at a given depth within the soil layer, the following functional relationship may be used to relate r_d to the frequency of the input motion:

$$\ln(r_d) = a - bf \tag{B-2}$$

where "f" is the frequency of the input motion and "a" and "b" are coefficients which appear to depend on depth below the ground surface. The information in Figure B-4 can also be expressed in terms of the period of the input motion, where $T = 1/f$, as follows:

$$\ln(r_d) = \alpha + \beta T \tag{B-3}$$

This period of the input motion can be related (in an approximate way) to earthquake magnitude based on the concept of predominant period initially proposed by Seed et al. (1969), or on the mean period recently proposed by Rathje et al. (1998). The study by Seed et al. (1969) shows essentially a linear relationship between the predominant period and earthquake magnitude. Rathje et al. (1998) also indicated an almost linear relationship up to about magnitude 7. Accordingly, it would seem reasonable to replace T by magnitude, M, in deriving expressions relating r_d to depth and magnitude, i.e., equation (B-3), after a slight rearrangement, is expressed as follows:

$$r_d = \exp[\alpha(z) + \beta(z)M] \tag{B-4}$$

This form will now be tested against the values of r_d calculated for a number of soil profiles subjected to recorded motions.

B-3. CALCULATION OF THE STRESS REDUCTION COEFFICIENT, r_d , USING RECORDED EARTHQUAKE GROUND MOTIONS

B-3.1. Soil sites used in the analyses

Six soil sites were selected for the purpose of testing and further developing the r_d expression in equation B-4. These sites are identified as A1, A2, B1, B2, C1 and C2. Sites A1 and A2 are presented in Figure B-5; sites B1 and B2 in Figure B-6, site C1 in Figure B-7, and site C2 in Figure B-8. Sites A1 and A2 were selected to represent a relatively shallow soil profile (100 ft \approx 30 m) with site A1 consisting of a relatively loose sands ($D_R = 40\%$) and A2 much denser ($D_R = 70\%$). Profiles B1 and B2 were selected to represent deeper soil profiles and constructed by extending profiles A1 and A2 250 ft (\approx 75 m) deeper. Site C1 was constructed mostly using the layering and properties obtained for the soil profile underlying the strong motion instrument at Treasure Island site in the San Francisco Bay Area. Site C2 was modeled approximately after the layering and properties obtained for the upper 420 ft (\approx 130 m) of the soil profile underlying the strong motion instrument at the La Cienega site in Los Angeles.

The layering, maximum shear wave velocities, and values of total unit weight used for each layer are shown in Figures B-5 through B-8. The modulus reduction and damping curves used in the response calculations are shown in Figures B-9 and B-10.

The response of each soil site was calculated using the accelerograms listed in Section B-3.2 as input rock outcrop motions in one-dimensional equivalent linear site response analysis.

B-3.2. Accelerograms used for input rock outcrop motions

Three sets of recorded accelerograms were selected to use as input rock outcrop motions to these sites. One set was selected from accelerograms recorded during magnitude $M \approx 7.5$ earthquakes, one set from accelerograms recorded during magnitude $M \approx 6.5$ earthquakes, and the third set from accelerograms recorded during magnitude $M \approx 5.5$ earthquakes. The strong motion stations at which the accelerograms selected for $M \approx 7.5$ earthquakes are listed in Table B-1; those for $M \approx 6.5$ and $M \approx 5.5$ earthquakes are listed in Tables B-2 and B-3, respectively. As noted in each table, the two horizontal components recorded at each station were used in the response calculations. Thus, the number of cases analyzed is:

Magnitude	Sites	Accelerograms	Number of cases
7.5	6	34	200
6.5	6	32	192
5.5	6	20	120
Grand total:			512

The spectral shape (i.e., spectral acceleration divided by the peak zero-period acceleration) for each of the $M \approx 7.5$ accelerograms, and the median shape for the entire set are presented in Figure B-11. The median spectral shape shown in Figure B-11 is compared to the target spectral shapes for $M = 7.5$ at distances of 3, 10, 50 and 100 km in Figure B-12 using pre-NGA attenuation relationships for a "rock site" and a strike slip source. Note that similar comparison were made to target spectra at these distances for a "rock

site" and a reverse source using the same pre-NGA attenuation relationships and that comparison is very similar to that shown in Figure B-12 for the strike slip source.

The peak accelerations for the $M \approx 7.5$ accelerograms range from about 0.05 g to about 0.85 g, with an average value of about 0.28 g and a median value of about 0.18; approximately 30% of the values are greater than 0.3 g and 20% are greater than 0.4 g.

The spectral shape for each of the $M \approx 6.5$ accelerograms, and the median shape for the entire set are presented in Figure B-13. The median spectral shape shown in Figure B-13 is compared to the target spectral shapes for $M = 6.5$ at distances of 3, 10, 50 and 100 km in Figure B-14 using pre-NGA attenuation relationships for a "rock site" and a strike slip source.

The peak accelerations for the $M \approx 6.5$ accelerograms range from about 0.04 g to about 0.84 g, with an average value of about 0.28 g and a median value of about 0.26; approximately 35% of the values are greater than 0.3 g and 20% are greater than 0.4 g.

The spectral shape for each of the $M \approx 5.5$ accelerograms, and the median shape for the entire set are presented in Figure B-15. The median spectral shape shown in Figure B-16 is compared to the target spectral shapes for $M = 5.5$ at distances of 3, 10, 50 and 100 km in Figure B-16 using pre-NGA attenuation relationships for a "rock site" and a strike slip source.

The peak accelerations for the $M \approx 5.5$ accelerograms range from about 0.04 g to about 0.43 g, with an average value of about 0.12 g and a median value of about 0.11; approximately 20% of the values are greater than 0.11 g.

Therefore, the range of the spectral shapes of the selected accelerograms and the median shape of these spectra are reasonable for the events (i.e., $M \approx 5.5, 6.5$ and 7.5 earthquakes) under consideration.

B-3.3 Results for $M = 7.5$ earthquakes

The values of r_d were calculated using the results of the site response analyses in the upper 95 ft (≈ 29 m) of each soil profile. The maximum shear stress, $\tau_{\max}(z)$, obtained from the site response analysis at depth z , was divided by the product of the total stress, $\sigma_v(z)$, at that depth times the peak horizontal surface acceleration, $a_{\max}(z=0)$, obtained from the site response analysis, to calculate the value of $r_d(z)$ at that depth. That is:

$$r_d(z) = \frac{\tau_{\max}(z)}{\sigma_v(z) \cdot a_{\max}(z=0)} \quad (\text{B-5})$$

Figure B-17 shows the values of r_d calculated for the six sites described in Section B-3.1 using the 34 accelerograms listed in Table B-1 for $M \approx 7.5$ earthquakes as input rock outcrop motions to each site. While the r_d values for site A1 trend toward the smallest and those for site C2 trend toward the largest among these results, there is no clear separation in r_d values for these sites. Therefore, it appears reasonable to treat the results for all six sites together.

The results shown in Figure B-17 indicate that there is a significant spread in the calculated r_d values at any depth for any one site or for all the sites combined. Therefore, an important aspect in utilizing results such as those shown in this figure is the choice of the percentile to represent the variations of r_d with

depth for $M = 7.5$. This choice is required so that an expression relating r_d with depth can be obtained for use in interpreting the liquefaction/no liquefaction case histories to derive a field-based liquefaction triggering correlation and in forward applications once such a correlation has been established. In this regard, it is important to note that: (1) the available liquefaction case histories primarily correspond to depths less than about 12 m, whereas the forward application of r_d relationships can involve depths greater than 12 m, and (2) the choice of percentile has a small effect on r_d values at shallow depths and a greater effect on the r_d values as depth increases. The choice of a relatively low percentile, say the 50th percentile, for the r_d relationship is reasonable for the interpretation of case histories but may not be adequate for forward applications. The choice of a higher percentile value, say the 84th percentile, is unconservative in interpreting case histories but does provide conservatism for forward applications.

The evaluations summarized in this Appendix were started in 1996 and built upon and expanded the work in this area initiated by Dr. Golesorkhi (1989). At that time, it was felt that the average curve published by Seed and Idriss (1971), which had been used for thousands of liquefaction evaluations over the prior 25 years, is a reasonable curve to "preserve" and that it would be desirable to select the x^{th} percentile from the results shown in Figure B-17 that would provide a reasonable approximation to that curve. Note that the analyses completed in 1996 did not include the motions recorded during the Chi-Chi or the Kocaeli earthquakes. At that time, the best fit was obtained for $x = 67\%$.

The motions recorded during the Chi-Chi or the Kocaeli earthquakes became available in late 1999 and were used at that time to calculate the values of r_d for sites A1 through C2. The inclusion of these motions again provided a best fit with $x = 67\%$ as depicted in Figure B-18.

Accordingly, the 67th percentile was adopted for use in deriving an expression relating r_d to magnitude, M , as a function of depth, z [i.e., using a form of equation (B-4)]. The following expressions were obtained for the parameters $\alpha(z)$ and $\beta(z)$:

$$\alpha(z) = -1.012 - 1.126 \sin\left(\frac{z}{11.73} + 5.133\right) \quad (\text{B-6})$$

$$\beta(z) = 0.106 + 0.118 \sin\left(\frac{z}{11.28} + 5.142\right) \quad (\text{B-7})$$

where z is in units of m and the arguments inside the sine terms are in radians. These parameters provide an excellent fit to the 67th percentile values of r_d for $M = 7.5$ as shown in Figure B-19.

B-3.3 Results for $M = 6.5$ and 5.5 earthquakes

The fit obtained using equations (B-6) and (B-7) for $M = 6.5$ and for $M = 5.5$ are presented in Figures B-20 and B-21. The derived equation for $M = 6.5$ provides a very good fit to the 67th-percentile values of r_d calculated for all sites using input motions recorded during $M \approx 6.5$ earthquakes as illustrated in Figure B-20. The fit is not as good, however, for the 67th-percentile values of r_d calculated for all sites using input motions recorded during $M \approx 5.5$ earthquakes, as shown in Figure B-21. The difference in r_d for $M = 5.5$ is of the order of 2% at a depth of 3 m increasing to about 8% at a depth of 15 m.

B-3.4 Expression derived to relate r_d to depth and earthquake magnitude for interpreting case histories and for use in forward calculations

Based on the above considerations, the following expression was derived to calculate r_d as a function of depth and earthquake magnitude.

$$\begin{aligned} r_d &= \exp[\alpha(z) + \beta(z) \cdot M] \\ \alpha(z) &= -1.012 - 1.126 \sin\left(\frac{z}{11.73} + 5.133\right) \\ \beta(z) &= 0.106 + 0.118 \sin\left(\frac{z}{11.28} + 5.142\right) \end{aligned} \quad (\text{B-8})$$

where z is in units of m and the arguments inside the sine terms are in radians. The variations of r_d with depth for $M = 5.5, 6.5, 7.5$ and 8 calculated using equation (B-8) are presented in Figure B-22. This expression is only applicable to depths less than 30 m.

Equation (B-8) was used by Idriss and Boulanger (2004, 2008) to interpret the case histories of liquefaction/no liquefaction and to construct the liquefaction triggering correlation discussed in the main body of this report. Equation (B-8) is recommended for use in conjunction with that correlation in forward assessments of liquefaction potential at a site.

B-3.5 Expression for the 50th percentile (median) values of r_d

The range and 50th percentile (median) values of r_d , calculated for sites A1 through C2 using input motions recorded during $M \approx 7.5$ earthquakes, are presented in Figure B-23. The median values shown in figure C-23 were also used to derive an expression for r_d as a function of depth and earthquake magnitude; the resulting expression is:

$$\begin{aligned} r_d &= \exp[\alpha(z) + \beta(z) \cdot M] \\ \alpha(z) &= -1.082 - 1.196 \sin\left(\frac{z}{11.73} + 5.133\right) \\ \beta(z) &= 0.106 + 0.118 \sin\left(\frac{z}{11.28} + 5.142\right) \end{aligned} \quad (\text{B-9})$$

Note that equation (B-9) is identical to equation (B-8) except for the coefficients for the parameter $\alpha(z)$, and that again z is in units of m and the arguments inside the sine terms are in radians. This expression is also only applicable to depths less than 30 m.

The median values of r_d calculated using equation (B-9) for $M = 7.5$ provides a very good fit to the 50th-percentile values of r_d , calculated for all sites using input motions recorded during $M \approx 7.5$ earthquakes as illustrated in Figure B-24. Similar fits are obtained for $M = 6.5$ and $M = 5.5$ as shown in Figure B-25.

The variations of the median values of r_d with depth for $M = 5.5, 6.5, 7.5$ and 8 calculated using equation (B-9) are presented in Figure B-26.

B-4.0 SUMMARY

This Appendix summarizes the approach and presents the results of the analyses completed in 1996 – 1999 to derive the expressions presented in Idriss (1999) for calculating r_d as a function of depth and earthquake magnitude. These expressions were used by Idriss and Boulanger (2004, 2008) to interpret the case histories of liquefaction/no liquefaction and to construct the liquefaction triggering correlation discussed in the main body of this report. The expressions for r_d summarized in this Appendix are recommended for use in conjunction with that correlation in forward assessments of liquefaction potential at a site.

In addition, expressions relating the median values of r_d with depth and earthquake magnitude are derived and have been utilized in sensitivity analyses as described in Section 6.0 of the main report.

Table B-1
 Accelerograms used in analyses – earthquake magnitude ≈ 7.5 *

Earthquake	Magnitude, M	Recording Station
1952 Kern County	7.4	Taft
		Santa Barbara
		Pasadena
1978 Tabas	7.4	Tabas
		Daybook
1992 Landers	7.3	Barstow
		Desert Spring
		Joshua Tree
		Lucerne
		Morango Valley
1999 Chi-Chi	7.6	Yermo Fire Station
		TCU045
		TCU085
		TCU102
1999 Kocaeli	7.5	TCU105
		Gebze
		Izmit

* The two horizontal components recorded at each station were used in the analyses for a total of 34 accelerograms.

Table B-2
 Accelerograms used in analyses – earthquake magnitude $\approx 6\frac{1}{2}$ **

Earthquake	Magnitude	Station
1968 Borrego	6.6	San Onofre
1971 San Fernando	6.6	Castaic
		Griffith Park
		Lake Hughes #4
		Lake Hughes #9
		Orion
		UCLA
1976 Gazli	6.8	Karakyr
1994 Northridge	6.7	Arleta
		Castaic
		Century City
		Griffith
		Lake Hughes #4
		Lake Hughes #9
		Sylmar
		UCLA

** The two horizontal components recorded at each station were used in the analyses for a total of 32 accelerograms.

Table B-3
 Accelerograms used in analyses – earthquake magnitude $\approx 5\frac{1}{2}$ ☆☆

Earthquake	Magnitude	Station
1957 San Francisco	5.3	Golden Gate
1970 Lytle Creek	5.3	Cedar Springs
1974 Hollister		Gilroy 1
1979 Coyote Lake	5.7	Gilroy 1
		Gilroy 6
		Halls Valley
		San Juan Bautista
1986 Hollister	5.5	Sago South
		Hollister Differential Array No. 1
		Hollister Differential Array No. 3

☆☆ *The two horizontal components recorded at each station were used in the analyses for a total of 20 accelerograms.*

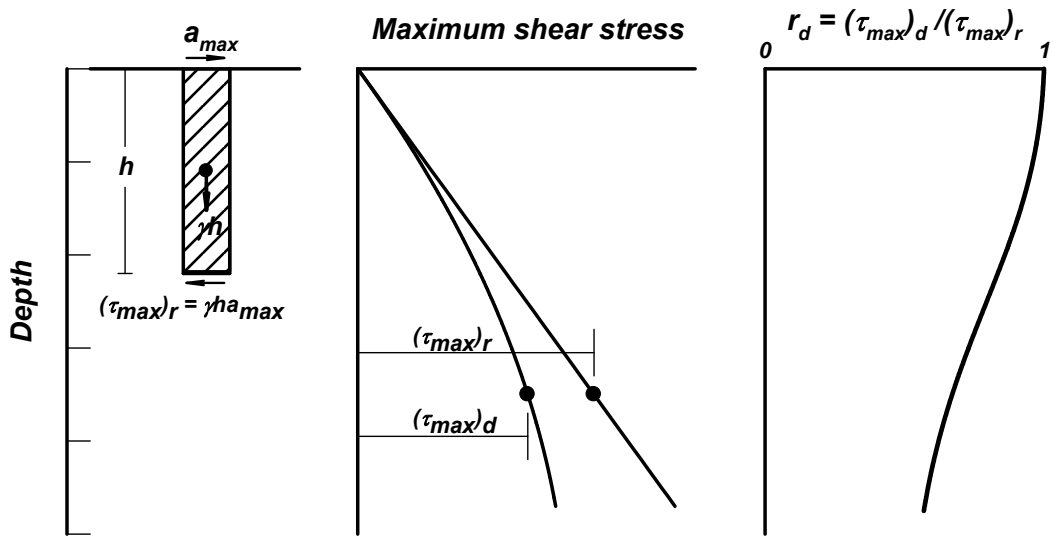


Figure B-1. Schematic for determining maximum shear stress, τ_{max} , and the stress reduction coefficient, r_d

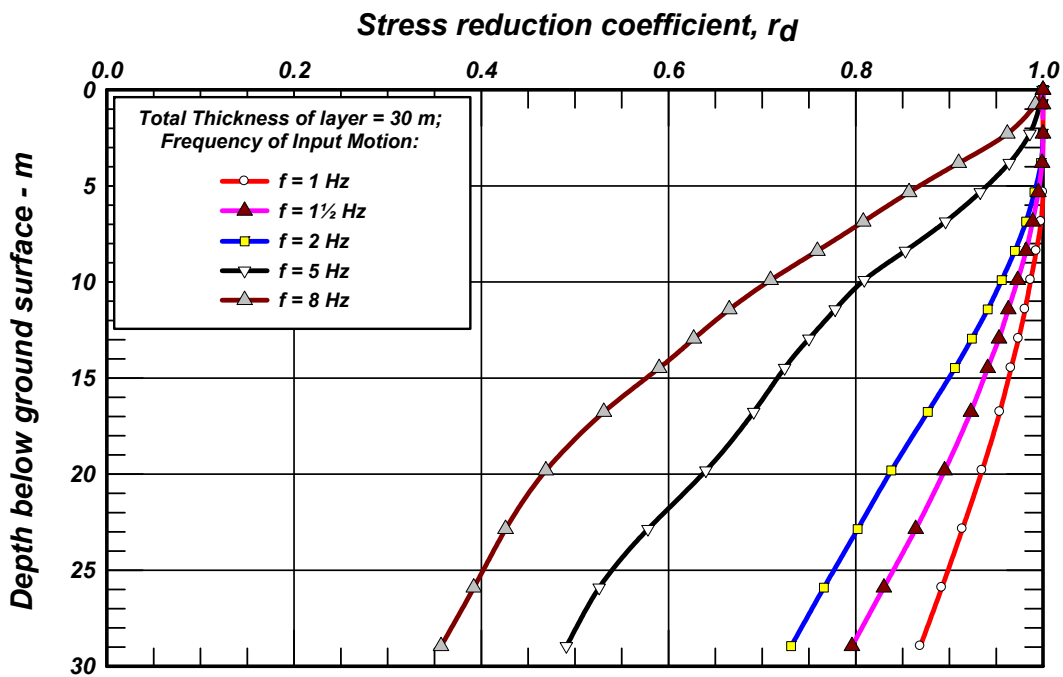


Figure B-2. Variations of the stress reduction coefficient with depth for the 30-m deep layers for various values of the frequency of input motion.

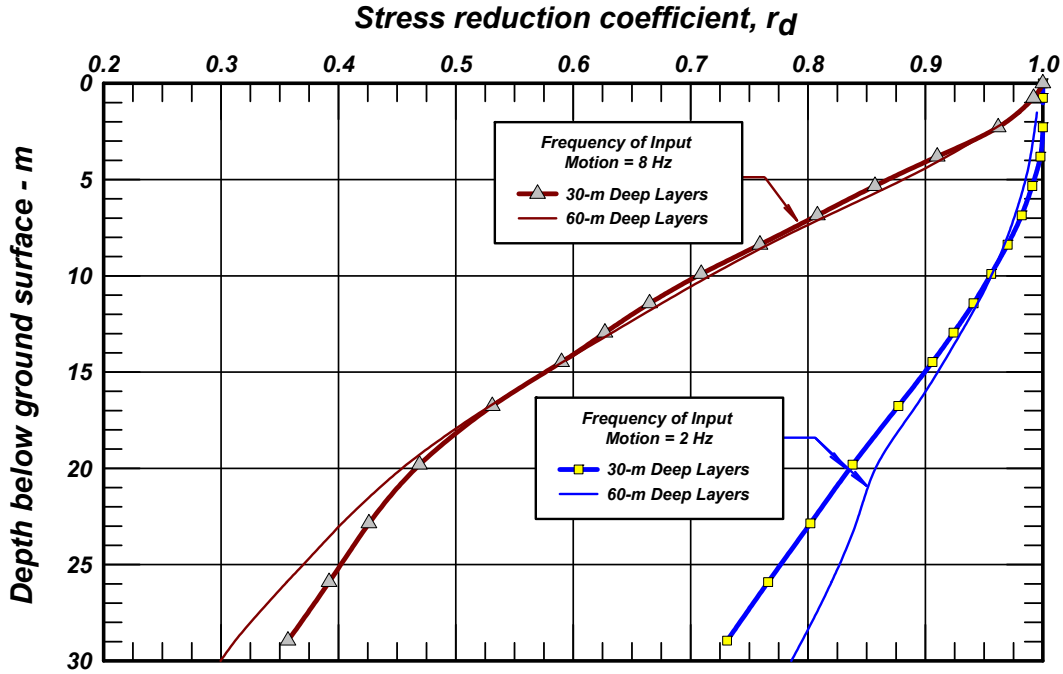


Figure B-3. Comparison of stress reduction coefficients calculated for 30-m deep layers with those calculated for 60-m deep layers using an input motion having a frequency of 2 Hz and input motion having a frequency of 8 Hz.

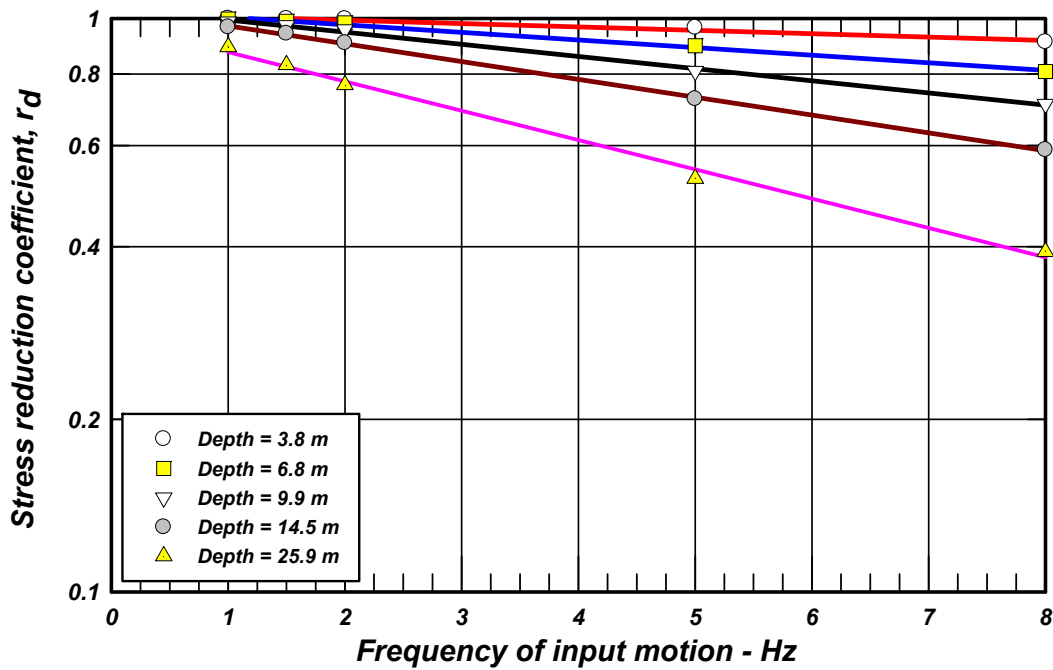


Figure B-4. Variations of stress reduction coefficient for the 30-m deep layers with frequency of input motion at various depths within the soil layer.

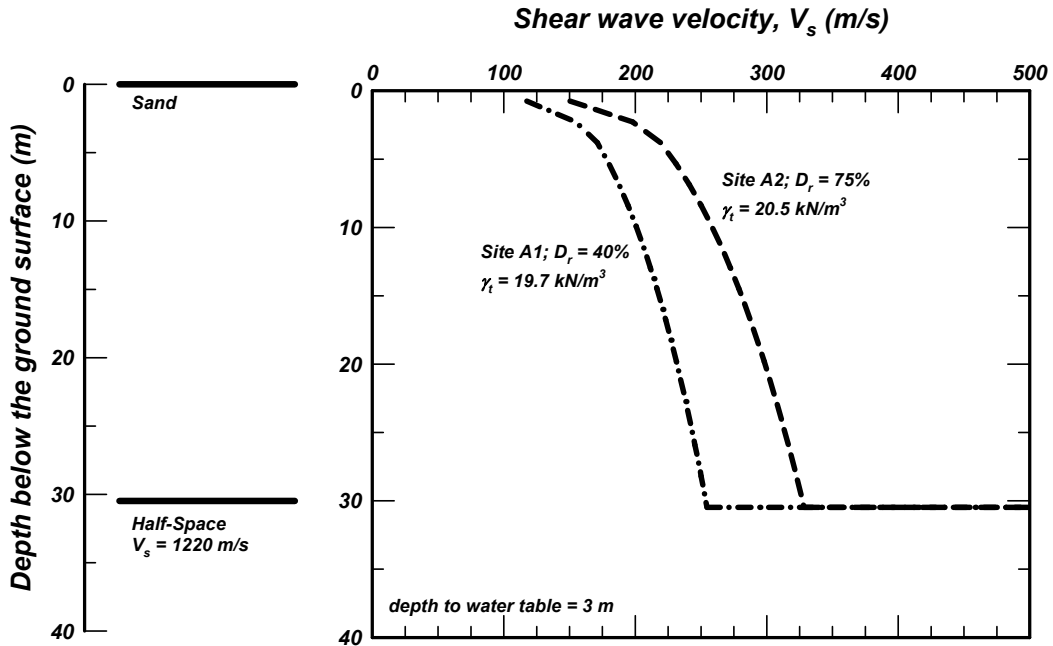


Figure B-5. Soil sites A1 and A2.

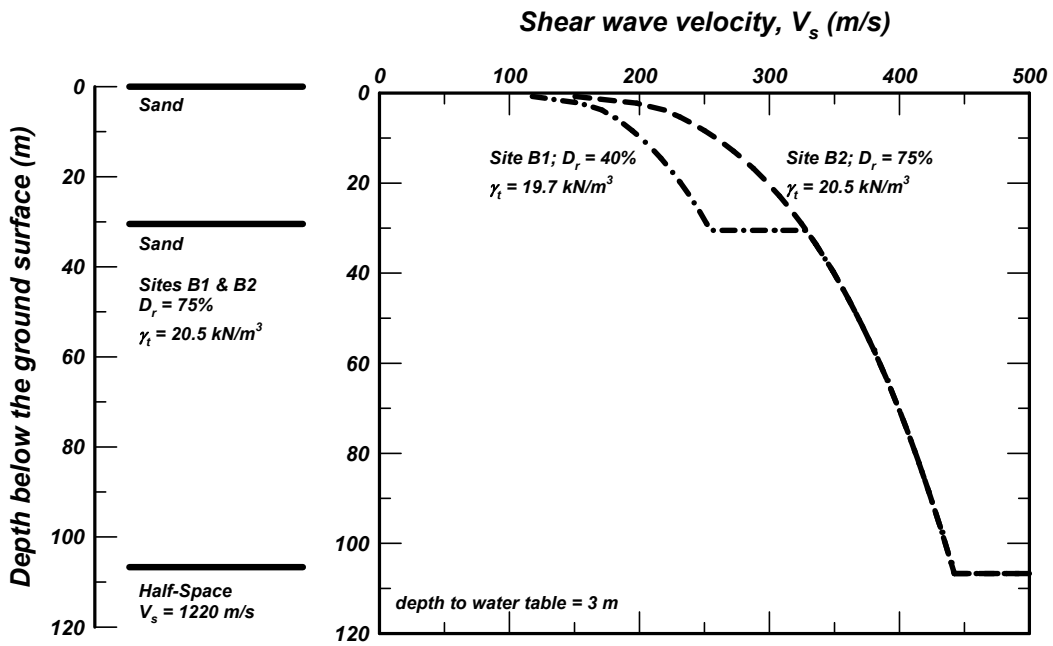


Figure B-6. Soil sites B1 and B2.

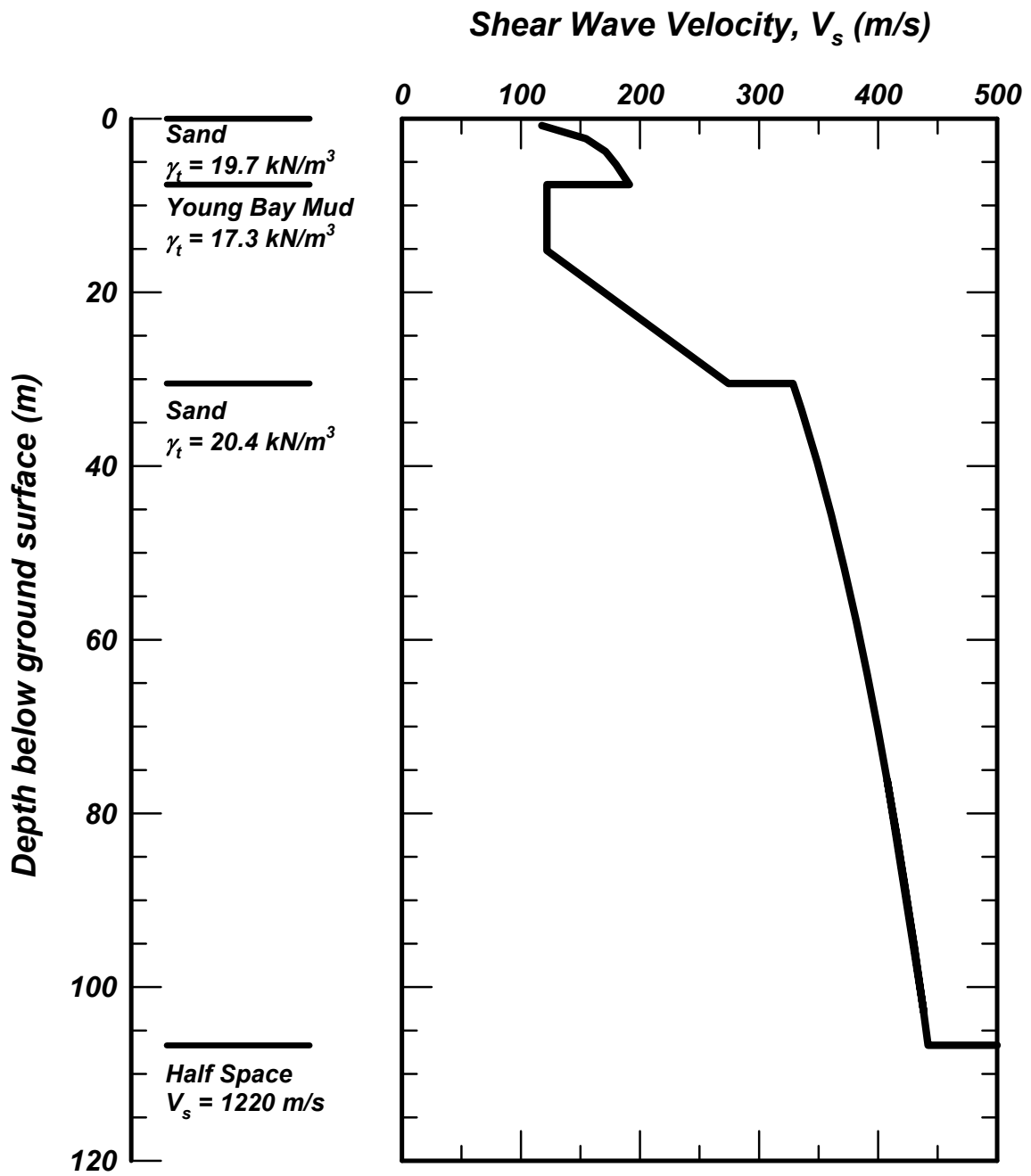


Figure B-7. Soil site C1.

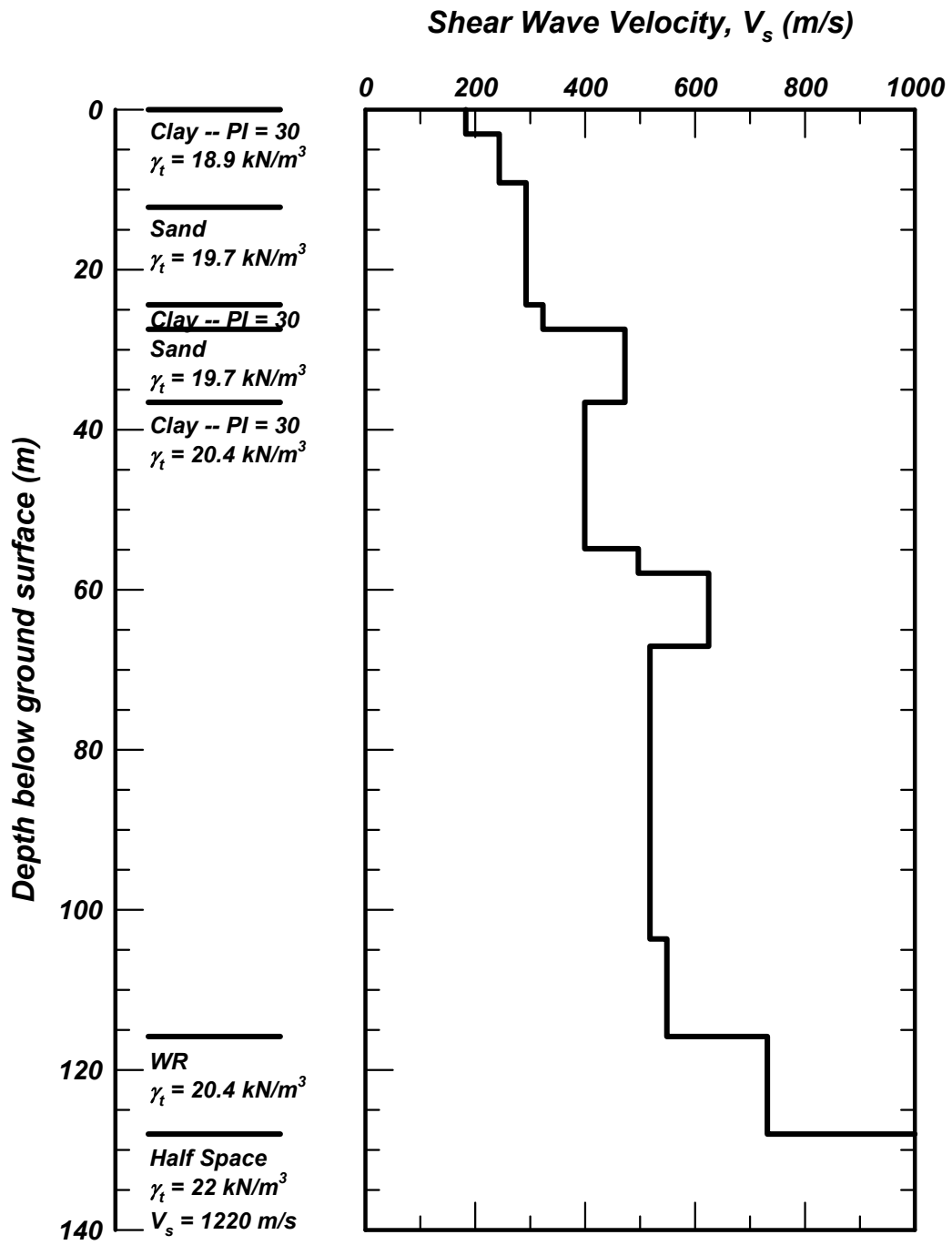


Figure B-8. Soil site C2.

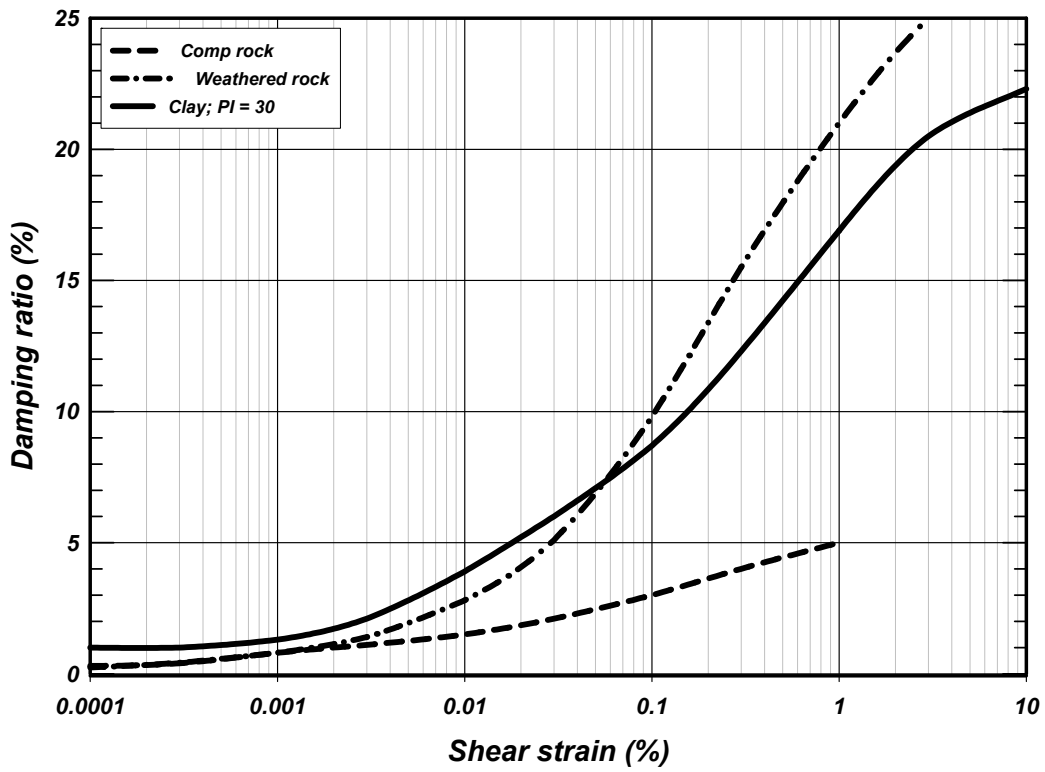
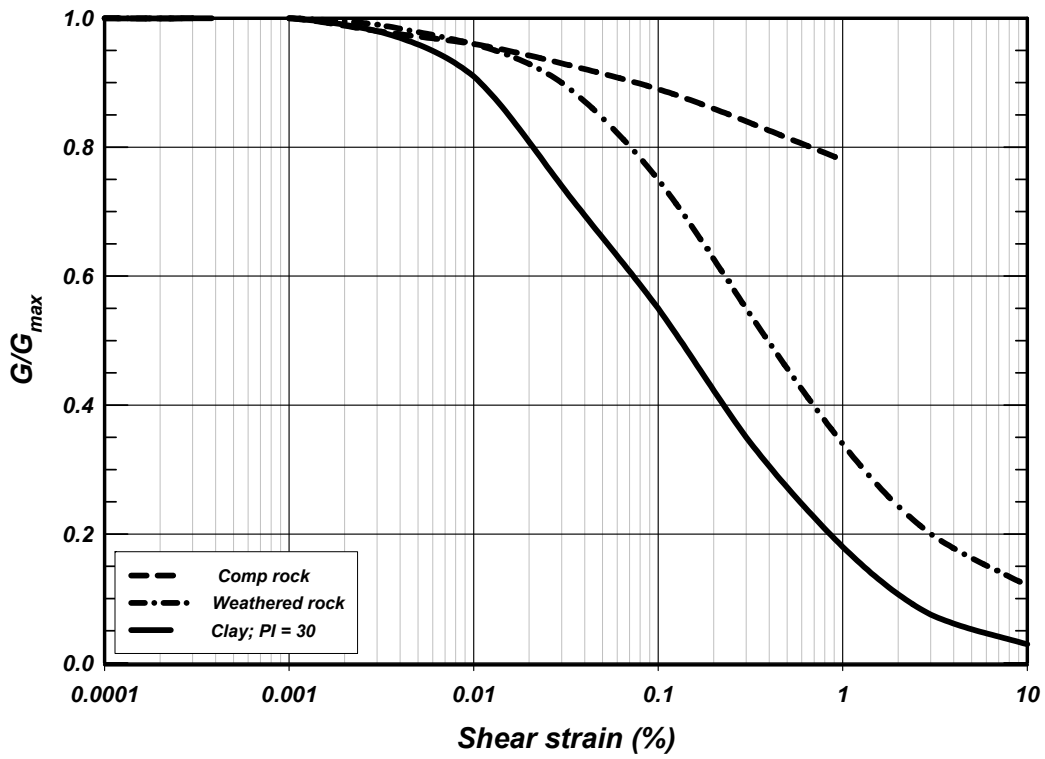


Figure B-9. Modulus reduction and damping curves used for competent rock, weathered rock and clay with PI = 30

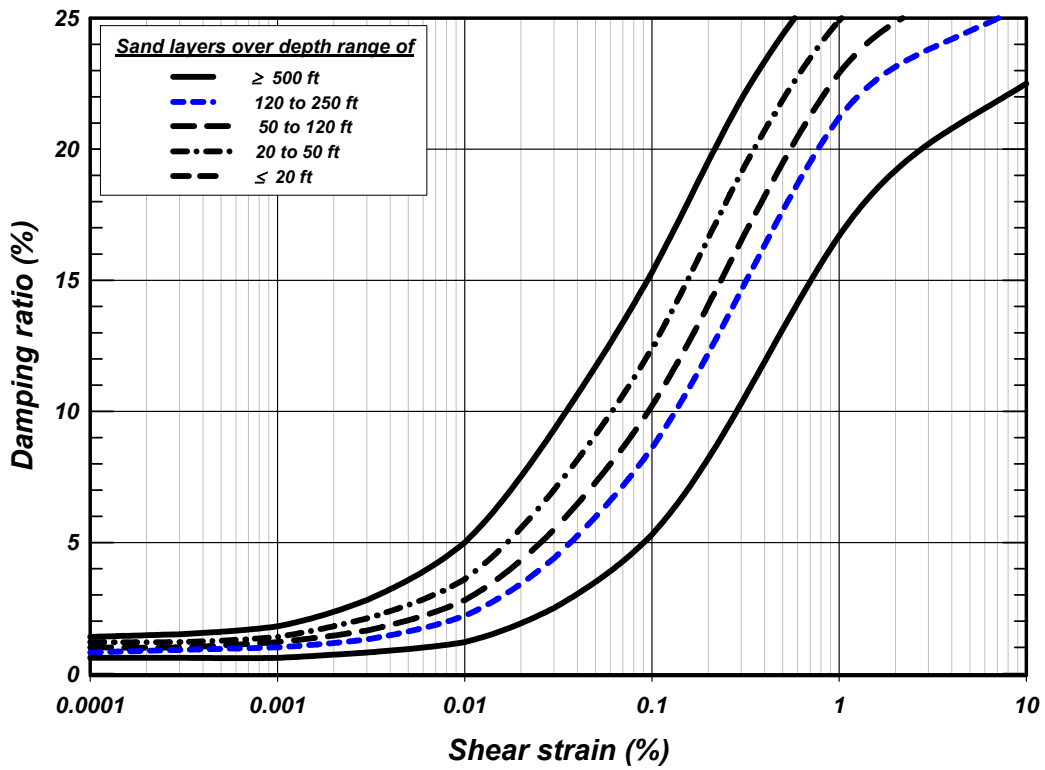
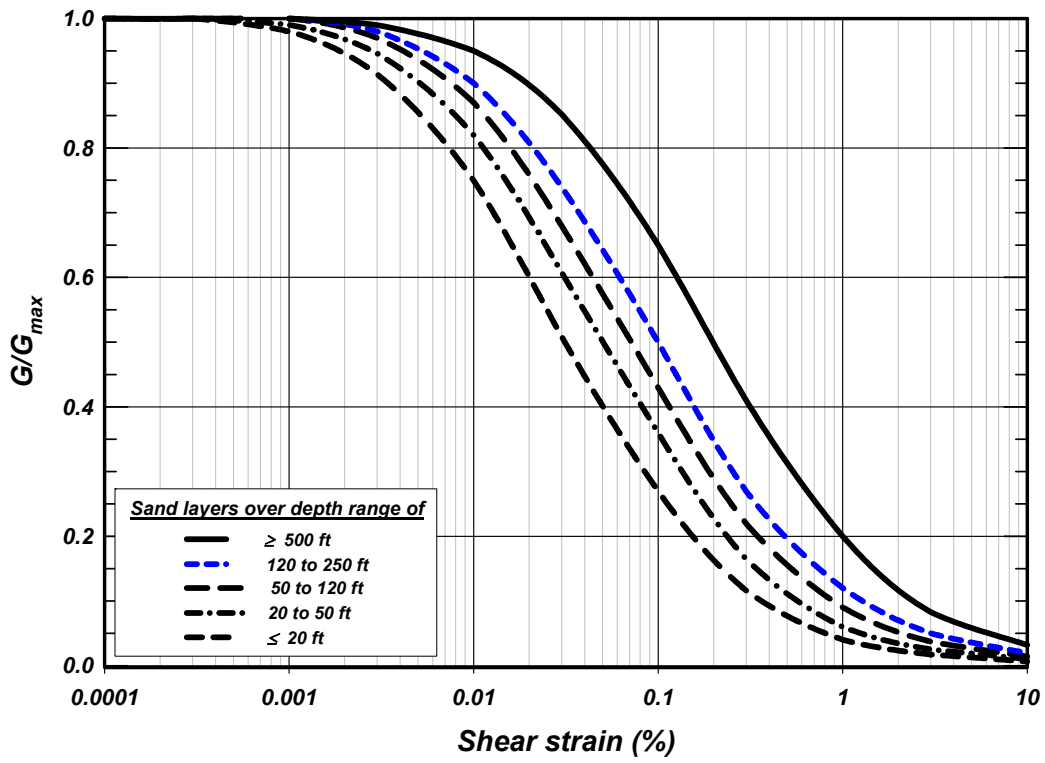


Figure B-10. Modulus reduction and damping curves used for sand layers (after EPRI, 1993)

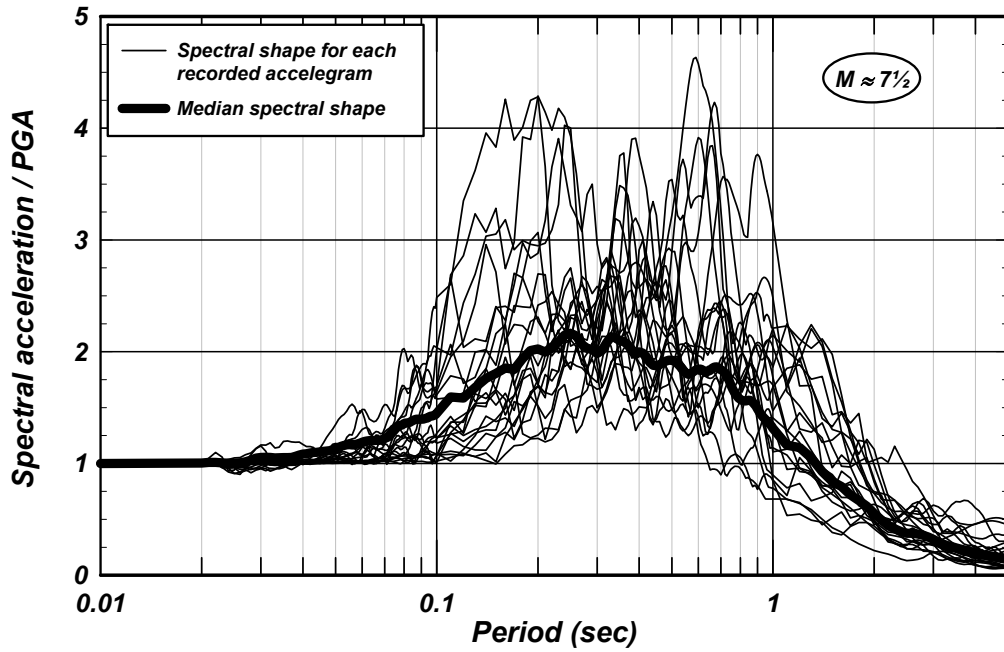


Figure B-11. Spectral shapes for accelerograms recorded during magnitude, $M \approx 7\frac{1}{2}$, earthquakes used in this study.

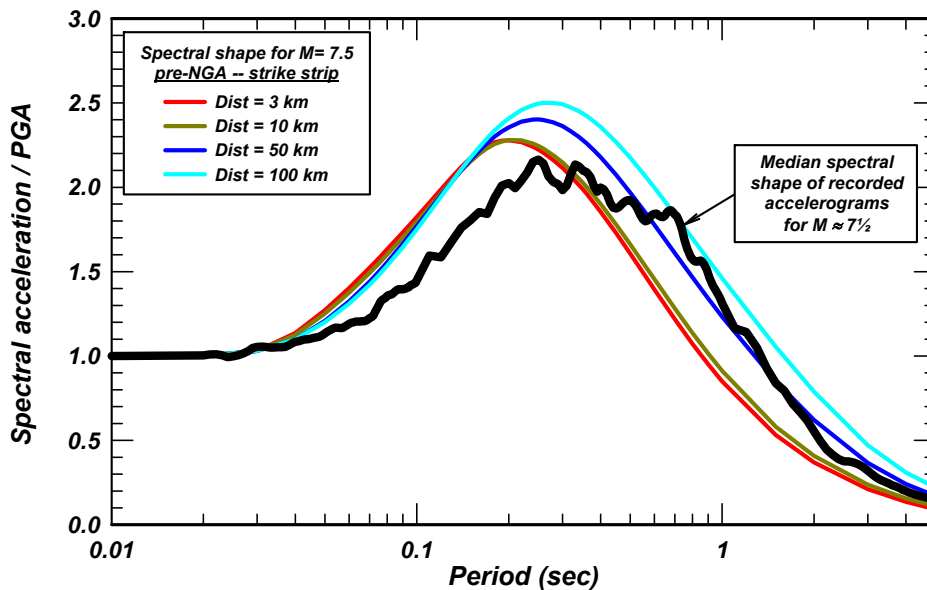


Figure B-12. Comparison of median spectral shape for recorded accelerograms, used as input rock outcrop for $M \approx 7.5$ earthquakes, with target spectral shapes for $M = 7.5$ calculated using pre-NGA attenuation relationships for a strike strip source.

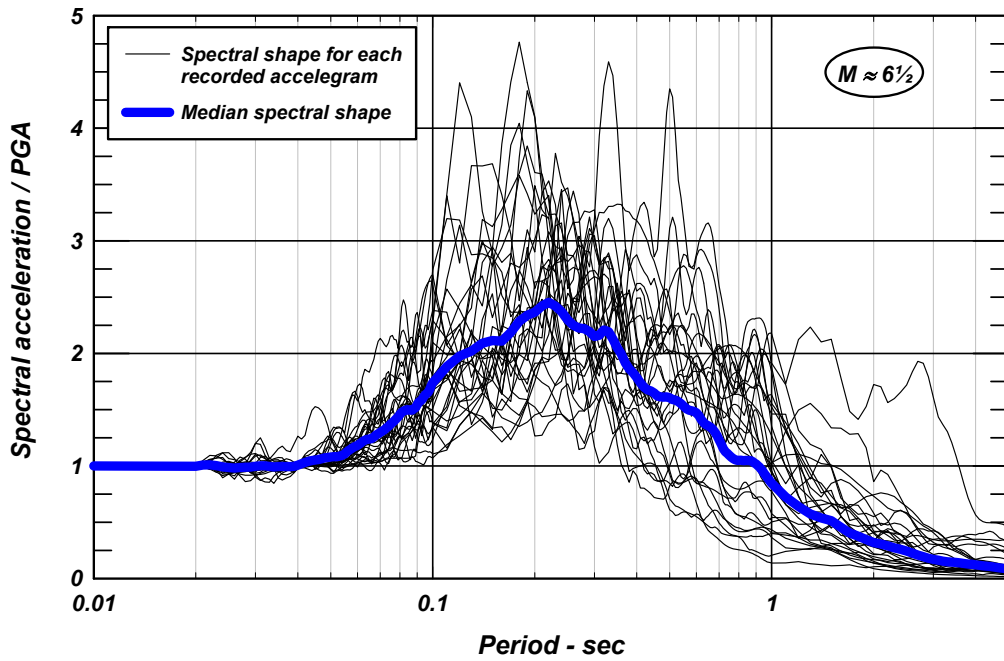


Figure B-13. Spectral shapes for accelerograms recorded during magnitude, $M \approx 6\frac{1}{2}$, earthquakes used in this study.

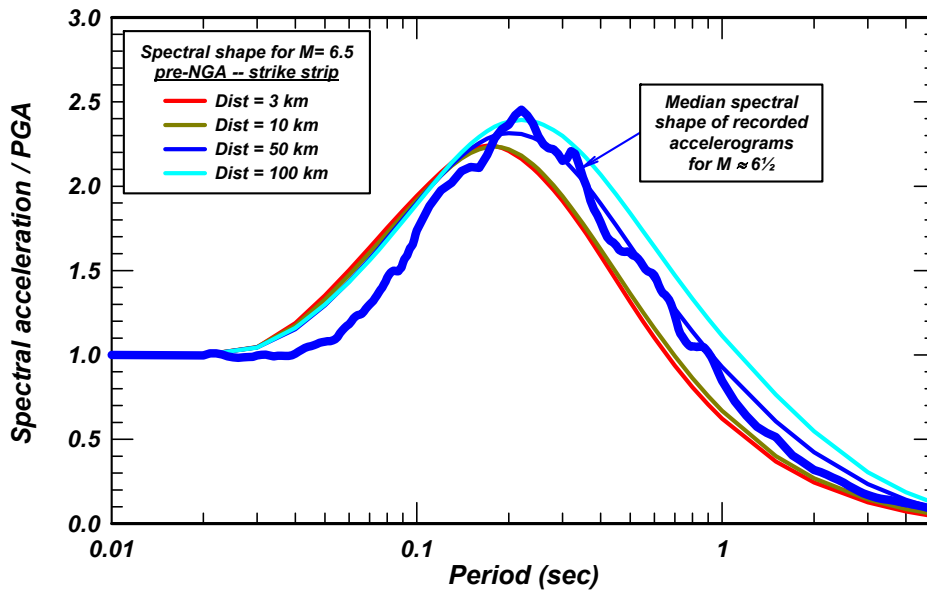


Figure B-14. Comparison of median spectral shape for recorded accelerograms, used as input rock outcrop for $M \approx 6.5$ earthquakes, with target spectral shapes for $M = 6.5$ calculated using pre-NGA attenuation relationships for a strike strip source.

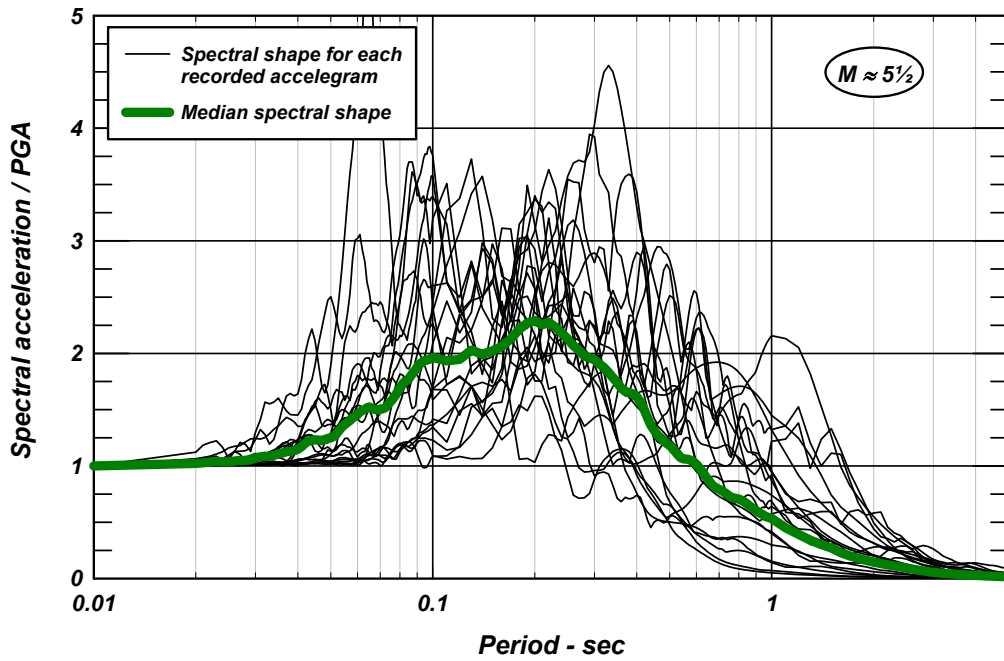


Figure B-15. Spectral shapes for accelerograms recorded during magnitude, $M \approx 5\frac{1}{2}$, earthquakes used in this study.

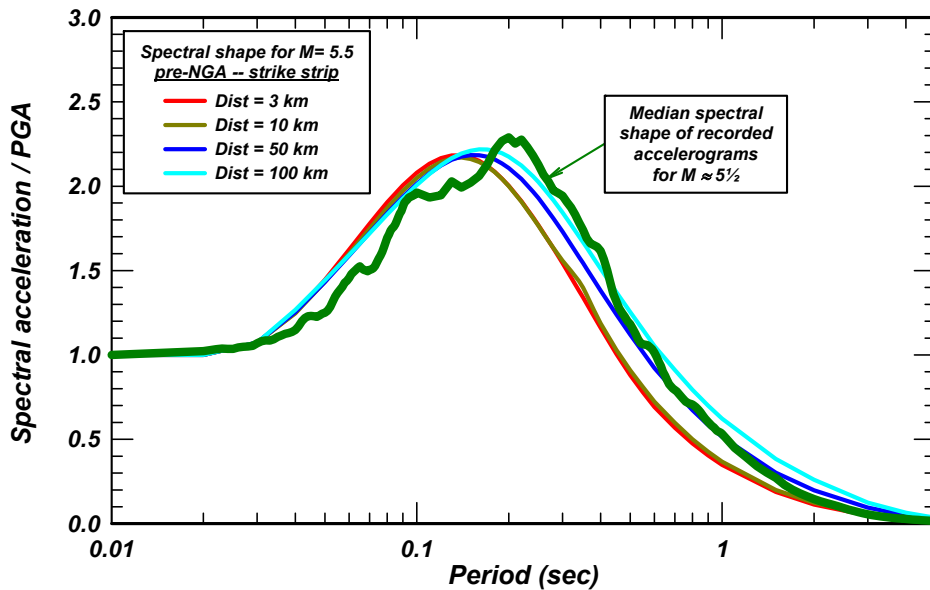


Figure B-16. Comparison of median spectral shape for recorded accelerograms, used as input rock outcrop for $M \approx 5.5$ earthquakes, with target spectral shapes for $M = 5.5$ calculated using pre-NGA attenuation relationships for a strike strip source.

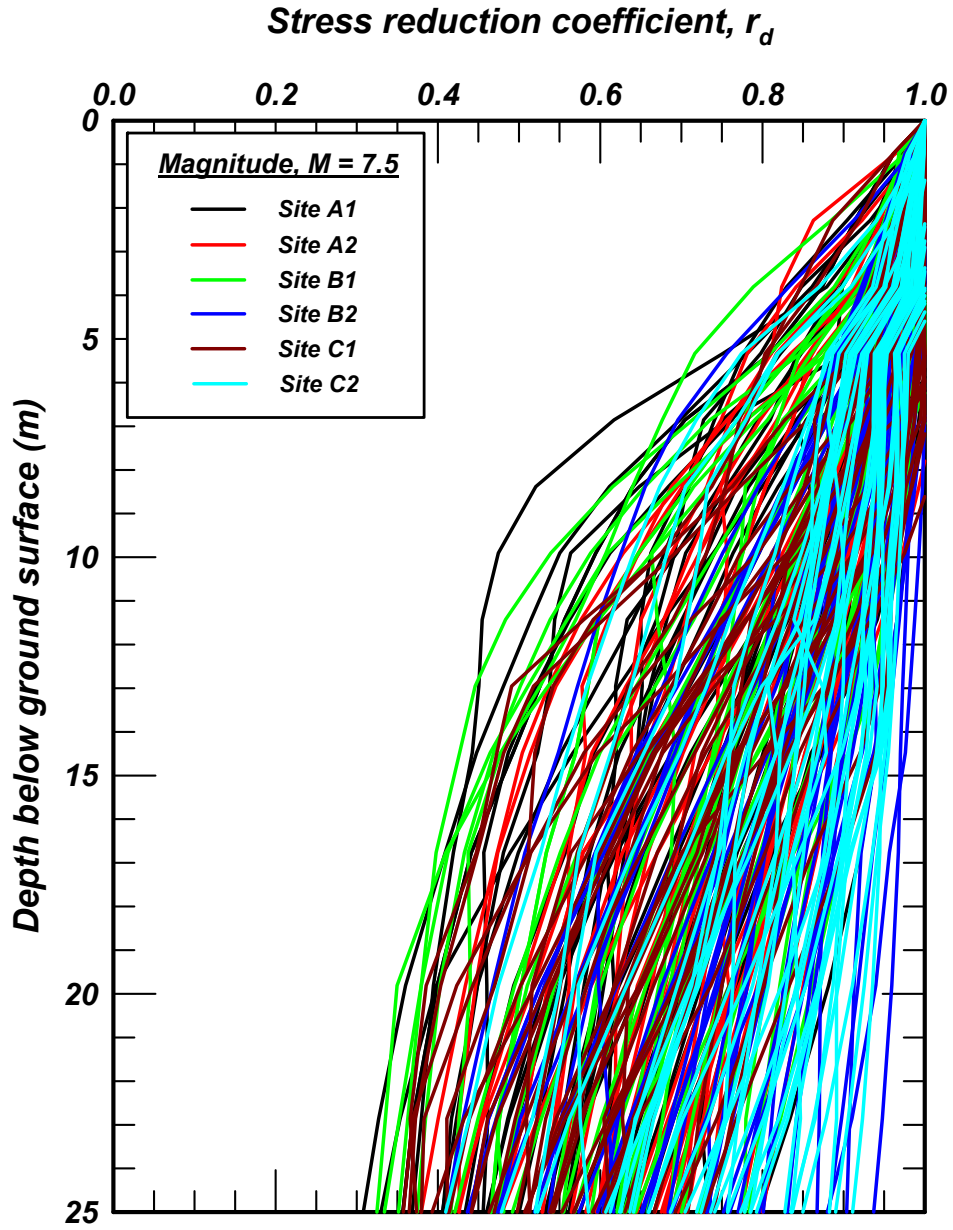


Figure B-17. Values of r_d calculated for Sites A1, A2, B1, B2, C1 and C2 using input motions recorded during $M \approx 7.5$ earthquakes.

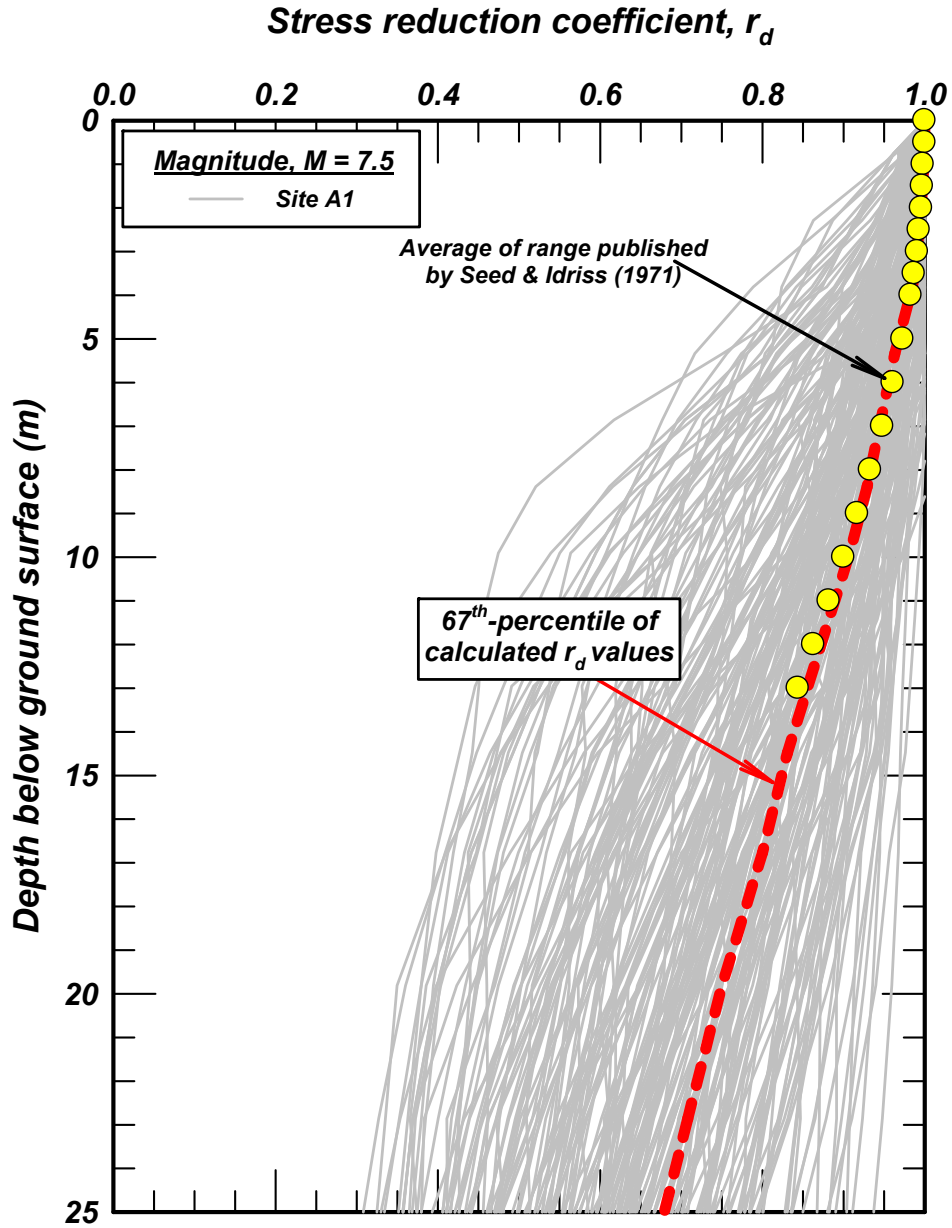


Figure B-18. Range and 67th-percentile values of r_d , calculated for all sites using input motions recorded during $M \approx 7.5$ earthquakes, and average of range published by Seed and Idriss (1971).

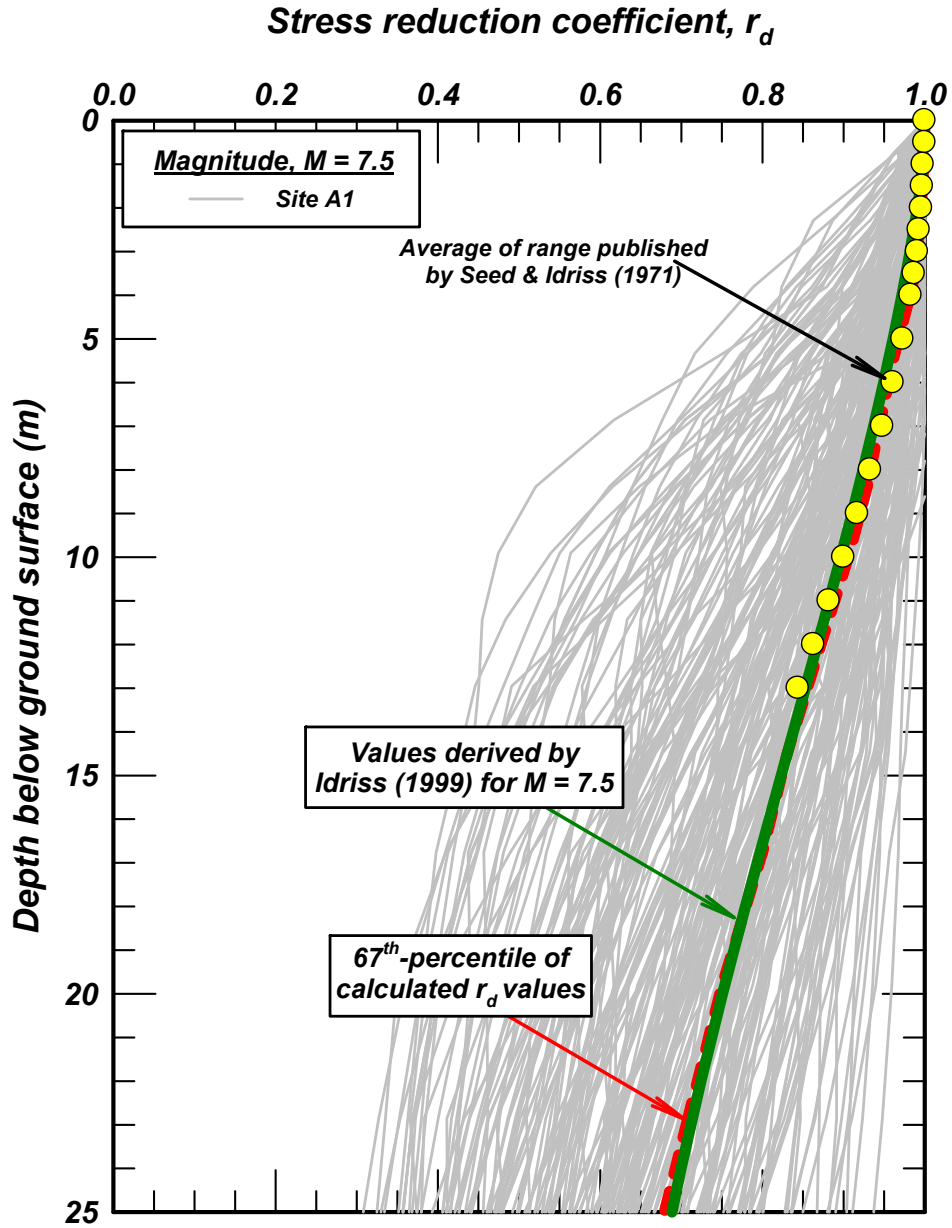


Figure B-19. Range and 67th-percentile values of r_d , calculated for all sites using input motions recorded during $M \approx 7.5$ earthquakes, average of range published by Seed and Idriss (1971), and curve derived by Idriss (1999) for $M = 7.5$.

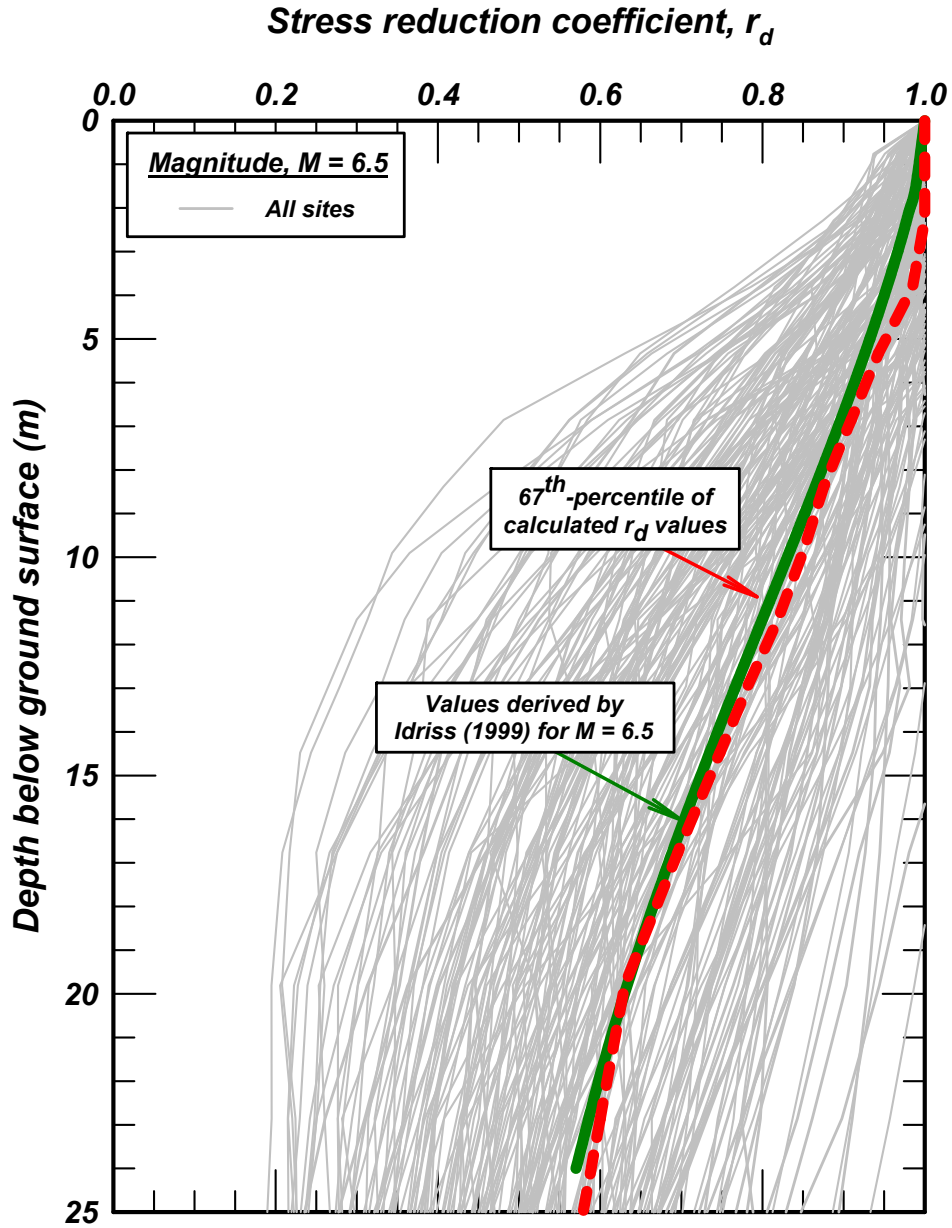


Figure B-20. Range and 67th-percentile values of r_d , calculated for all sites using input motions recorded during $M \approx 6.5$ earthquakes, and curve derived by Idriss (1999) for $M = 6.5$.

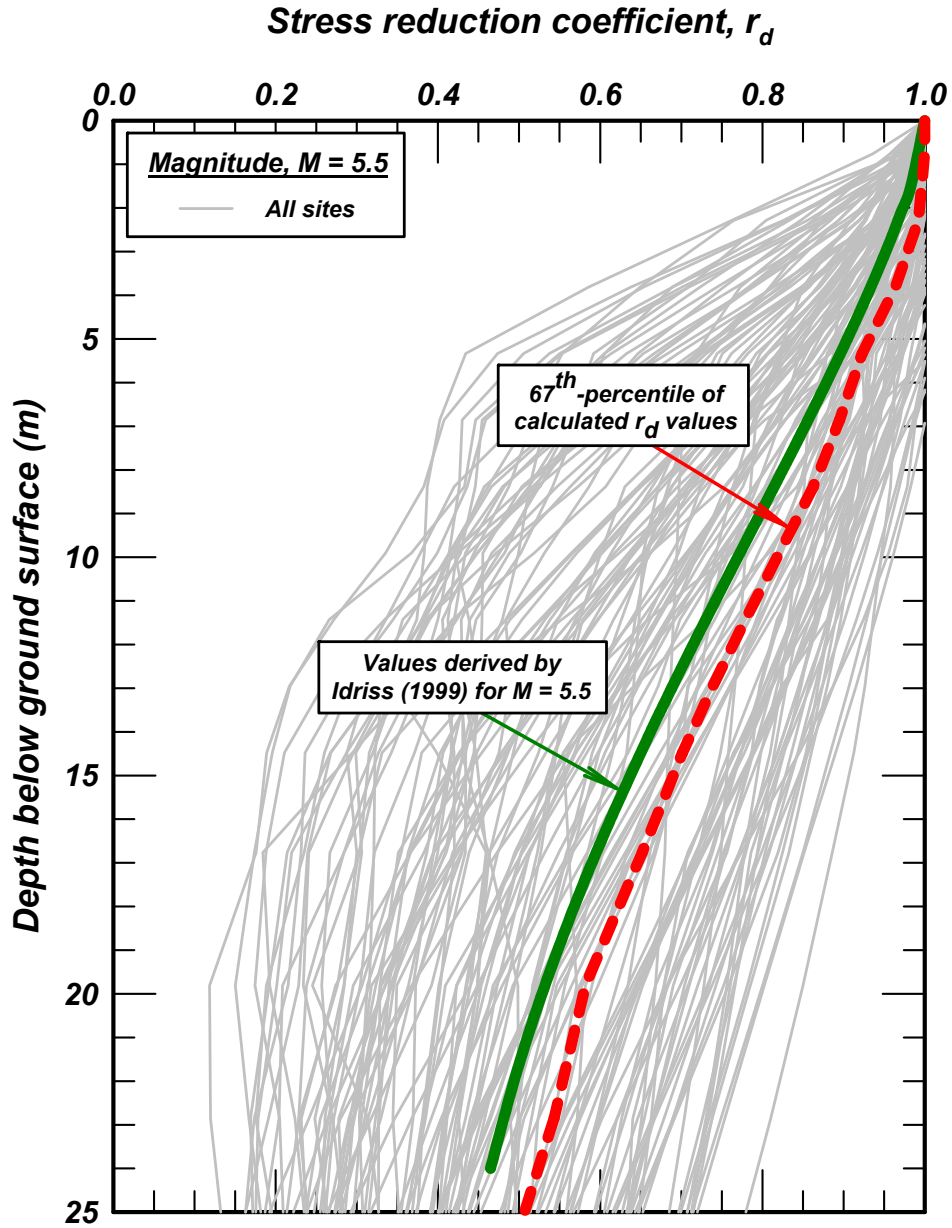


Figure B-21. Range and 67th-percentile values of r_d , calculated for all sites using input motions recorded during $M \approx 5.5$ earthquakes, and curve derived by Idriss (1999) for $M = 5.5$.

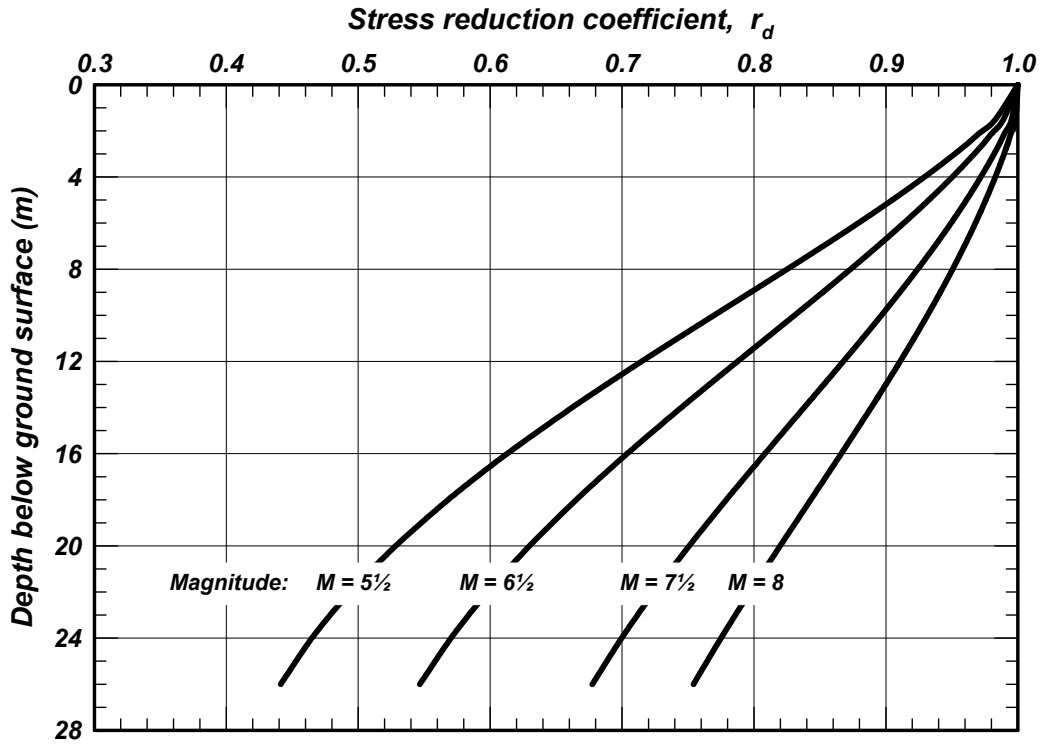


Figure B-22. Values of r_d , calculated for $M = 5\frac{1}{2}$, $6\frac{1}{2}$, $7\frac{1}{2}$ and 8 using equations derived by Idriss (1999), and used in the interpretations of liquefaction/no liquefaction case histories by Idriss and Boulanger (2004, 2008).

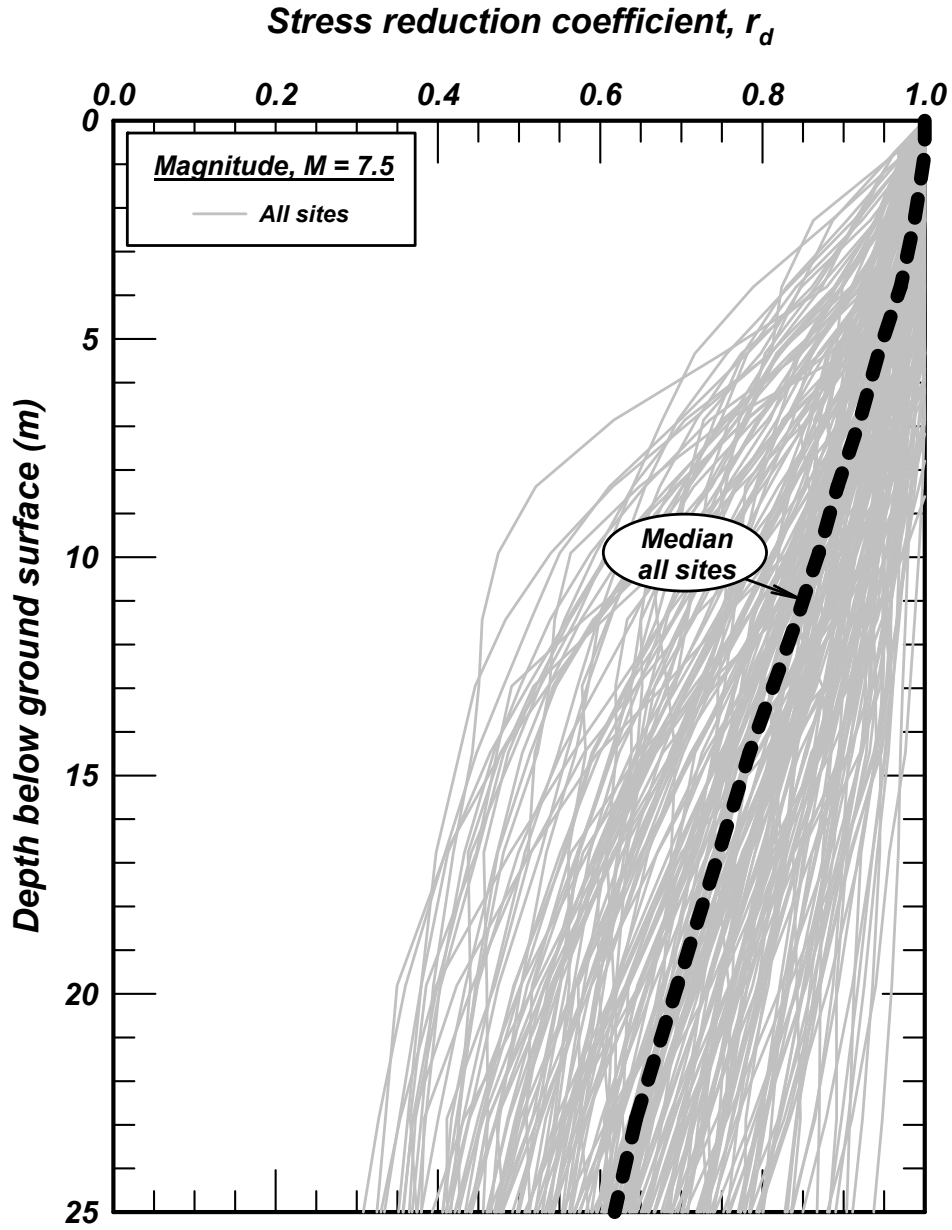


Figure B-23. Range and median values of r_d , calculated for all sites using input motions recorded during $M \approx 7.5$ earthquakes.

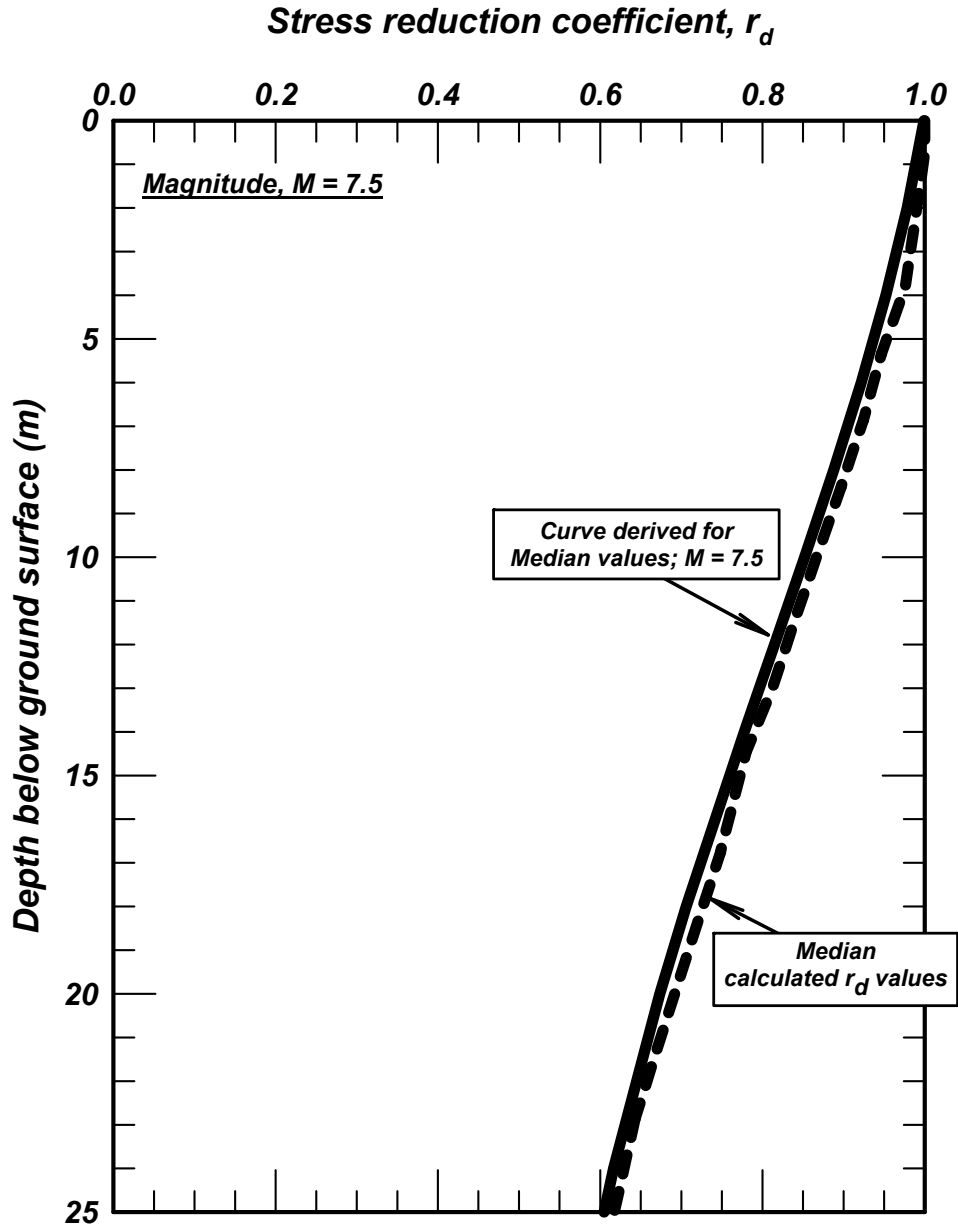


Figure B-24. Median values of r_d , calculated for all sites using input motions recorded during $M \approx 7.5$ earthquakes, and curve derived to fit these median values.

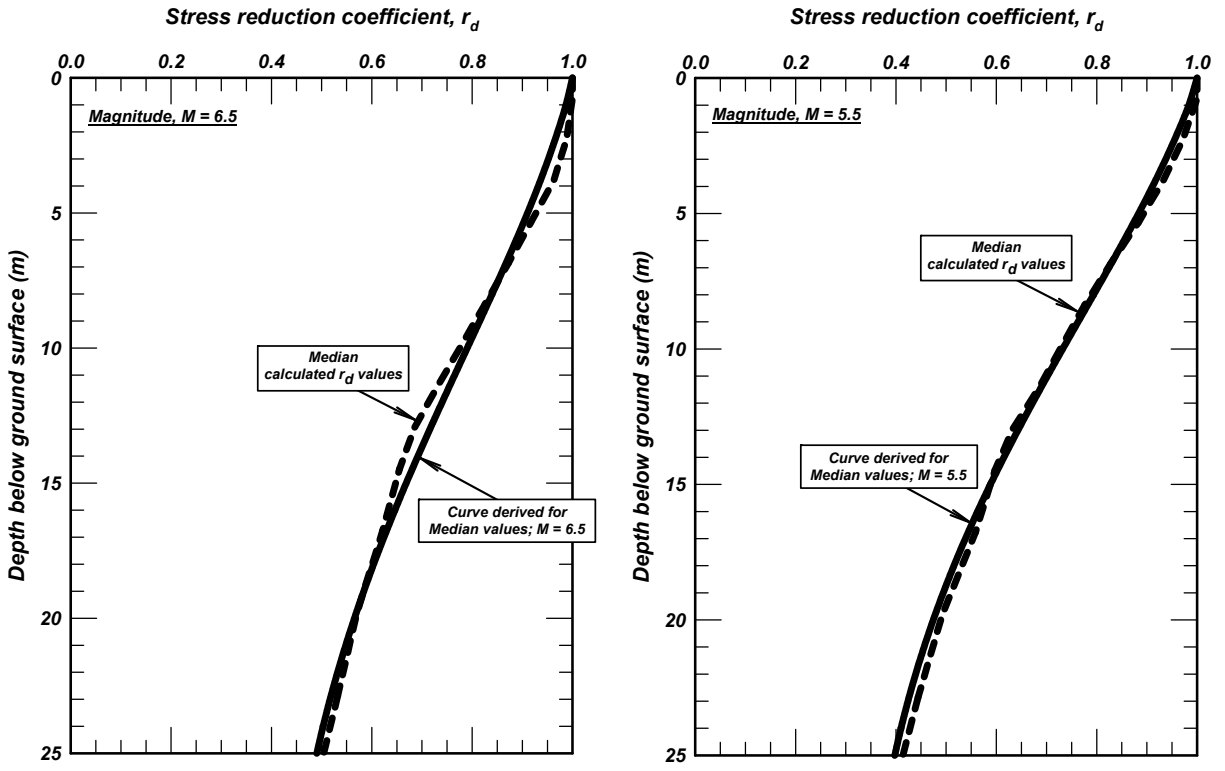


Figure B-25. Median values of r_d , calculated for all sites using input motions recorded during $M \approx 6.5$ and $M \approx 5.5$ earthquakes, and curves derived to fit these median values.

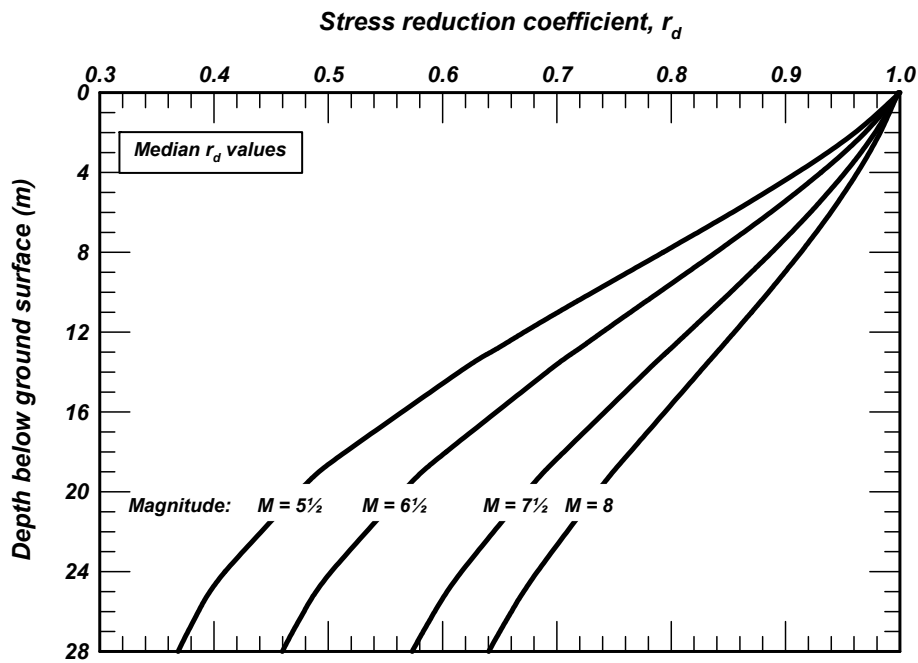


Figure B-26. Median values of r_d , calculated for $M = 5\frac{1}{2}$, $6\frac{1}{2}$, $7\frac{1}{2}$ and 8 using equations derived in this Appendix.

APPENDIX C:
COMPUTATIONS OF REPRESENTATIVE $(N_1)_{60CS}$ VALUES

Earthquake & site	Avg depth (m)	Depth GWT (m)	σ_v (kPa)	σ'_v (kPa)	(N_m)	$(N_1)_{60}$	C_B	C_E	C_N	C_R	C_S	FC (%)	$(N_1)_{60cs}$	$\Delta(N_1)_{60cs}$	γ_{tot} above water table	γ_{tot} below water table	Primary source of data
-------------------	---------------	---------------	------------------	-------------------	---------	--------------	-------	-------	-------	-------	-------	--------	----------------	----------------------	----------------------------------	----------------------------------	------------------------

1976 M=7.6 Tangshan earthquake - July 27

<u>Coastal Region</u>	3.0	1.1	58	39	7	9.7	1	1.0	1.63	0.85	1	12	11.8		18.9	19.6	Shengcong et al (1983), Seed et al (1984), Cetin et al (2000)
	4.0	1.1	78	49	8	9.9	1	1.0	1.45	0.85	1	12	12.0		18.9	19.6	
	5.0	1.1	97	59	13	15.8	1	1.0	1.28	0.95	1	12	17.9		18.9	19.6	
	6.0	1.1	117	69	10	11.5	1	1.0	1.21	0.95	1	12	13.6		18.9	19.6	
Averages =	4.5				9.5	11.7							12.0	13.8			

Compute representative values given the above average $(N_1)_{60cs}$:

4.5	1.1	87	54	9.0	11.7	1	1.0	1.37	0.95	1	12	13.8	2.1	18.9	19.6
-----	-----	----	----	-----	------	---	-----	------	------	---	----	------	-----	------	------

Differ = -5%

1977 M=7.4 Argentina - Nov 23

<u>San Juan B-3</u>	11.1	6.7	199	156	13	7.6	1	0.8	0.78	1	1	5	7.6		17.3	18.9	Idriss et al (1979), Seed et al. (1984)
---------------------	------	-----	-----	-----	----	-----	---	-----	------	---	---	---	-----	--	------	------	---

Note: Seed et al. (1984) reported N=12 at 39 ft, but original boring shows a single N=13 at 36.5 feet in sand.

1978 M=7.7 Miyagiken-Oki earthquake - June 12

<u>Ishinomaki - 2</u>	2.0	1.4	36	30	4	5.6	1	1.09	1.70	0.75	1	10	6.7		17.3	19.7	Ishihara et al (1980), Seed et al (1984), Cetin et al (2000)
	3.0	1.4	56	40	4	5.9	1	1.09	1.70	0.8	1	10	7.1		17.3	19.7	
	4.0	1.4	75	50	4	5.6	1	1.09	1.51	0.85	1	10	6.8		17.3	19.7	
	5.0	1.4	95	60	4	5.1	1	1.09	1.37	0.85	1	10	6.2		17.3	19.7	
Averages =	3.5				4.0	5.5							10.0	6.7			

Compute representative values given the above average $(N_1)_{60cs}$:

3.5	1.4	66	45	3.7	5.5	1	1.09	1.61	0.85	1	10	6.7	1.1	17.3	19.7
-----	-----	----	----	-----	-----	---	------	------	------	---	----	-----	-----	------	------

Differ = -7%

Earthquake & site	Avg depth (m)	Depth GW (m)	σ_v (kPa)	σ'_v (kPa)	(N_m)	$(N_1)_{60}$	C_B	C_E	C_N	C_R	C_S	FC (%)	$(N_1)_{60cs}$	$\Delta(N_1)_{60cs}$	γ_{tot} above water table	γ_{tot} below water table	Primary source of data
<u>Ishinomaki - 4</u>	2.0	1.4	37	31	16	23.3	1	1.21	1.60	0.75	1	10	24.4		18.1	20.0	Ishihara et al (1980), Seed et al (1984), Cetin et al (2000)
	3.0	1.4	57	42	15	21.1	1	1.21	1.45	0.8	1	10	22.3		18.1	20.0	
	4.0	1.4	77	52	16	21.8	1	1.21	1.32	0.85	1	10	22.9		18.1	20.0	
	5.0	1.4	97	62	15	19.1	1	1.21	1.24	0.85	1	10	20.3		18.1	20.0	
	6.0	1.4	117	72	15	20.0	1	1.21	1.16	0.95	1	10	21.1		18.1	20.0	
	7.0	1.4	137	82	16	20.1	1	1.21	1.09	0.95	1	10	21.2		18.1	20.0	
Averages =	4.5				15.5	20.9						10.0	22.0				
Compute representative values given the above average $(N_1)_{60cs}$:																	
	4.5	1.4	87	57	14.2	20.9	1	1.21	1.28	0.95	1	10	22.0	1.1	18.1	20.0	
Differ = -8%																	
<u>Nakamura Dyke N-4</u>	1.3	0.5	24	16	5	6.8	1	1.00	1.70	0.8	1	5	6.8		18.1	18.9	Iwasaki (1986), Tohno & Yasuda (1981), Seed et al (1984), Cetin et al
	2.3	0.5	43	25	3	4.3	1	1.00	1.70	0.85	1	5	4.3		18.1	18.9	
	3.3	0.5	62	35	5	7.2	1	1.00	1.70	0.85	1	5	7.2		18.1	18.9	
	4.3	0.5	81	44	6	9.1	1	1.00	1.59	0.95	1	5	9.1		18.1	18.9	
Averages =	2.8				4.8	6.9						5.0	6.9				
Compute representative values given the above average $(N_1)_{60cs}$:																	
	2.8	0.5	53	30	4.7	6.9	1	1.00	1.70	0.85	1	5	6.9	0.0	18.1	18.9	
Differ = 0%																	

Earthquake & site	Avg depth (m)	Depth GWT (m)	σ_v (kPa)	σ'_v (kPa)	(N_m)	$(N_1)_{60}$	C_B	C_E	C_N	C_R	C_S	FC (%)	$(N_1)_{60cs}$	$\Delta(N_1)_{60cs}$	γ_{tot} above water table	γ_{tot} below water table	Primary source of data	
<u>Yuriage Br 2</u>	2.0	1.2	36	29	10	14.3	1	1.12	1.70	0.75	1	7	14.4		17.3	19.7	Iwasaki et al (1978), Tohno & Yasuda (1981),	
	3.0	1.2	56	39	13	18.1	1	1.12	1.55	0.8	1	7	18.2		17.3	19.7		
	4.0	1.2	76	49	20	25.5	1	1.12	1.34	0.85	1	7	25.6		17.3	19.7		
Averages =	2.5					11.5	16.2											
Compute representative values given the above average $(N_1)_{60cs}$:																		
	2.5	1.2	46	34	10.1	16.2	1	1.12	1.68	0.85	1	7	16.3	0.1	17.3	19.7		
Differ = -12%																		
<i>1979 ML=6.5 Imperial Valley earthquake - Oct 15</i>																		
<u>Heber Road - Unit A1</u>	2.7	1.8	49	40	29	36.6	1	1.13	1.32	0.85	1	17	40.5		17.3	19.7	Bennett et al (1981), Youd & Bennett (1983), Seed et al (1984), Cetin et al (2000)	
	4.0	1.8	74	53	36	41.5	1	1.13	1.20	0.85	1	10	42.7		17.3	19.7		
	2.1	1.8	37	34	28	35.8	1	1.13	1.41	0.8	1	10	36.9		17.3	19.7		
Averages =	2.9					31.0	38.0											
Compute representative values given the above average $(N_1)_{60cs}$:																		
	2.9	1.8	53	42	30.4	37.8	1	1.13	1.30	0.85	1	12	40.0	2.2	17.3	19.7		
Differ = -2%																		
<u>Radio Tower B1</u>	3.4	2.1	62	50	2	2.9	1	1.13	1.49	0.85	1	64	8.5		18.1	18.9	Bennett et al (1984), Seed et al (1984), Cetin et al (2000)	
	5.1	2.1	95	66	7	9.3	1	1.13	1.24	0.95	1	23	14.2		18.1	18.9		
Averages =	3.4					2.0	2.9											
Compute representative values given the above average $(N_1)_{60cs}$:																		
	3.4	2.1	62	50	2.0	2.9	1	1.13	1.49	0.85	1	64	8.5	5.6	18.1	18.9		
Differ = 0%																		

Earthquake & site	Avg depth (m)	Depth GWT (m)	σ_v (kPa)	σ'_v (kPa)	(N_m)	$(N_1)_{60}$	C_B	C_E	C_N	C_R	C_S	FC (%)	$(N_1)_{60cs}$	$\Delta(N_1)_{60cs}$	γ_{tot} above water table	γ_{tot} below water table	Primary source of data
-------------------	---------------	---------------	------------------	-------------------	---------	--------------	-------	-------	-------	-------	-------	--------	----------------	----------------------	----------------------------------	----------------------------------	------------------------

1983 M=6.8 Nihonkai-Chubu earthquake - June 21

<u>Takeda Elementary Sch.</u>	3.3	0.35	62	33	8	14.1	1	1.22	1.70	0.85	1	0	14.1		17.3	18.9	Yasuda & Tohno
	4.3	0.35	81	42	7	12.7	1	1.22	1.57	0.95	1	0	12.7		17.3	18.9	(1988), Cetin et al
	5.3	0.35	100	51	8	13.1	1	1.22	1.41	0.95	1	0	13.1		17.3	18.9	(2000)
Averages =	4.3				7.7	13.3						0.0	13.3				

Compute representative values given the above average $(N_1)_{60cs}$:

4.3	0.35	81	42	7.4	13.3	1	1.22	1.56	0.95	1	0	13.3	0.0	17.3	18.9
-----	------	----	----	-----	------	---	------	------	------	---	---	------	-----	------	------

Differ = -4%

1987 M=6.2 & M=6.5 Superstition Hills earthquakes - 01 and 02 - Nov 24

<u>Wildlife B</u>	2.3	1.2	43	32	4	6.1	1	1.13	1.70	0.8	1	69	11.7	5Ng	18.5	19.1	Holzer (USGS personal communication), Cetin et al (2000)
	3.0	1.2	57	39	6	9.2	1	1.13	1.59	0.85	1	33	14.6	2Ng2	18.5	19.1	
	3.0	1.2	57	39	5	7.8	1	1.13	1.63	0.85	1	20	12.3	5Ng	18.5	19.1	
	3.4	1.2	63	42	3	4.6	1	1.13	1.60	0.85	1	33	10.1	1Ns	18.5	19.1	
	3.4	1.2	63	42	5	7.6	1	1.13	1.58	0.85	1	17	11.5	2Ng1	18.5	19.1	
	3.4	1.2	63	42	10	14.2	1	1.13	1.48	0.85	1	25	19.3	3Ns	18.5	19.1	
	3.7	1.2	69	45	6	8.6	1	1.13	1.49	0.85	1	33	14.1	2Ng3	18.5	19.1	
	3.8	1.2	72	46	13	17.4	1	1.13	1.39	0.85	1	20	21.9	5Ng	18.5	19.1	
	4.3	1.2	81	51	5	6.9	1	1.13	1.43	0.85	1	33	12.3	1Ns	18.5	19.1	
	4.3	1.2	81	51	11	14.4	1	1.13	1.37	0.85	1	20	18.9	2Ng1	18.5	19.1	
	4.3	1.2	81	51	7	9.4	1	1.13	1.40	0.85	1	33	14.9	2Ng2	18.5	19.1	
	4.3	1.2	81	51	9	11.9	1	1.13	1.38	0.85	1	25	17.0	3Ns	18.5	19.1	
	4.6	1.2	87	54	10	14.3	1	1.13	1.33	0.95	1	20	18.8	5Ng	18.5	19.1	
	4.9	1.2	92	56	4	5.8	1	1.13	1.36	0.95	1	33	11.3	2Ng3	18.5	19.1	
	5.2	1.2	98	59	4	5.7	1	1.13	1.33	0.95	1	33	11.2	1Ns	18.5	19.1	
	5.2	1.2	98	59	17	22.4	1	1.13	1.23	0.95	1	25	27.5	3Ns	18.5	19.1	
	5.3	1.2	101	61	6	8.3	1	1.13	1.29	0.95	1	33	13.8	5Ng	18.5	19.1	
	5.5	1.2	104	62	10	13.4	1	1.13	1.25	0.95	1	33	18.9	2Ng2	18.5	19.1	
	6.1	1.2	116	68	9	11.7	1	1.13	1.21	0.95	1	33	17.1	1Ns	18.5	19.1	
	6.1	1.2	116	68	12	15.3	1	1.13	1.19	0.95	1	33	20.8	2Ng3	18.5	19.1	
	6.1	1.2	116	68	12	15.4	1	1.13	1.19	0.95	1	25	20.4	3Ns	18.5	19.1	

Earthquake & site	Avg depth (m)	Depth GWT (m)	σ_v (kPa)	σ'_v (kPa)	(N_m)	$(N_1)_{60}$	C_B	C_E	C_N	C_R	C_S	FC (%)	$(N_1)_{60cs}$	$\Delta(N_1)_{60cs}$	γ_{tot} above water table	γ_{tot} below water table	Primary source of data
<u>Miller Farm</u>	4.6	4.9	89	92	11	12.4	1	1.13	1.05	0.95	1.0	19	16.7		18.1	19.7	Holzer et al (1994), Bennett & Tinsley (1995).
<u>CMF-3</u>	5.6	4.9	103	96	6	6.6	1	1.13	1.03	0.95	1.0	41	12.2		18.1	19.7	
	6.7	4.9	124	107	13	13.6	1	1.13	0.98	0.95	1.0	22	18.4		18.1	19.7	
Averages =	6.2				9.5	10.1							31.5	15.3			
Compute representative values given the above average $(N_1)_{60cs}$:																	
	6.2	4.90	114	101	9.2	9.9	1	1.13	1.00	0.95	1.0	32	15.3	5.4	18.1	19.7	
Differ = -3%																	
<u>Miller Farm</u>	7.0	4.7	130	108	20	20.9	1	1.13	0.97	0.95	1.0	13	23.4		18.1	19.7	Holzer et al (1994), Bennett & Tinsley (1995).
<u>CMF-5</u>																	
Single N value for this borehole. Adjacent CPT does suggest that the sand layer is relatively uniform in its penetration resistance.																	
<u>Miller Farm</u>	4.6	4.4	83	81	11	13.0	1	1.13	1.10	0.95	1.0	45	18.6		18.1	19.7	Holzer et al (1994), Bennett & Tinsley (1995).
<u>CMF-8</u>	6.0	4.4	110	95	9	10.0	1	1.13	1.03	0.95	1.0	17	13.8		18.1	19.7	
	7.5	4.4	140	110	9	9.3	1	1.13	0.96	0.95	1.0	14	12.2		18.1	19.7	
Averages =	6.0				9.7	10.8							25	14.9			
Compute representative values given the above average $(N_1)_{60cs}$:																	
	6.0	4.40	111	95	8.8	9.8	1	1.13	1.03	0.95	1.0	25	14.9	5.1	18.1	19.7	
Differ = -8%																	
<u>Miller Farm</u>	7.5	3.0	141	96	12.0	13.2	1	1.13	1.02	0.95	1.0	20	17.7		17.3	19.7	Holzer et al (1994), Bennett & Tinsley (1995).
<u>CMF-10</u>	9.3	3.0	175	114	25.0	27.1	1	1.13	0.96	1.00	1.0	20	31.6		17.3	19.7	
Averages =	8.4				18.5	20.2							20	24.6			
Compute representative values given the above average $(N_1)_{60cs}$:																	
	8.4	3.00	158	105	19.0	20.2	1	1.13	0.99	0.95	1	20	24.6	4.5	17.3	19.7	
Differ = 3%																	

Earthquake & site	Avg depth (m)	Depth GWT (m)	σ_v (kPa)	σ'_v (kPa)	(N_m)	$(N_1)_{60}$	C_B	C_E	C_N	C_R	C_S	FC (%)	$(N_1)_{60cs}$	$\Delta(N_1)_{60cs}$	γ_{tot} above water table	γ_{tot} below water table	Primary source of data
<u>State Beach</u>	3.36	2.6	60	52	14	19.9	1	1.25	1.34	0.85	1	1	19.9		17.3	19.6	Boulanger et al (1995, 1997)
<u>UC-B2</u>	4.12	2.6	75	60	16	21.3	1	1.25	1.25	0.85	1	1	21.3		17.3	19.6	
	4.88	2.6	90	67	11	15.9	1	1.25	1.22	0.95	1	1	15.9		17.3	19.6	
	5.64	2.6	105	75	13	17.8	1	1.25	1.15	0.95	1	1	17.8		17.3	19.6	
	6.41	2.6	120	82	13	17.0	1	1.25	1.10	0.95	1	1	17.0		17.3	19.6	
Averages =	4.9				13.4	18.4						1	18.4				
Compute representative values given the above average $(N_1)_{60cs}$:																	
	4.9	2.60	90	67	12.8	18.4	1	1.25	1.20	0.95	1	1	18.4	0.0	17.3	19.6	
Differ = -4%																	
<u>Treasure Island (2 borings)</u>	2.7	1.5	48	36	8	13.6	1	1.13	1.61	0.85	1.1	20	18.1		17.3	18.1	Pass (1994), Youd & Shakal (1994), Cetin et al (2000)
	2.7	1.5	48	36	9	15.1	1	1.13	1.59	0.85	1.1	20	19.6		17.3	18.1	
	4.0	1.5	71	47	1	1.7	1	1.13	1.58	0.85	1.1	20	6.2		17.3	18.1	
	4.2	1.5	75	48	5	7.7	1	1.13	1.47	0.85	1.1	20	12.2		17.3	18.1	
	5.2	1.5	93	57	8	12.4	1	1.13	1.31	0.95	1.1	20	16.9		17.3	18.1	
	5.2	1.5	93	57	5	8.0	1	1.13	1.35	0.95	1.1	20	12.4		17.3	18.1	
	6.0	1.5	107	63	0	0.0	1	1.13	1.34	0.95	1.1	20	4.5		17.3	18.1	
	6.4	1.5	115	67	6	8.8	1	1.13	1.24	0.95	1.1	20	13.2		17.3	18.1	
	7.0	1.5	126	71	7	9.8	1	1.13	1.19	0.95	1.1	20	14.3		17.3	18.1	
	7.6	1.5	136	76	3	4.1	1	1.13	1.17	0.95	1.1	20	8.6		17.3	18.1	
	7.9	1.5	142	79	5	6.7	1	1.13	1.14	0.95	1.1	20	11.2		17.3	18.1	
	8.8	1.5	158	86	6	8.1	1	1.13	1.08	1	1.1	20	12.6		17.3	18.1	
	9.1	1.5	164	89	2	2.7	1	1.13	1.08	1	1.1	20	7.2		17.3	18.1	
Averages =	6.5				4.4	6.4						20	10.8				
Compute representative values given the above average $(N_1)_{60cs}$:																	
	6.5	1.49	116	67	4.3	6.4	1	1.13	1.24	0.95	1.1	20	10.8	4.5	17.3	18.1	
Differ = -1%																	

Earthquake & site	Avg depth (m)	Depth GW (m)	σ_v (kPa)	σ'_v (kPa)	(N_m)	$(N_1)_{60}$	C_B	C_E	C_N	C_R	C_S	FC (%)	$(N_1)_{60cs}$	$\Delta(N_1)_{60cs}$	γ_{tot} above water table	γ_{tot} below water table	Primary source of data
-------------------	---------------	--------------	------------------	-------------------	---------	--------------	-------	-------	-------	-------	-------	--------	----------------	----------------------	----------------------------------	----------------------------------	------------------------

1993 M=7.6 Kushiro-Oki earthquake - Jan 15

<u>Kushiro Port</u>	2.8	2.0	46	39	17	27.2	1	1.30	1.45	0.85	1	5	27.2		16.0	18.1	Iai et al. (1995)
<u>Seismo St.</u>	3.8	2.0	65	47	17	25.5	1	1.30	1.36	0.85	1	5	25.5		16.0	18.1	
	4.8	2.0	83	55	16	25.2	1	1.30	1.27	0.95	1	5	25.2		16.0	18.1	
Averages =	3.8				16.7	25.9						5	25.9				

Compute representative values given the above average $(N_1)_{60cs}$:

3.8	2.00	65	47	17.4	25.9	1	1.30	1.35	0.85	1	5	25.9	0.0	16.0	18.1
-----	------	----	----	------	------	---	------	------	------	---	---	------	-----	------	------

Differ = 4%

1994 M=6.7 Northridge earthquake - Jan 17

<u>Balboa B1v.</u>	8.2	7.2	150	140	10	9.2	1	1.13	0.85	0.95	1	51	14.8		18.1	19.6	Bennett et al (1998), Holzer et al (1998), Cetin et al (2000)
<u>Unit C</u>	8.3	7.2	152	141	17	15.8	1	1.13	0.87	0.95	1	48	21.4		18.1	19.6	
	8.4	7.2	154	142	9	8.2	1	1.13	0.84	0.95	1	48	13.8		18.1	19.6	
	9.2	7.2	170	150	20	19.3	1	1.13	0.85	1	1	54	24.9		18.1	19.6	
Averages =	8.5				14.0	13.1						50	18.7				

Compute representative values given the above average $(N_1)_{60cs}$:

8.5	7.20	156	143	13.6	13.1	1	1.13	0.86	1	1	50.3	18.7	5.6	18.1	19.6
-----	------	-----	-----	------	------	---	------	------	---	---	------	------	-----	------	------

Differ = -3%

Earthquake & site	Avg depth (m)	Depth GWT (m)	σ_v (kPa)	σ'_v (kPa)	(N_m)	$(N_1)_{60}$	C_B	C_E	C_N	C_R	C_S	FC (%)	$(N_1)_{60cs}$	$\Delta(N_1)_{60cs}$	γ_{tot} above water table	γ_{tot} below water table	Primary source of data
-------------------	---------------	---------------	------------------	-------------------	---------	--------------	-------	-------	-------	-------	-------	--------	----------------	----------------------	----------------------------------	----------------------------------	------------------------

1995 M=6.9 Hyogoken-Nambu (Kobe) earthquake - Jan 16

<u>Site 1</u>	5.3	2.4	103	74	43	54.1	1	1.22	1.09	0.95	1	0	54.1				Tokimatsu (2010)
	6.3	2.4	124	85	41	49.8	1	1.22	1.05	0.95	1	6.7	49.9				

Averages = 5.80 113 80 42.0 51.9 Average= 3.4 52.0

Compute representative values given the above average $(N_1)_{60cs}$:

5.8	2.4	113	80	42.1	52.0	1	1.22	1.07	0.95	1	3.4	52.0	0.0	varies	varies
-----	-----	-----	----	------	------	---	------	------	------	---	-----	------	-----	--------	--------

Differ = 0%

<u>Site 2</u>	5.3	2.9	100	76	33	41.5	1	1.22	1.09	0.95	1	8	41.8				Tokimatsu (2010)
	6.3	2.9	120	87	41	49.5	1	1.22	1.04	0.95	1	0	49.5				
	7.3	2.9	140	97	36	42.3	1	1.22	1.01	0.95	1	7	42.4				
	8.3	2.9	159	106	40	48.2	1	1.22	0.99	1.00	1	30	53.6				
	9.3	2.9	178	115	28	32.8	1	1.22	0.96	1.00	1	22	37.6				
	11.3	2.9	217	134	24	26.5	1	1.22	0.91	1.00	1	22	31.2				

Averages = 8.0 152 103 33.7 40.1 Average= 15 42.7

Compute representative values given the above average $(N_1)_{60cs}$:

8.0	2.9	152	103	34.2	39.5	1	1.22	1.00	0.95	1	14.8	42.7	3.2	varies	varies
-----	-----	-----	-----	------	------	---	------	------	------	---	------	------	-----	--------	--------

Differ = 2%

Earthquake & site	Avg depth (m)	Depth GWT (m)	σ_v (kPa)	σ'_v (kPa)	(N_m)	$(N_1)_{60}$	C_B	C_E	C_N	C_R	C_S	FC (%)	$(N_1)_{60cs}$	$\Delta(N_1)_{60cs}$	γ_{tot} above water table	γ_{tot} below water table	Primary source of data
<u>Site 3</u>	4.3	2.5	78.4	60.7	39	51.7	1	1.22	1.14	0.95	1	5	51.7				Tokimatsu (2010)
	5.3	2.5	99.0	71.5	40	50.8	1	1.22	1.10	0.95	1	4	50.8				
	6.3	2.5	119.6	82.3	46	56.3	1	1.22	1.06	0.95	1	0	56.3				
	7.3	2.5	140.2	93.1	34	40.4	1	1.22	1.03	0.95	1	4	40.4				
Averages =	5.8		109	77	39.8	49.8						Average=	3	49.8			
Compute representative values given the above average $(N_1)_{60cs}$:																	
	5.8	2.5	109	77	40.0	49.8	1	1.22	1.08	0.95	1	3.3	49.8	0.0	varies	varies	
Differ = 1%																	
<u>Site 4</u>	3.3	2.1	55.1	42.8	26	35.7	1	1.22	1.32	0.85	1	0	35.7				Tokimatsu (2010)
	4.3	2.1	75.7	53.6	24	34.4	1	1.22	1.24	0.95	1	3.6	34.4				
	5.3	2.1	96.3	64.4	30	39.8	1	1.22	1.15	0.95	1	0	39.8				
Averages =	4.3		76	54	26.7	36.6						Average=	1	36.6			
Compute representative values given the above average $(N_1)_{60cs}$:																	
	4.3	2.1	76	54	25.8	36.6	1	1.22	1.23	0.95	1	1.2	36.6	0.0	varies	varies	
Differ = -3%																	

Earthquake & site	Avg depth (m)	Depth GW (m)	σ_v (kPa)	σ'_v (kPa)	(N_m)	$(N_1)_{60}$	C_B	C_E	C_N	C_R	C_S	FC (%)	$(N_1)_{60cs}$	$\Delta(N_1)_{60cs}$	γ_{tot} above water table	γ_{tot} below water table	Primary source of data
<u>Site 5</u>	7.3	3.0	141.0	98.9	6	7.1	1	1.22	1.01	0.95	1	0	7.1				Tokimatsu (2010)
	8.6	3.0	167.7	112.9	5	5.7	1	1.22	0.94	1.00	1	0	5.7				
	9.3	3.0	182.3	120.5	4	4.4	1	1.22	0.90	1.00	1	0	4.4				
	10.3	3.0	202.6	131.2	7	7.4	1	1.22	0.86	1.00	1	5	7.4				
Averages =	8.9		173	116	5.5	6.1							1	6.1			
Compute representative values given the above average $(N_1)_{60cs}$:																	
	8.9	3.0	173	116	5.4	6.1	1	1.22	0.92	1.00	1	1.3	6.1	0.0	varies	varies	
Differ = -1%																	
<u>Site 6</u>	3.3	2.3	58.0	48.2	10	14.9	1	1.22	1.44	0.85	1	3	14.9				Tokimatsu (2010)
	4.3	2.3	77.1	57.5	18	25.5	1	1.22	1.22	0.95	1	30	30.9				
	6.3	2.3	115.4	76.1	18	23.3	1	1.22	1.12	0.95	1	14	26.1				
	7.3	2.3	134.5	85.5	14	17.4	1	1.22	1.07	0.95	1	30	22.8				
	8.3	2.3	152.3	93.4	10	12.7	1	1.22	1.04	1.00	1	30	18.0				
Averages =	5.9		107	72	14.0	18.8							21	22.5			
Compute representative values given the above average $(N_1)_{60cs}$:																	
	5.9	2.3	107	72	13.4	17.8	1	1.22	1.15	0.95	1	21.4	22.5	4.7	varies	varies	
Differ = -5%																	

Earthquake & site	Avg depth (m)	Depth GWT (m)	σ_v (kPa)	σ'_v (kPa)	(N_m)	$(N_1)_{60}$	C_B	C_E	C_N	C_R	C_S	FC (%)	$(N_1)_{60cs}$	$\Delta(N_1)_{60cs}$	γ_{tot} above water table	γ_{tot} below water table	Primary source of data
<u>Site 7</u>	3.3	3.2	62	60	8	10.9	1	1.22	1.32	0.85	1	0	10.9				Tokimatsu (2010)
	4.3	3.2	82	71	21	27.8	1	1.22	1.14	0.95	1	0	27.8				
	6.3	3.2	124	93	32	38.1	1	1.22	1.03	0.95	1	12	40.1				
	7.3	3.2	144	104	23	26.4	1	1.22	0.99	0.95	1	0	26.4				
	8.3	3.2	165	114	21	24.4	1	1.22	0.95	1.00	1	0	24.4				
Averages =	3.3		62	60	8	11						0	10.9				
Compute representative values given the above average $(N_1)_{60cs}$:																	
	3.3	3.2	62	60	8.0	10.9	1	1.22	1.32	0.85	1	0	10.9	0.0	varies	varies	
Differ = 0%																	
<u>Site 8</u>	4.0	3.0	66.7	56.4	18	26.2	1	1.22	1.26	0.95	1	0	26.2				Tokimatsu (2010)
	5.0	3.0	84.8	64.6	15	21.1	1	1.22	1.21	0.95	1	0	21.1				
	6.0	3.0	103.1	73.2	19	25.1	1	1.22	1.14	0.95	1	0	25.1				
Averages =	5.0		85	65	17.3	24.1						0	24.1				
Compute representative values given the above average $(N_1)_{60cs}$:																	
	5.0	3.0	85	65	17.4	24.1	1	1.22	1.20	0.95	1	0.0	24.1	0.0	varies	varies	
Differ = 0%																	

Earthquake & site	Avg depth (m)	Depth GWT (m)	σ_v (kPa)	σ'_v (kPa)	(N_m)	$(N_1)_{60}$	C_B	C_E	C_N	C_R	C_S	FC (%)	$(N_1)_{60cs}$	$\Delta(N_1)_{60cs}$	γ_{tot} above water table	γ_{tot} below water table	Primary source of data
<u>Site 9</u>	3.3	2.8	59.3	54.1	8	11.5	1	1.22	1.39	0.85	1	7	11.6				Tokimatsu (2010)
	4.3	2.8	78.9	63.9	5	7.5	1	1.22	1.30	0.95	1	0	7.5				
	5.3	2.8	98.6	73.7	13	17.5	1	1.22	1.16	0.95	1	0	17.5				
Averages =	4.3		79	64	8.7	12.2						2	12.2				
Compute representative N values given the above average $(N_1)_{60cs}$:																	
	4.3	2.8	79	64	8.3	12.2	1	1.22	1.27	0.95	1	2.3	12.2	0.0	varies	varies	
Differ = -4%																	
<u>Site 10</u>	6.0	4.5	108.8	93.7	20	23.9	1	1.22	1.03	0.95	1	5	23.9				Tokimatsu (2010)
	7.0	4.5	127.4	102.5	27	31.2	1	1.22	1.00	0.95	1	10	32.3				
	8.0	4.5	145.8	111.0	20	23.5	1	1.22	0.96	1.00	1	10	24.7				
	9.0	4.5	164.3	119.8	26	29.9	1	1.22	0.94	1.00	1	10	31.0				
Averages =	7.5		137	107	23.3	27.1						9	28.0				
Compute representative values given the above average $(N_1)_{60cs}$:																	
	7.5	4.5	137	107	24.1	27.4	1	1.22	0.98	0.95	1	8.8	28.0	0.6	varies	varies	
Differ = 4%																	

Earthquake & site	Avg depth (m)	Depth GWT (m)	σ_v (kPa)	σ'_v (kPa)	(N_m)	$(N_1)_{60}$	C_B	C_E	C_N	C_R	C_S	FC (%)	$(N_1)_{60cs}$	$\Delta(N_1)_{60cs}$	γ_{tot} above water table	γ_{tot} below water table	Primary source of data
<u>Site 11</u>	3.8	1.5	63.8	41.2	7	11.6	1	1.22	1.60	0.85	1	5	11.6				Tokimatsu (2010)
	4.5	1.5	76.4	46.5	5	8.9	1	1.22	1.54	0.95	1	5	8.9				
	5.3	1.5	89.1	51.8	6	10.0	1	1.22	1.44	0.95	1	5	10.0				
	6.0	1.5	101.5	56.8	4	6.5	1	1.22	1.40	0.95	1	5	6.5				
	6.8	1.5	114.1	62.1	6	9.1	1	1.22	1.31	0.95	1	5	9.1				
	7.5	1.5	126.9	67.6	7	10.1	1	1.22	1.24	0.95	1	5	10.1				
	8.3	1.5	139.6	72.9	6	8.8	1	1.22	1.20	1.00	1	5	8.8				
	9.0	1.5	152.1	78.0	5	7.1	1	1.22	1.16	1.00	1	5	7.1				
	9.8	1.5	164.3	82.9	3	4.2	1	1.22	1.13	1.00	1	5	4.2				
Averages =	6.8		114	62	5.4	8.5							5	8.5			
Compute representative values given the above average $(N_1)_{60cs}$:																	
	6.8	1.5	114	62	5.6	8.5	1	1.22	1.31	0.95	1	5.0	8.5	0.0	varies	varies	
Differ = 2%																	
<u>Site 12</u>	4.3	3.2	73.0	62.2	20	27.9	1	1.22	1.20	0.95	1	4	27.9				Tokimatsu (2010)
	5.3	3.2	92.2	71.6	19	25.0	1	1.22	1.13	0.95	1	30	30.3				
	6.3	3.2	111.3	80.9	19	24.1	1	1.22	1.10	0.95	1	8	24.5				
Averages =	5.3		92	72	19.3	25.7							14	27.6			
Compute representative values given the above average $(N_1)_{60cs}$:																	
	5.3	3.2	92	72	18.6	24.7	1	1.22	1.14	0.95	1	14.0	27.6	2.9	varies	varies	
Differ = -4%																	

Earthquake & site	Avg depth (m)	Depth GWT (m)	σ_v (kPa)	σ'_v (kPa)	(N_m)	$(N_1)_{60}$	C_B	C_E	C_N	C_R	C_S	FC (%)	$(N_1)_{60cs}$	$\Delta(N_1)_{60cs}$	γ_{tot} above water table	γ_{tot} below water table	Primary source of data
<u>Site 13</u>	5.0	2.3	89.5	63.0	10	14.6	1	1.22	1.26	0.95	1	0	14.6				Tokimatsu (2010)
	6.0	2.3	106.8	70.5	8	11.0	1	1.22	1.19	0.95	1	20	15.5				
	7.0	2.3	124.4	78.3	10	13.1	1	1.22	1.13	0.95	1	20	17.5				
	8.0	2.3	141.9	85.9	9	11.9	1	1.22	1.08	1.00	1	20	16.3				
Averages =	6.5		116	74	9.3	12.6							Average=	15	16.0		
Compute representative values given the above average $(N_1)_{60cs}$:																	
	6.5	2.3	116	74	9.5	12.7	1	1.22	1.16	0.95	1	15.0	16.0	3.3	varies	varies	
Differ = 3%																	
<u>Site 14</u>	4.3	3.1	76.2	64.4	17	23.7	1	1.22	1.20	0.95	1	7	23.8				Tokimatsu (2010)
	5.3	3.1	95.3	73.7	15	19.7	1	1.22	1.14	0.95	1	30	25.1				
Averages =	4.8		86	69	16.0	21.7							Average=	19	24.5		
Compute representative values given the above average $(N_1)_{60cs}$:																	
	4.8	3.1	86	69	15.0	20.3	1	1.22	1.17	0.95	1	19	24.5	4.2	varies	varies	
Differ = -6%																	
<u>Site 15</u>	4.7	3.7	82.4	72.6	12	16.3	1	1.22	1.17	0.95	1	5	16.3				Tokimatsu (2010)
	5.4	3.7	97.2	80.0	14	18.1	1	1.22	1.11	0.95	1	0	18.1				
	6.9	3.7	126.6	94.7	19	22.6	1	1.22	1.03	0.95	1	9	23.4				
Averages =	5.7		102	82	15.0	19.0							Average=	5	19.2		
Compute representative values given the above average $(N_1)_{60cs}$:																	
	5.7	3.7	102	82	15.1	19.2	1	1.22	1.10	0.95	1	5	19.2	0.0	varies	varies	
Differ = 1%																	

Earthquake & site	Avg depth (m)	Depth GWT (m)	σ_v (kPa)	σ'_v (kPa)	(N_m)	$(N_1)_{60}$	C_B	C_E	C_N	C_R	C_S	FC (%)	$(N_1)_{60cs}$	$\Delta(N_1)_{60cs}$	γ_{tot} above water table	γ_{tot} below water table	Primary source of data
<u>Site 16</u>	4.0	2.5	71.1	55.9	18	26.3	1	1.22	1.26	0.95	1	5	26.3				Tokimatsu (2010)
	5.0	2.5	89.1	64.1	17	23.8	1	1.22	1.21	0.95	1	5	23.8				
Averages =	4.5		80	60	17.5	25.0						5	25.0				
Compute representative values given the above average $(N_1)_{60cs}$:																	
	4.5	2.5	80	60	17.5	25.0	1	1.22	1.23	0.95	1	5	25.0	0.0	varies	varies	
Differ = 0%																	
<u>Site 17</u>	3.0	0.8	53.3	31.2	10	17.6	1	1.22	1.70	0.85	1	5	17.6				Tokimatsu (2010)
	3.8	0.8	66.1	36.7	7	12.2	1	1.22	1.69	0.85	1	5	12.2				
	4.5	0.8	79.5	42.7	13	21.8	1	1.22	1.44	0.95	1	5	21.8				
	5.3	0.8	93.1	49.0	20	30.2	1	1.22	1.30	0.95	1	5	30.2				
	6.0	0.8	106.6	55.1	16	23.8	1	1.22	1.28	0.95	1	5	23.8				
Averages =	4.5		80	43	13.2	21.1						5	21.1				
Compute representative values given the above average $(N_1)_{60cs}$:																	
	4.5	0.8	80	43	12.6	21.1	1	1.22	1.45	0.95	1	5	21.1	0.0	varies	varies	
Differ = -5%																	

Earthquake & site	Avg depth (m)	Depth GW (m)	σ_v (kPa)	σ'_v (kPa)	(N_m)	$(N_1)_{60}$	C_B	C_E	C_N	C_R	C_S	FC (%)	$(N_1)_{60cs}$	$\Delta(N_1)_{60cs}$	γ_{tot} above water table	γ_{tot} below water table	Primary source of data
<u>Site 18</u>	9.0	7.7	170.0	156.8	33	34.8	1	1.22	0.87	1.00	1	0	34.8				Tokimatsu (2010)
	10.0	7.7	189.3	166.2	44	47.1	1	1.22	0.88	1.00	1	0	47.1				
	11.0	7.7	208.4	175.5	42	44.1	1	1.22	0.86	1.00	1	0	44.1				
	12.0	7.7	227.6	185.0	43	44.6	1	1.22	0.85	1.00	1	0	44.6				
Averages =	10.5		199	171	40.5	42.6						0	42.6				
Compute representative values given the above average $(N_1)_{60cs}$:																	
	10.5	7.7	199	171	40.5	42.6	1	1.22	0.86	1.00	1	0	42.6	0.0	varies	varies	
Differ = 0%																	
<u>Site 19</u>	7.0	6.1	128.1	119.3	20	21.7	1	1.22	0.93	0.95	1	10	22.8				Tokimatsu (2010)
	8.0	6.1	146.4	127.7	19	21.0	1	1.22	0.91	1.00	1	10	22.2				
Averages =	7.5		137	124	19.5	21.3						10	22.5				
Compute representative values given the above average $(N_1)_{60cs}$:																	
	7.5	6.1	137	124	20.0	21.3	1	1.22	0.92	0.95	1	10	22.5	1.1	varies	varies	
Differ = 3%																	

Earthquake & site	Avg depth (m)	Depth GWT (m)	σ_v (kPa)	σ'_v (kPa)	(N_m)	$(N_1)_{60}$	C_B	C_E	C_N	C_R	C_S	FC (%)	$(N_1)_{60cs}$	$\Delta(N_1)_{60cs}$	γ_{tot} above water table	γ_{tot} below water table	Primary source of data
<u>Site 22</u>	4.0	2.4	77	61	33	44.0	1	1.22	1.15	0.95	1	0	44.0				Tokimatsu (2010)
	5.0	2.4	96	70	38	48.5	1	1.22	1.10	0.95	1	0	48.5				
	6.0	2.4	114	79	24	30.4	1	1.22	1.09	0.95	1	10	31.5				
	7.0	2.4	132	87	18	22.2	1	1.22	1.06	0.95	1	10	23.3				
	8.0	2.4	151	96	36	44.5	1	1.22	1.01	1.00	1	10	45.7				
Averages =	6.0		114	79	29.8	37.9							Average=	6	38.6		
Compute representative values given the above average $(N_1)_{60cs}$:																	
	6.0	2.4	114	79	30.8	38.6	1	1.22	1.08	0.95	1	6	38.6	0.0	varies	varies	
Differ = 3%																	
<u>Site 23</u>	4.00	3.0	73	63	18	25.1	1	1.22	1.20	0.95	1	10	26.3				Tokimatsu (2010)
	5.00	3	92	72	50	63.3	1	1.22	1.09	0.95	1	0	63.3				
	6.00	3	110	81	18	22.9	1	1.22	1.10	0.95	1	10	24.0				
Averages =	5.0		92	72	18	24.0							Average=	10.0	25.1		
Compute representative values given the above average $(N_1)_{60cs}$:																	
	5.0	3.0	92	72	18.1	24.0	1	1.22	1.15	0.95	1	10	25.1	1.1	varies	varies	
Differ = 0%																	

Earthquake & site	Avg depth (m)	Depth GW (m)	σ_v (kPa)	σ'_v (kPa)	(N_m)	$(N_1)_{60}$	C_B	C_E	C_N	C_R	C_S	FC (%)	$(N_1)_{60cs}$	$\Delta(N_1)_{60cs}$	γ_{tot} above water table	γ_{tot} below water table	Primary source of data
<u>Site 24</u>	3.0	2.4	54	47	16	22.8	1	1.22	1.38	0.85	1	0	22.8				Tokimatsu (2010)
	4	2.4	72	56	18	26.4	1	1.22	1.26	0.95	1	0	26.4				
Averages =	3.5		63	51	17	24.6						0.0	24.6				
Compute representative values given the above average $(N_1)_{60cs}$:																	
	3.5	2.4	63	51	18.0	24.6	1	1.22	1.32	0.85	1	0	24.6	0.0	varies	varies	
Differ = 6%																	
<u>Site 25</u>	3.0	2.2	54	46	26	35.0	1	1.22	1.30	0.85	1	5	35.0				Tokimatsu (2010)
	4.0	2.2	73	55	26	36.7	1	1.22	1.22	0.95	1	0	36.7				
Averages =	3.5		64	50	26	35.8						2.5	35.8				
Compute representative values given the above average $(N_1)_{60cs}$:																	
	3.5	2.2	64	50	27.5	35.8	1	1.22	1.25	0.85	1	3	35.8	0.0	varies	varies	
Differ = 6%																	
<u>Site 26</u>	3.0	0.9	54	33	21	32.2	1	1.22	1.48	0.85	1	0	32.2				Tokimatsu (2010)
	4.0	0.9	72	42	28	41.8	1	1.22	1.29	0.95	1	0	41.8				
Averages =	3.5		63	37	25	37.0						0.0	37.0				
Compute representative values given the above average $(N_1)_{60cs}$:																	
	3.5	0.9	63	37	26.0	37.0	1	1.22	1.37	0.85	1	0	37.0	0.0	varies	varies	
Differ = 6%																	

Earthquake & site	Avg depth (m)	Depth GW (m)	σ_v (kPa)	σ'_v (kPa)	(N_m)	$(N_1)_{60}$	C_B	C_E	C_N	C_R	C_S	FC (%)	$(N_1)_{60cs}$	$\Delta(N_1)_{60cs}$	γ_{tot} above water table	γ_{tot} below water table	Primary source of data
<u>Site 27</u>	2.0	1.1	34.1	24.8	29	43.9	1	1.22	1.46	0.85	1	10	45.1				Tokimatsu (2010)
	3.0	1.1	52.71	33.58	26	37.8	1	1.22	1.40	0.85	1	10	38.9				
Averages =	2.5		43	29	28	40.8							Average= 10.0	42.0			
Compute representative values given the above average $(N_1)_{60cs}$:																	
	2.5	1.1	43	29	27.6	40.8	1	1.22	1.43	0.85	1	10	42.0	1.1	varies	varies	
Differ = 0%																	
<u>Site 28</u>	2.0	1.8	35	32	10	17.6	1	1.22	1.69	0.85	1	5	17.6				Tokimatsu (2010)
	3.0	1.8	52	40	10	16.1	1	1.22	1.55	0.85	1	5	16.1				
	4.0	1.8	71	49	18	27.5	1	1.22	1.32	0.95	1	10	28.6				
	5.0	1.8	89	57	15	22.1	1	1.22	1.27	0.95	1	10	23.2				
Averages =	3.5		62	44	13	20.8							Average= 7.5	21.4			
Compute representative values given the above average $(N_1)_{60cs}$:																	
	3.5	1.8	62	44	14.3	21.1	1	1.22	1.42	0.85	1	8	21.4	0.2	varies	varies	
Differ = 8%																	

Earthquake & site	Avg depth (m)	Depth GW (m)	σ_v (kPa)	σ'_v (kPa)	(N_m)	$(N_1)_{60}$	C_B	C_E	C_N	C_R	C_S	FC (%)	$(N_1)_{60cs}$	$\Delta(N_1)_{60cs}$	γ_{tot} above water table	γ_{tot} below water table	Primary source of data
-------------------	---------------	--------------	------------------	-------------------	---------	--------------	-------	-------	-------	-------	-------	--------	----------------	----------------------	----------------------------------	----------------------------------	------------------------

<u>Site 29</u>	3.0	2.0	53.1	43.3	12	18.3	1	1.22	1.47	0.85	1	0	18.3				Tokimatsu (2010)
	3.8	2.0	66.7	49.5	14	19.9	1	1.22	1.37	0.85	1	0	19.9				
	4.5	2.0	79.9	55.4	10	15.5	1	1.22	1.34	0.95	1	0	15.5				

Averages = 3.8 67 49 12 17.9 Average= 0.0 17.9

Compute representative values given the above average $(N_1)_{60cs}$:

3.8 2.0 67 49 12.4 17.9 1 1.22 1.39 0.85 1 0 17.9 0.0 varies varies

Differ = 4%

<u>Site 30</u>	7.0	1.5	118	64	24	32.5	1	1.22	1.17	0.95	1	10	33.6				Tokimatsu (2010)
	8.0	1.5	137	73	35	46.5	1	1.22	1.09	1.00	1	10	47.6				
	9.0	1.5	156	82	29	37.7	1	1.22	1.07	1.00	1	10	38.9				
	10.0	1.5	175	91	35	43.9	1	1.22	1.03	1.00	1	10	45.1				

Averages = 8.5 146 78 31 40.1 Average= 10.0 41.3

Compute representative values given the above average $(N_1)_{60cs}$:

8.5 1.5 146 78 30.5 40.1 1 1.22 1.08 1.00 1 10 41.3 1.1 varies varies

Differ = -1%

Earthquake & site	Avg depth (m)	Depth GW (m)	σ_v (kPa)	σ'_v (kPa)	(N_m)	$(N_1)_{60}$	C_B	C_E	C_N	C_R	C_S	FC (%)	$(N_1)_{60cs}$	$\Delta(N_1)_{60cs}$	γ_{tot} above water table	γ_{tot} below water table	Primary source of data
<u>Site 31</u>	3.0	1.2	53.9	36.3	31	42.9	1	1.22	1.33	0.85	1	0	42.9				Tokimatsu (2010)
	4.0	1.2	73.1	45.6	40	57.2	1	1.22	1.23	0.95	1	0	57.2				
	5.0	1.2	92.1	54.8	36	49.0	1	1.22	1.18	0.95	1	0	49.0				
Averages =	4.0		73	46	36	49.7							0.0	49.7			
Compute representative values given the above average $(N_1)_{60cs}$:																	
	4.0	1.2	73	46	34.8	49.7	1	1.22	1.23	0.95	1	0	49.7	0.0	varies	varies	
Differ = -3%																	
<u>Site 32</u>	2.0	1.4	34.0	28.2	18	29.8	1	1.22	1.60	0.85	1	0	29.8				Tokimatsu (2010)
	3.0	1.4	52.4	36.7	19	28.6	1	1.22	1.45	0.85	1	10	29.7				
	4.0	1.4	70.5	45.0	16	25.4	1	1.22	1.37	0.95	1	10	26.6				
	5.0	1.4	88.8	53.5	21	30.6	1	1.22	1.26	0.95	1	5	30.6				
Averages =	3.5		61	41	19	28.6							6.3	29.2			
Compute representative values given the above average $(N_1)_{60cs}$:																	
	3.5	1.4	61	41	20.1	29.1	1	1.22	1.40	0.85	1	6	29.2	0.0	varies	varies	
Differ = 9%																	

Earthquake & site	Avg depth (m)	Depth GWL (m)	σ_v (kPa)	σ'_v (kPa)	(N_m)	$(N_1)_{60}$	C_B	C_E	C_N	C_R	C_S	FC (%)	$(N_1)_{60cs}$	$\Delta(N_1)_{60cs}$	γ_{tot} above water table	γ_{tot} below water table	Primary source of data
<u>Site 33</u>	7.0	2.0	123.4	74.3	21	27.1	1	1.22	1.11	0.95	1	50	32.7				Tokimatsu (2010)
	8.0	2.0	141.8	83.0	23	29.9	1	1.22	1.07	1.00	1	50	35.6				
	9.0	2.0	160.2	91.5	21	26.5	1	1.22	1.04	1.00	1	50	32.2				
Averages =	8.0		142	83	22	27.9						Average=	50.0	33.5			
Compute representative values given the above average $(N_1)_{60cs}$:																	
	8.0	2.0	142	83	21.3	27.9	1	1.22	1.07	1.00	1	50	33.5	5.6	varies	varies	
Differ = -2%																	
<u>Site 34</u>	4.0	1.8	69.4	47.8	20	30.4	1	1.22	1.31	0.95	1	5	30.4				Tokimatsu (2010)
	5.0	1.8	87.4	56.0	16	23.5	1	1.22	1.27	0.95	1	10	24.7				
	6.0	1.8	105.7	64.5	19	26.2	1	1.22	1.19	0.95	1	10	27.3				
	7.0	1.8	123.8	72.8	18	23.8	1	1.22	1.14	0.95	1	10	25.0				
	8.0	1.8	142.0	81.1	17	22.7	1	1.22	1.09	1.00	1	10	23.9				
	9.0	1.8	160.0	89.4	16	20.6	1	1.22	1.05	1.00	1	10	21.7				
	10.0	1.8	178.1	97.6	17	21.1	1	1.22	1.02	1.00	1	10	22.2				
Averages =	7.0		124	73	18	24.0						Average=	9.3	25.0			
Compute representative values given the above average $(N_1)_{60cs}$:																	
	7.0	1.8	124	73	18.3	24.2	1	1.22	1.14	0.95	1	9	25.0	0.8	varies	varies	
Differ = 4%																	

Earthquake & site	Avg depth (m)	Depth GW (m)	σ_v (kPa)	σ'_v (kPa)	(N_m)	$(N_1)_{60}$	C_B	C_E	C_N	C_R	C_S	FC (%)	$(N_1)_{60cs}$	$\Delta(N_1)_{60cs}$	γ_{tot} above water table	γ_{tot} below water table	Primary source of data
<u>Site 35</u>	3.0	2.1	52.0	42.7	13	19.8	1	1.22	1.47	0.85	1	5	19.8				Tokimatsu (2010)
	4.0	2.1	69.9	50.8	13	20.4	1	1.22	1.35	0.95	1	0	20.4				
	5.0	2.1	87.5	58.6	10	15.0	1	1.22	1.30	0.95	1	10	16.2				
	6.0	2.1	105.4	66.6	13	18.2	1	1.22	1.21	0.95	1	10	19.3				
Averages =	4.5		79	55	12	18.3						Average=	6.3	18.9			
Compute representative values given the above average $(N_1)_{60cs}$:																	
	4.5	2.1	79	55	12.3	18.9	1	1.22	1.32	0.95	1	6	18.9	0.0	varies	varies	
Differ = 1%																	
<u>Site 36</u>	3.0	0.9	52.0	31.7	20	31.3	1	1.22	1.51	0.85	1	5	31.3				Tokimatsu (2010)
	4.0	0.9	70.4	40.4	20	32.0	1	1.22	1.38	0.95	1	0	32.0				
Averages =	3.5		61	36	20	31.6						Average=	2.5	31.6			
Compute representative values given the above average $(N_1)_{60cs}$:																	
	3.5	0.9	61	36	21.2	31.6	1	1.22	1.44	0.85	1	3	31.6	0.0	varies	varies	
Differ = 6%																	

Earthquake & site	Avg depth (m)	Depth GW (m)	σ_v (kPa)	σ'_v (kPa)	(N_m)	$(N_1)_{60}$	C_B	C_E	C_N	C_R	C_S	FC (%)	$(N_1)_{60cs}$	$\Delta(N_1)_{60cs}$	γ_{tot} above water table	γ_{tot} below water table	Primary source of data
<u>Site 37</u>	2.0	4.0	34.8	34.8	17	26.7	1	1.22	1.51	0.85	1	0	26.7				Tokimatsu (2010)
	3.0	4.0	53.0	53.0	16	21.9	1	1.22	1.32	0.85	1	0	21.9				
	4.0	4.0	70.7	70.7	11	15.2	1	1.22	1.19	0.95	1	0	15.2				
	5.0	4.0	89.0	79.2	17	21.9	1	1.22	1.11	0.95	1	0	21.9				
	6.0	4.0	107.1	87.5	17	21.0	1	1.22	1.07	0.95	1	0	21.0				
Averages =	5.0		89	79	15	19.3						0.0	19.3				
Compute representative values given the above average $(N_1)_{60cs}$:																	
	5.0	4.0	89	79	15.0	19.3	1	1.22	1.12	0.95	1	0	19.3	0.0	varies	varies	
Differ = 0%																	
<u>Site 38</u>	6.0	3.0	107.3	77.8	13	17.0	1	1.22	1.13	0.95	1	5	17.0				Tokimatsu (2010)
	7.0	3.0	125.2	86.0	16	19.9	1	1.22	1.08	0.95	1	5	19.9				
	8.0	3.0	143.0	93.9	13	16.4	1	1.22	1.04	1.00	1	5	16.4				
	9.0	3.0	161.1	102.2	19	23.1	1	1.22	1.00	1.00	1	5	23.1				
	10.0	3.0	179.1	110.4	16	18.8	1	1.22	0.96	1.00	1	5	18.8				
Averages =	8.0		143	94	15	19.1						5.0	19.1				
Compute representative values given the above average $(N_1)_{60cs}$:																	
	8.0	3.0	143	94	15.1	19.1	1	1.22	1.03	1.00	1	5	19.1	0.0	varies	varies	
Differ = -2%																	

Earthquake & site	Avg depth (m)	Depth GW (m)	σ_v (kPa)	σ'_v (kPa)	(N_m)	$(N_1)_{60}$	C_B	C_E	C_N	C_R	C_S	FC (%)	$(N_1)_{60cs}$	$\Delta(N_1)_{60cs}$	γ_{tot} above water table	γ_{tot} below water table	Primary source of data
<u>Site 39</u>	4.0	2.6	74.6	60.9	44	58.3	1	1.22	1.14	0.95	1	0	58.3				Tokimatsu (2010)
	5.0	2.6	94.1	70.5	50	63.7	1	1.22	1.10	0.95	1	0	63.7				
Averages =	4.5		84	66	47	61.0						0.0	61.0				
Compute representative values given the above average $(N_1)_{60cs}$:																	
	4.5	2.6	84	66	47.0	61.0	1	1.22	1.12	0.95	1	0	61.0	0.0	varies	varies	
Differ = 0%																	
<u>Site 40</u>	3.0	2.8	56.4	54.5	36	44.2	1	1.22	1.18	0.85	1	0	44.2				Tokimatsu (2010)
	4.0	2.8	75.1	63.3	26	35.2	1	1.22	1.17	0.95	1	0	35.2				
Averages =	3.5		66	59	31	39.7						0.0	39.7				
Compute representative values given the above average $(N_1)_{60cs}$:																	
	3.5	2.8	66	59	32.5	39.7	1	1.22	1.18	0.85	1	0	39.7	0.0	varies	varies	
Differ = 5%																	

Earthquake & site	Avg depth (m)	Depth GWT (m)	σ_v (kPa)	σ'_v (kPa)	(N_m)	$(N_1)_{60}$	C_B	C_E	C_N	C_R	C_S	FC (%)	$(N_1)_{60cs}$	$\Delta(N_1)_{60cs}$	γ_{tot} above water table	γ_{tot} below water table	Primary source of data
-------------------	---------------	---------------	------------------	-------------------	---------	--------------	-------	-------	-------	-------	-------	--------	----------------	----------------------	----------------------------------	----------------------------------	------------------------

<u>Site 41</u>	2.3	2.0	38.2	35.7	11	18.3	1	1.22	1.61	0.85	1	0	18.3				Tokimatsu (2010)
	3.0	2.0	51.4	41.6	10	15.9	1	1.22	1.53	0.85	1	0	15.9				
	3.8	2.0	64.4	47.2	7	10.9	1	1.22	1.50	0.85	1	0	10.9				
	4.5	2.0	77.4	52.8	8	12.9	1	1.22	1.39	0.95	1	0	12.9				
	5.3	2.0	90.6	58.7	10	15.1	1	1.22	1.30	0.95	1	0	15.1				
	6.0	2.0	103.9	64.7	12	17.1	1	1.22	1.23	0.95	1	0	17.1				
Averages =	4.1		71	50	10	15.0						0.0	15.0				

Compute representative values given the above average $(N_1)_{60cs}$:

4.1	2.0	71	50	9.2	15.0	1	1.22	1.41	0.95	1	0	15.0	0.0	varies	varies		
		Differ =		-5%													

<u>Site 42</u>	4.0	1.2	67	39	7	13.0	1	1.22	1.60	0.95	1	10	14.2				Tokimatsu (2010)
	5.0	1.2	84	46	7	12.0	1	1.22	1.48	0.95	1	10	13.2				
	6.0	1.2	101	54	7	11.2	1	1.22	1.39	0.95	1	10	12.4				
Averages =	5.0		84	46	7	12.1						10.0	13.2				

Compute representative values given the above average $(N_1)_{60cs}$:

5.0	1.2	84	46	7.0	12.1	1	1.22	1.48	0.95	1	10	13.2	1.1	varies	varies
		Differ =		1%											

Earthquake & site	Avg depth (m)	Depth GW (m)	σ_v (kPa)	σ'_v (kPa)	(N_m)	$(N_1)_{60}$	C_B	C_E	C_N	C_R	C_S	FC (%)	$(N_1)_{60cs}$	$\Delta(N_1)_{60cs}$	γ_{tot} above water table	γ_{tot} below water table	Primary source of data
<u>Site 43</u>	4.2	2.2	71	52	10	15.6	1	1.22	1.35	0.95	1	20	20.1				Tokimatsu (2010)
	5.15	2.2	89	59	10	14.7	1	1.22	1.27	0.95	1	20	19.2				
Averages =	4.7		80	55	10	15.2							Average= 20.0	19.6			
Compute representative values given the above average $(N_1)_{60cs}$:																	
	4.7	2.2	80	55	10.0	15.2	1	1.22	1.31	0.95	1	20	19.6	4.5	varies	varies	
Differ = 0%																	
<u>Site 44</u>	3.0	1.6	51	36	4	7.1	1	1.22	1.70	0.85	1	5	7.1				Tokimatsu (2010)
	4.0	1.6	67	43	6	10.9	1	1.22	1.57	0.95	1	5	10.9				
	5.0	1.6	84	50	4	7.0	1	1.22	1.51	0.95	1	5	7.0				
Averages =	4.0		67	43	5	8.3							Average= 5.0	8.3			
Compute representative values given the above average $(N_1)_{60cs}$:																	
	4.0	1.6	67	43	4.4	8.3	1	1.22	1.61	0.95	1	5	8.3	0.0	varies	varies	
Differ = -5%																	

Earthquake & site	Avg depth (m)	Depth GWT (m)	σ_v (kPa)	σ'_v (kPa)	(N_m)	$(N_1)_{60}$	C_B	C_E	C_N	C_R	C_S	FC (%)	$(N_1)_{60cs}$	$\Delta(N_1)_{60cs}$	γ_{tot} above water table	γ_{tot} below water table	Primary source of data
-------------------	---------------	---------------	------------------	-------------------	---------	--------------	-------	-------	-------	-------	-------	--------	----------------	----------------------	----------------------------------	----------------------------------	------------------------

1983 M=7.7 Nihonkai-Chubu earthquake - May 26

<u>Gaiko 1</u>	2.4	1.5	44	35	6	10.6	1	1.22	1.70	0.85	1	9	11.3		17.3	19.6	Iai et al. (1989)
	3.5	1.5	66	46	5	8.1	1	1.22	1.57	0.85	1	2	8.1		17.3	19.6	
	4.3	1.5	81	53	6	9.8	1	1.22	1.41	0.95	1	2	9.8		17.3	19.6	
	6.4	1.5	123	74	5	6.9	1	1.22	1.20	0.95	1	2	6.9		17.3	19.6	
	7.3	1.5	140	83	8	10.3	1	1.22	1.11	0.95	1	2	10.3		17.3	19.6	
	8.4	1.5	162	94	8	10.2	1	1.22	1.04	1	1	2	10.2		17.3	19.6	
	10.3	1.5	199	112	6	6.9	1	1.22	0.94	1	1	2	6.9		17.3	19.6	
	12.5	1.5	242	134	6	6.2	1	1.22	0.85	1	1	2	6.2		17.3	19.6	

Averages = 6.9 132 79 6.3 8.6 Average= 2.88 8.7

Compute representative values given the above average $(N_1)_{60cs}$:

6.9 1.5 132 79 6.6 8.7 1 1.22 1.15 0.95 1 2.88 8.7 0.0 17.3 19.6

Differ = 5%

<u>Gaiko 2</u>	4.3	1.5	81	53	2	3.3	1	1.22	1.44	0.95	1	20	7.8		17.3	19.6	Iai et al. (1989)
	5.4	1.5	103	64	2	3.0	1	1.22	1.30	0.95	1	20	7.5		17.3	19.6	
	6.3	1.5	120	73	4	5.6	1	1.22	1.22	0.95	1	4	5.6		17.3	19.6	
	7.3	1.5	140	83	4	5.2	1	1.22	1.13	0.95	1	4	5.2		17.3	19.6	
	8.3	1.5	159	92	5	6.5	1	1.22	1.06	1	1	4	6.5		17.3	19.6	
	9.4	1.5	181	103	6	7.3	1	1.22	0.99	1	1	4	7.3		17.3	19.6	
	10.5	1.5	202	114	6	6.8	1	1.22	0.93	1	1	4	6.8		17.3	19.6	
	12.4	1.5	239	132	8	8.4	1	1.22	0.86	1	1	4	8.4		17.3	19.6	
	14.4	1.5	279	152	9	8.8	1	1.22	0.80	1	1	4	8.8		17.3	19.6	
	16.4	1.5	318	172	4	3.6	1	1.22	0.74	1	1	20	8.1		17.3	19.6	

Averages = 9.8 189 107 6.0 6.9 Average= 4.0 6.9

Compute representative values given the above average $(N_1)_{60cs}$:

9.8 1.5 189 107 5.9 6.9 1 1.22 0.97 1.00 1 4 6.9 0.0 17.3 19.6

Differ = -2%

Earthquake & site	Avg depth (m)	Depth GWT (m)	σ_v (kPa)	σ'_v (kPa)	(N_m)	$(N_1)_{60}$	C_B	C_E	C_N	C_R	C_S	FC (%)	$(N_1)_{60cs}$	$\Delta(N_1)_{60cs}$	γ_{tot} above water table	γ_{tot} below water table	Primary source of data
<u>Ohama No. 2 (2)</u>	2.7	0.72	51	32	1	1.8	1	1.22	1.70	0.85	1	2	1.8		17.3	19.6	Iai et al. (1989)
	3.8	0.72	72	42	2	3.5	1	1.22	1.70	0.85	1	2	3.5		17.3	19.6	
	4.6	0.72	88	50	3	5.3	1	1.22	1.53	0.95	1	2	5.3		17.3	19.6	
	6.5	0.72	125	69	6	8.6	1	1.22	1.24	0.95	1	2	8.6		17.3	19.6	
	8.6	0.72	167	90	6	7.9	1	1.22	1.07	1	1	2	7.9		17.3	19.6	
Averages =	5.2		100	56	3.6	5.4						2	5.4				
Compute representative values given the above average $(N_1)_{60cs}$:																	
	5.2	0.7	100	56	3.3	5.4	1	1.22	1.43	0.95	1	2	5.4	0.0	17.3	19.6	
Differ = -9%																	
<u>Ohama No. 3 (1)</u>	1.3	1.37	24	25	6	10.0	1	1.22	1.70	0.8	1	2	10.0		17.3	19.6	Iai et al. (1989)
	2.5	1.37	45	34	2	3.5	1	1.22	1.70	0.85	1	2	3.5		17.3	19.6	
	4.4	1.37	83	53	5	8.3	1	1.22	1.44	0.95	1	2	8.3		17.3	19.6	
	5.4	1.37	103	63	5	7.6	1	1.22	1.31	0.95	1	2	7.6		17.3	19.6	
	6.5	1.37	123	74	6	8.3	1	1.22	1.20	0.95	1	2	8.3		17.3	19.6	
	8.4	1.37	161	92	7	9.0	1	1.22	1.05	1	1	2	9.0		17.3	19.6	
10.3	1.37	199	111	11	12.8	1	1.22	0.95	1	1	7	12.9		17.3	19.6		
Averages =	5.4		103	63	5.0	7.4						2	7.4				
Compute representative values given the above average $(N_1)_{60cs}$:																	
	5.4	1.4	103	63	4.8	7.4	1	1.22	1.31	0.95	1	2	7.4	0.0	17.3	19.6	
Differ = -3%																	

Earthquake & site	Avg depth (m)	Depth GW (m)	σ_v (kPa)	σ'_v (kPa)	(N_m)	$(N_1)_{60}$	C_B	C_E	C_N	C_R	C_S	FC (%)	$(N_1)_{60cs}$	$\Delta(N_1)_{60cs}$	γ_{tot} above water table	γ_{tot} below water table	Primary source of data
<u>Ohama No. 3 (3)</u>	1.5	1.35	25	24	5	8.3	1	1.22	1.70	0.8	1	2	8.3		17.3	19.6	Iai et al. (1989)
	2.8	1.35	51	37	2	3.5	1	1.22	1.70	0.85	1	2	3.5		17.3	19.6	
	3.4	1.35	64	44	3	5.2	1	1.22	1.67	0.85	1	2	5.2		17.3	19.6	
	4.4	1.35	83	53	2	3.5	1	1.22	1.52	0.95	1	2	3.5		17.3	19.6	
	5.6	1.35	106	65	5	7.5	1	1.22	1.29	0.95	1	2	7.5		17.3	19.6	
	7.3	1.35	141	82	5	6.6	1	1.22	1.13	0.95	1	2	6.6		17.3	19.6	
	9.4	1.35	182	103	6	7.3	1	1.22	0.99	1	1	2	7.3		17.3	19.6	
	11.5	1.35	222	123	11	12.2	1	1.22	0.91	1	1	2	12.2		17.3	19.6	
	13.3	1.35	258	140	4	4.0	1	1.22	0.81	1	1	2	4.0		17.3	19.6	
Averages =	5.5		104	64	3.8	5.6						2	5.6				
Compute representative values given the above average $(N_1)_{60cs}$:																	
	5.5	1.4	104	64	3.7	5.6	1	1.22	1.32	0.95	1	2	5.6	0.0	17.3	19.6	
Differ = -5%																	
<u>Ohama No. 3 (4)</u>	1.4	1.46	25	26	8	13.3	1	1.22	1.70	0.8	1	2	13.3		17.3	19.6	Iai et al. (1989)
	2.6	1.46	48	36	3	5.3	1	1.22	1.70	0.85	1	2	5.3		17.3	19.6	
	3.3	1.46	62	44	5	8.3	1	1.22	1.61	0.85	1	2	8.3		17.3	19.6	
	4.3	1.46	81	53	6	9.9	1	1.22	1.42	0.95	1	2	9.9		17.3	19.6	
	5.4	1.46	102	64	6	9.0	1	1.22	1.29	0.95	1	2	9.0		17.3	19.6	
	7.3	1.46	140	83	13	16.6	1	1.22	1.10	0.95	1	2	16.6		17.3	19.6	
Averages =	3.9		73	49	5.0	8.1						2	8.1				
Compute representative values given the above average $(N_1)_{60cs}$:																	
	3.9	1.5	73	49	5.2	8.1	1	1.22	1.50	0.85	1	2	8.1	0.0	17.3	19.6	
Differ = 4%																	

Earthquake & site	Avg depth (m)	Depth GWT (m)	σ_v (kPa)	σ'_v (kPa)	(N_m)	$(N_1)_{60}$	C_B	C_E	C_N	C_R	C_S	FC (%)	$(N_1)_{60cs}$	$\Delta(N_1)_{60cs}$	γ_{tot} above water table	γ_{tot} below water table	Primary source of data
<u>Nakajima No. 1 (5)</u>	1.4	1.46	25	26	8	13.3	1	1.22	1.70	0.8	1	2	13.3		17.3	19.6	Iai et al. (1989)
	2.4	1.46	43	34	5	8.8	1	1.22	1.70	0.85	1	2	8.8		17.3	19.6	
	3.4	1.46	62	44	9	14.1	1	1.22	1.52	0.85	1	2	14.1		17.3	19.6	
	4.4	1.46	84	54	20	29.2	1	1.22	1.26	0.95	1	2	29.2		17.3	19.6	
	6.4	1.46	121	73	3	4.2	1	1.22	1.20	0.95	1	20	8.6		17.3	19.6	
	7.5	1.46	143	84	5	6.5	1	1.22	1.11	0.95	1	8	6.8		17.3	19.6	
	8.3	1.46	158	92	7	9.0	1	1.22	1.05	1	1	10	10.2		17.3	19.6	
	10.3	1.46	198	111	8	9.3	1	1.22	0.95	1	1	10	10.4		17.3	19.6	
	12.3	1.46	238	131	8	8.5	1	1.22	0.87	1	1	13	11.0		17.3	19.6	
	13.2	1.46	255	140	17	17.9	1	1.22	0.86	1	1	10	19.1		17.3	19.6	
Averages =	6.5	1.5	124	74	6.6	9.2						Average=	8.38	10.4			
Compute representative values given the above average $(N_1)_{60cs}$:																	
	6.5	1.5	124	74	7.3	9.9	1	1.22	1.18	0.95	1	8.38	10.4	0.5	17.3	19.6	
Differ = 10%																	
<u>Nakajima No. 2 (1)</u>	2.3	1.45	41	33	6	10.6	1	1.22	1.70	0.85	1	3	10.6		17.3	19.6	Iai et al. (1989)
	4.5	1.45	85	55	5	8.2	1	1.22	1.41	0.95	1	3	8.2		17.3	19.6	
	5.6	1.45	105	65	11	15.7	1	1.22	1.23	0.95	1	3	15.7		17.3	19.6	
	6.4	1.45	123	74	18	23.7	1	1.22	1.14	0.95	1	3	23.7		17.3	19.6	
	8.4	1.45	161	93	7	9.0	1	1.22	1.05	1	1	3	9.0		17.3	19.6	
	10.4	1.45	200	112	5	5.7	1	1.22	0.94	1	1	3	5.7		17.3	19.6	
	12.4	1.45	240	133	20	21.8	1	1.22	0.89	1	1	3	21.8		17.3	19.6	
Averages =	7.1		136	81	10.3	13.5						Average=	3	13.5			
Compute representative values given the above average $(N_1)_{60cs}$:																	
	7.1	1.5	136	81	10.4	13.5	1	1.22	1.12	0.95	1	3	13.5	0.0	17.3	19.6	
Differ = 1%																	

Earthquake & site	Avg depth (m)	Depth GW (m)	σ_v (kPa)	σ'_v (kPa)	(N_m)	$(N_1)_{60}$	C_B	C_E	C_N	C_R	C_S	FC (%)	$(N_1)_{60cs}$	$\Delta(N_1)_{60cs}$	γ_{tot} above water table	γ_{tot} below water table	Primary source of data
-------------------	---------------	--------------	------------------	-------------------	---------	--------------	-------	-------	-------	-------	-------	--------	----------------	----------------------	----------------------------------	----------------------------------	------------------------

<u>Nakajima No. 2 (2)</u>	2.4	1.5	43	34	6.00	10.6	1	1.22	1.70	0.85	1	7	10.7		17.3	19.6	Iai et al. (1989)
	3.3	1.5	62	44	11.00	16.9	1	1.22	1.48	0.85	1	7	17.0		17.3	19.6	
	4.2	1.5	79	53	2.00	3.5	1	1.22	1.52	0.95	1	7	3.7		17.3	19.6	
	5.2	1.5	99	62	4.00	6.2	1	1.22	1.33	0.95	1	7	6.3		17.3	19.6	

Averages = 3.8 71 48 5.8 9.3 Average= 7 9.4

Compute representative values given the above average $(N_1)_{60cs}$:

3.8 1.5 71 48 6.0 9.3 1 1.22 1.50 0.85 1 7 9.4 0.1 17.3 19.6

Differ = 4%

<u>Nakajima No. 3(3)</u>	1.4	1.58	27	29	4.00	6.6	1	1.22	1.70	0.8	1	2	6.6		17.3	19.6	Iai et al. (1989)
	2.5	1.58	45	36	4.00	7.1	1	1.22	1.70	0.85	1	2	7.1		17.3	19.6	
	3.3	1.58	62	44	4.00	6.7	1	1.22	1.62	0.85	1	2	6.7		17.3	19.6	
	4.2	1.58	78	53	4.00	6.8	1	1.22	1.46	0.95	1	2	6.8		17.3	19.6	
	5.4	1.58	103	65	10.00	14.4	1	1.22	1.24	0.95	1	2	14.4		17.3	19.6	
	6.4	1.58	121	74	8.00	10.9	1	1.22	1.18	0.95	1	2	10.9		17.3	19.6	
	8.4	1.58	161	94	13.00	16.4	1	1.22	1.04	1	1	2	16.4		17.3	19.6	
	10.4	1.58	200	113	10.00	11.5	1	1.22	0.94	1	1	2	11.5		17.3	19.6	
	12.4	1.58	238	133	11.00	11.7	1	1.22	0.87	1	1	2	11.7		17.3	19.6	

Averages = 6.0 115 71 7.6 10.2 Average= 2 10.2

Compute representative values given the above average $(N_1)_{60cs}$:

6.0 1.6 115 71 7.3 10.2 1 1.22 1.21 0.95 1 2 10.2 0.0 17.3 19.6

Differ = -3%

Earthquake & site	Avg depth (m)	Depth GWL (m)	σ_v (kPa)	σ'_v (kPa)	(N_m)	$(N_1)_{60}$	C_B	C_E	C_N	C_R	C_S	FC (%)	$(N_1)_{60cs}$	$\Delta(N_1)_{60cs}$	γ_{tot} above water table	γ_{tot} below water table	Primary source of data
<u>Nakajima No. 3(4)</u>	2.3	1.51	41	34	5.00	8.8	1	1.22	1.70	0.85	1	2	8.8		17.3	19.6	Iai et al. (1989)
	3.3	1.51	61	43	6.00	9.9	1	1.22	1.59	0.85	1	2	9.9		17.3	19.6	
	4.3	1.51	81	54	5.00	8.3	1	1.22	1.43	0.95	1	2	8.3		17.3	19.6	
	5.5	1.51	105	65	10.00	14.4	1	1.22	1.24	0.95	1	2	14.4		17.3	19.6	
	6.4	1.51	121	74	12.00	16.2	1	1.22	1.16	0.95	1	2	16.2		17.3	19.6	
	8.3	1.51	160	93	9.00	11.5	1	1.22	1.05	1	1	2	11.5		17.3	19.6	
	10.1	1.51	195	110	10.00	11.7	1	1.22	0.96	1	1	2	11.7		17.3	19.6	
Averages =	5.7		109	68	8.1	11.5						Average=	2	11.5			
Compute representative values given the above average $(N_1)_{60cs}$:																	
	5.7	1.5	109	68	8.0	11.5	1	1.22	1.24	0.95	1	2	11.5	0.0	17.3	19.6	
Differ = -1%																	
<u>Ohama No. 1(1)</u>	1.4	1.2	24	22	18.00	29.9	1	1.22	1.70	0.8	1	2	29.9		17.3	19.6	Iai et al. (1989)
	2.4	1.2	43	32	9.00	15.9	1	1.22	1.70	0.85	1	3	15.9		17.3	19.6	
	3.5	1.2	65	43	10.00	15.7	1	1.22	1.51	0.85	1	2	15.7		17.3	19.6	
	4.4	1.2	83	52	13.00	20.2	1	1.22	1.34	0.95	1	2	20.2		17.3	19.6	
	5.4	1.2	103	62	17.00	24.1	1	1.22	1.22	0.95	1	3	24.1		17.3	19.6	
	6.4	1.2	123	72	22.00	29.0	1	1.22	1.14	0.95	1	3	29.0		17.3	19.6	
Averages =	3.9		74	47	12.3	18.9						Average=	2.5	18.9			
Compute representative values given the above average $(N_1)_{60cs}$:																	
	3.9	1.2	74	47	13.0	18.9	1	1.22	1.41	0.85	1	2.5	18.9	0.0	17.3	19.6	
Differ = 6%																	

Earthquake & site	Avg depth (m)	Depth GW (m)	σ_v (kPa)	σ'_v (kPa)	(N_m)	$(N_1)_{60}$	C_B	C_E	C_N	C_R	C_S	FC (%)	$(N_1)_{60cs}$	$\Delta(N_1)_{60cs}$	γ_{tot} above water table	γ_{tot} below water table	Primary source of data
<u>Ohama No. 1(2)</u>	2.4	1.2	44	33	10.00	17.5	1	1.22	1.69	0.85	1	2	17.5		17.3	19.6	Iai et al. (1989)
	4.4	1.2	84	52	20.00	29.5	1	1.22	1.27	0.95	1	2	29.5		17.3	19.6	
	6.3	1.2	121	71	25.00	32.8	1	1.22	1.13	0.95	1	3	32.8		17.3	19.6	
	8.5	1.2	163	92	27.00	34.1	1	1.22	1.03	1	1	6	34.1		17.3	19.6	
	10.4	1.2	202	111	28.00	33.1	1	1.22	0.97	1	1	6	33.1		17.3	19.6	
Averages =	3.4		64	42	15.0	23.5						2	23.5				
Compute representative values given the above average $(N_1)_{60cs}$:																	
	3.4	1.2	64	42	15.9	23.5	1	1.22	1.43	0.85	1	2	23.5	0.0	17.3	19.6	
Differ = 6%																	
<u>Ohama No. 1(3)</u>	1.6	1.2	29	25	14.00	23.2	1	1.22	1.70	0.8	1	1	23.2		17.3	19.6	Iai et al. (1989)
	2.5	1.2	46	34	11.00	18.8	1	1.22	1.65	0.85	1	1	18.8		17.3	19.6	
	3.6	1.2	68	45	19.00	27.0	1	1.22	1.37	0.85	1	1	27.0		17.3	19.6	
	4.8	1.2	91	56	20.00	29.0	1	1.22	1.25	0.95	1	4	29.0		17.3	19.6	
	5.6	1.2	107	64	21.00	28.9	1	1.22	1.19	0.95	1	4	28.9		17.3	19.6	
Averages =	2.6		48	34	14.7	23.0						1	23.0				
Compute representative values given the above average $(N_1)_{60cs}$:																	
	2.6	1.2	48	34	14.1	23.0	1	1.22	1.57	0.85	1	1	23.0	0.0	17.3	19.6	
Differ = -4%																	

Earthquake & site	Avg depth (m)	Depth GW (m)	σ_v (kPa)	σ'_v (kPa)	(N_m)	$(N_1)_{60}$	C_B	C_E	C_N	C_R	C_S	FC (%)	$(N_1)_{60cs}$	$\Delta(N_1)_{60cs}$	γ_{tot} above water table	γ_{tot} below water table	Primary source of data
<u>Ohama No. 1(4)</u>	2.2	1.2	40	30	21.00	32.0	1	1.22	1.47	0.85	1	20	36.5		17.3	19.6	Iai et al. (1989)
	3.3	1.2	61	41	19.00	27.1	1	1.22	1.38	0.85	1	20	31.6		17.3	19.6	
	4.2	1.2	80	50	22.00	32.5	1	1.22	1.27	0.95	1	1	32.5		17.3	19.6	
	5.2	1.2	99	60	25.00	34.6	1	1.22	1.19	0.95	1	3	34.6		17.3	19.6	
	6.2	1.2	118	69	28.00	36.6	1	1.22	1.13	0.95	1	4	36.6		17.3	19.6	
	7.1	1.2	137	79	32.00	40.0	1	1.22	1.08	0.95	1	4	40.0		17.3	19.6	
Averages =	5.2		99	60	25.0	34.6						Average=	2.67	34.6			
Compute representative values given the above average $(N_1)_{60cs}$:																	
	5.2	1.2	99	60	25.0	34.6	1	1.22	1.19	0.95	1	2.67	34.6	0.0	17.3	19.6	
Differ = 0%																	
<u>Ohama No. 1(5)</u>	1.3	1.2	23	22	25.00	38.9	1	1.22	1.60	0.8	1	1	38.9		17.3	19.6	Iai et al. (1989)
	2.1	1.2	39	30	25.00	37.9	1	1.22	1.46	0.85	1	1	37.9		17.3	19.6	
	3.2	1.2	60	40	25.00	35.1	1	1.22	1.35	0.85	1	1	35.1		17.3	19.6	
Averages =	2.2		41	31	25.0	37.3						Average=	1	37.3			
Compute representative values given the above average $(N_1)_{60cs}$:																	
	2.2	1.2	41	31	24.7	37.3	1	1.22	1.46	0.85	1	1	37.3	0.0	17.3	19.6	
Differ = -1%																	

Earthquake & site	Avg depth (m)	Depth GWT (m)	σ_v (kPa)	σ'_v (kPa)	(N_m)	$(N_1)_{60}$	C_B	C_E	C_N	C_R	C_S	FC (%)	$(N_1)_{60cs}$	$\Delta(N_1)_{60cs}$	γ_{tot} above water table	γ_{tot} below water table	Primary source of data
<u>Ohama No. 1 (58-22)</u>	2.5	1.2	46	33	12.00	20.3	1	1.22	1.63	0.85	1	4	20.3		17.3	19.6	Iai et al. (1989)
	3.5	1.2	66	43	14.00	21.0	1	1.22	1.45	0.85	1	2	21.0		17.3	19.6	
	4.5	1.2	86	53	15.00	22.8	1	1.22	1.31	0.95	1	3	22.8		17.3	19.6	
	5.4	1.2	103	62	13.00	18.8	1	1.22	1.25	0.95	1	1	18.8		17.3	19.6	
	6.5	1.2	125	73	14.00	18.8	1	1.22	1.16	0.95	1	2	18.8		17.3	19.6	
Averages =	4.5		85	53	13.6	20.3						2.4	20.3				
Compute representative values given the above average $(N_1)_{60cs}$:																	
	4.5	1.2	85	53	13.2	20.3	1	1.22	1.33	0.95	1	2.4	20.3	0.0	17.3	19.6	
Differ = -3%																	
<u>Ohama No. Rvt (1)</u>	1.6	1.45	27	26	15.00	24.9	1	1.22	1.70	0.8	1	1	24.9		17.3	19.6	Iai et al. (1989)
	3.6	1.45	66	46	17.00	24.3	1	1.22	1.38	0.85	1	1	24.3		17.3	19.6	
	5.6	1.45	106	66	18.00	24.8	1	1.22	1.19	0.95	1	3	24.8		17.3	19.6	
	7.5	1.45	143	84	16.00	20.1	1	1.22	1.08	0.95	1	2	20.1		17.3	19.6	
Averages =	4.5		86	55	16.5	23.5						1.75	23.5				
Compute representative values given the above average $(N_1)_{60cs}$:																	
	4.5	1.5	86	55	15.8	23.5	1	1.22	1.28	0.95	1	1.75	23.5	0.0	17.3	19.6	
Differ = -4%																	

Earthquake & site	Avg depth (m)	Depth GWT (m)	σ_v (kPa)	σ'_v (kPa)	(N_m)	$(N_1)_{60}$	C_B	C_E	C_N	C_R	C_S	FC (%)	$(N_1)_{60cs}$	$\Delta(N_1)_{60cs}$	γ_{tot} above water table	γ_{tot} below water table	Primary source of data
-------------------	---------------	---------------	------------------	-------------------	---------	--------------	-------	-------	-------	-------	-------	--------	----------------	----------------------	----------------------------------	----------------------------------	------------------------

<u>Ohama No.</u>	1.7	1.6	30	29	17.00	26.9	1	1.22	1.62	0.8	1	0	26.9		17.3	19.6	Iai et al. (1989)
<u>Rvt (2)</u>	3.7	1.6	68	48	15.00	21.4	1	1.22	1.38	0.85	1	2	21.4		17.3	19.6	
	5.7	1.6	107	68	6.00	8.7	1	1.22	1.25	0.95	1	9	9.4		17.3	19.6	
	7.7	1.6	147	87	24.00	29.4	1	1.22	1.06	0.95	1	3	29.4		17.3	19.6	
	9.6	1.6	184	106	20.00	24.0	1	1.22	0.98	1	1	4	24.0		17.3	19.6	
	11.7	1.6	225	126	21.00	23.4	1	1.22	0.91	1	1	8	23.8		17.3	19.6	

Averages = 6.7 127 77 17.2 22.3 Average= 4.33 22.5

Compute representative values given the above average $(N_1)_{60cs}$:

6.7 1.6 127 77 17.3 22.5 1 1.22 1.12 0.95 1 4.33 22.5 0.0 17.3 19.6

Differ = 1%

<u>Ohama No.</u>	1.8	1.45	33	29	16.00	25.6	1	1.22	1.64	0.8	1	0	25.6		17.3	19.6	Iai et al. (1989)
<u>Rvt (3)</u>	3.5	1.45	64	45	15.00	22.0	1	1.22	1.41	0.85	1	1	22.0		17.3	19.6	
	5.4	1.45	103	64	22.00	30.1	1	1.22	1.18	0.95	1	0	30.1		17.3	19.6	
	7.3	1.45	140	82	26.00	32.4	1	1.22	1.07	0.95	1	2	32.4		17.3	19.6	
	9.5	1.45	182	104	25.00	30.3	1	1.22	0.99	1	1	14	33.2		17.3	19.6	

Averages = 3.6 67 46 17.7 25.9 Average= 0.33 25.9

Compute representative values given the above average $(N_1)_{60cs}$:

3.6 1.5 67 46 18.3 25.9 1 1.22 1.37 0.85 1 0.33 25.9 0.0 17.3 19.6

Differ = 4%

Earthquake & site	Avg depth (m)	Depth GWT (m)	σ_v (kPa)	σ'_v (kPa)	(N_m)	$(N_1)_{60}$	C_B	C_E	C_N	C_R	C_S	FC (%)	$(N_1)_{60cs}$	$\Delta(N_1)_{60cs}$	γ_{tot} above water table	γ_{tot} below water table	Primary source of data
<u>Akita station (1)</u>	1.4	1.75	30	34	13.00	20.4	1	1.22	1.61	0.8	1	3	20.4		17.3	19.6	Iai et al. (1989)
	2.4	1.75	43	37	12.00	19.6	1	1.22	1.57	0.85	1	4	19.6		17.3	19.6	
	3.3	1.75	61	46	12.00	17.9	1	1.22	1.44	0.85	1	1	17.9		17.3	19.6	
Averages =	2.9		52	41	12.0	18.7							2.5	18.7			
Compute representative values given the above average $(N_1)_{60cs}$:																	
	2.9	1.8	52	41	12.0	18.7	1	1.22	1.50	0.85	1	2.5	18.7	0.0	17.3	19.6	
Differ = 0%																	
<u>Akita station (2)</u>	1.5	1.75	30	33	9.00	14.9	1	1.22	1.70	0.8	1	3	14.9		17.3	19.6	Iai et al. (1989)
	2.4	1.75	43	37	8.00	13.8	1	1.22	1.66	0.85	1	4	13.8		17.3	19.6	
	3.4	1.75	63	46	9.00	13.8	1	1.22	1.48	0.85	1	1	13.8		17.3	19.6	
Averages =	2.9		53	41	8.5	13.8							2.5	13.8			
Compute representative values given the above average $(N_1)_{60cs}$:																	
	2.9	1.8	53	41	8.5	13.8	1	1.22	1.56	0.85	1	2.5	13.8	0.0	17.3	19.6	
Differ = 0%																	
<u>Aomori Port</u>	1.3	1.14	23	22	4.00	6.6	1	1.22	1.70	0.8	1	4	6.6		17.3	19.6	Iai et al. (1989)
	2.4	1.14	44	32	10.00	17.6	1	1.22	1.70	0.85	1	4	17.6		17.3	19.6	
	3.3	1.14	63	41	6.00	10.1	1	1.22	1.62	0.85	1	4	10.1		17.3	19.6	
	4.3	1.14	81	50	10.00	16.2	1	1.22	1.40	0.95	1	4	16.2		17.3	19.6	
	5.4	1.14	103	61	10.00	14.8	1	1.22	1.28	0.95	1	7	14.9		17.3	19.6	
Averages =	3.3		63	41	8.0	13.1							4.6	13.1			
Compute representative values given the above average $(N_1)_{60cs}$:																	
	3.3	1.1	63	41	8.0	13.1	1	1.22	1.58	0.85	1	4.6	13.1	0.0	17.3	19.6	
Differ = 0%																	

Earthquake & site	Avg depth (m)	Depth GW (m)	σ_v (kPa)	σ'_v (kPa)	(N_m)	$(N_1)_{60}$	C_B	C_E	C_N	C_R	C_S	FC (%)	$(N_1)_{60cs}$	$\Delta(N_1)_{60cs}$	γ_{tot} above water table	γ_{tot} below water table	Primary source of data
-------------------	---------------	--------------	------------------	-------------------	---------	--------------	-------	-------	-------	-------	-------	--------	----------------	----------------------	----------------------------------	----------------------------------	------------------------

<u>Hakodate</u>	2.8	1.6	51	39	3.00	5.2	1	1.22	1.66	0.85	1	34	10.7		17.3	19.6	Iai et al. (1989)
	3.8	1.6	71	50	4.00	6.0	1	1.22	1.45	0.85	1	34	11.5		17.3	19.6	
	4.8	1.6	90	59	2.00	3.1	1	1.22	1.36	0.95	1	98	8.6		17.3	19.6	
	5.8	1.6	110	69	2.00	2.9	1	1.22	1.24	0.95	1	98	8.4		17.3	19.6	
	6.7	1.6	128	78	5.00	6.7	1	1.22	1.15	0.95	1	20	11.1		17.3	19.6	
	7.8	1.6	149	88	6.00	7.5	1	1.22	1.07	0.95	1	20	11.9		17.3	19.6	
Averages =	4.3		81	54	2.8	4.3						Average=	66	9.8			

Compute representative values given the above average $(N_1)_{60cs}$:

4.3	1.6	81	54	2.6	4.2	1	1.22	1.41	0.95	1	66	9.8	5.6	17.3	19.6
-----	-----	----	----	-----	-----	---	------	------	------	---	----	-----	-----	------	------

Differ = -6%

1968 M=7.5 earthquake (April 1) and 1984 M=6.9 earthquake (Aug 7)

<u>Hososhima</u>	1.9	2	35	36	4.00	6.6	1	1.22	1.70	0.8	1	36	12.2		17.3	19.6	Iai et al. (1989)
	3.9	2	72	53	13.00	17.6	1	1.22	1.31	0.85	1	36	23.1		17.3	19.6	
	6.0	2	112	73	20.00	26.0	1	1.22	1.12	0.95	1	36	31.5		17.3	19.6	
	7.9	2	151	93	23.00	27.5	1	1.22	1.03	0.95	1	36	33.0		17.3	19.6	
	9.9	2	190	112	19.00	22.3	1	1.22	0.96	1	1	36	27.8		17.3	19.6	
	11.9	2	228	131	18.00	19.8	1	1.22	0.90	1	1	36	25.3		17.3	19.6	
Averages =	2.9		53	45	8.5	12.1						Average=	36	17.6			

Compute representative values given the above average $(N_1)_{60cs}$:

2.9	2.0	53	45	8.0	12.1	1	1.22	1.46	0.85	1	36	17.6	5.5	17.3	19.6
-----	-----	----	----	-----	------	---	------	------	------	---	----	------	-----	------	------

Differ = -6%

Earthquake & site	Avg depth (m)	Depth GWT (m)	σ_v (kPa)	σ'_v (kPa)	(N_m)	$(N_1)_{60}$	C_B	C_E	C_N	C_R	C_S	FC (%)	$(N_1)_{60cs}$	$\Delta(N_1)_{60cs}$	γ_{tot} above water table	γ_{tot} below water table	Primary source of data
-------------------	---------------	---------------	------------------	-------------------	---------	--------------	-------	-------	-------	-------	-------	--------	----------------	----------------------	----------------------------------	----------------------------------	------------------------

1982 M=6.9 Urakawa-Oki earthquake - Mar 21

<u>Tokachi</u>	0.3	1.62	28	41	4.00	6.2	1	1.22	1.70	0.75	1	5	6.2		17.3	19.6	Iai et al. (1989)
	0.9	1.62	28	35	7.00	10.9	1	1.22	1.70	0.75	1	5	10.9		17.3	19.6	
	1.8	1.62	31	30	10.00	16.6	1	1.22	1.70	0.8	1	5	16.6		17.3	19.6	
	2.9	1.62	53	41	11.00	17.4	1	1.22	1.53	0.85	1	5	17.4		17.3	19.6	
Averages =	2.4		42	35	10.5	17.0						5	17.0				

Compute representative values given the above average $(N_1)_{60cs}$:

2.4	1.6	42	35	10.0	17.0	1	1.22	1.64	0.85	1	5	17.0	0.0	17.3	19.6
-----	-----	----	----	------	------	---	------	------	------	---	---	------	-----	------	------

Differ = -5%